PALEOGEOGRAPHIC RECONSTRUCTION OF PART OF EASTERN GONDWANALAND: PETROFACIES AND DETRITAL GEOCHRONOLOGIC STUDY OF PERMO-CARBONIFEROUS GONDWANAN SEQUENCES OF INDIA AND BANGLADESH

by

Nur Uddin Md. Khaled Chowdhury

A thesis submitted to the Graduate faculty of
Auburn University
in partial fulfillment of the
requirements for the Degree of
Master of Science in Geology

Auburn, Alabama
December 13, 2014

Keywords: Gondwana, Permo-Carboniferous, Petrofacies, $^{40}Ar/^{39}Ar$ Geochronology, India and Bangladesh

Approved by:

Ashraf Uddin (Chair), Professor of Geology and Geography
Charles E. Savrda, Professor of Geology and Geography
David T. King, Jr., Professor of Geology and Geography
Willis E. Hames, Professor of Geology and Geography

Abstract

PALEOGEOGRAPHIC RECONSTRUCTION OF PART OF EASTERN GONDWANALAND: PETROFACIES AND DETRITAL GEOCHRONOLOGIC STUDY OF PERMO-CARBONIFEROUS GONDWANAN SEQUENCES OF INDIA AND BANGLADESH

This study has been carried out focusing on petrofacies and geochronology of Permo-Carboniferous Gondwanan sequences of Barapukuria, Dighipara, and Khalaspir coal basins in the Bengal Basin and Jharia Basin in the Eastern India in order to better reconstruct regional detrital and tectonic histories of Late Paleozoic Gondwanan basins of South Asia.

Sandstone petrographic studies of Permo-Carboniferous Gondwanan sequences reveal differences in sandstone modes between sediments from India and the Bengal Basin. Modal compositions vary among various basins and among sandstones from different stratigraphic levels of the same basin. These compositional differences may be attributed to differences in source rocks.

Heavy mineral assemblages in Gondwanan sequences of Bangladesh and India are dominated by a few mineral groups, including garnet, apatite, zircon, rutile, tourmaline, sphene, epidote, siderite and opaques. Microprobe studies of garnets show all analyzed grains are almandine rich and indicate sources from amphibolite facies, granulite facies, and pegmatites. Ca-Fe(tot)-Mg plots suggest that tourmaline grains

were derived from Ca-poor metapelites, metapsammites, and quartz tourmaline rocks, with one exception. The exceptional sample from Dighipara appears to have derived from Ca-rich metapelites, metapsammites, and calc-silicate rocks.

Laser $^{40}Ar/^{39}Ar$ analyses of detrital muscovites show mostly polymodal distributions of cooling ages indicating multiple source terranes. Age distributions for Indian sediments significantly differ from those of the Bengal Basin samples. Age distributions from Bengal samples strongly fall in a narrow zone of Cambro-Ordovician (470 – 520 Ma). In contrast, Indian samples are more scattered (480 – 1830 Ma) and include more Neoproterozoic cooling ages. However, Indan samples also include significant age distributions of Cambro-Ordovician. Within the Indian basin, the age distributions of the older Talchir Formation significantly differ from those of the younger Barakar sandstones. Stratigraphic changes in the modes of age distributions for muscovites may reflect changes in source terranes through time. Similarities between the ages of the present study to published geochronology of the Kuunga orogen, Shingbhum craton, Meghalayan craton, and/or Eastern Ghats Mobile Belt are interpreted to indicate these regions are the most probable sources of Gondwanan sediments in Bengal Basin and the Jharia Basin of eastern India.

Acknowledgments

It is my pleasure to thank all those who assisted directly and indirectly with my thesis. I am pleased to thank the almighty God who has been with me all the way and given me the scope to study about the mystery of the Earth. It was a really enjoyable experience to work with Dr. Ashraf Uddin, my thesis advisor. I appreciate all his help and support that he provided to me for last two years. Dr. Uddin helped me not only as the principal advisor but also as a real guardian to get the best outcome of this research.

I would also like to express my heartfelt thanks to Dr. Charles E. Savrda, David T. King, Jr., and Willis E. Hames for their contributions to this research as my thesis committee members. Dr. Savrda helped with significant editing in this thesis. Dr. Hames helped me understand many aspects of detrital geochronology. I am grateful to Dr. King, for giving me a better handle on stratigraphy. Also, I would like to thank all other faculty members of Geology and Geography at Auburn University.

Auburn University, American Association of Petroleum Geologists, and the Geological Society of America provided financial assistance without which this research would not have been possible. I would like to express my heartfelt gratitude to Dr. Abhijit Basu from Indiana University and Dr. Sukanta Dey, Indian School of Mines for their help in collecting samples from the Jharia Basin, India. Mrs. Munira Akhter, former director general of Geological Survey of Bangladesh (GSB) and Mr. Akhtarul Ahsan

(Rohan) helped me tremendously to collect sediment core samples from Bengal Basin. I very much appreciate their help.

I want to thank Mr. Chris Fleisher of University of Georgia for his help with microprobe analysis. I am also grateful to Ms. Sheila Arington and Delaine Tease for their support with administrative work. I thank Dr. Zeki Billor for his guidance in muscovite separation. I also want to thank Ruhollah Keshvardoost and Ziaul Haque for their enormous support and help during this work. I would also like to thank all graduate students and my colleagues, for their help and support.

Finally, I would like to thank my parents, without whom nothing would have been possible for me, and my siblings for all their continuous support and encouragement.

Table of Contents

List of Tables

List of Figures

List of Abbreviations

ZTR	Zircon, Tourmaline, Rutile
ANIMAL	Auburn Noble Isotope Mass Analysis Laboratory
EMP	Electron Microprobe
BSE	Back Scattered Electron

CHAPTER 1: INTRODUCTION

1.1 INTRODUCTION

Studies of sandstone composition are powerful tools in tracing sediment provenance (Dickinson and Suczek, 1979; Johnsson, 1993). Petrofacies (Facies distinguished primarily on the basis of appearance or composition without respect to form, boundaries, or mutual relations, [Weller, 1958, p.627]) studies of detrital sequences can help interpret paleogeography, paleoclimate, ancient plate tectonic settings, and uplift and exhumation histories (Graham et al., 1976; Dickinson and Suczek, 1979; Johnsson, 1993; Sitaula, 2009; Alam, 2011).

Provenance studies focusing on detrital mineralogy are an important tool for revealing basin evolution and denudation history of orogenic belts. Sandstone compositional analyses, in which proportions of detrital framework grains within sand (stone) samples are plotted on different ternary diagrams (such as Q_tFL, Q_mFL_t, and Q_mPK), can help distinguish various tectonic settings of source areas (Ingersoll and Busby, 1995; Ingersoll et al., 1995). Various factors other than source rock may have significant control on composition of detrital sediments. These include modes of transportation, depositional environments, climate, and diagenesis (Suttner, 1974). Even though the interactions between these factors are complex, they typically behave in similar ways in any given setting (Dickinson and Suczek, 1979; Dickinson et al., 1983; Johnsson, 1993).

As sediments are transported long distances from their source areas, feldspar grains and lithic fragments become separated from relict quartz and are chemically

broken down. This results in quartz-rich sandstones that are characteristic of continental interiors and passive-margin platform settings, and massive, mud-rich deltas characteristic of passive continental margin slope settings. In contrast, magmatic arc depositional systems tend to have short transport distances, which reduce physical sediment sorting and chemical weathering, and results in sandstones that are less enriched in quartz and more abundant in lithics.

Studies of detrital geochronology of certain minerals (e.g., muscovite, zircon, apatite, etc.) in sands provide valuable insight into cooling ages of detrital minerals and thus yield essential information on unroofing histories of source terranes and sediment routing networks (i.e., Peavy, 2008; Sitaula, 2009; Alam, 2011; Moore, 2012).

The southern supercontinent that existed from 550 to 167 million years is known as the Gondwanaland. The Indian subcontinent, along with Australia and Antarctica, constituted Eastern Gondwanaland, whereas the South American and African continents comprised the primary components of Western Gondwanaland (Fig. 1.1). Medlicott (1873) first assigned the name 'Gondwana' to a suite of rocks he studied in the Satpura Basin in Madhya Pradesh, India. He coined the term ‘Gondwana’ after an aboriginal tribe of Central India.

Permo-Carboniferous Gondwanan sequences are well-distributed in the Indian subcontinent, South Africa, Madagascar, Australia, Antarctica and South America, bearing proof that the southern continents were once united in the form of Gondwanaland. Deposition of Gondwanan sediments in Peninsular India was initiated during the Late Carboniferous after a hiatus spanning about 250 million years,

subsequent to the deposition of Neoproterozoic to Early Cambrian Vindhyan and Kurnool sediments (Vaidyanadhan and Ramakrishnan, 2008). In the Indian subcontinent, these sequences were initially deposited in one master basin that later was segmented during Gondwanan extensional tectonics (Veevers and Tewari, 1995).

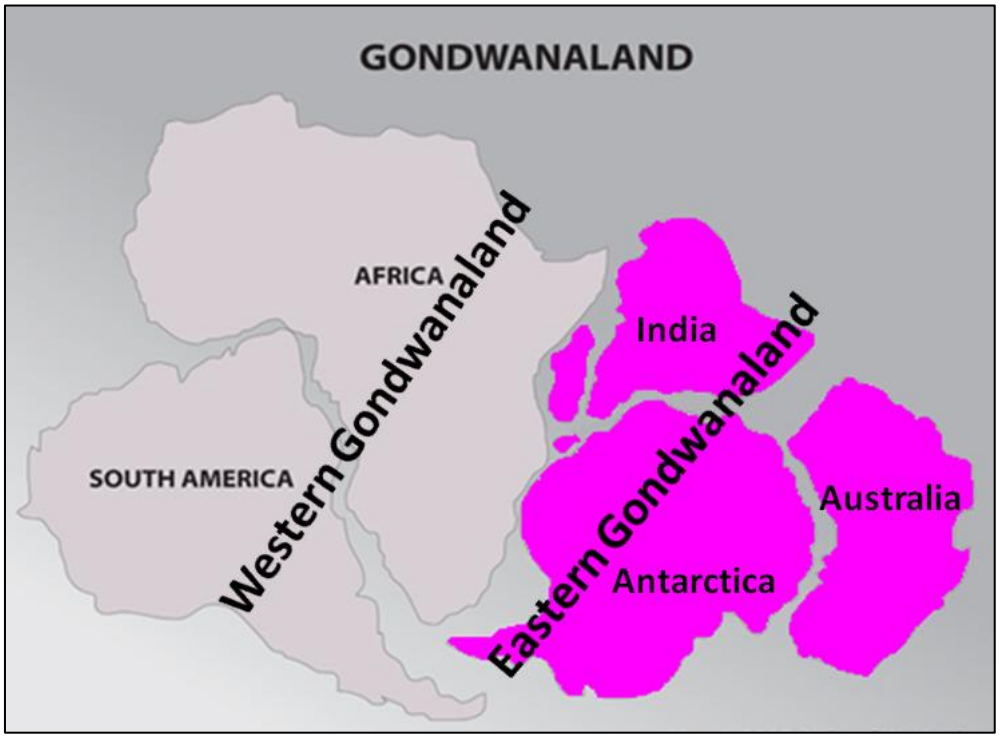

Figure 1.1 Paleogeographic map of Gondwanaland (after Rogers et al., 1995).

1.2 LOCATION OF THE STUDY AREA

The present study is focused on Gondwanan sequences of India and Bangladesh (Fig. 1.2). Samples of these Permo-Carboniferous sequences were collected from outcrops in the Jharia basin (also known as Damodar basin), India. The Damodar basin in eastern India consists of a series of approximately east-west elongated isolated Gondwanan basins that are also known as the Damodar system. The Jharia basin is located in the eastern part (of Damodar system (Fig. 1.2).

None of the Gondwanan sequences are exposed in Bangladesh. However, these sequences are encountered in several wells in the Indian Platform region of the Bengal basin (Fig. 1.3). Gondwanan sediments from northwestern Bangladesh were collected from three coal basins; i.e., Barapukuria, Khalaspir, and Dighipara basins (Figs. 1.2 and 1.3). Core samples were acquired at repositories of the Geological Survey of Bangladesh (GSB) from three drill wells; i.e. GDH-41 (Barapukuria), GDH-45 (Khalaspir), and GDH-62 (Dighipara).

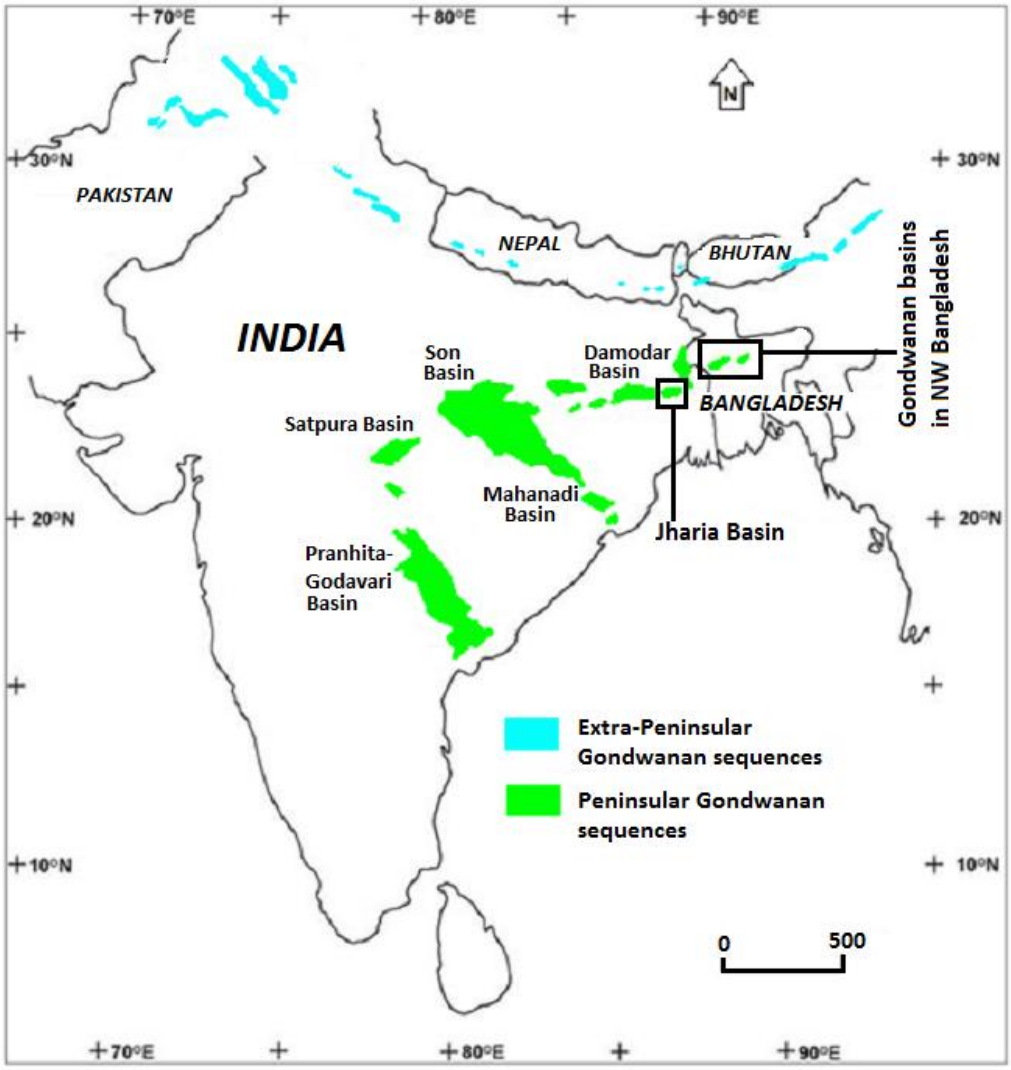

Figure 1.2 Location map showing distribution of Gondwanan basins in the Indian subcontinent (after Frakes et al., 1975). Studied areas are indicated by open rectangles.

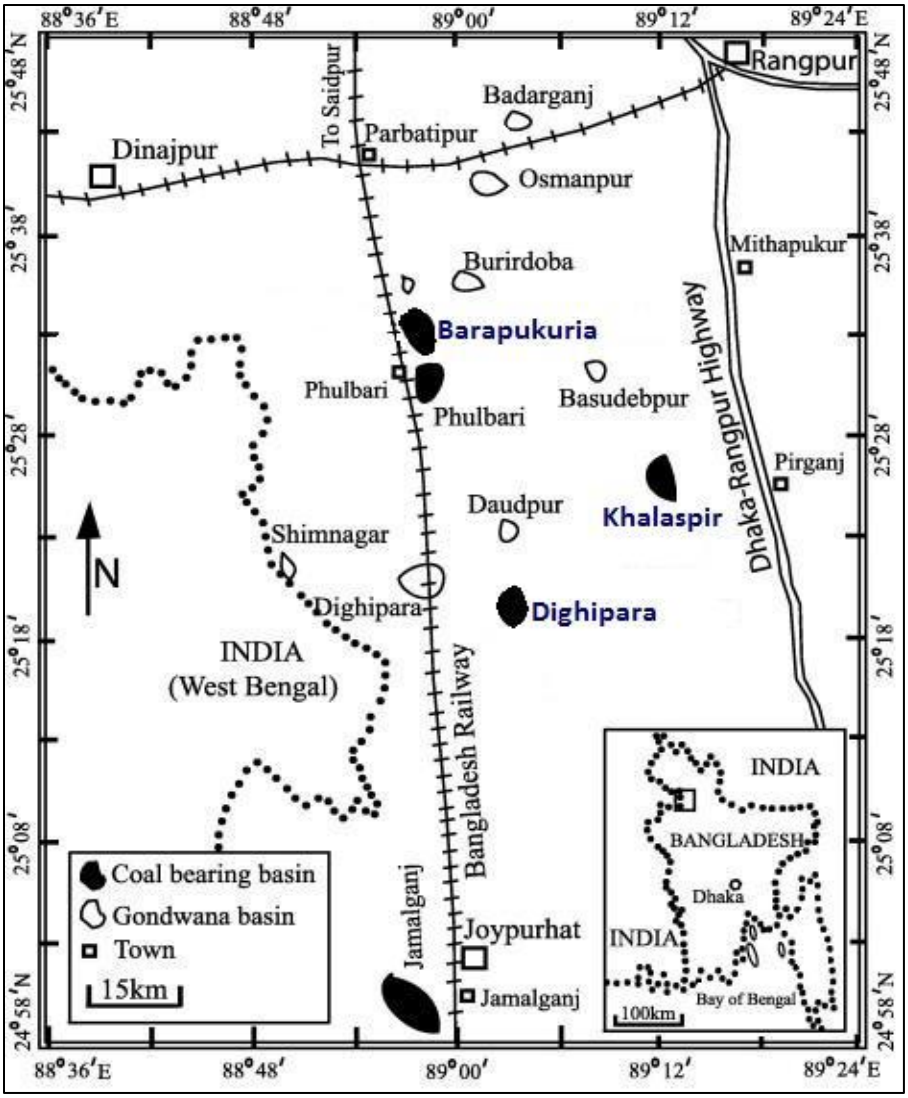

Figure 1.3 Permo-Carboniferous Gondwana basins in Indian platform part of northwest Bangladesh (after Farhaduzzaman et al., 2013). Core samples for this study were collected from wells drilled in Barapukuria, Khalaspir, and Dighipara basins.

1.3 PREVIOUS WORK

The Gondwanan sequences of Peninsular India have been well studied by previous workers. Wadia (1919) reported basic information about Indian geology, including the geology of Peninsular India. Veevers and Tewari (1995) modeled the Gondwanan master basin that developed between the Tethys and the Gondwanaland

interior. Acharyya (2000) worked on the India-Asia collision and resulting amalgamation of Gondwana-derived blocks in the Himalayan Foreland basin. Dutta (2002) contributed by constructing a composite stratigraphic section for the Gondwanan units of Peninsular India.

Uddin and Islam (1992) and Hossain et al. (2002) studied sedimentological aspects of Gondwanan sequences of Bangladesh to decipher their depositional environments. Palynological studies carried out on these sequences correlated them to the middle part of the regional Raniganj Stage of India and the Upper Permian of the Salt Range of Pakistan (Stover, 1964; Islam, 1990). Additionally, geological and geophysical surveys have been carried out in the Gondwanan basins since the early 1950's, and, as a result, a number of economic mineral deposits have been identified in this region (Akhtar, 2000). Mukhopadhyay et al. (2010) worked on stratigraphic correlation between different Gondwanan basins of India based on major tectonic events and changes in the depositional environments. Farhaduzzaman et al. (2013) studied maceral content and petrographic characteristics to evaluate paleofacies and paleoenvironments of the Barapukuria and Dighipara basins in Bangladesh. They suggested that the paleodepositional settings for Permo-Carboniferous coal deposits were mostly swamps with alternating oxic to anoxic conditions. Multiple transitions from icehouse to greenhouse states are documented for these Late Paleozoic sequences (Frakes et al., 1992).

A recent study on mineralogical and geochemical changes based on mineralogical Indices of alteration (MIA) and chemical indices of alteration (CIA) in

sediments from the Khalaspir basin in Bangladesh indicates a distinct shift from a dry and cool climate to a warm and humid climate during the Permo-Carboniferous (Roy and Roser, 2013).

Petrographic studies of Gondwanan sequences of Talchir Basin, India (Hota et al., 2011) suggest that sandstone types in the Barakar Formation, Barren Measures, and Kaharbari Formation are sublitharenites, subarkoses, and quartzarenites, respectively (Fig. 1.4). Petrographic studies by Huque et al. (2003) indicate that sandstones from drill-well GDH 40 of Barapukuria, Bangladesh are arkosic and subarkosic. Sitaula (2009) studied petrofacies and detrital geochronology of Gondwanan quartz arenitic and arkosic sandstones of similar depositional age from two areas of Nepal and indicated contrasting sources for these sediments (Fig. 1.4). Alam (2011) indicated that Gondwanan sediments of Barapukuria and Khalaspir basins in NW Bangladesh are mostly lithic arkoses to lithic subarkoses and suggested three different sources with a predominant source from an area with modes of cooling age at circa 495-500 Ma. These cooling ages in detrital grains however, are conspicuously absent from Permo-Carboniferous sediments of Nepal. These recent findings from Bangladesh and Nepal raise questions about whether the regional Gondwanan sequences of South Asia are all coeval. Differences in sandstone compositions among various Gondwanan basins of the Indian subcontinent may be attributed to differences in (1) source terranes, (2) routing systems or drainage patterns, and (3) geomorphic and structural positions of the basins.

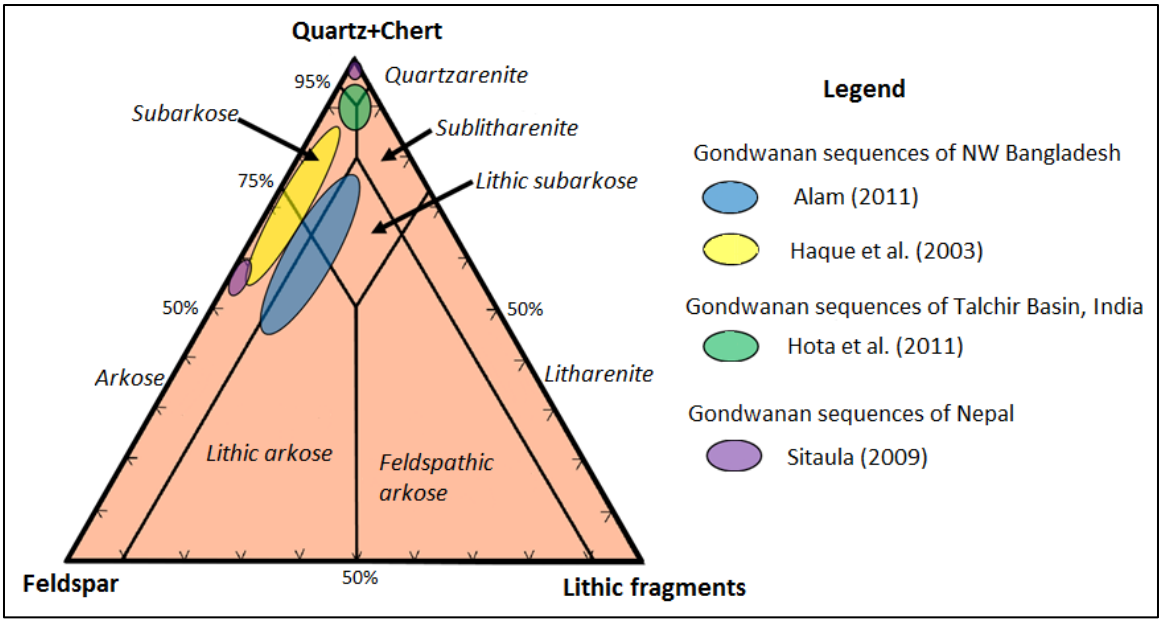

Figure 1.4 Petrographic compositions of sandstones from different Gondwanan basins in the Indian subcontinent (compiled from Huque et al., 2003; Sitaula, 2009; Hota et al., 2011; Alam, 2011). Fields are taken from McBride (1963).

1.4 OBJECTIVES

The Gondwanan basins in the Indian subcontinent are relics of the original master basins that were disrupted during and after the deposition (Veever and Tewari, 1995). Two recent thesis studies on Permo-Carboniferous sandstones from Nepal and Bangladesh provided contrasting provenance information (Sitaula, 2009; Alam, 2011). Data obtained from Permo-Carboniferous sandstone samples from Bangladesh indicate provenances ranging from cratonic for older samples to orogenic for younger sandstones (Alam, 2011). Provenance data derived from Gondwanan sandstones from Nepal also indicate cratonic to orogenic sources. However, coeval units from eastern and western parts of Nepal show marked differences in sand composition and cooling ages of detrital minerals (Sitaula, 2009). Cooling ages of many of these minerals may

have been affected by Miocene Himalayan tectonism. The present thesis research focuses on petrofacies and geochronology of Gondwanan sequences of Bangladesh and India in order to better reconstruct regional detrital and tectonic histories of Late Paleozoic Eastern Gondwanaland basins. Data from Gondwanan sandstones of India will fill an information gap between Nepal and Bangladesh.

Understanding the detrital history of Gondwanan sequences in India and Bangladesh is also important in revealing rift-to-drift phase transitions of various segments of Eastern Gondwanaland. Additionally, from an economic geology point of view, Gondwanan sequences of Bangladesh and India are important because these sequences host significant coal deposits in this region, and some of the coal basins are prospective for coal-bed methane.

Sandstone petrographic studies were performed on representative sandstone samples from different stratigraphic levels to understand textural and compositional maturity and to evaluate provenance history. Studies of heavy mineral assemblages, mineral chemistry on selected heavy minerals, and bulk whole-rock geochemistry were done to infer provenance and weathering history of the sediments. Data obtained from different basins in Bangladesh and India are compared to discriminate their provenance history and better reconstruct the regional paleogeography. Detrital $^{40}Ar/^{39}Ar$ age dating of muscovite grains was carried out to reveal temporal relationship and probable tectonic histories of source terranes.

CHAPTER 2: GENERAL GEOLOGY OF THE STUDY AREA

2.1 INTRODUCTION

The Gondwanan sequences in Peninsular India are distributed in many isolated graben/ half-graben basins. Clastic sediments of varying thicknesses (~200 m to ~4000 m) were deposited within these basins with the major depocenters confined to the existing river valleys and with paleodirection towards the west or northwest (Wadia, 1919; Vaidyanadhan and Ramakrishnan, 2008). The Gondwanan sediments of Peninsular India are mostly continental deposits (Medlicott, 1873; Fox, 1931; Ghosh and Bandyopadhaya, 1967; Chatterjee and Ghosh, 1970; Ghosh and Mitra, 1970; Ghosh, 2002). Gondwanan sediments also have been reported from the western (Afganistan, Pakistan, etc.) and the eastern Himalayas (Nepal, Sikkim, Bhutan, Assam, etc.) these are known as extra-peninsular Gondwanan sequences. However, the Triassic sediments are missing in the Gondwanan sequences of extra-Peninsular India. In addition, Gondwanan sediments have been identified in cores from the offshore Bay of Bengal along the lineament of the Godavari and Mahanadi River valleys (Mukhopadhyay et al., 2010).

Gondwanan sequences of Peninsular India and northwest Bangladesh are well preserved compare to those in the extra-Peninsular India, which are locally intensely folded and compressed. The fundamental characteristics of Gondwanan sequences as noted by Vaidyanadhan and Ramakrishnan (2008) are (a) a basal glacial boulder deposit overlain by alternating sandstone, coal, and shale, (b) preservation of sediments in fault-bounded intra-cratonic basins, (c) mostly fluvio-lacustrine depositional environments,

(d) presence of *Glossopteris* and *Ptilophyllum* flora, and (e) northerly or northwesterly paleoslope directions.

2.2 DISTRIBUTION AND TECTONIC EVOLUTION OF GONDWANAN SEQUENCES OF PENINSULAR INDIA

Peninsular India experienced rifting during Permian–Triassic Gondwanan sedimentation. The Gondwanan sequences of peninsular India accumulated in numerous discrete intracratonic basins during this period (Chakraborty and Ghosh, 2005, 2008; Khan and Shahnawaz, 2013). Boundary faults developed at the marginal part of the basins along Pre-Cambrian lineaments (Veevers and Tewari 1995; Dasgupta, 2002). Intrabasinal faults also affected syndepositional sedimentation (Chakraborty et al., 2003).

The major Gondwanan basins of Peninsular India are the Pranhita Godavari, Mahanadi, Koel - Damodar, Son, Satpura, and Rajmahal basins (Fig. 2.1). All these basins in the Indian subcontinent are distributed along certain well-defined linear belts (Fox, 1931), as a result of deposition of sediments in river valleys. The three major linear belts along which Gondwanan Basins of Peninsular India occur are: (1) the east-west trending Koel-Damodar valley basin along the valley of the Damodar River, (2) the NW-SE trending Son-Mahanadi valley basin along the Mahanadi River, and (3) the NW-SE Pranhita-Godavari valley basin (Wadia, 1919; Chakraborty et al., 2003; Vaidyanadhan and Ramakrishnan, 2008). The Rajmahal Basin in eastern India and Gondwanan sequences of northwestern Bangladesh are considered to be a continuation of Damodar

valley basin (Uddin, 1996). Many of the stratigraphic units of the Indian Gondwana Supergroup exhibit striking lateral changes in thickness and facies over relatively short distances. According to Dutta (2002), development of Gondwanan basins in India was influenced by extensional forces that acted along the lineaments between the cratonic blocks of India.

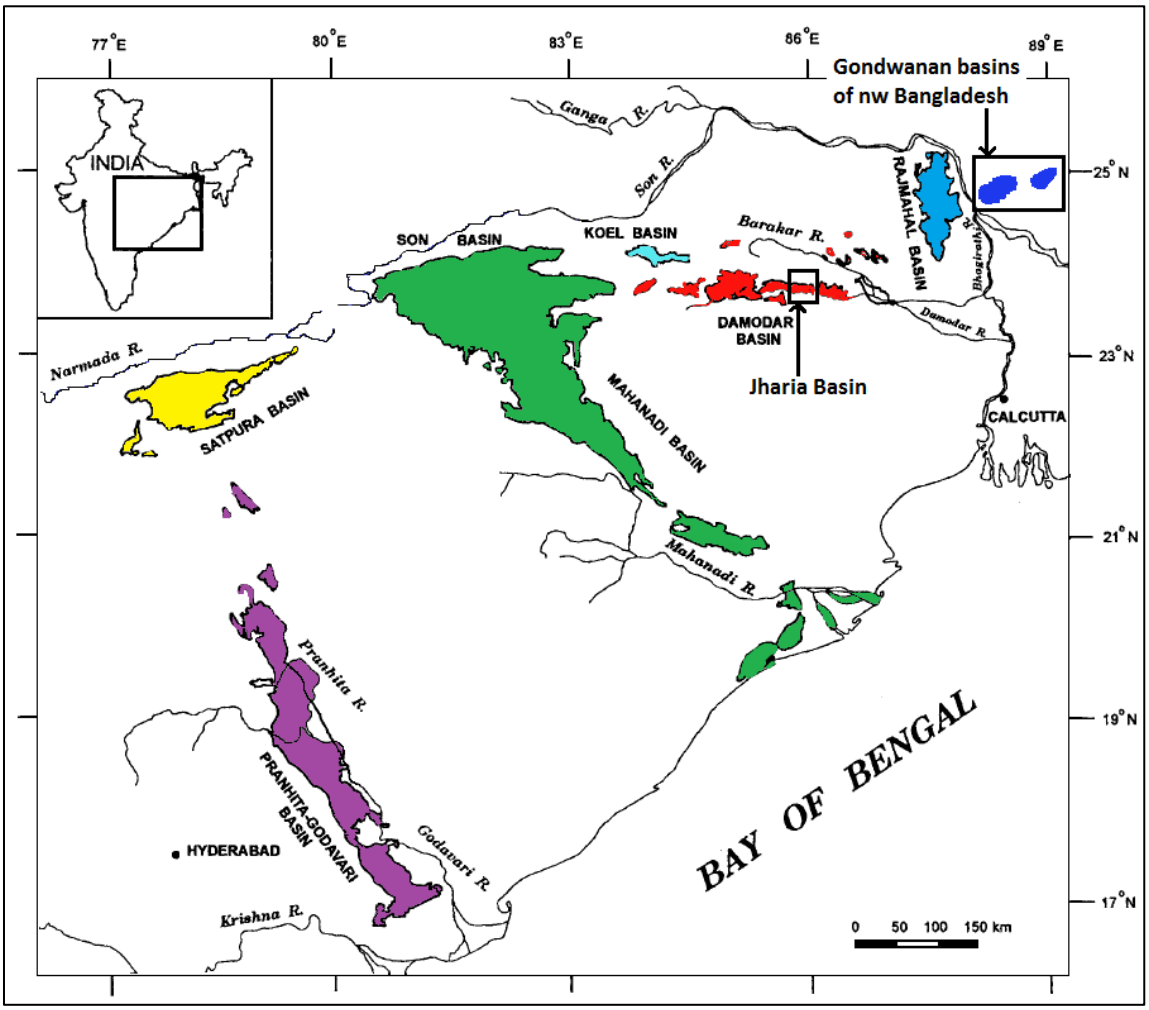

Figure 2.1 Distribution of Gondwanan basins in Peninsular India (after Veevers and Tewari, 1995; Dutta, 2002; and Mukhopadhyay et al., 2010) including study area of the Jharia basin and northwestern Bangladesh (indicated by open rectangles).

The Gondwana group of India is divided into three classic divisions-- the lower, middle and upper, which correspond in a general way to the Permian, Triassic, and Jurassic of Europe, respectively (Wadia, 1919). These units have been further divided into different formations. The oldest Gondwanan unit is the Talchir Formation, which is composed primarily of coarse-grained sandstones and conglomerates with some interbedded mudrocks in the upper section. The younger Gondwanan units overlying the Talchir Formation are the Barakar Formation, the Barren Measures, the Raniganj Formation and the Panchet Formation, in ascending order (Table 2.1). The Barakar and Raniganj formations are composed mostly of alternating sandstones and mudrocks with interbedded coal seams. The Barren Measures and the Panchet Formation also are composed of alternating sandstones and mudrocks but do not contain any coal seam. Other than the lowermost Talchir Formation, which records glacial deposition, most Permo-Carboniferous deposits in Gondwanan basins in India were deposited in fluvial environments (Dutta, 2002).

The evolution of these basins is related to mountain building and other crustal movements. Normal faulting in extensional lineaments between the cratonic blocks of India is considered as the main mechanism of Gondwanan basin development in India (Dutta, 2002). Most of the Gondwanan basins are half-grabens bounded by high angle (~60) normal faults on one side (Tewari, 1999; Vaidyanadhan and Ramakrishnan, 2008). The evolutionary tectonic activities of these basins have taken place in several stages, as illustrated in Figure 2.2.

Table 2.1 Existing scheme of correlation of Gondwanan formations at various localities (after Mukhopadhyay et al., 2010).

<table>
<tr><th colspan="2">Age</th><th>Damodar-Koel Valley</th><th>Rajmahal</th><th colspan="2">Mahanadi</th><th>Son</th><th>Satpura</th><th colspan="2">Godavari</th></tr>
<tr><td colspan="2" rowspan="2">Lower Creteceous</td><td rowspan="2"></td><td></td><td rowspan="2" colspan="2"></td><td>Bansa Bed</td><td>Jalalpur</td><td rowspan="2" colspan="2">Chikiala/ Gangapur</td></tr>
<tr><td rowspan="4">Dubrajpur</td><td></td><td></td></tr>
<tr><td rowspan="5">Jurassic</td><td rowspan="3">Late</td><td rowspan="4"></td><td rowspan="3"></td><td rowspan="3"></td><td rowspan="3"></td><td rowspan="2">Bogra</td><td></td></tr>
<tr><td rowspan="2">Kotla</td></tr>
<tr><td rowspan="3"></td><td rowspan="3"></td></tr>
<tr><td rowspan="2">Middle
Early</td><td rowspan="2"></td><td rowspan="2">Dharmaram</td><td rowspan="6">Maleri Group</td></tr>
<tr><td>Bandhavgarh</td><td></td><td></td></tr>
<tr><td rowspan="5">Triassic</td><td rowspan="2">Late</td><td rowspan="3"></td><td>Parsora</td><td rowspan="2"></td><td rowspan="2"></td><td rowspan="2"></td><td rowspan="2"></td></tr>
<tr><td rowspan="2">Supra Panchet</td><td rowspan="2">Kamthi</td><td rowspan="4">Kamthi</td><td>Tiki</td><td>Maleri</td></tr>
<tr><td rowspan="2">Middle</td><td rowspan="3">Pali</td><td rowspan="2">Dewna</td><td>Bhimaram</td></tr>
<tr><td rowspan="2"></td><td rowspan="2"></td><td>Yerrapalli</td></tr>
<tr><td>Early</td><td rowspan="2"></td><td rowspan="2">Panchamari</td><td rowspan="2">Upper Kamthi
Middle
Kamthi</td><td rowspan="2">Kamthi</td></tr>
<tr><td rowspan="3">Permian</td><td rowspan="2">Late</td><td>Panchet</td><td></td><td></td><td></td></tr>
<tr><td>Raniganj</td><td></td><td>Raniganj</td><td>Raniganj</td><td>Bijuri</td><td>Lower Kamthi</td><td></td></tr>
<tr><td>Barren Measures</td><td></td><td>Barren Measures</td><td>Barren Measures</td><td>Motur</td><td>Barren Measures</td><td>Barak</td></tr>
<tr><td>Early</td><td>Barakar</td><td>Barakar</td><td colspan="2">Barakar</td><td>Barakar</td><td>Barakar</td><td>Barakar</td><td></td></tr>
<tr><td colspan="2">Late Carbonifeorus</td><td>Talchir</td><td>Talchir</td><td colspan="2">Talchir</td><td>Talchir</td><td>Talchir</td><td colspan="2">Talchir</td></tr>
</table>

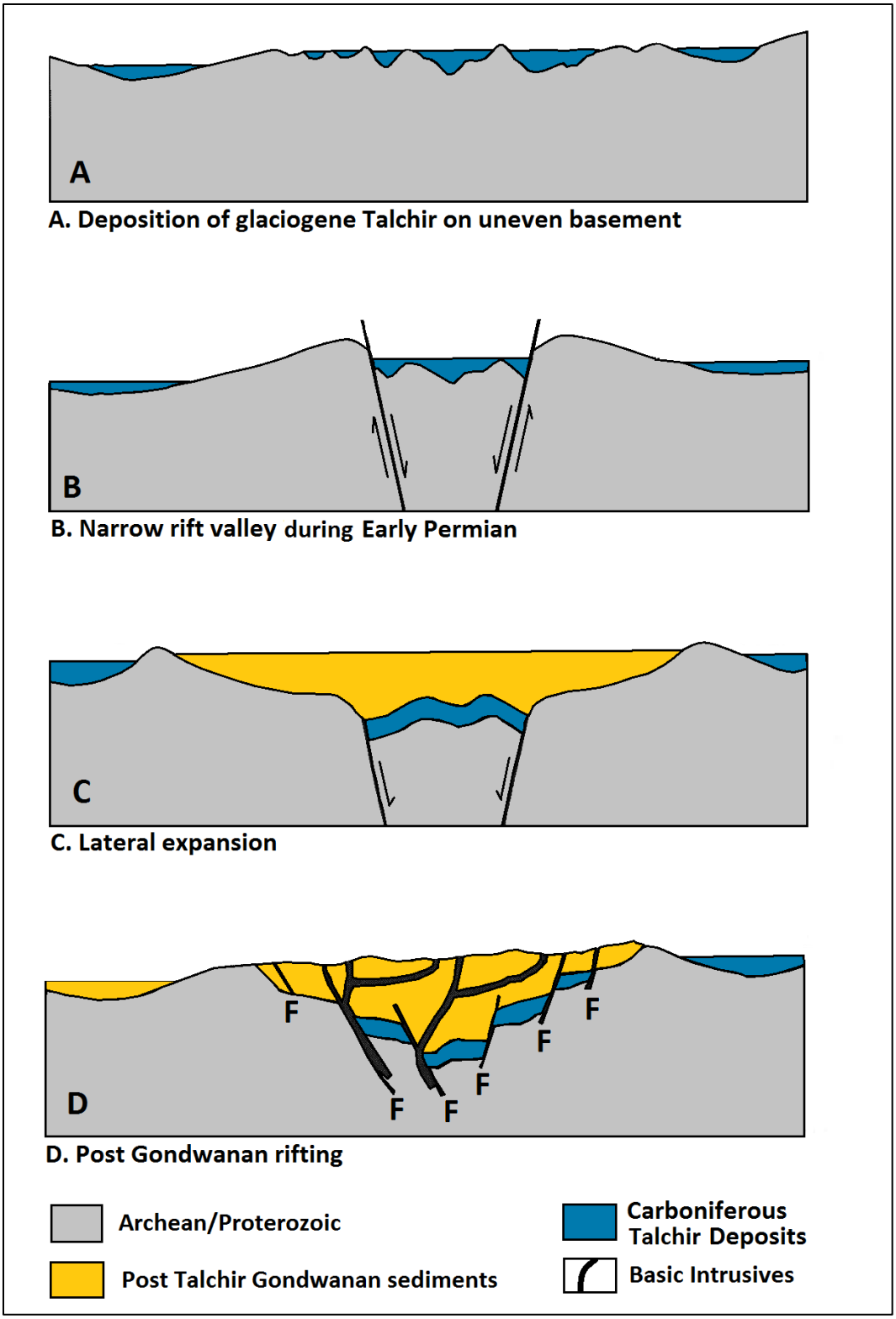

Figure 2.2 Illustrations showing tectonic evolution of Gondwanan basins in Peninsular India (after Casshyap and Tewari, 1988, 1991; Casshyap et al., 1993; Tewari and Maejima, 2010).

On the Indian subcontinent, Gondwanan sedimentation initiated during the Late Carboniferous in different intracratonic rifted basins (Veevers and Tewari, 1995). Gondwanan sedimentation started with glacial/glaciogene deposition of the Talchir Formation (Fig. 2.2; A). Paleoslope directions were northerly or northwesterly during this time (Casshyap et al., 1993; Dasgupta, 2002). According to Maejima et al. (2004), during the Permo-Carboniferous, isostatic rebound due to deglaciation might have provided initial depression.

During Early Permian deglaciation, narrow valleys formed (Veevers and Tewari, 1995) by reactivation of Proterozoic rifts (Fig. 2.2; B). Deposition of sediments of the Lower Barakar or Kaharbari Formation occurred in braided stream systems after initial rifting in Early Permian (Tewari and Maejima, 2010). The northwesterly paleoslope prevailed during that time.

During Mid-Permian to Early Jurassic, rift valleys subdued beyond depositional limit due to lateral expansion and valleys became broader (Fig. 2.2; C). Northwesterly paleoslopes were maintained through the Carboniferous and Early Permian. Faulting was renewed during the Mid-Triassic.

Permian rifting reactivated during the breakup of Greater India during the Late Jurassic to Early Cretaceous (Fig. 2.2; D). This rifting terminated sedimentation in Gondwanan basins (Tewari and Maejima, 2010). Marginal basins were characterized by alluvial fan deposition, and the direction of paleoslope reversed towards the southeast at this stage.

2.3 JHARIA BASIN

The Jharia is a WNW–ESE trending, slightly elongate, rhombic basin and its southern boundary is marked by a fault zone. The strata define a broad, gentle syncline plunging towards west. Trends of the intrabasinal normal faults vary from NW–SE to NNE–SSW. The basin profile indicates fault-controlled subsidence (Verma et al., 1979).

2.3.1 Structural framework of the Jharia Basin

A geological map of Jharia basin (after Fox, 1930) is shown in Figure 2.3. The Jharia Coal Basin is a sickle-shaped (Fig. 2.3) east-west trending Gondwanan basin formed as a part of the Damodar valley basin in northeast India. This basin contains almost all of the metallurgical coal of India. The basin is roughly 38 km long in the east-west direction and 19 km long in the north-south direction (Verma et al., 1979). Approximately 3000 m of Permian Gondwanan deposits unconformably overlie Archean gneissic basement. This succession includes, in ascending order, the Talchir Formation, fluvial and fluviolacustrine sediments of the Barakar, Barren Measures and Raniganj formations (Fox, 1930), all of which were deposited in an intracratonic extensional setting (Ghosh and Mukhopadhyay, 1985).

The northern margin of the coalfield has a gentle arcuate shape extending from Matigara in the west to Patharigara in the east (Verma et al., 1979; Ghosh and Mukhopadhyay, 1985). The Barakar and the Talchir formations along the northern margin dip towards the south and have a normal depositional contact with the

metamorphic basement (Verma et al., 1979; Chakraborty and Ghosh, 2005). The thickness of the Talchir Formation varies from 0.15 km to 0.55 km.

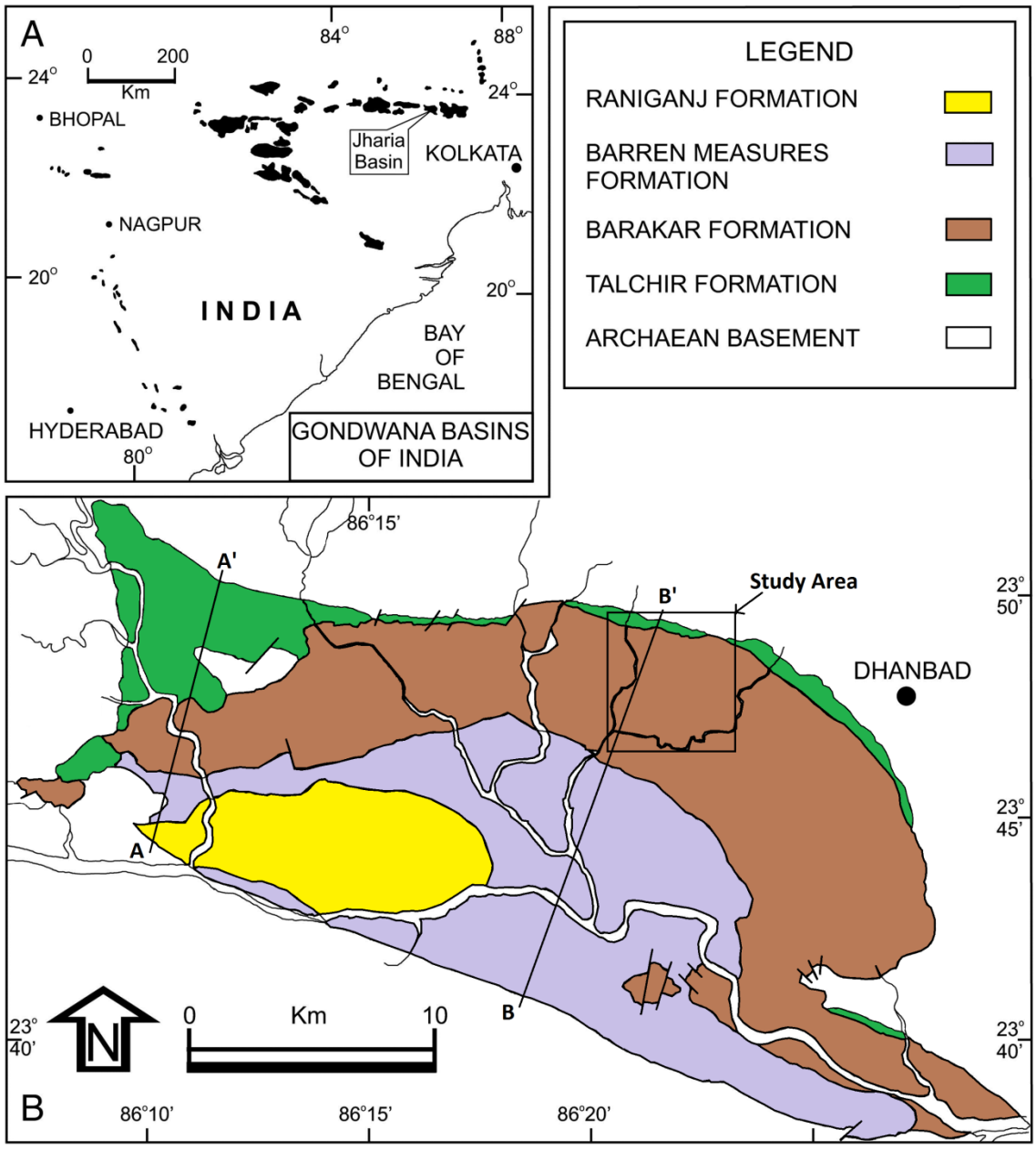

Figure 2.3 Geological map of Jharia Basin, India (after Fox, 1930). The field area is outlined here with a rectangle.

The Talchir Formation is very well exposed near the western, northern and the eastern margins of the basin. The southern boundary of the field constitutes a steeply

dipping boundary fault (Figs. 2.4 and 2.5) which extends almost in a straight line (WNW-ESE) for approximately 35 km long. Here, strata dip towards the north, away from this boundary. Talchir deposits have not been found along the southern boundary of this coalfield (Verma et al., 1979).

The Gondwanan basins of peninsular India nucleated along preexisting zones of weakness in the Precambrian basement (Chakraborty et al., 2003). The Jharia basin is a 'half-graben' basin with a strong master boundary fault on the southern side. Numerous faults have been identified in the Jharia coalfield, many of which are normal tensional faults related to the southern boundary fault (Verma et al., 1979, Chakraborty et al., 2003). Several strike-slip faults, some of which are 'sag-faults', and several dip and oblique faults also have been identified. Faults are often associated with mica-peridotite intrusives. Faulting and folding of the Jharia coalfield occurred during Mesozoic, more specifically during the Jurassic. This faulting activity ceased entirely when igneous activity began. According to Fox (1930), several domes are present in the Jharia coalfield (such as Dugda High in Fig. 2.4). Several geological cross-sections have been constructed based on geological and geophysical studies (Verma and Ghosh, 1974; Verma et al., 1979; Ghosh and Mukhopadhyay, 1985; Chakraborty et al., 2003) along various profiles. Some of these are shown in Figures 2.4 and 2.5.

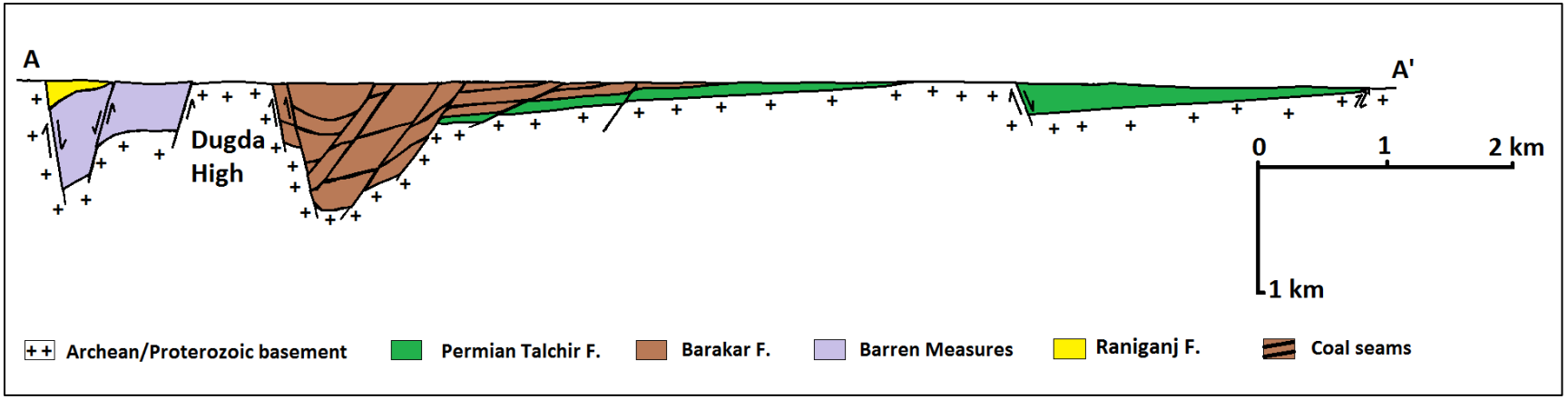

Figure 2.4 Geological cross section along AA' (location shown in Fig. 2.3), Jharia Basin (after Verma et al., 1979; Ghosh and Mukhopadhyay, 1985). Several domes and toughs formed due to reactivation of faulting at different stages.

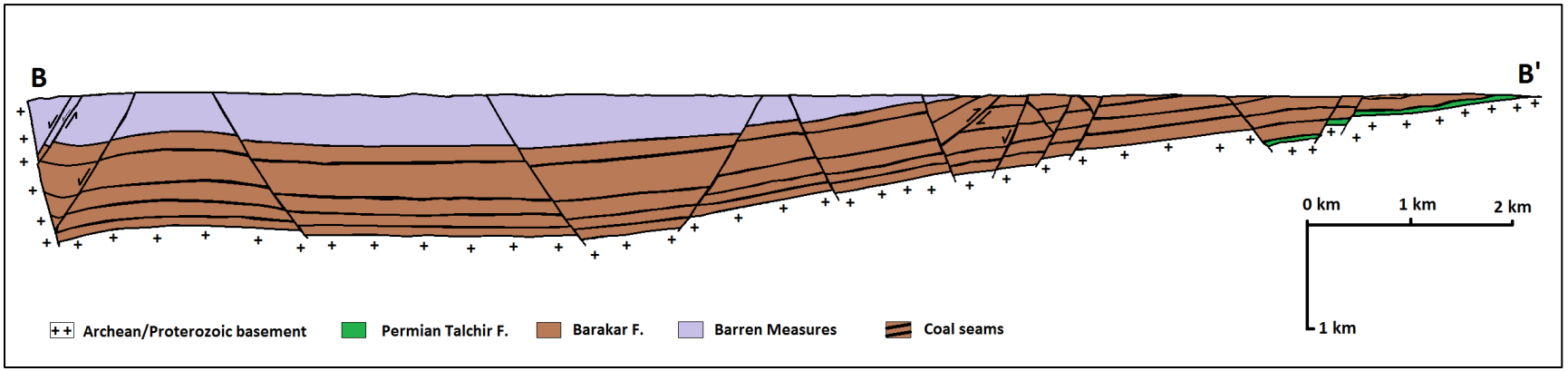

Figure 2.5 Geological cross section along BB' (location shown in Fig. 2.3), Jharia Basin (after Verma et al., 1979; Ghosh and Mukhopadhyay, 1985). Sediment thickness increases towards the southern fault boundary (left in above figures).

2.3.2 Stratigraphy of the Jharia coal basin

The oldest Gondwanan unit is the Talchir Formation, which is composed primarily of coarse-grained sandstones and conglomerates with some interbedded mudrocks in the upper part. Younger Gondwanan units overlying the Talchir Formation are the Barakar Formation, the Barren Measures, and the Raniganj Formation, in ascending order (Table 1).

Table 2.2 Stratigraphy of the Jharia coal basin (after Fox, 1930 and Verma et al., 1979). Studied sequences are shaded in green.

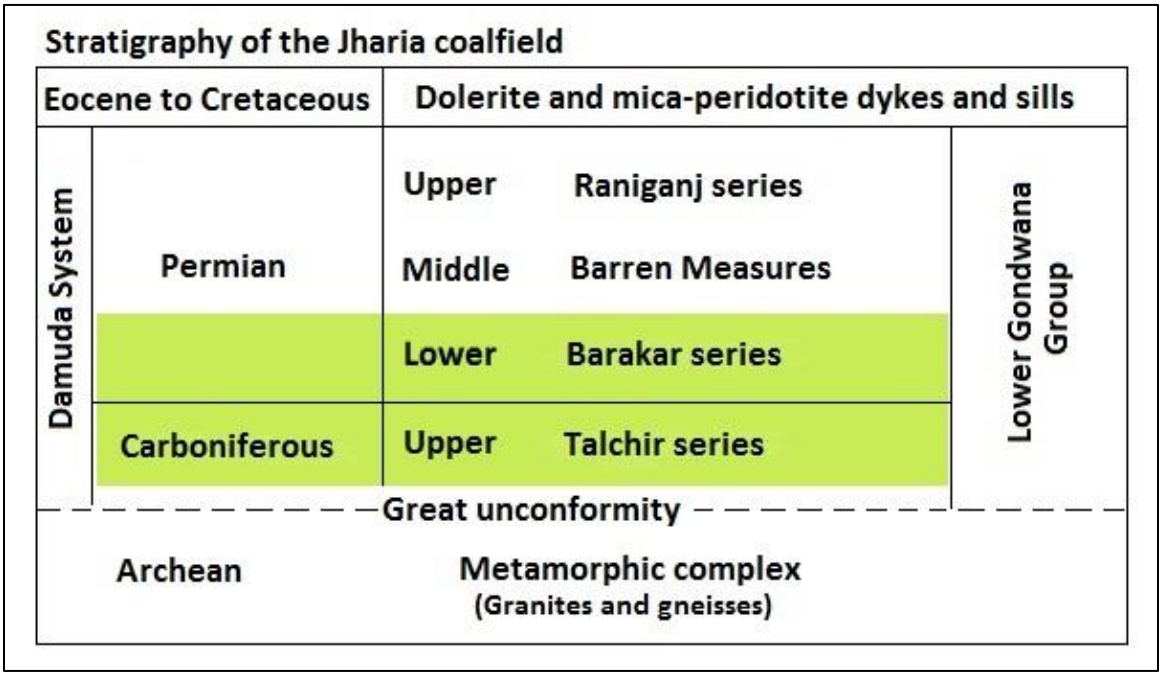

Talchir Formation: These Carboniferous deposits are composed of boulder bed/tillite, greenish gray sandstone, and light green shale that unconformably or nonconformably overlie the Precambrian basement (Veevers and Tewari, 1995; Vaidyanadhan and Ramakrishnan, 2008). The boulder bed contains angular and poorly sorted pebble- to boulder-sized clasts that show locally massive but typically stratified

fabrics. Textural immaturity of these clasts indicates derivation from adjacent basement rocks. Mostly massive to thinly bedded sandstones locally exhibit cross-bedding, ripple-marks, and flaser bedding. Shale dominates downslope away from the basin margin and up-section above the basal tillite. In addition to a *Glossopteris* flora, this formation also contains some marine fossils (e.g., *Eurydesma*, *Fenestella*) that indicate marine incursions in to the basin during Carboniferous (Vaidyanadhan and Ramakrishnan, 2008; Mukhopadhyay et al., 2010).

Barakar Formation: The Lower Permian Barakar Formation, which is the main repository of coal in this basin, rests on Talchir Formation. The Barakar Formation is characterized by fining-upward cycles of sandstone, carbonaceous shale, and coal. The sandstone shows planar and trough cross-beds reflecting paleocurrent directions towards the west or northwest. *Glossopteris* flora is common in carbonaceous shale and coal seams.

Barren Measures: Due to the absence of coal seams, this formation is named the Barren Measures. The Barren Measures is composed of alternating units of cross-bedded sandstone, micaceous siltstone, and ironstone shale deposited in meandering streams setting.

Raniganj Formation: The Raniganj Formation consists of sandstones, shales, and coal seams that overlie the Barren Measures. It reflects a return to the style of deposition of the Barakar Formation. However, sandstones in the Raniganj Formation are finer than those of the Barakar Formation.

2.4 GONDWANAN SEQUENCES OF BANGLADESH

The Bengal Basin of Bangladesh has been broadly divided into three major tectonic regions: (1) the stable platform in the northwest (Indian Platform flank zone); (2) the deep basin in the middle; and (3) the eastern fold-belt (Uddin and Lundberg, 2004; Imam, 2005). In Bangladesh, Gondwanan sediments were deposited in several graben/half-graben basins only in the stable platform.

Gondwanan sequences of Bangladesh record a history of pre-Himalayan orogenesis and dispersal and distribution of Gondwanaland. The Gondwanan sequences in northwestern Bangladesh are known as the Kuchma and Paharpur formations. Based on palynological study, the Paharpur and Kuchma formations were deposited during Early Permian and are considered as equivalent to lower Gondwanan sequences of India (Akhtar, 2000). According to Akhtar and Kosanke (2000), sediments of both the Paharpur and Kuchma formations were deposited in fluvial environments. The Jurassic Rajmahal Trap unconformably overlies the Gondwana Group. Gondwanan sequences are nowhere exposed in Bangladesh. However, these sequences are encountered in several wells in the Indian Platform region of the Bengal basin (Akhter, 2000).

Generalized stratigraphy of Northwest Bangladesh

In northwestern Bangladesh, Precambrian igneous and metamorphic rocks underlie all sedimentary rock units. Precambrian basement occurs at a shallow depth of ~130 meters below the surface in the northwestern part of the Indian Platform area and dips southward under increasingly thicker Permian to Recent sedimentary cover.

Thicknesses of the sedimentary sequences in the central Indian Platform area are up to ~1 km and increase to about 6 km in the southeastern part of the Indian Platform. The generalized stratigraphy of the Indian Platform is shown in Table 1.

Table 2.3 Generalized stratigraphy of northwest Bangladesh (after Uddin and Lundberg, 1998). Studied sequences are shaded in yellow.

CHRONOSTRATIGRAPHY	GROUP	FORMATION	THICKNESS (m)	LITHOLOGY
PLEISTOCENE		BARID CLAY	40	Reddish clay
PLIOCENE		DUPI TILA	170	Loosely compact sandstone
MIOCENE		JAMALGANJ	400	Alternating sandstone and shale
OLIGOCENE		BOGRA	160	Sandstone and shale
EOCENE	JAINTIA	KOPILI SHALE	170	Mostly shale
		SYLHET LIMESTONE	240	Nummulitic limestone
		CHERRA	370	Mostly sandstone
JURASSIC		SHIBGANJ TRAPWASH	130	Basaltic volcanic rock
		RAJMAHAL TRAP	540	
PERMO-CARBONIFEROUS	GONDWANA	PAHARPUR	1000	Mostly hard sandstone and coal
		KUCHMA		
PRECAMBRIAN CRYSTALLINE BASEMENT				Igneous and metamorphic rock

The oldest sedimentary unit of Bangladesh is the Permo-Carboniferous Lower Gondwana Group, which rests unconformably on Precambrian crystalline basement. The Gondwanan sequences of Bangladesh, which include the Kuchma and Paharpur formations, are composed predominantly of hard feldspathic sandstones with some coal

layers, conglomerates and shales. This group is about 1000 m thick and is found within fault-bounded basins, including the Barapukuria, Phulbari, Khalaspir, Dighipara, and Jamalganj basins.

The Jurassic Rajmahal Trap, which is composed of volcanic basaltic rocks, rests on top of Gondwanan Paharpur Formation. Rajmahal Trap, which is 100 to 500 m thick, is named after Rajmahal Hill in adjacent India where this unit is exposed at the surface. The Shibganj Trapwash consists of weathered volcanic rock fragments from the underlain Rajmahal Trap and ferruginous sandstone and mudstone.

The Jaintia Group, which varies in thickness from ~150 to 800 m, is encountered in several drill holes in northwestern Bangladesh. This group is the oldest exposed sedimentary sequence of Bangladesh. Three formations are included in this group: Cherra Formation, Sylhet Limestone, and Kopili Shale. The upper Paleocene to lower Eocene Chera Formation, also known as the Tura Sandstone, is composed of sandstone with minor shale and occasional thin coal layers. The Sylhet Limestone is the most fossiliferous unit in Bangladesh. Common forams include *Nummulites, Discocycina,* and *Alveolina*, etc. The Kopili Shale is overlain by the Oligocene Bogra Formation, which is composed of alternating sandstone, shale and carbonaceous siltstone. The Miocene Jamalganj Formation is characterized by interbedded sandstone, shale and siltstone. Both the Bogra and Jamalganj formations were deposited in deltaic settings. The Pliocene Dupi Tila Formation is primarily composed of pebbly coarse-grained fluvial

sandstones. The Dupi Tila Formation is overlain by the Pleistocene Barind Clay Formation, which is composed of reddish-brown clay.

CHAPTER 3: SANDSTONE PETROGRAPHY

3.1 INTRODUCTION

Sedimentary rocks are principal sources of information in deciphering paleotectonic history of the Earth's crust. Studies of clastic rocks, particularly of sandstone composition, have been utilized to reveal orogenic progression, unroofing history, and plate tectonic evolution (Ingersoll and Suczek, 1979; Johnsson, 1993).

Sandstone petrography is one of the most commonly used techniques in studying provenance history of sediments. Compositional analyses of clastic sediments have been used for a long time to evaluate the nature of the source terranes. Detrital framework grains of sandstones, plotted on different ternary diagrams, can be used to discriminate various tectonic settings and to interpret plate interactions in the geologic past (Graham et al., 1976; Ingersoll, 1978; Dickinson and Suczek, 1979; Kumar, 2004).

This chapter describes sandstone petrology and modal analysis of the Gondwanan Talchir and Barakar formations from India, and the Kuchma and Paharpur formations from Bangladesh. Provenance studies using sandstone modal analyses are based on the assumption that sedimentary processes such as modes of transportation, depositional environments, climates, and diagenesis have not altered mineralogical composition significantly (Basu, 1976; Kumar, 2004; Sitaula, 2009; Alam, 2011). Hence, all these factors need to be considered when interpreting sediment provenance (Suttner, 1974; Johnsson, 1993). Variables controlling sandstone composition act on the source rock in different ways with different magnitudes. For instances, low-energy depositional environments and relatively short transport in a low-relief river may have

very little effect on sand (stone) composition. In contrast, humid climates and high-energy transport regimes may have a greater impact on the composition of derived sand (stones). Moreover, mixing of sediments from various sources complicates the interpretation of provenance (Velbel, 1985). Multiple basin analytical techniques such as thermochronology, whole-rock chemistry, and mineral chemistry along with traditional modal analysis are needed for multiple source identification (Morton and Hallsworth, 1999, Peavy, 2008, Alam, 2011).

3.2 METHODS

A key component of this study was sandstone petrographic analysis oriented towards interpretation of provenance (Ingersoll et al., 1984). Fieldwork was completed in India and Bangladesh from December 2012 to January 2013. A total of twenty-one (21) samples from different stratigraphic levels of Gondwanan sequences were collected from exposures (Fig. 3.1) in an abandoned coal field in the Damodar (Jharia) basin of India. Twenty-seven (27) samples were collected from three different drill cores (e.g., Barapukuria coal mine, Khalaspir and Dighipara coal field area) in northwest Bangladesh (Fig. 1.4). Cores were housed at the repositories of the Geological Survey of Bangladesh. Out of the total forty-eight (48) samples, fifteen (15) are mostly mudstone and siltstone and were not used for petrographic study.

Figure 3.1 Exposure of Barakar sequences in the Jharia coal field, India. Photo was taken during the fieldwork in January, 2013.

The samples were prepared in the rock preparation lab in the Department of Geology and Geography at Auburn University and sent to Spectrum Laboratories to prepare petrographic thin sections. Mineral assemblages were analyzed with a petrographic microscope. Modal analyses were performed by point-counting using the the Gazzi-Dickinson method (Dickinson and Suczek, 1979) in order to minimize control by grain size on sand-grain composition. A total of 300 representative points were counted in each thin section. Framework grains were normalized to 100% using all the end members for quartz, feldspar, and lithic fragments. Careful attention was paid to the classification of lithic fragments and feldspar types (Pettijohn et al., 1973; Uddin and Lundberg, 1998). Thin sections were stained with potassium rhodizonate and sodium

cobaltinitrite to distinguish feldspars types. Modal sandstone compositional data were plotted on ternary diagrams (QtFL, QmFLt, QmPK, LsLvLm, QpLvmLsm, etc.) to evaluate tectonic provenance (Dickinson and Suczek, 1979). The following parameters were evaluated: Qt = total quartz; Qm = monocrystalline quartz grains; Qp = polycrystalline quartz grains, including chert grains; F = total feldspar grains; P = plagioclase feldspar grains; K = potassium feldspar grains; L = lithic fragments; Lt = total lithic fragments; Ls = sedimentary lithic fragments; Lv = volcanic lithic fragments; Lm = metamorphic lithic fragments; Lsm = sedimentary and metasedimentary lithic fragments; Lvm = volcanic, hypabyssal, metavolcanic lithic fragments; Lm_1 =very low- to low-grade metamorphic lithic fragments, and Lm_2 = low- to intermediate-grade metamorphic lithic fragments.

Table 3.1 Redefined modal parameters of sand and sandstone (after Graham et al., 1976; Dickinson and Suczek, 1979; Dorsey, 1988; Uddin and Lundberg, 1998).

Qt = Qm + Qp, Where, Qt = total quartzose grains Qm = monocrystalline quartz (> 0.625 mm) Qp = polycrystalline quartz (including chert)
Feldspar Grains (F=P+K), where, F = total feldspar grains P = plagioclase feldspar grains K = potassium feldspar grains
Unstable Lithic Fragments (Lt = Ls + Lv + Lm), where, Lt = total unstable lithic fragments and chert grains Lv = volcanic/metavolcanic lithic fragments Ls = sedimentary/metasedimentary lithic fragments Lm_1 = very low- to low-grade metamorphic lithic fragments Lm_2 = low- to intermediate-grade metamorphic lithic fragments

3.3 PETROGRAPHY

Gondwanan sequences in the Indian subcontinent record the history of pre-Himalayan orogenesis and of dispersal and distribution of eastern Gondwanaland. The Gondwanan Group of northwestern Bengal Basin, which consists of the Kuchma and Paharpur formations, records sedimentation during the early Permian that is equivalent to Lower Gondwanan sequence (Islam et al., 1992).

3.3.1 PETROGRAPHY OF TALCHIR FORMATION, JHARIA BASIN, INDIA

The Lower Permian Talchir Formation consists of boulder bed/tillite, rhythmite, greyish green shale, and light green sandstone. The boulder bed is composed of angular, poorly sorted, pebble- to boulder-sized clasts within sandy matrix. The greyish green shale is silty, laminated and varved. Light green sandstone is micaceous, rippled, and cross-stratified.

Two sandstone samples from this formation were subjected to petrographic study. Stratigraphic positions of these samples are shown in Figure 3.2. Sandstones of the Talchir Formation are composed mostly of quartz and feldspar. Grains are very poorly sorted with some pebble-to cobble-sized grains present in the thin sections. The average modal composition of Talchir sandstone is $Qt_{66}F_{21}L_{13}$. Quartz grains are subangular to subrounded. Monocrystalline quartz with mostly straight extinction dominates over the polycrystalline grains. Plagioclase and K-feldspar are abundant and some of the feldspar has been calcified (Fig. 3.3). Mica is also present. Most of the lithic grains observed are sedimentary, mainly mudstone and argillite. The Talchir sandstone

contains approximately 15% matrix, which consists of clay formed by alteration of feldspars.

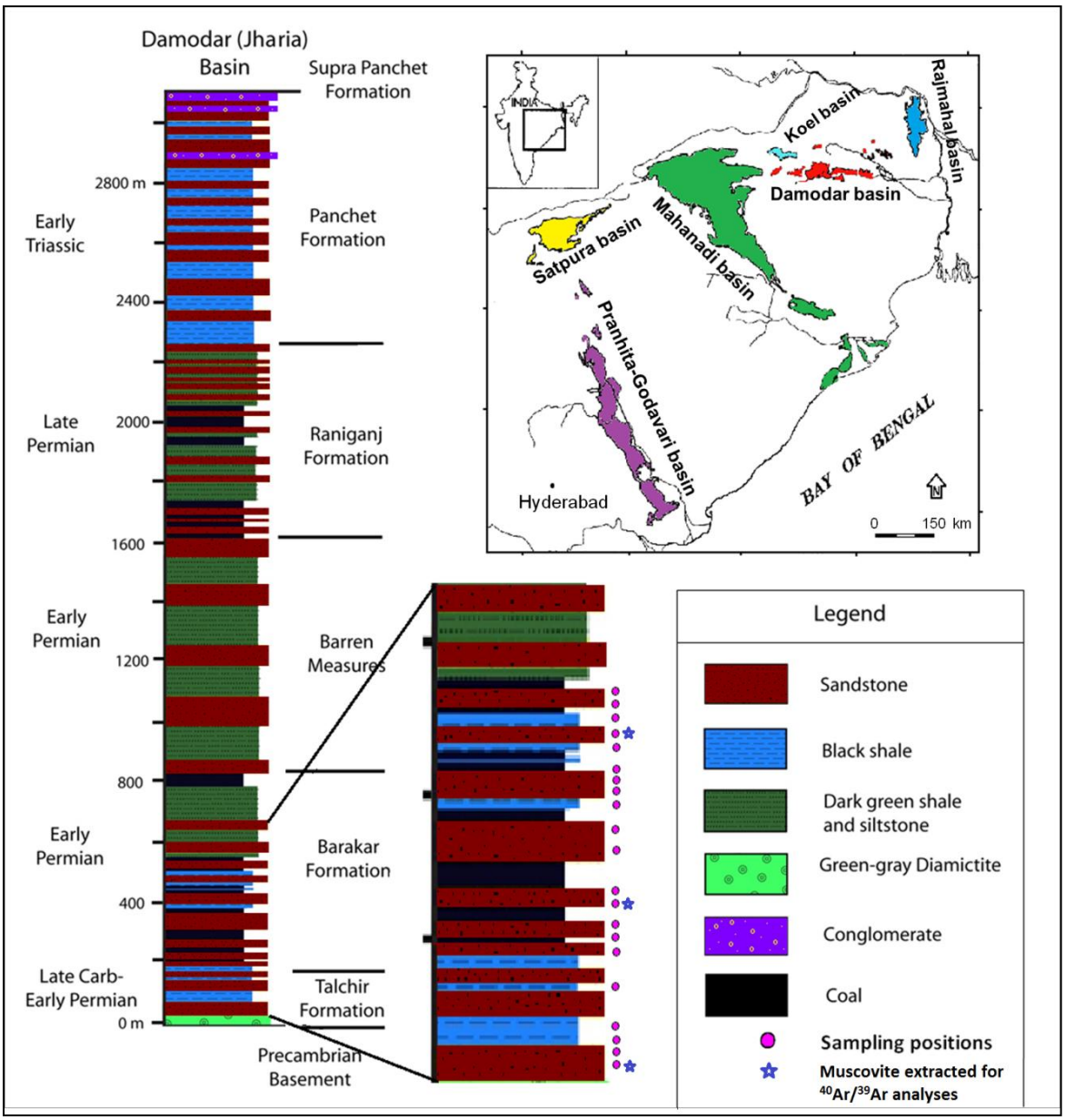

Figure 3.2 Stratigraphic column of Gondwanan sequences in the Damodar (Jharia) Basin. The inset map shows locations of Gondwanan basins in eastern India including the study area in the Damodar (Jharia) basin. Stratigraphic positions of the sediment samples collected for this study are shown by purple dots on the enlarged view. Blue asterisk indicates stratigraphic locations of samples collected for $^{40}Ar/^{39}Ar$ analyses (after Veevers and Tewari, 1995; Dutta, 2002; and Mukhopadhyay et al., 2010).

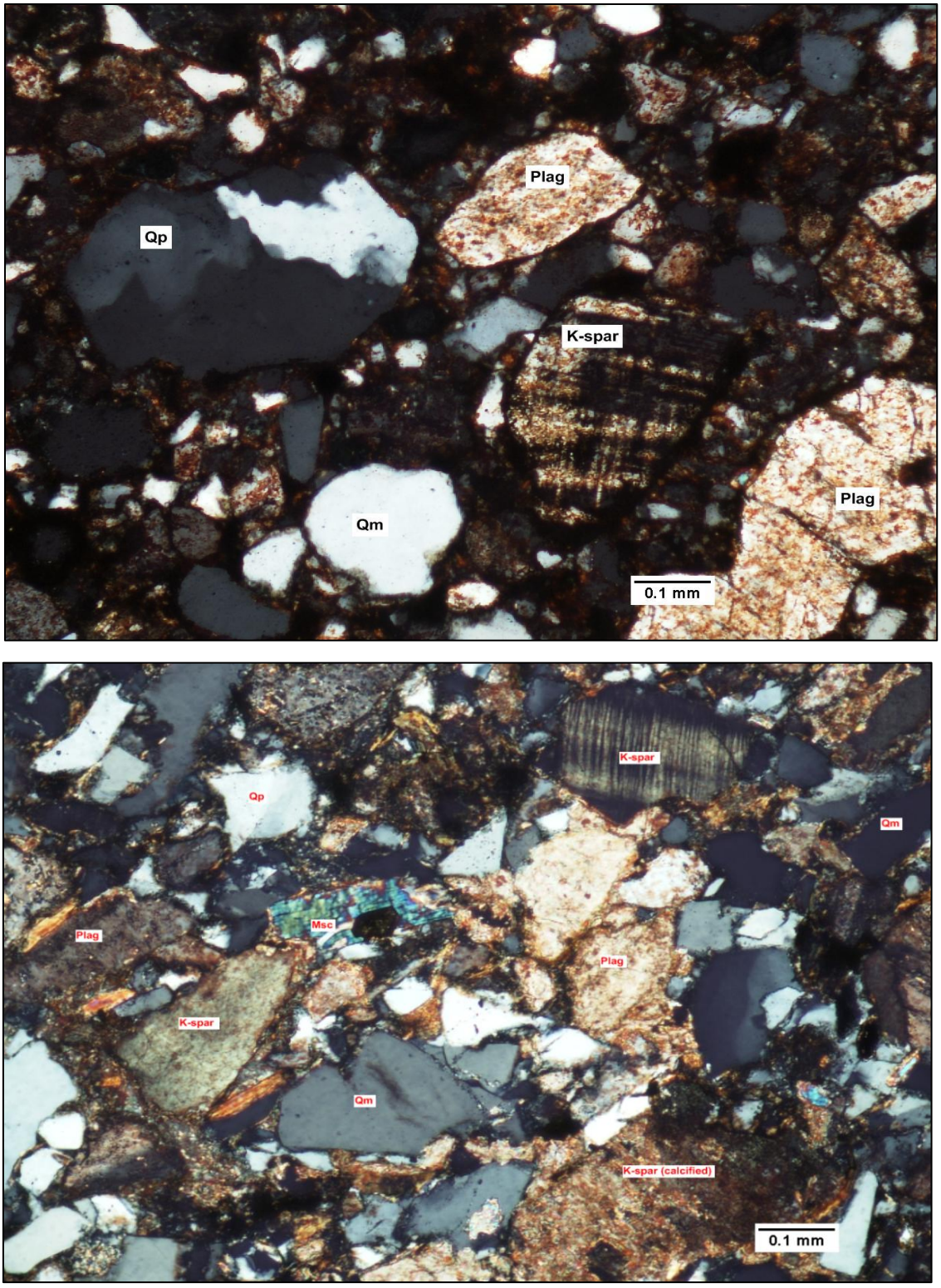

Figure 3.3 Representative photomicrographs of Gondwanan Talchir sandstones from Jharia basin, India (Qm = monocrystalline quartz, Qp = polycrystalline quartz, K-spar= potassium feldspar, Plag= plagioclase).

3.3.2 PETROGRAPHY OF BARAKAR FORMATION, JHARIA BASIN, INDIA

The Barakar Formation is the main repository of coal deposits in Gondwanan sediments of India. This formation is characterized by fining upward cycles of sandstone, shale, carbonaceous shale and coal deposits. Thick coal seams developed in the lower and middle part of these cyclothems. Sandstone shows massive and cross-beds with paleocurrent direction towards north or northwest. *Glossopteris* flora is recorded from this formation (Vaidyanadhan and Ramakrishnan, 2008).

Thirteen (13) sand (stone) samples were collected from the Barakar Formation. Stratigraphic positions of these samples are shown in Figure 3.2. Barakar sandstone are composed mostly of quartz and lithic grains. No feldspar was identified from this sandstone. The average modal composition is $Qt_{86}F_0L_{14}$. Monocrystalline quartz dominates over polycrystalline grains. Most of the monocrystalline quartz grains show non-undulose to slightly undulose extinction. Overgrowths on quartz were observed. Some quartz grains were calcitized. Most framework grains are moderately to well sorted and subangular to subrounded, although some grains are angular. Significant siderite contents were identified from several thin sections (Fig. 3.4). Based on grain size, the Barakar sandstone can be divided into two broad parts; a lower part, containing very coarse sand- to pebble-sized quartz grains (Fig 3.5), and an upper part consisting of fine- to coarse-grained quartz. The matrix content increases and sorting decreases from stratigraphically older to younger sandstones. Mica are abundant.

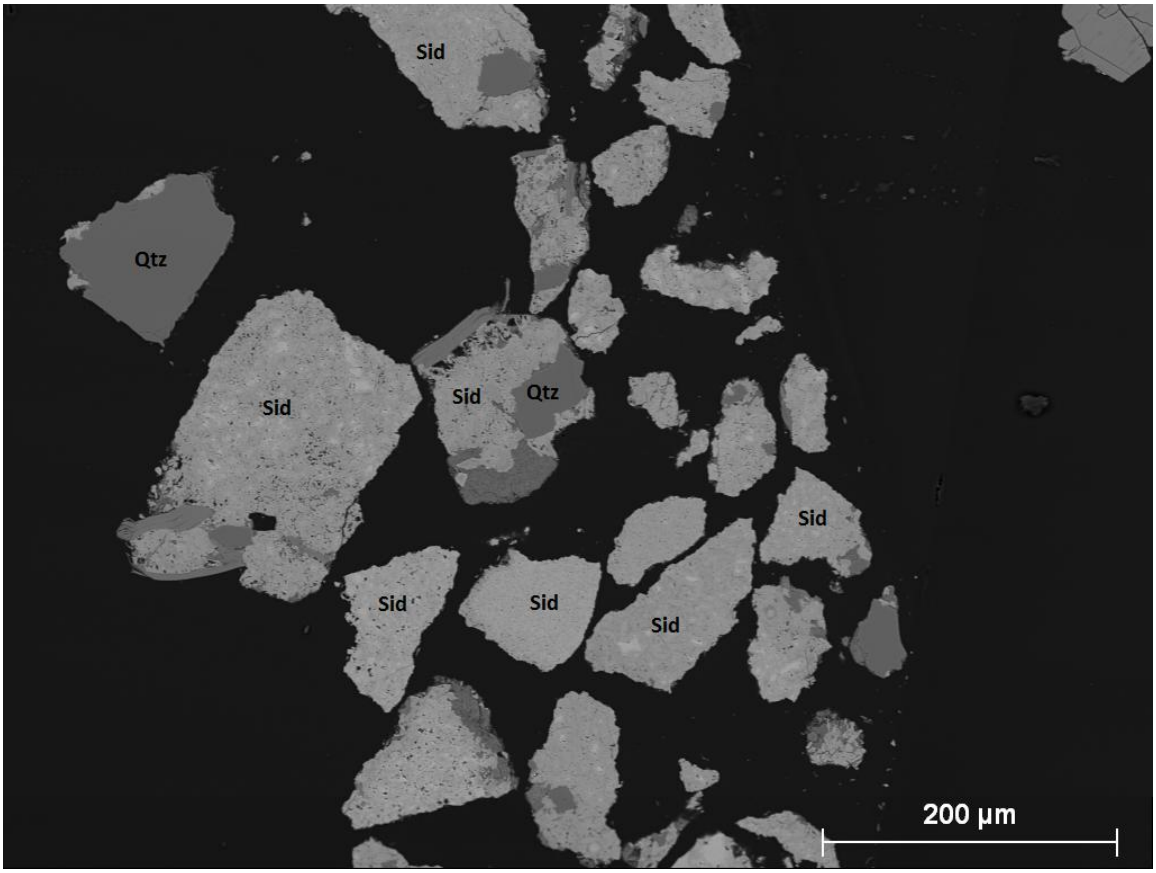

Figure 3.4 Backscattered image of siderite-rich Gondwanan Barakar sandstones from Jharia basin, India (Sid = siderite, Qtz = quartz).

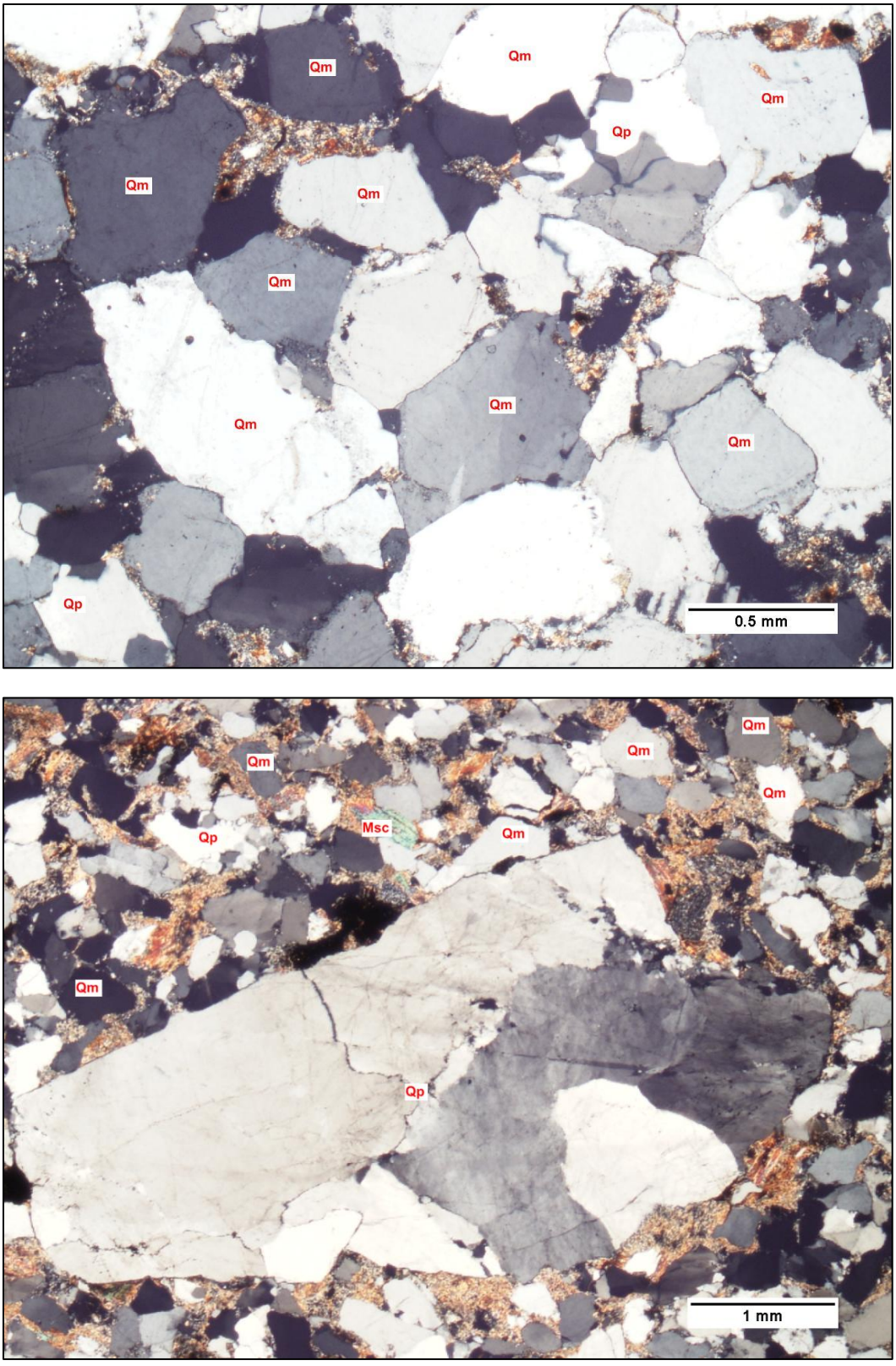

Figure 3.5 Representative photomicrographs of Barakar sandstones from Jharia basin, India (Qm = monocrystalline quartz, Qp = polycrystalline quartz, Msc =muscovite).

3.3.3 PETROGRAPHY OF BARAPUKURIA COAL BASIN, BANGLADESH

Rocks of the Gondwanan group of Barapukuria Basin are usually assigned to the Kuchma and Paharpur formations. The lithological character and thick coal beds with characteristic *Glossopteris* and *Gangamopteris* floras suggest that these strata might be equivalent to Lower Gondwanan rocks found in India and other parts of the world (Islam et al., 1992). The Barapukuria basin area is covered with Holocene alluvium and Pleistocene Barind Clay. The stratigraphic succession of this basin has been established on the basis of borehole data (Bakr et al., 1996; Islam et al., 1987). The sedimentary units encountered in boreholes include the Gondwanan Group (Permian), Dupi Tila Formation (Pliocene), Barind Clay (Pleistocene), and Holocene alluvium.

Overall grain size generally decreases upward through the Gondwanan sequences. The lower part of the group is characterized by conglomerates that unconformably overlie the Archean basement complex. Clasts are mostly angular to subrounded granules, pebbles, and cobbles. Sandstone and carbonaceous material locally interbedded with the conglomerates (Bakr et al., 1996).

A total of seven (7) core samples were collected at different stratigraphic levels from the exploratory drill well GDH-41 (Fig. 3.6). The samples studied from Barapukuria coal mine are mostly sub-arkosic to quartz arenitic, although a few of them are litharenitic. Core samples are quartz-rich but also include, in descending order, feldspar, mica, organic matter and lithic fragments. Only sedimentary lithic fragments were identified. Sands overall are very poorly sorted, angular to subangular, and immature. Average modal composition of Barapukuria sandstones is $Qt_{66}F_{17}L_{17}$. Monocrystalline

quartz crystals are more abundant than polycrystalline quartz. Boehl lamellae are present in some quartz grains. Some of the quartz grains are semicomposite with slightly undulose extinction. K-feldspar is dominant over plagioclase feldspars. The appearances of feldspars vary from fresh to highly altered (Fig. 3.7).

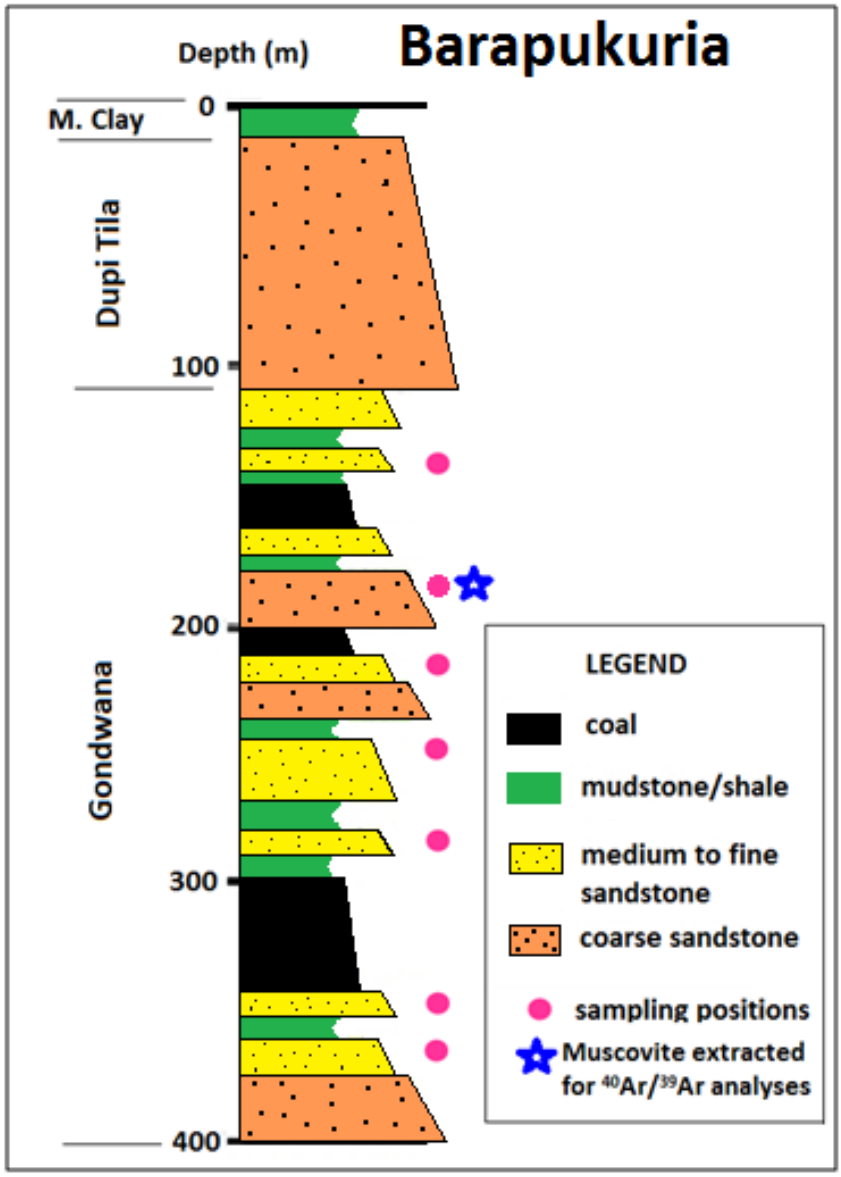

Figure 3.6 Generalized stratigraphic column of Gondwanan sequence in Barapukuria drill-well GDH-41, Bangladesh. Sediment sampling positions for this study are shown by pink dots. Blue star indicates stratigraphic location of sample collected for $^{40}Ar/^{39}Ar$ analyses (after Bakr et al., 1996).

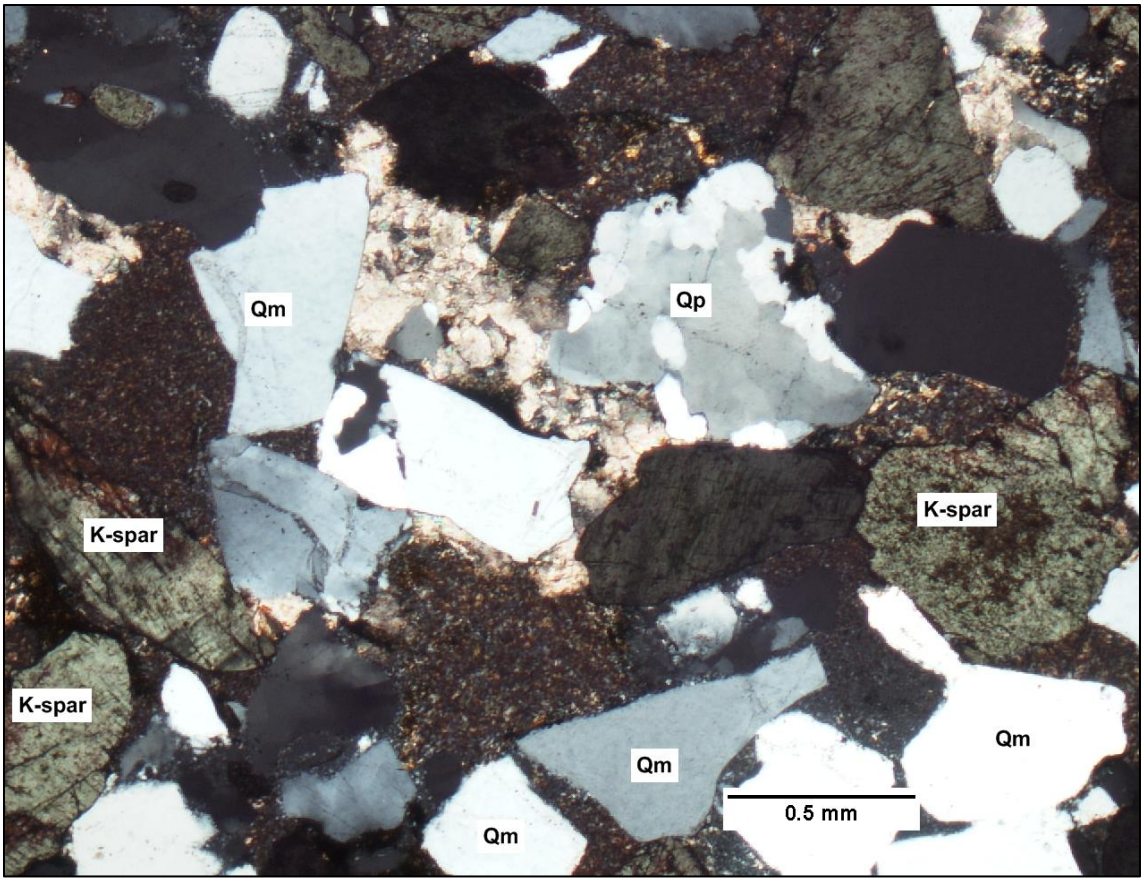

Figure 3.7 Representative photomicrograph of a Gondwanan sandstone from Barapukuria coal basin, Bangladesh (Qm = monocrystalline quartz, Qp = polycrystalline quartz, K-spar= potassium feldspar).

3.3.4 PETROGRAPHY OF DIGHIPARA COAL BASIN, BANGLADESH

The Dighipara basin is a north-south elongated half-graben, bounded by major north-south-oriented boundary faults at the eastern margin. The stratigraphic column (Fig. 3.8) is similar to that of the Barapukuria basin (Hasan and Islam, 2003). The Permian Gondwanan Group underlies archaean basement and is unconformably overlain by the Pliocene Dupi Tila Formation and the Pleistocene Barind (Madhupur) Clay Formation. The Gondwana Group in the study area is approximately 475 m thick and includes a number of coal seams (Imam, 2005). The Gondwanan sandstones in the Dighipara basin are crossbedded and are interpreted to have been deposited in a high-

energy fluvial environment. Mudstones are interpreted to have been deposited in low-energy delta-plain settings, while the coal accumulated in very low-energy swamp settings (Alam et al., 2003; Imam, 2005).

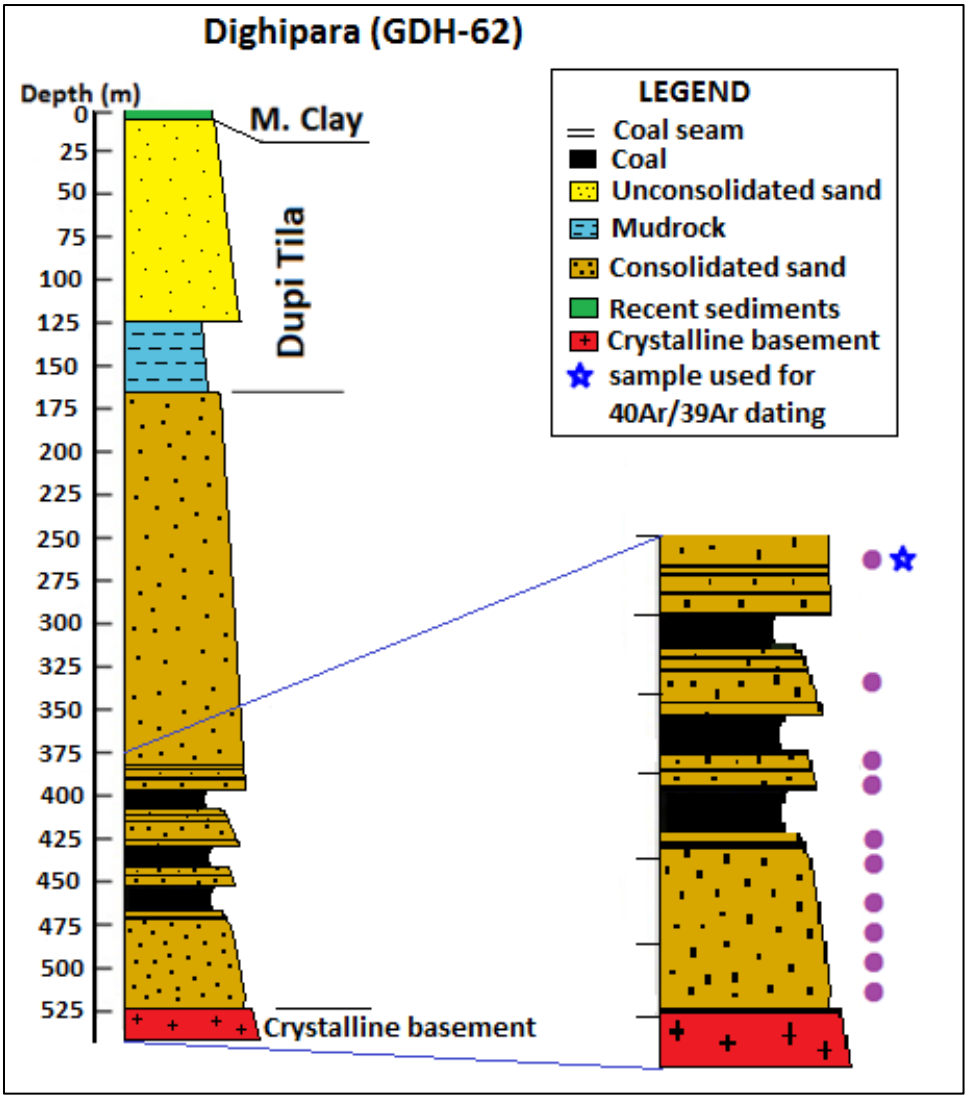

Figure 3.8 Generalized stratigraphic column of the Gondwanan sequence in Dighipara drill-well GDH-62, Bangladesh. Sediment-sampling positions for this study are shown by pink dots. Blue star indicates stratigraphic location of sample collected for $^{40}Ar/^{39}Ar$ analyses (after Bakr et al., 1996).

A total of six (6) sand (stone) samples were analyzed out of the ten (10) samples collected from the Dighipara well. Sandstones are primarily poorly to very poorly sorted

arkoses. Lithic fragments are scarce. The average modal composition is $Qt_{77}F_{19}L_4$. Quartz grains are angular to subangular, indicating short distances of transport. Unlike in other samples of this study, polycrystalline quartz dominates over monocrystalline grains (Fig. 3.9). Many of the feldspars may have been altered into clay minerals. Quartz overgrowths within K-feldspar were found. Significant amount of feldspar are calcitized. Fluid/mud injection through the sediments has been observed (Fig. 3.10).

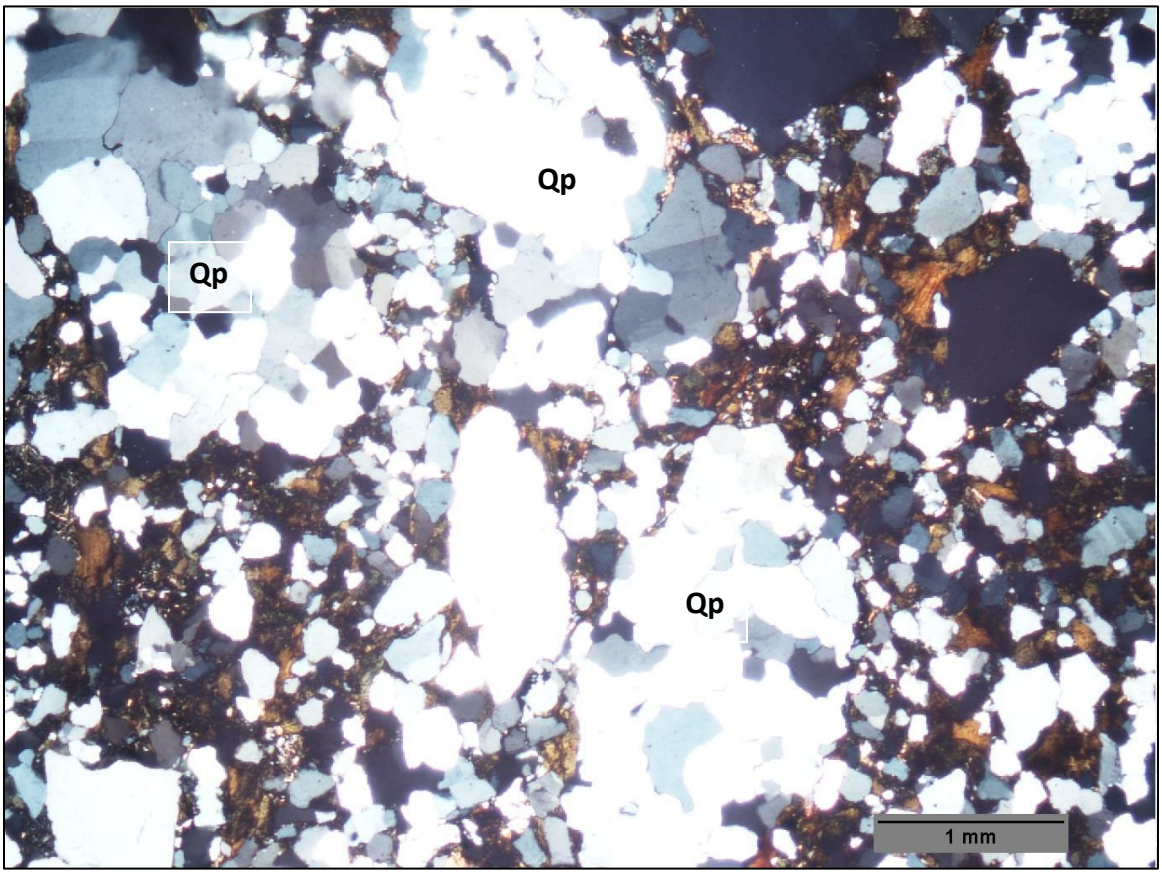

Figure 3.9 Representative photomicrograph of Gondwanan sandstone from Dhigipara coal basin, Bangladesh (Qp = polycrystalline quartz).

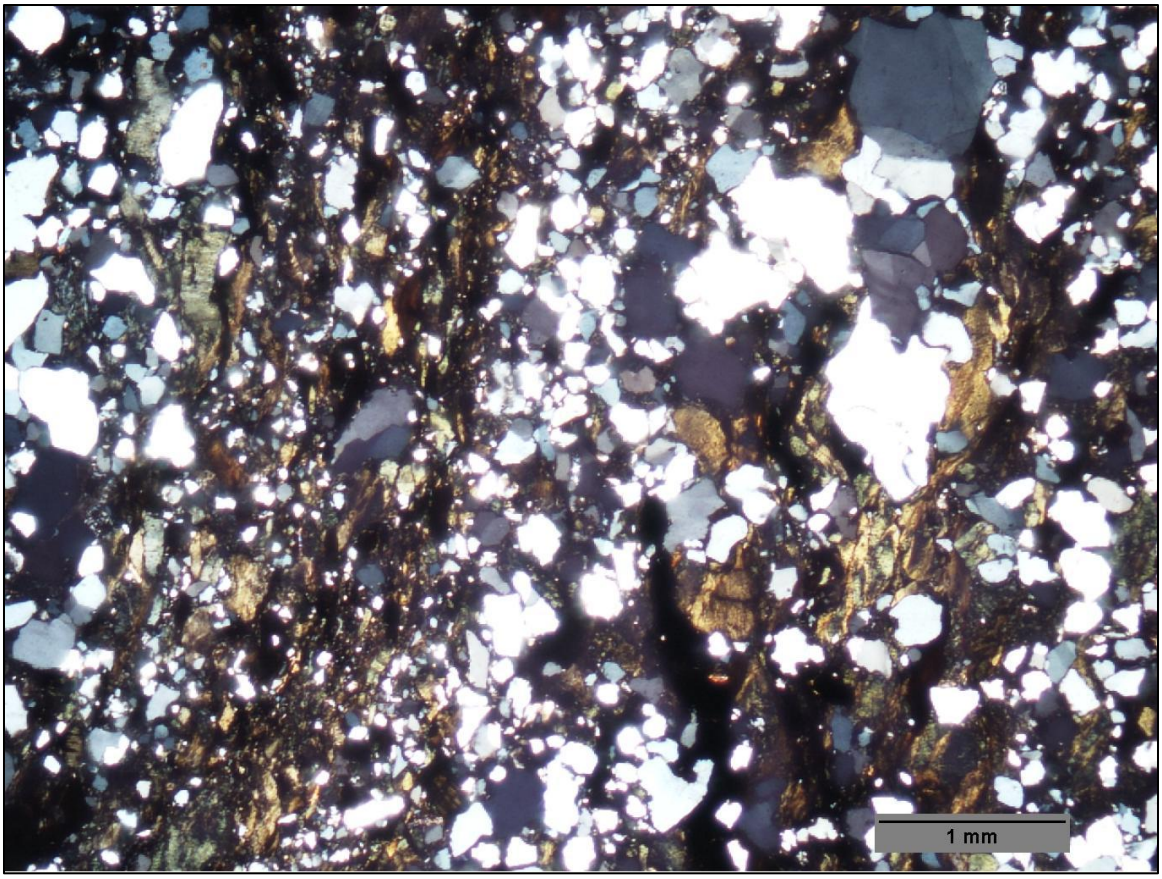

Figure 3.10 Representative photomicrograph of Gondwanan sandstone from Dhigipara coal basin, Bangladesh.

3.3.5 PETROGRAPHY OF KHALASPIR COAL BASIN, BANGLADESH

The Khalaspir coal mine is located about 80 km southeast of Barapukuria (Fig. 1.3). The Paharpur Formation and Kuchma Formation in the Khalshpir basin are considered to be equivalent to the Raniganj Group and Barakar Group, respectively, in India based on their lithology and coal geochemistry (Zaher and Rahman, 1980). The depositional sequences of the Gondwanan Group in the Khalaspir basin consist of alternating sandstones and mudstones with coal layers of variable thickness. The bottom parts of the sequences are characterized by pebbly sandstones and conglomerates. Grain size generally decreases up section.

A total of ten (10) core samples were collected from the GDH-45 well at Khalaspir from different stratigraphic levels. Stratigraphic positions of these samples are shown in Figure 3.11. Quartz is the most dominant framework grain in sandstones from this core. Other framework grains include feldspar, mica, organic matter, and lithic fragments, in a descending order (Fig. 3.12). Average modal composition of the Khalaspir core sandstones is $Qt_{72}F_{14}L_{14.}$ Quartz grains are subangular to rounded, and monocrystalline quartz is dominant over polycrystalline quartz. Coarser polycrystalline quartz grains are observed locally.

Both plagioclase and K-feldspar are observed in significant amounts but K-feldspar dominates over plagioclase. Feldspar grains are variably alterated to sericite or clay minerals and some are calcitized. Muscovite and biotite are also present. Sedimentary lithic fragments, including mudstones, are abundant. Mud clasts are reddish because of leaching of iron-rich solutions and eventual development of iron crusts. Matrix is more common than siliceous cements.

Quartz grains in some samples exhibit Boehm lamellae. Such features in quartz crystals are caused by intense strain and deformation of grains (Mange and Maurer, 1989). Probable mud injections were observed. This may be related to a combination of high rates of sedimentation and tectonic compression. The mud injections may have formed by rise of fluidized sediments along faults (Milkov, 2000).

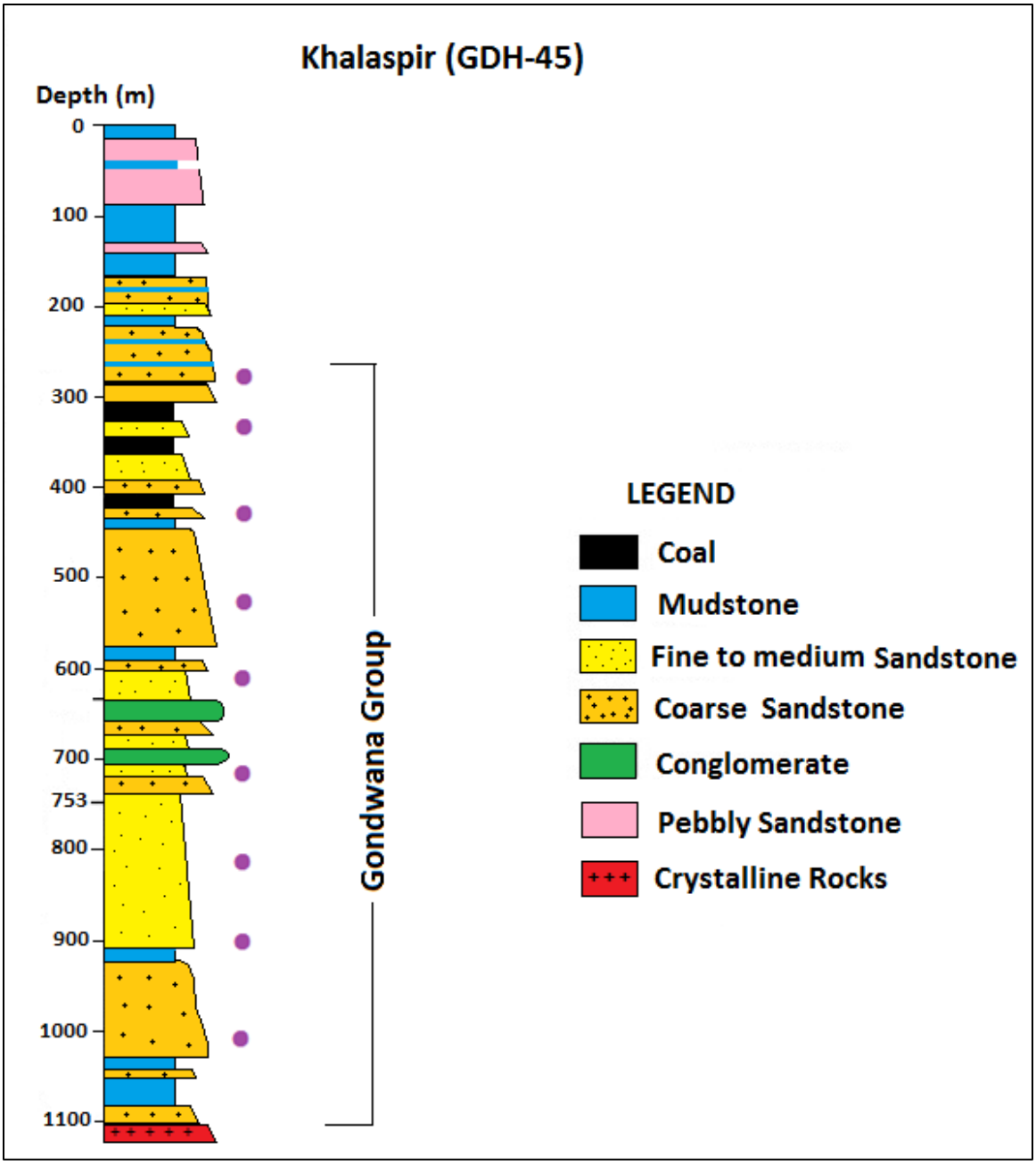

Figure 3.11 Generalized stratigraphic column of Gondwanan sequences of Khalaspir drill-well GDH-45, Bangladesh. Sediment sampling positions for this study are shown by pink dots (after Islam et al., 1992; Roy and Roser, 2013).

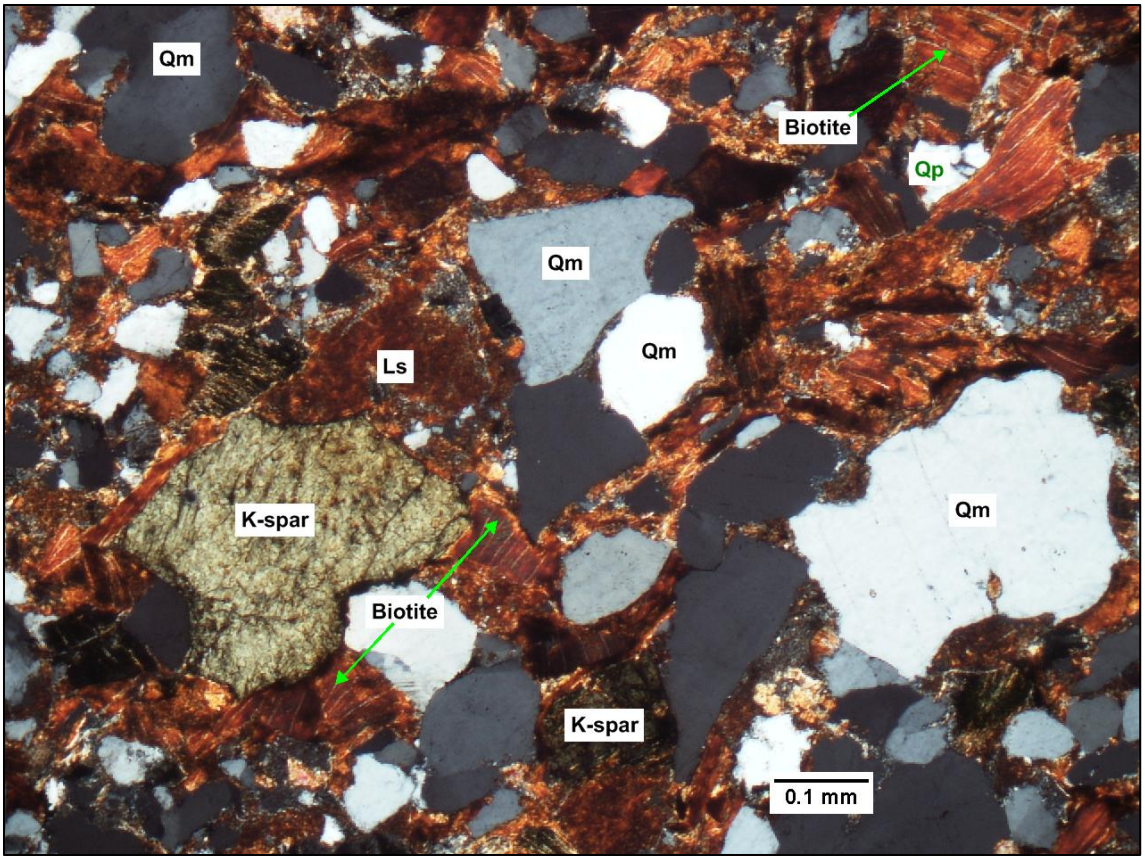

Figure 3.12 Representative photomicrograph of Gondwanan sandstone from Khalaspir coal basin, Bangladesh (Qm = monocrystalline quartz, Qp = polycrystalline quartz, Ls = sedimentary lithic fragment, K-spar= potassium feldspar).

3.4 SANDSTONE MODES

Thirty-three (33) sandstone samples (18 from Bangladesh and 15 from India) were analyzed from different stratigraphic levels of Gondwanan sequences of India and Bangladesh. Modal compositions of these sediments are shown in Table 3.2. Average sandstone modes from three different coal basins in northwest Bangladesh and the Barakar and Talchir formations from Jharia basin in northeast India are plotted in Figure 3.13 (McBride, 1963). Sandstone modes of the Talchir Formation and Barapukuria and Khalaspir samples fall in the lithic subarkose field. However, Barakar and Dighipara samples fall in the sublitharenite and subarkose fields, respectively.

Table 3.2 Normalized modal compositions of Gondwanan sandstones from different basins in Bangladesh and India.

Sample Location	Sample No.	Qt	F	L	Qm	F	Lt	Qm	P	K
	B-K-2	90	1	9	89	1	10	99	0	1
	B-K-3	81	7	12	59	7	34	89	0	11
KHALASPIR	B-K-5	74	2	24	49	2	49	96	1	3
	B-K-6	65	8	27	27	8	65	77	0	23
	B-K-7	62	31	7	39	31	30	56	20	24
	B-K-10	58	35	7	53	35	12	60	20	20
	Average	72	14	14	53	14	33	80	7	14
	STDEV	12	15	9	21	15	21	18	10	10
	B-B-1	71	16	13	55	16	29	77	1	22
	B-B-2	62	30	8	48	30	22	62	0	38
BARA PUKURIA	B-B-3	48	16	36	46	16	38	74	3	23
	B-B-4	75	18	7	42	18	40	69	1	30
	B-B-6	72	21	7	54	21	25	71	1	28
	B-B-7	66	2	32	55	2	43	97	0	3
	Average	66	17	17	50	17	33	75	1	24
	STDEV	10	9	13	5	9	9	12	1	12
DIGHIPARA	B-D-1	86	6	8	45	6	49	87	3	10
	B-D-3	93	5	2	28	5	67	85	0	15
	B-D-4	83	7	10	36	7	57	84	0	16
	B-D-8	65	34	1	2	34	64	5	1	94
	B-D-10	56	44	0	2	44	54	3	85	12
	Average	77	19	4	23	19	58	53	18	29
	STDEV	15	18	4	20	18	7	45	38	36
All Bengal	Average	71.00	16.65	12.35	42.88	16.65	40.47	70.06	8.00	21.94
samples	STDEV	12.55	13.64	10.76	20.71	13.64	17.81	27.96	20.86	21.16
TALCHIR	I-T-1	60	20	20	42	20	38	68	23	9
	I-T-2	71	22	7	43	22	35	66	19	15
	Average	66	21	13	43	21	37	67	21	12
	STDEV	8	1	9	1	1	2	1	3	4
	I-B-1	98	0	2	75	0	25	100	0	0
	I-B-2	99	0	1	81	0	19	100	0	0
	I-B-3	100	0	0	81	0	19	100	0	0
	I-B-4	99	0	1	62	0	38	100	0	0
	I-B-5	96	0	4	64	0	36	100	0	0
BARAKAR	I-B-6	96	0	4	52	0	48	100	0	0
	I-B-7	76	0	24	52	0	48	100	0	0
	I-B-8	91	0	9	50	0	50	100	0	0
	I-B-10	96	0	4	37	0	63	100	0	0
	I-B-12	56	0	44	19	0	81	100	0	0
	I-B-13	27	0	73	10	0	90	100	0	0
	I-B-14	93	0	7	28	0	72	100	0	0
	I-B-16	97	0	3	37	0	63	100	0	0
	Average	86	0	14	50	0	50	100	0	0
	STDEV	22	0	22	23	0	23	0	0	0
All Indian	Average	83.67	2.80	13.53	48.87	2.80	48.33	95.60	2.80	1.60
samples	STDEV	21.50	7.40	20.24	21.33	7.40	21.72	11.62	7.43	4.37

(STDEV= standard deviation)

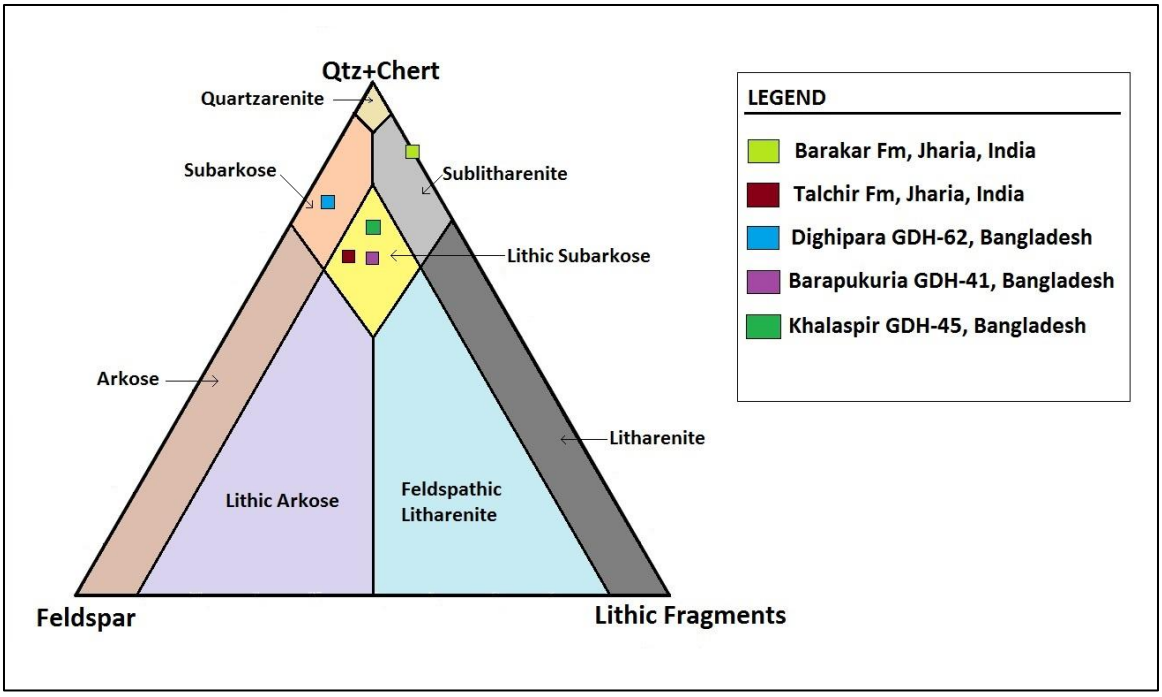

Figure 3.13 Average modal compositions of the Gondwanan sandstones from India and Bangladesh.

Sandstones from Bangladesh and Talchir Formation in India are angular to subangular grains and both texturally and compositionally more immature than coeval sandstones from Barakar Formation in India. Monocrystalline quartz was dominant over polycrystalline quartz in both Indian and Bangladesh samples. However, Bengal samples contain higher percentage of polycrystalline quartz with >3 crystals per grain, which indicates low-rank metamorphic source rocks (Blatt, 1967; Basu et al., 1975). High amount of monocrystalline nonundulose quartz in Barakar sandstones indicate plutonic sources (Blatt and Christie, 1963; Blatt, 1967; Basu et al., 1975). Although significant amounts of feldspar were observed from the Bangladesh samples and the Talchir Formation of India, no feldspar was found in the samples from the Barakar Formation (India).

3.5 PETROFACIES EVOLUTION

Several tectonic provenance fields (transitional continental, basement uplift, recycled orogenic and dissected arc) were identified for these mostly poorly-sorted subarkosic and sublitharenitic samples. Sandstone modal analysis shows that Gondwanan sediments from Bangladesh areas (~$Qt_{66}F_{20}L_{14}$) plot mostly in the 'recycled orogenic' to 'transitional continental' provenance fields of Dickinson (1985), whereas Indian Gondwanan samples (~$Qt_{84}F_3L_{13}$) plot in the 'craton interior' to 'recycled orogenic' fields (Fig. 3.13). However, in the QmFLt plot, Bengal samples falls in the recycled orogenic, transitional recycled, mixed, dissected arc and transitional arc settings, whereas Indian samples fall in the recycled orogenic and transitional recycled fields (Fig. 3.14). QmPK plots indicate that potassium feldspar is dominant over plagioclase feldspar (Fig. 3.15).

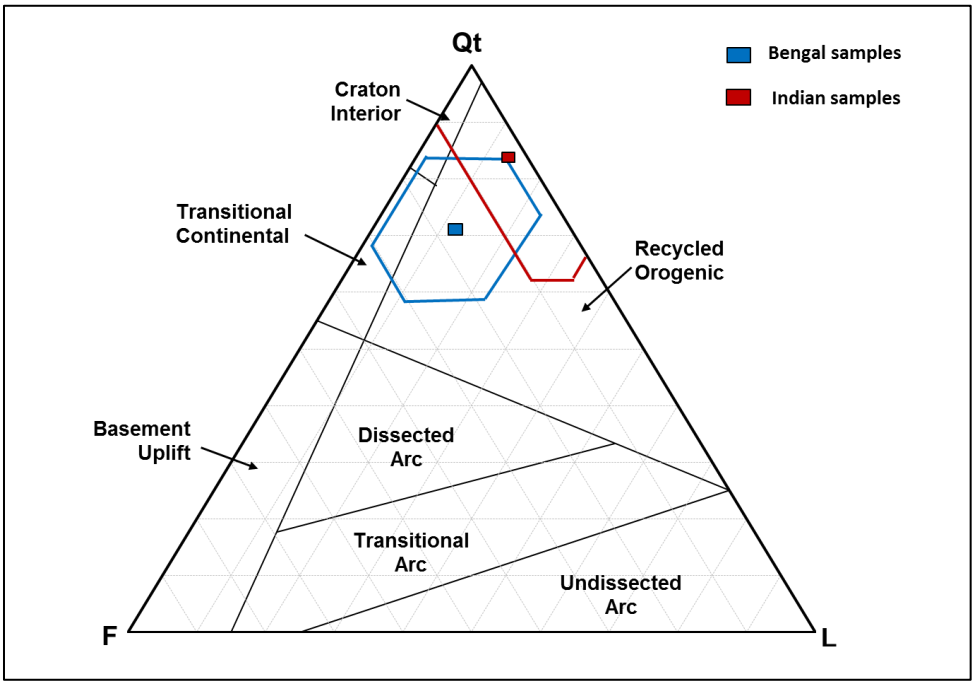

Figure 3.14 Q_tFL plots of Gondwanan sandstone samples showing mean and standard deviation polygons (provenance fields from Dickinson, 1985).

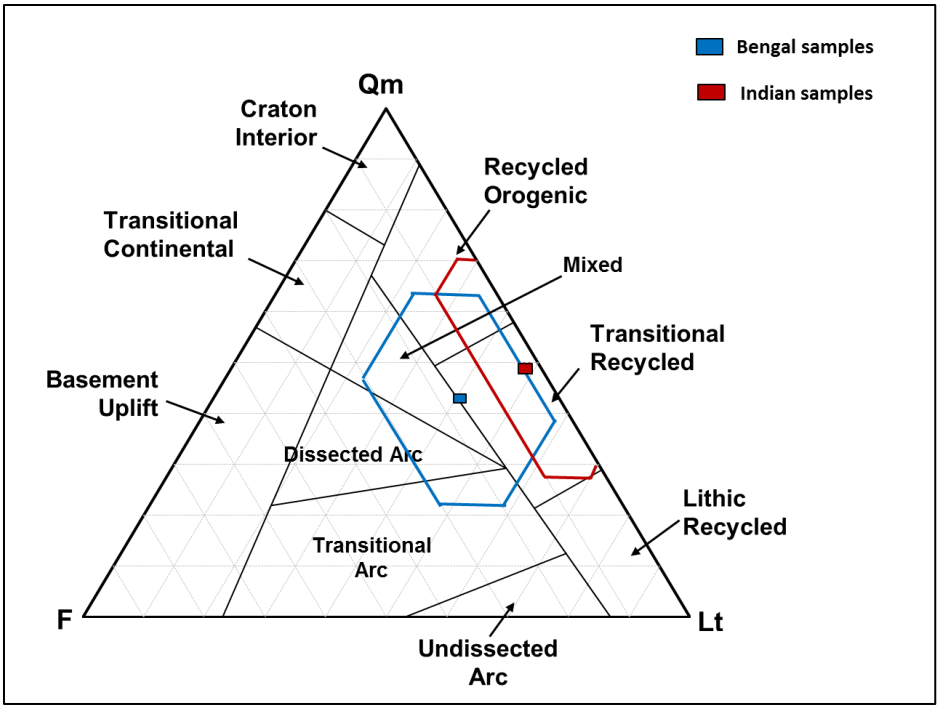

Figure 3.15 Q_mFL_t plots of Gondwanan sandstone samples showing mean and standard deviation polygons (provenance fields from Dickinson, 1985).

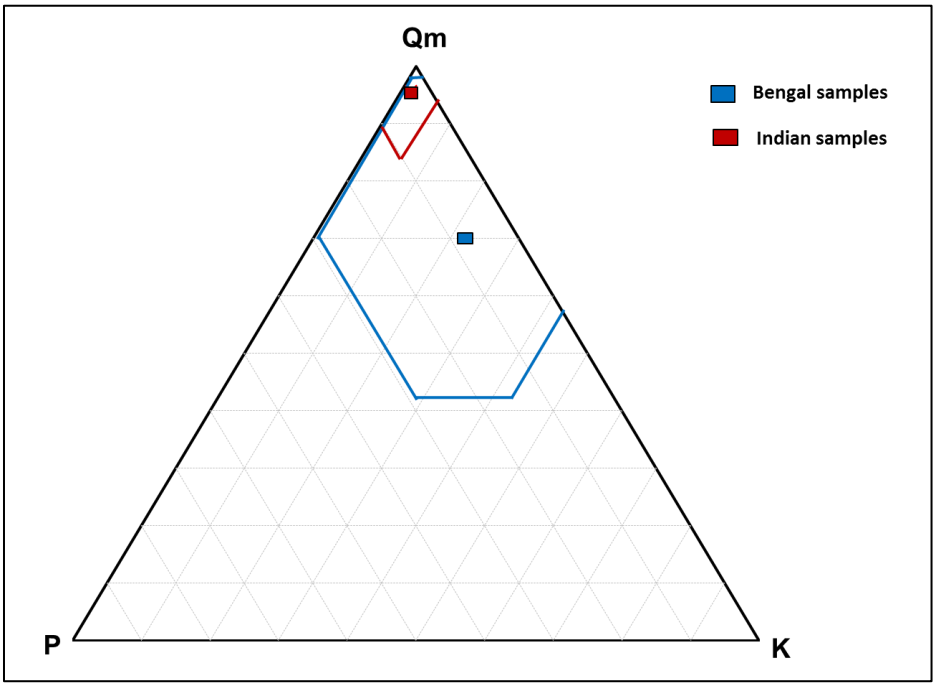

Figure 3.16 Q_mPK plots of Gondwanan sandstone samples showing mean and standard deviation polygons (provenance fields from Dickinson, 1985).

Sandstone modal analysis suggests that multiple sources have contributed sediments to these Gondwanan basins in both Bangladesh and India. Sediment sources from continental blocks are either on stable shields and platforms or from uplifted blocks along plate boundaries. In the study area, these sediments may have been derived from the adjacent Indian craton. Given the north or northwesterly paleoslopes for the Lower Gondwanan sediments, the Singbhum cratons, Meghalayan craton (Shilong Plateau), and Eastern Ghats Mobile Belt are the probable sources for these sediments. Figure 3.17 illustrates distribution of Gondwanan sediments in the Indian subcontinent and their probable source terranes in the adjacent area.

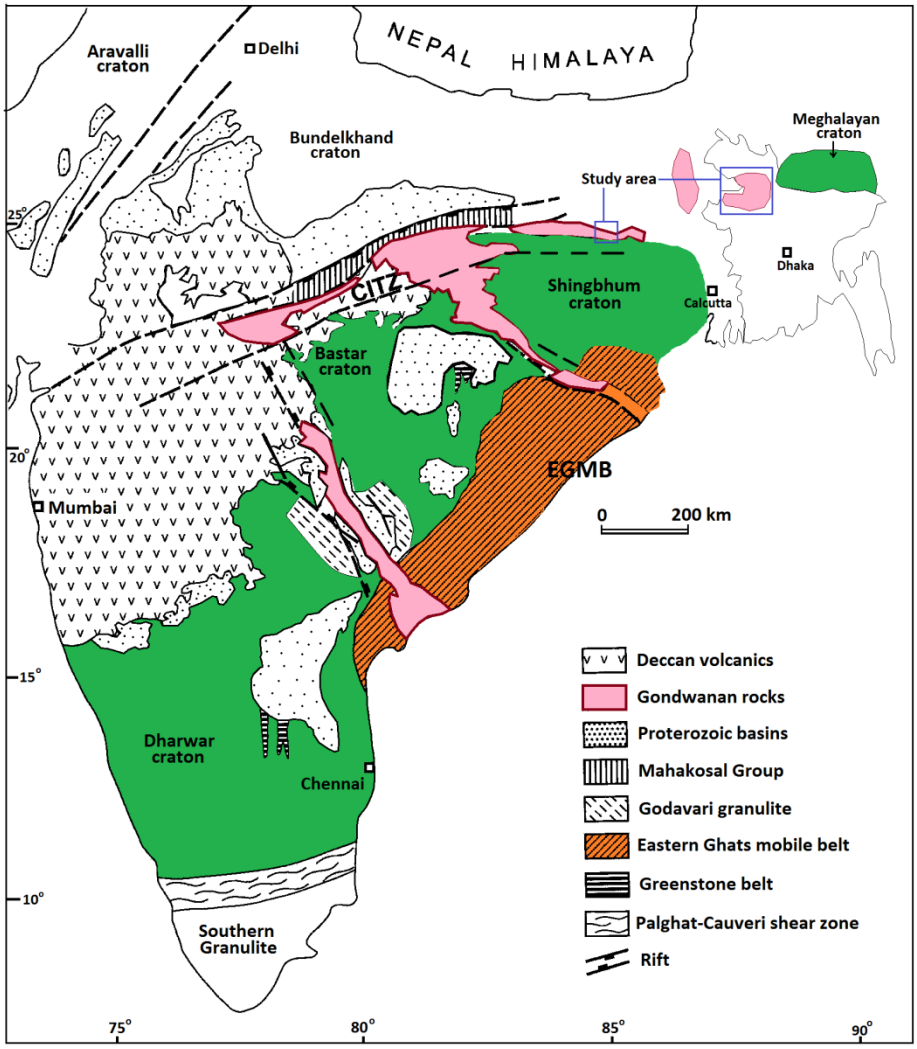

Figure 3.17 Gondwanan sequences of Bangladesh and India, and their probable nearby sources including Shingbhum craton, Meghalayan craton, and Eastern Ghats mobile belt (compiled from Dutta, 2002; Meert et al., 2010).

The Pinjarra Orogen, which was located between Western Australia and eastern India (Fig. 3.18), also could have been a source of sediments in the study area (Collins, 2003; Cawood, 2005; and Collins and Pisarevsky, 2005). The Prydz Bay Belt, Napier complex, and/or Rayner complex in eastern Antarctica also may have contributed to these basins in the Indian subcontinent. Figure 3.18 illustrates probable source terranes in the adjacent Antarctica and Australia.

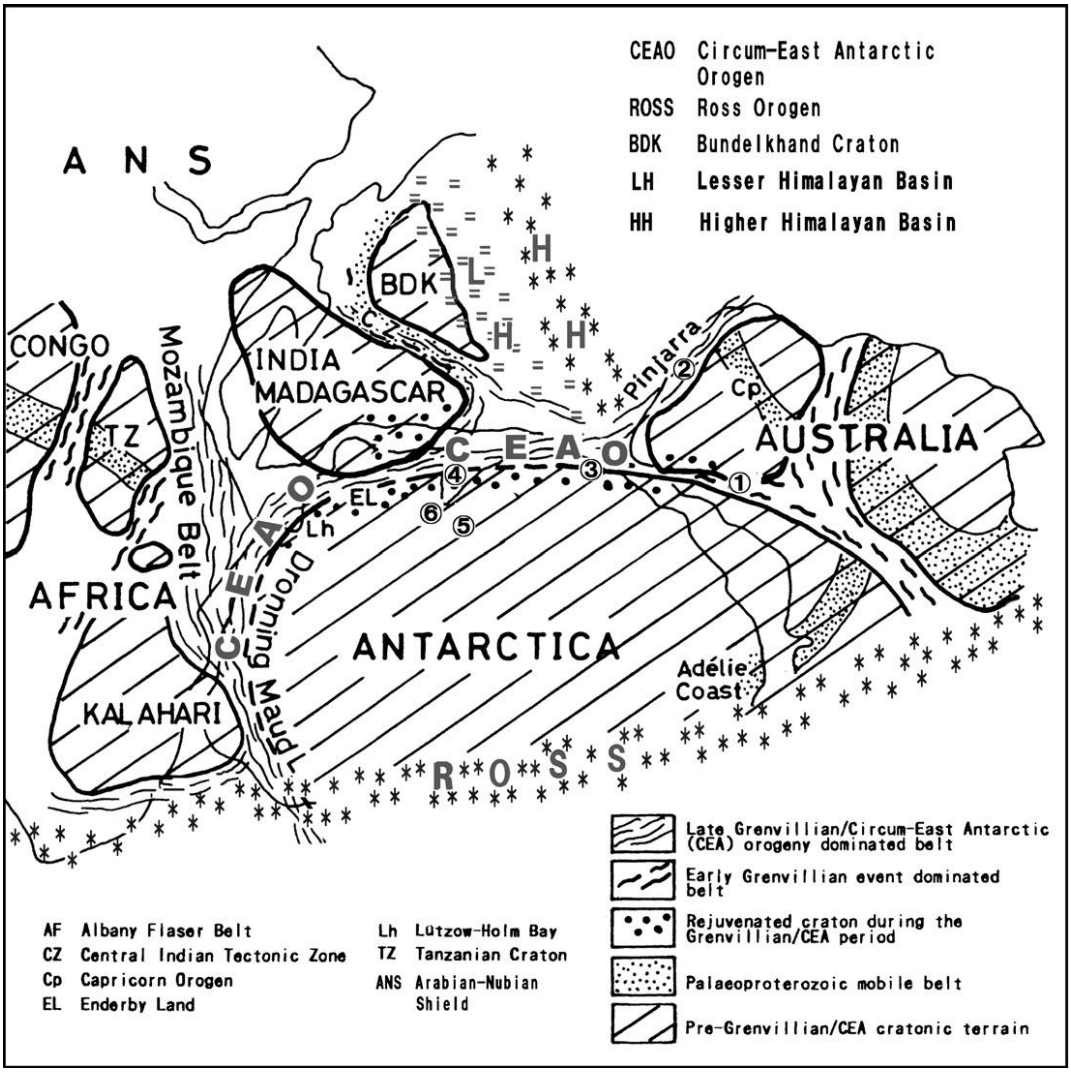

Figure 3.18 Paleogeographic map showing assembly ①: Albany–Flaser Belt, ②: Leeuwin-Darling Zone, ③: Denmann Glacier area, ④: Prydz Bay, ⑤: Grove Mountains, ⑥: Prince Charles Mountains (from Yoshida and Upreti, 2006).

CHAPTER 4: HEAVY MINERAL ANALYSES

4.1 INTRODUCTION

Heavy mineral analysis has been used widely in provenance studies of siliciclastic rocks. Studies of sediment composition can help constrain source-rock lithology. Common minerals (like quartz and feldspars) that constitute the bulk sediment composition are contributed by a variety of rocks. However, many heavy minerals are

restricted to specific source rocks. Thus, heavy mineral suites can provide clues to decipher provenance lithology (Rahman and Ahmed, 1996; Tiwari and Yadav, 1993; Hota and Maejima, 2009; Sevastjanova et al., 2012). Different sources within the same tectonic setting even can be distinguished by heavy mineral analyses (Morton, 1985; Najman and Garzanti, 2000; Garzanti et al., 2007).

Among the large varieties of heavy mineral species found in sandstones, approximately thirty are used in source-rock identification (Morton, 1985; Mange and Maurer, 1992). Heavy mineral assemblages are generally resistant enough to endure transport (Morton and Hallsworth, 1999; Uddin et al., 2007). Several sedimentary processes such as weathering of source rock, mechanical breakdown and hydraulics during transportation, alluvial storage, and burial diagenesis may change the original relative abundances of heavy mineral assemblages (Morton, 1985; Morton and Hallsworth, 1999). However, some minerals are more stable (Table 4.1), including apatite, TiO_2 polymorphs (rutile, anatase and brookite), tourmaline, and zircon (Morton, 1984, Mange and Maurer, 1992; Morton and Hallsworth, 1999).

Table 4.1 Relative stability of minerals with similar hydraulic and diagenetic behaviors (stability increases towards the top part of the table).

Stability in weathering profiles (Grimm, 1973; Bateman and Catt, 1985; Dryden and Dryden, 1946)	Mechanical stability during transport (Freise, 1931)	Burial persistence North Sea (Morton, 1984, 1986)	Chemical weathering (Pettijohn, 1941)

Zircon, Rutile Tourmaline, Andalusite, Kyanite, Staurolite Garnet Epidote Calcic Amphibole Clinopyroxene Orthopyroxene Apatite	Tourmaline Corundum Chrome-spinel Spinel Rutile Staurolite Augite Topaz Garnet Epidote Apatite Zircon Kyanite Olivine Andalusite Diopside Monazite	Apatite, Monazite, Spinel, TiO_2 minerals, Tourmaline, Zircon Chloritoid, Garnet Staurolite Kyanite Titanite Epidote Calcic Amphibole Andalusite Sillimanite Pyroxene Olivine	TiO_2 minerals Zircon Tourmaline Sillimanite Andalusite Kyanite Staurolite Topaz Titanite Monazite Garnet Epidote Calcic amphibole Orthopyroxene Clinopyroxene Olivine Apatite

Morton and Hallsworth (1994) proposed the method of varietal studies of heavy minerals that focuses on the relative abundances of more stable species (i.e., those that are less impacted by diagenesis and hydraulic behavior). Determination of relative proportions of specific minerals that behave in a similar way during diagenesis and transportation can be very useful (Morton and Hallsworth, 1994). Several mineral ratios and indices have been proposed by Morton and Hallsworth (1994). These include ATi (apatite and tourmaline index), GZi (garnet and zircon index), CZi (chrome spinel and zircon index), MZi (monazite, zircon index), and RZi (TiO_2 group and zircon ratio). However, these methods are not applicable if the rock unit does not contain abundant heavy minerals. In the absence of full suites of heavy minerals, study can be accomplished by determining the relative abundance of all important heavy mineral species preserved in each stratigraphic unit, recognizing dominant members of the

mineral groups, and establishing index minerals from different stratigraphic levels (Peavy, 2008; Rahman, 2008; Alam, 2011).

Semi-quantitative analyses of heavy mineral assemblages in representative sandstones from Permo-Carboniferous Gondwanan sediments were performed in order to assess source rock types and to help reconstruct paleogeography of Southeast Asia.

4.2 METHODS

Samples were crushed in Himalayan Research Laboratory, Auburn University using a pestle and mortar. Careful attention was paid so that individual grains were not fragmented. A total of thirty five (35) samples were used for this study. Samples were disintegrated by drying in an oven and then sieving to extract 0-4 phi size fractions. The samples were weighed and added to the heavy liquid in a separating funnel. The heavy liquid tetrabromoethane ($C_2B_2Br_4$, density 2.89-2.96 gm/cc) was used to separate the heavy minerals from the lighter fractions. The mixture was stirred several times to ensure that the grains were thoroughly wetted and not coagulated. As time passed, the heavy minerals settled down to the bottom of the funnel and the lighter fractions appeared floating above the heavy liquid at the top of the separating funnel. After 24 hours, the stopcock was opened slowly and the liquid bearing the heavy mineral fraction in the bottom part of the separating funnel was allowed to flow slowly through a filter paper. The separated heavy fractions were washed carefully with acetone and dried in the open air and oven for 2 hours. Lighter fractions also were cleaned with acetone, dried, and stored. The heavy mineral fractions of samples were weighed to calculate weight percentage (Fig. 4.1) and processed for magnetic separation.

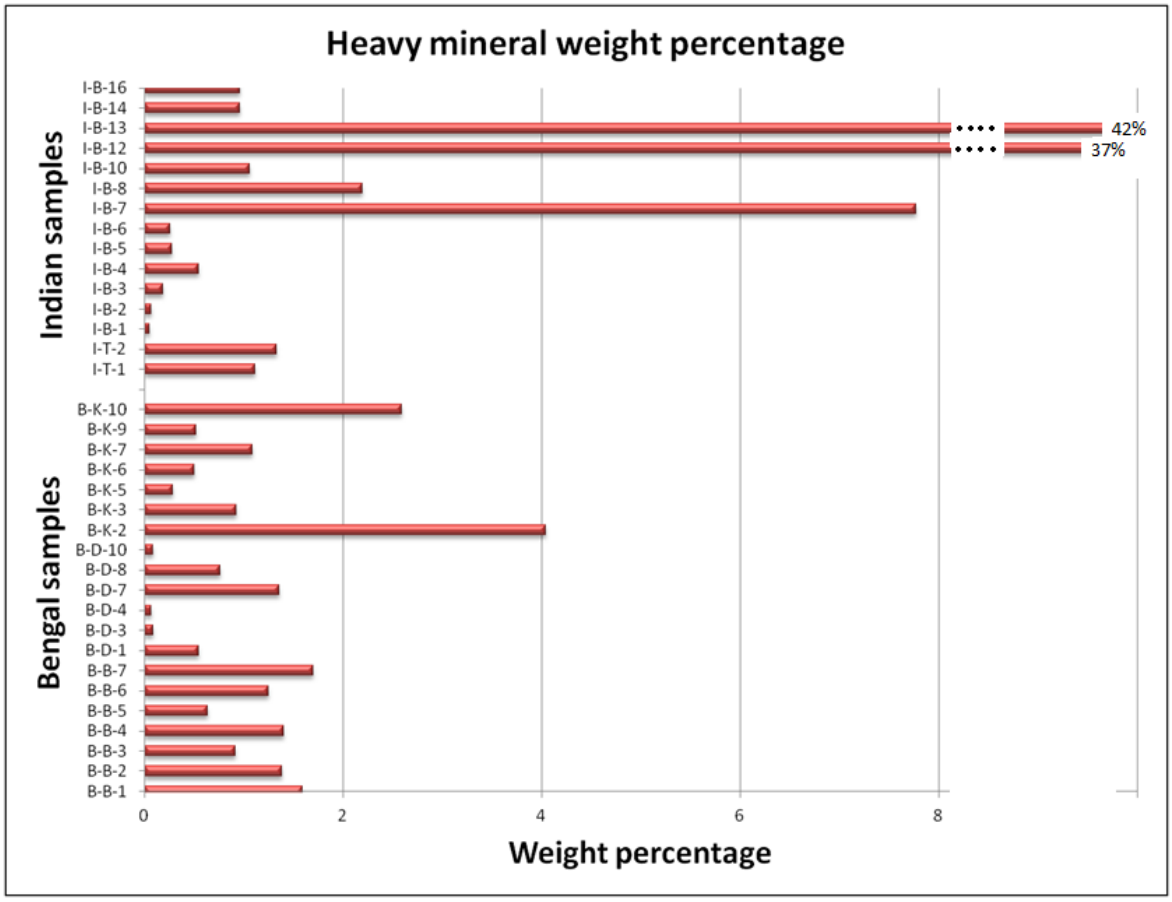

Figure 4.1 Heavy mineral weight percentages in Gondwanan sandstones from India and Bangladesh.

Magnetic separation of heavy minerals was carried out using a Frantz magnetic separation in the Department of Geology and Geography at Auburn University. Five different groups (Table 4.2) were separated based on magnetic susceptibility (Hess, 1966). Separation was done by applying different slide slope angles and current values. These groups include Group-1: Strongly Magnetic (SM); Group-2 and 3: Moderately Magnetic (MM) but different current values; Group-4: Weakly Magnetic (WM); and Group-5: Poorly Magnetic (PM).

Table 4.2 Five heavy mineral grains based on different magnetic susceptibility (Hess, 1966)

Side slope 15˚				Side slope 5˚	
Strongly magnetic	Moderately magnetic		Weakly magnetic	Poorly magnetic	
Hand magnet	0.4 Amps	0.8 Amps	1.2 Amps	1.2 Amps	
Magnetite Pyrrhotite Fe-oxides	Illmenite Garnet Olivine Chromite Chloritoid	Hornblende Hypersthene Augite Actinolite Staurolite Epidote Biotite Chlorite Tourmaline (dark)	Diopside Tremolite Enstatite Spinel Staurolite (light) Muscovite Zoisite Clinozoisite Tourmaline (light)	Sphene Leucoxene Apatite Andalusite Monazite Xenotine	Zircon Rutile Anatase Brookite Pyrite Corundum Topaz Fluorite Kyanite Silimanite Anhydrite Beryl
Group 1	Group 2	Group 3	Group 4	Group 5	

Group-1 consists of strongly magnetic minerals including magnetite, pyrrhotite and Fe-oxides. This group was separated using a hand magnet. Group-2 minerals include illmenite, garnet, olivine, chromite and chloritoid. This group was seperated using a 15^{o} side slope and a 0.4-Amp current. Group 3 minerals include hornblende, hypersthene, augite, actinolite, staurolite, epidote, biotite, chlorite, and tourmaline. These were separated from weakly to poorly magnetic minerals using a 0.8-amp current and a 15º side slope. Group 4 minerals, including diopside, tremolite, enstatite, spinel, staurolite (light), muscovite, zoisite, clinozoisite, and tourmaline (light), were separated from Group-5 using a 1.2-amp current and a 15º side slope. The remaining heavy minerals were classified as Group 5 (poorly magnetic), which were not separated further due their presence in small amounts. This group includes slightly magnetic minerals, such as

sphene, leucoxene, apatite, andalusite, monazite, and xenotine, and other non-magnetic minerals like zircon, rutile, pyrite, corundum, fluorite, kyanite, sillimanite, and beryl. Separation of heavy minerals belonging to all five groups was not achieved for all samples due to the absence or rarity of minerals from certain groups.

Separated heavy minerals were sent to Spectrum Laboratories in Vancouver, WA to prepare polished thin sections. Due to budget constraints, polished thin sections were prepared from only twenty (20) samples out of thirty five (35) samples. Each of the magnetically separated heavy mineral fractions was segregated in different areas of each thin section. Identification of minerals was carried out using a petrographic microscope and the modified Fleet method (Fleet, 1926). Numbers of grains from each layer were counted and then added together to calculate the percentage of different species of heavy minerals.

4.3 RESULTS

Semi-quantitative data for heavy minerals from Permo-Carboniferous Gondwanan sediments are presented in Table 4.3 and Table 4.4. Studied sequences show diverse assemblages of both opaque and transparent heavy minerals, although only a few dominate the assemblages. Opaque minerals in the present study are mostly oxides and hydroxides of iron (e.g., magnetite, hematite, limonite and ilmenite). Although similar varieties of transparent minerals observed in both Indian and Bengal samples, there are distinct differences in relative abundances of different mineral species. Mineral assemblages in the Barakar Formation are notably different from

Bengal samples and from the Talchir Formation from the same basin. Highly stable minerals zircon, tourmaline, and rutile (ZTR) are significantly more abundant in Barakar samples than in samples from the other areas (Table 4.5).

Heavy mineral assemblages in Gondwanan sandstones from Bangladesh and India are dominated by very stable minerals, including garnet, apatite, zircon, tourmaline, rutile along with siderite, opaques and leucoxenes. Mineral assemblages in the Talchir Formation also include epidote, sphene, monazite, muscovite, biotite and barite. The Talchir Formation contains an abundance of garnet, most of which are pink or colorless and mostly angular (Fig.4.2). After garnet, apatite is the most abundant heavy mineral in this formation. Apatite grains are more rounded (sub-rounded) compared to garnet and other minerals in the samples. Tourmaline grains identified in this formation are mostly bluish, greenish or pinkish (Fig.4.2).

Table 4.3 Heavy mineral distributions in Gondwanan sandstones from Talchir and Barakar Formation, Jharia basin, India.

Sample No	I - T - 1		I - T - 2		I - B - 2		I - B - 4		I - B - 6	
Rock Unit	Talchir Formation		Talchir Formation		Barakar Formation		Barakar Formation		Barakar Formation	
Heavy minerals	No of grains	Percentage	No of grains	Percentage	No of grains	Percentage	No of grains	Percentage	No of grains	Percentage
Zircon	5	1.15	21	1.24		0.00	9	4.81		0.00
Rutile	4	0.92		0.00	4	9.09	18	9.63	5	22.73
Tourmaline		0.00	53	3.14	23	52.27	49	26.20	10	45.45
Garnet	333	76.91	1418	84.00	6	13.64	2	1.07		0.00
Apatite	48	11.09	112	6.64		0.00		0.00		0.00
Epidote		0.00	3	0.18		0.00		0.00		0.00
Amphibole		0.00		0.00		0.00		0.00		0.00
Chrome-spinel		0.00		0.00		0.00		0.00		0.00
Chlorite		0.00		0.00		0.00		0.00		0.00
Sphene	2	0.46	31	1.84		0.00	1	0.53		0.00
Monazite	4	0.92	8	0.47		0.00		0.00		0.00
Muscovite		0.00	4	0.24		0.00	66	35.29	1	4.55
Biotite		0.00	1	0.06		0.00		0.00		0.00
Xenotine		0.00		0.00		0.00		0.00		0.00
Staurolite		0.00		0.00		0.00		0.00		0.00
Barite	14	3.23		0.00		0.00		0.00		0.00
Opaques	23	5.31	37	2.19	11	25.00	42	22.46	6	27.27
Total	433	100.00	1688	100.00	44	100.00	187	100.00	22	100.00
ZTR	9	2.08	74	4.38	27	61.36	76	40.64	15	68.18

Table 4.3 (cont.) Heavy mineral distributions in Gondwanan sandstones from Barakar Formation, Jharia basin, India.

Sample No	I - B - 7		I - B - 8		I - B - 12		I - B - 13		I - B - 14	
Rock Unit	Barakar Formation		Barakar Formation		Barakar Formation		Barakar Formation		Barakar Formation	
Heavy minerals	No of grains	Percentage	No of grains	Percentage	No of grains	Percentage	No of grains	Percentage	No of grains	Percentage
Zircon	4	2.03	6	5.50	4	0.74	4	1.02		0.00
Rutile	6	3.05	20	18.35	4	0.74	4	1.02	3	6.98
Tourmaline	8	4.06	75	68.81	13	2.42	2	0.51	15	34.88
Garnet		0.00		0.00		0.00		0.00		0.00
Apatite		0.00		0.00		0.00		0.00		0.00
Epidote		0.00		0.00		0.00		0.00		0.00
Amphibole		0.00		0.00		0.00	1	0.25		0.00
Chrome-spinel		0.00		0.00		0.00		0.00		0.00
Chlorite		0.00		0.00		0.00		0.00		0.00
Sphene		0.00		0.00		0.00		0.00		0.00
Monazite		0.00		0.00		0.00		0.00		0.00
Muscovite	166	84.26		0.00	516	96.09	354	90.08	12	27.91
Biotite		0.00		0.00		0.00		0.00		0.00
Xenotine		0.00		0.00		0.00		0.00		0.00
Staurolite		0.00	2	1.83		0.00		0.00		0.00
Barite	1	0.51		0.00		0.00		0.00		0.00
Opaques	12	6.09	6	5.50		0.00	28	7.12	13	30.23
Total	197	100.00	109	100.00	537	100.00	393	100.00	43	100.00
ZTR	18	9.14	101	92.66	21	3.91	10	2.54	18	41.86

Table 4.4 Heavy mineral distributions in Gondwanan sandstones from Dighipara and Barapukuria coal basins, Bangladesh.

Sample No	B - D - 1		B - D - 4		B - D - 7		B - D - 8		B - B - 1	
Rock Unit	Dighipara		Dighipara		Dighipara		Dighipara		Barapukuria	
Heavy minerals	No of grains	Percentage	No of grains	Percentage	No of grains	Percentage	No of grains	Percentage	No of grains	Percentage
Zircon	6	3.17	2	7.14		0.00	3	0.31	14	2.44
Rutile		0.00		0.00	3	0.62		0.00	24	4.18
Tourmaline	5	2.65		0.00	3	0.62	39	3.98		0.00
Garnet	87	46.03		0.00		0.00	124	12.67	78	13.59
Apatite		0.00		0.00	67	13.87	56	5.72		0.00
Epidote		0.00		0.00		0.00		0.00		0.00
Amphibole		0.00		0.00		0.00	710	72.52		0.00
Chrome-spinel		0.00		0.00	1	0.21		0.00		0.00
Chlorite		0.00		0.00	7	1.45	2	0.20		0.00
Sphene	2	1.06		0.00	3	0.62	2	0.20		0.00
Monazite		0.00		0.00		0.00		0.00	7	1.22
Muscovite	3	1.59		0.00		0.00		0.00	1	0.17
Biotite		0.00		0.00		0.00		0.00	1	0.17
Xenotine		0.00		0.00	4	0.83		0.00	3	0.52
Staurolite		0.00		0.00	2	0.41		0.00		0.00
Baryte		0.00	4	14.29	343	71.01		0.00		0.00
Opaques & Leucoxene	86	45.50	22	78.57	50	10.35	43	4.39	446	77.70
Total	189	100.00	28	100.00	483	100.00	979	100.00	574	100.00
ZTR	11	5.82	2	7.14	6	1.24	42	4.29	38	6.62

Table 4.4 (cont.) Heavy mineral distributions in Gondwanan sandstones from Khalaspir and Barapukuria coal basins, Bangladesh.

Sample No	B - K - 3		B - K - 6		B - K - 9		B - B - 3		B - B - 6	
Rock Unit	Khalaspir		Khalaspir		Khalaspir		Barapukuria		Barapukuria	
Heavy minerals	No of grains	Percentage	No of grains	Percentage	No of grains	Percentage	No of grains	Percentage	No of grains	Percentage
Zircon	7	4.29	23	5.03	6	1.32	5	1.59	14	2.64
Rutile	3	1.84	28	6.13		0.00	3	0.96		0.00
Tourmaline		0.00		0.00		0.00	2	0.64	11	2.07
Garnet		0.00	63	13.79	307	67.77	2	0.64		0.00
Apatite		0.00	111	24.29	63	13.91		0.00	35	6.59
Epidote		0.00		0.00	22	4.86		0.00	89	16.76
Amphibole		0.00		0.00		0.00		0.00	63	11.86
Chrome-spinel		0.00		0.00		0.00		0.00		0.00
Chlorite		0.00	4	0.88	7	1.55		0.00		0.00
Sphene		0.00		0.00	39	8.61		0.00	195	36.72
Monazite	4	2.45		0.00		0.00		0.00		0.00
Muscovite	2	1.23		0.00	1	0.22		0.00		0.00
Biotite		0.00	175	38.29	3	0.66	6	1.91	1	0.19
Xenotine		0.00		0.00		0.00		0.00		0.00
Staurolite		0.00		0.00		0.00		0.00		0.00
Barite		0.00		0.00		0.00	2	0.64		0.00
Opaques & Leucoxene	147	90.18	53	11.60	5	1.10	294	93.63	123	23.16
Total	163	100.00	457	100.00	453	100.00	314	100.00	531	100.00
ZTR	10	6.13	51	11.16	6	1.32	10	3.18	25	4.71

Table 4.5 Relative abundances (in percent) of heavy mineral suites in Gondwanan sandstones from Bangladesh and India.

Heavy minerals	Talchir Formation	Barakar Formation	Dighipara Basin	Khalaspir Basin	Barapukuria Basin
Zircon	1.20	1.76	2.66	3.55	2.22
Rutile	0.46	8.95	0.16	2.66	1.71
Tourmaline	1.57	29.33	1.81	-	0.90
Garnet	80.46	1.84	14.67	27.19	4.74
Apatite	8.86	-	4.90	12.73	2.20
Epidote	0.09	-	-	1.62	5.59
Amphibole	-	0.03	18.13	-	3.95
Chrome-spinel	-	-	0.05	-	-
Chlorite	-	-	0.41	0.81	-
Sphene	1.15	0.07	0.47	2.87	12.24
Monazite	0.70	-	-	0.82	0.41
Muscovite	0.12	42.27	0.40	0.48	0.06
Biotite	0.03	-	-	12.99	0.76
Xenotine	-	-	0.21	-	0.17
Staurolite	-	0.23	0.10	-	-
Barite	1.62	0.06	21.33	-	0.21
Opaques	3.75	15.46	34.70	34.30	64.83
Total	100.00	100.00	100.00	100.00	100.00
ZTR	3.23	40.04	4.62	6.21	4.84

Eight (8) samples of the Barakar Formation were used for heavy mineral analysis. Heavy minerals identified from these samples are zircon, rutile, tourmaline, garnet, muscovite, hornblende, sphene, staurolite, barite, siderite, and opaques and leucoxenes. The overall most abundant heavy mineral in Barakar Formation is siderite. The abundance siderite in the Barakar Formation has significantly increased the overall heavy mineral content (Fig. 4.1). However, these siderites may not be detrital, thus excluded from the normalized data chart.

ZTR content is very high (average = 40.04%) in Barakar sandstones compare to other areas. Among ZTR, tourmaline is the most abundant followed by rutile and zircon. High percentages of mica (muscovite) also are observed in this formation (Fig. 4.3). Garnet contents are very low compared to the Talchir Formation and Bangladesh samples. Only eight (8) grains of garnet were identified from the studied Barakar sandstones.

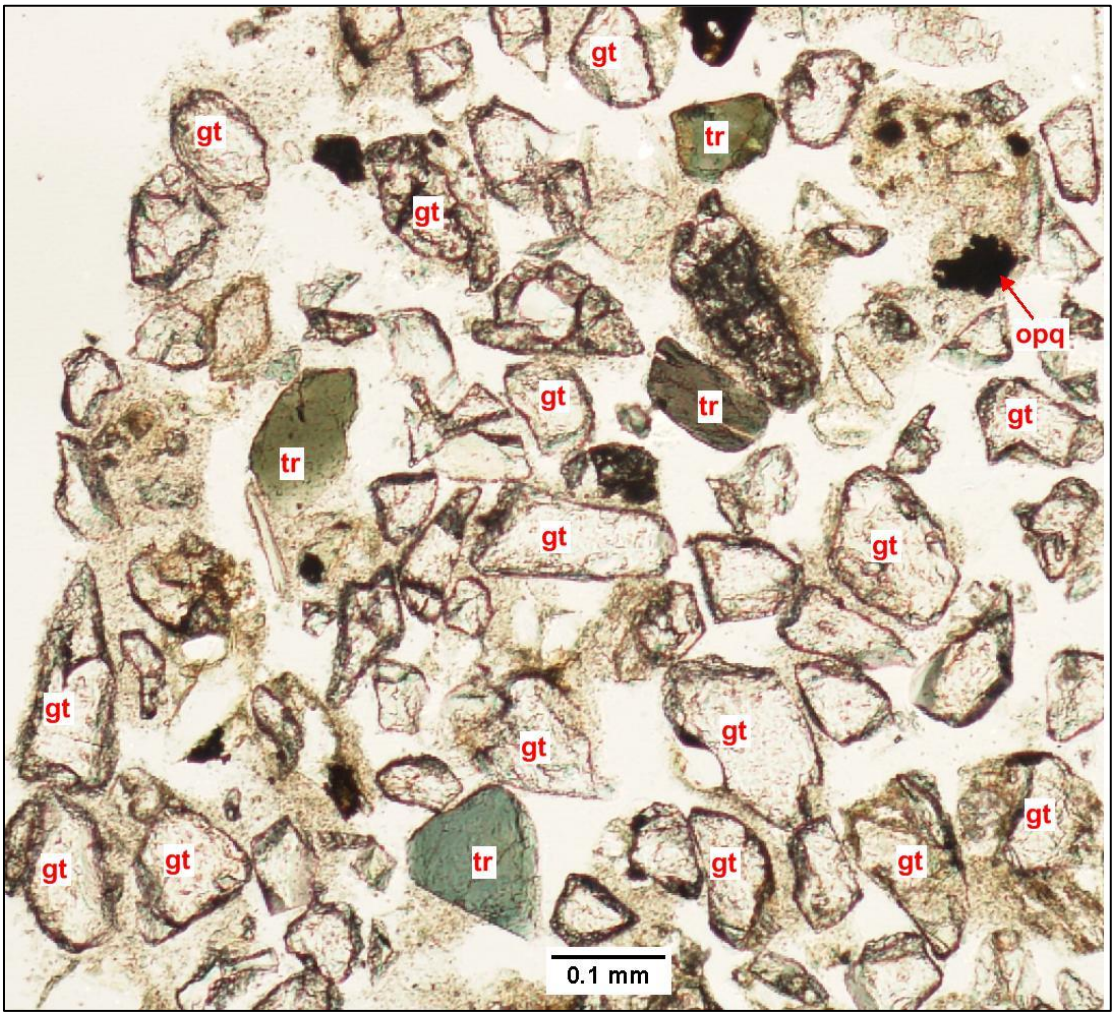

Figure 4.2 Representative photomicrograph of heavy mineral assemblages in sandstone from Talchir Formation (sample – I-T-2), Jharia basin, India (gt - garnet, tr – tourmaline, opq – opaque grains).

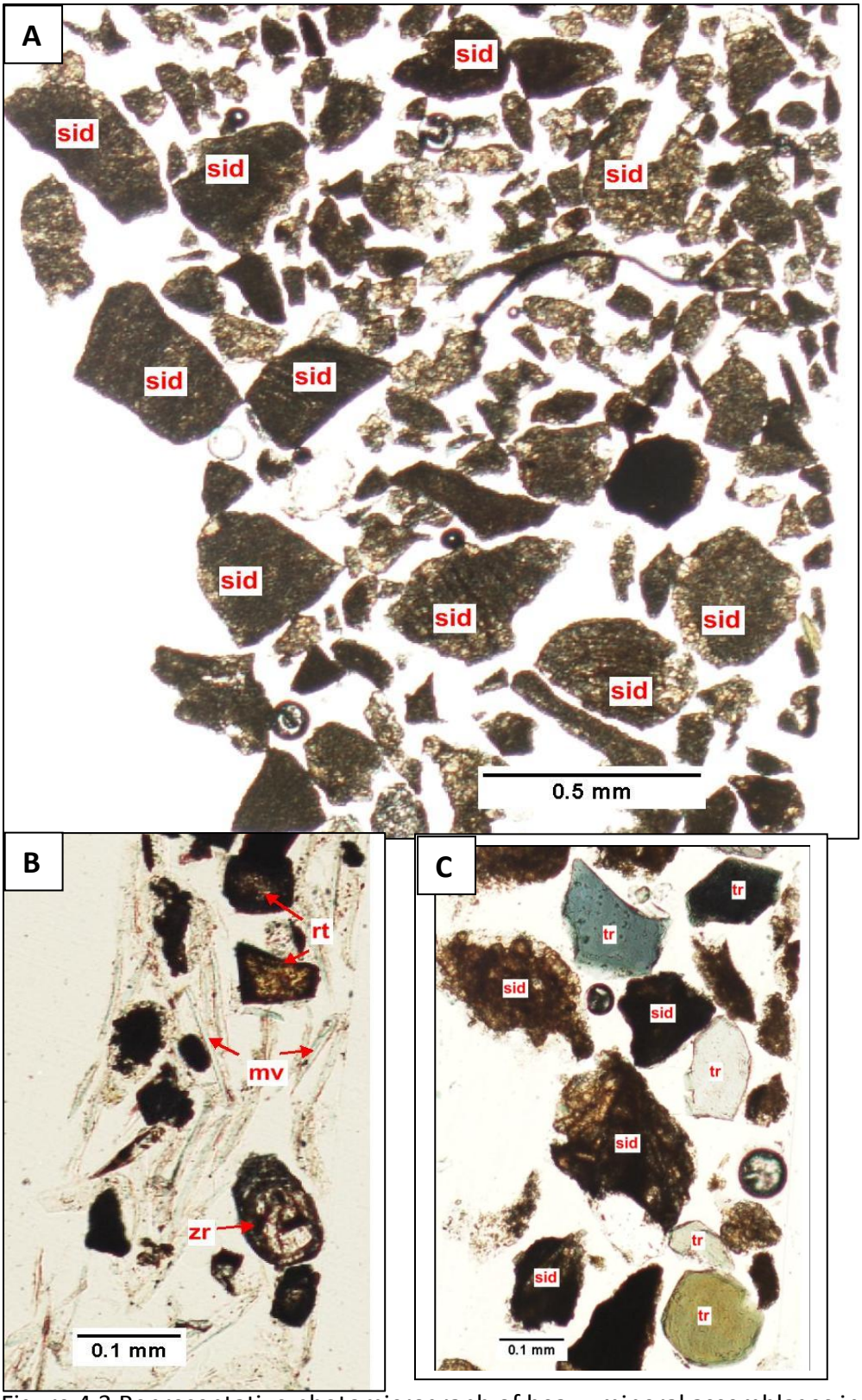

Figure 4.3 Representative photomicrograph of heavy mineral assemblages in sandstone from Barakar Formation (samples, A. - I-B-13, B. - I-B-4, C. - I-B-8), Jharia basin, India (sid - siderite, tr – tourmaline, rt – rutile, zr – zircon, mv – muscovite).

Dighipara samples from northwest Bangladesh have the lowest heavy mineral contents among the studied sandstones. A sharp contrast in heavy mineral abundance is observed in this area compared to the others. Four (4) sandstone samples were studied from this coal basin for heavy mineral analysis. Heavy mineral suites identified from this basin include opaques and leucoxenes, barite, amphibole, garnet, apatite, zircon, tourmaline, sphene, chlorite, muscovite, xenotine, rutile, staurolite, and chrome-spinel, in order of most to least abundant. One sample (B-D-8) shows very high amphibole content (72.52%), which is very uncommon in other Gondwanan sandstones; e.g., only one amphibole grain was identified from the Barakar Formation. Amphibole grains are mainly hornblende angular and elongate (Fig. 4.4-A) shape indicate limited transport from the source. Barite content (an average of 21.33%) is also significantly high. Among the four studied samples, two of them contain relatively higher percentages of garnet, while the other two do not contain any garnet. Changes in garnet abundance may be due to change in source terranes.

Heavy mineral assemblages in Barapukuria samples include leucoxene, sphene, epidote, garnet, amphibole, zircon, apatite, rutile, tourmaline, biotite, monazite, opaques, barite, xenotine, and muscovite, in order of decreasing abundance (Fig. 4.4-C). Opaque minerals are relatively rare in Barapukuria samples but leucoxene is common. Barapukuria samples contain high percentage of sphene (average of 12.24%) and epidote (average of 5.59%), both of which are rare in sandstones from other areas.

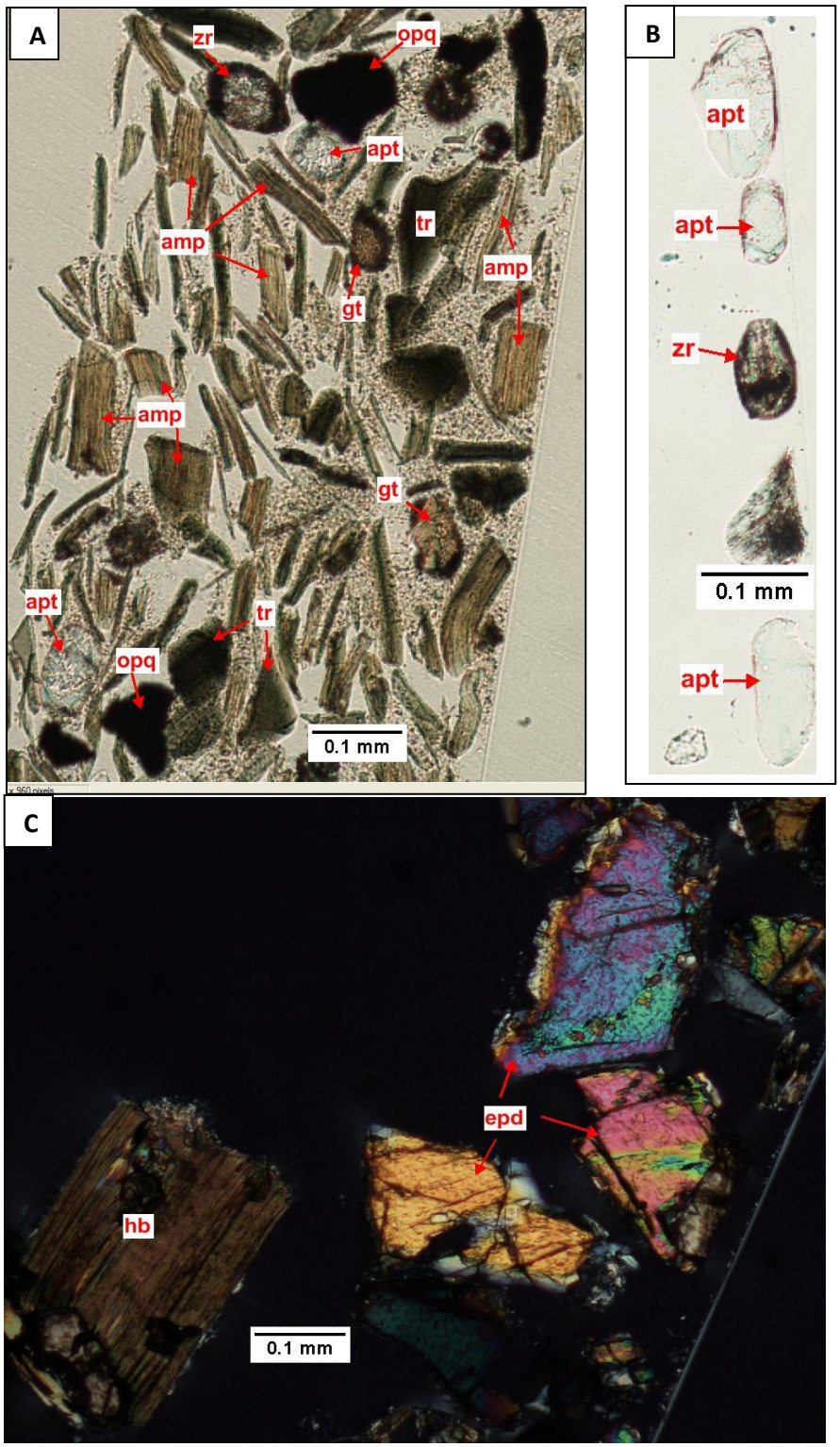

Figure 4.4 Representative photomicrograph of heavy mineral assemblages in sandstone from Dighipara (samples, A and B: B-D-8) and Barapukuria coal basin (sample, C: B-B-6), (amp-amphibole, apt-apatite, gt-garnet, epd-epidote, opq-opaque, hb-hornblende, zr – zircon).

Three (3) sandstone samples from Khalaspir coal basin (drill core GDH-45) were used for semi-quantitative heavy mineral studies. Among the most stable minerals (ZTR), zircon is more abundant than rutile and tourmaline was absent. Garnet is abundant (27.19%), compared to other Bengal samples and Barakar sandstones. Most of the garnet grains are angular and exhibit fractures and inclusions. These sandstones also contain significant amounts of biotite, which is uncommon in other areas.

Figure 4.5 Representative photomicrograph (cross nickle in 10X zoom) of heavy mineral assemblages in sandstone from Khalaspir basin, Bangladesh (epd - epidote, apt - apatite).

4.4 PROVENANCE

Heavy mineral assemblages consisting of ultrastable (zircon, tourmaline, rutile), stable (garnet, apatite, epidote) and unstable (hornblende) grains indicate different source rocks. Although Bengal and Indian samples have similar types of mineral assemblages, distinct differences in relative abundances of certain heavy minerals indicate differences in source materials. The majority of the heavy minerals are angular, indicating proximal source(s). However, some subrounded to rounded grains indicating distal source(s). Studies of paleo-currents for the Gondwanan sediments suggest a northerly or northwesterly paleo-slope direction. The Shingbhum craton, which is located at the southern boundary of these basins, might be a possible source. Other possible sources could be located in the Antarctica (Prydz Bay and/or Rayner province of East Antarctica), which was then amalgamated with India. The Kuunga orogen formed due to collision between Australia and East Antarctica, also may have contributed as a source terrane.

Garnet dominates in all of the studied Gondwanan sediments except for the Barakar Formation in Jharia basin (Fig. 4.6). Variations of garnet abundances in vertical sequences also are observed, and these may reflect changes in source rock. The Barakar sandtone contains the least amount of garnet but the highest percentage of tourmaline (Figs. 4.6 and 4.7). In contrast, The Talchir sandstones have the highest garnet contents but very low tourmaline contents (Figs. 4.6 and 4.7). This negative correlation between garnet and tourmaline content in Gondwanan sediments from different areas indicates

differences in source rocks rather than changes in other components such as depositional settings, climatic conditions etc.

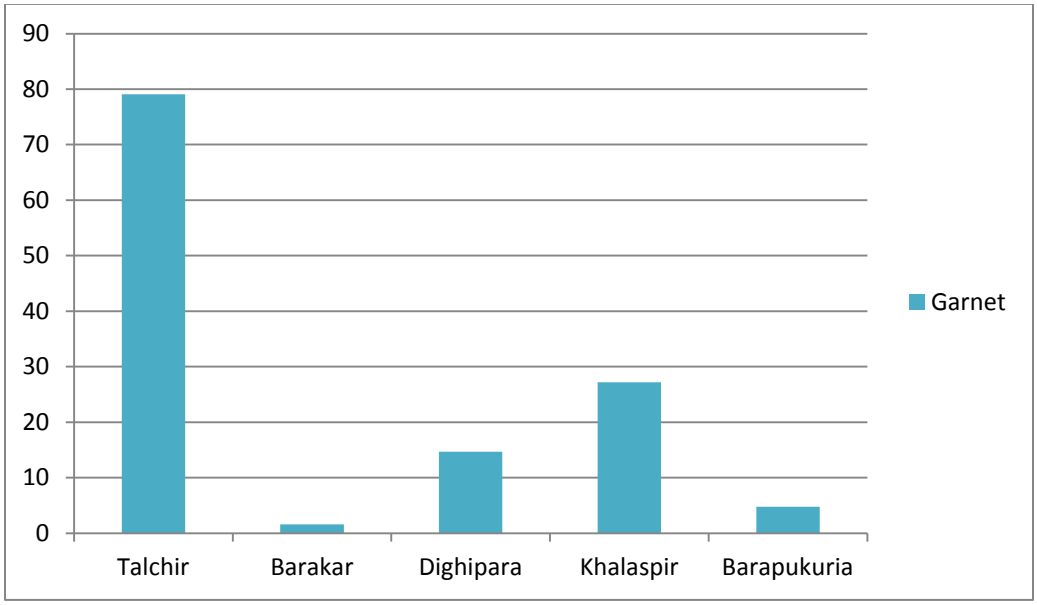

Figure 4.6 Variation in distribution of garnets among Gondwanan sandstones from India and Bangladesh.

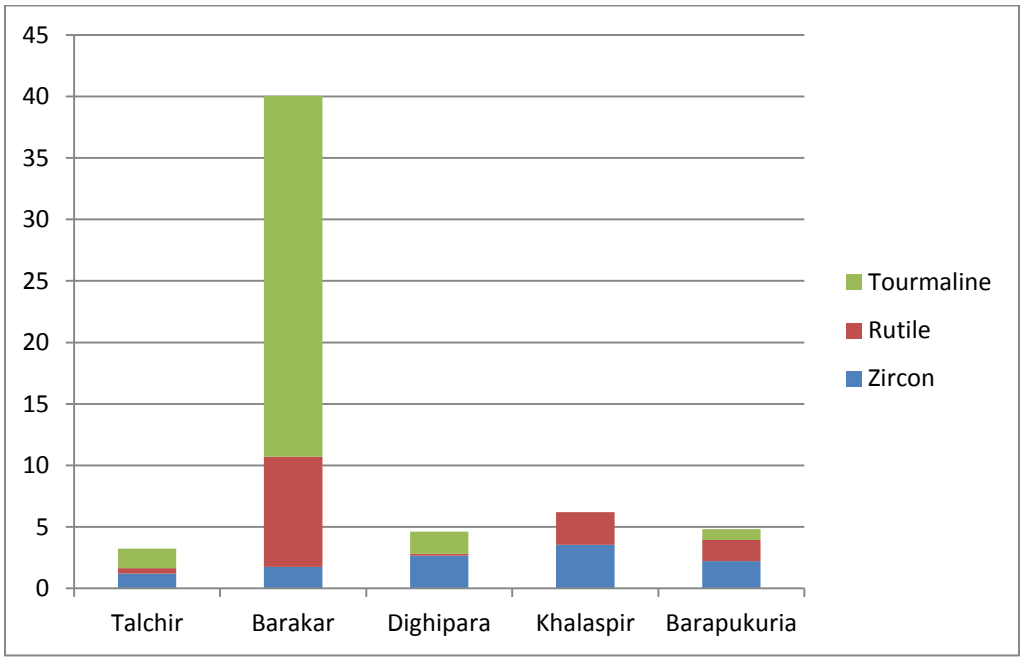

Figure 4.7 Distribution of highly stable minerals (ZTR) in sandstone from different Gondwanan units and basins in India and Bangladesh.

The 'ZTR index' (which is the combined percentage of zircon, tourmaline, and rutile among the transparent heavy minerals) is a useful tool to quantify mineralogical maturity in heavy mineral suits (Hubert, 1962). Calculated ZTR indices indicate that the Barakar sandstone is more mature than the other studied samples (Fig. 4.7). The Talchir sandstones are the least mineralogical maturity based on ZTR index (Fig. 4.7).

According to Morton and Hallsworth (1994), determining proportions of stable minerals with similar hydraulic behaviors provides a clearer picture of the nature of source terrane than conventional heavy mineral analyses. Ratios of highly stable mineral indices also suggest variations in sources among the studied basins. Barakar sandstones samples plot in discrete areas on the GZi to ATi, RZi to ATi, and MZi to ATi crossplots (Figs. 5.8, 5.9, and 5.10).

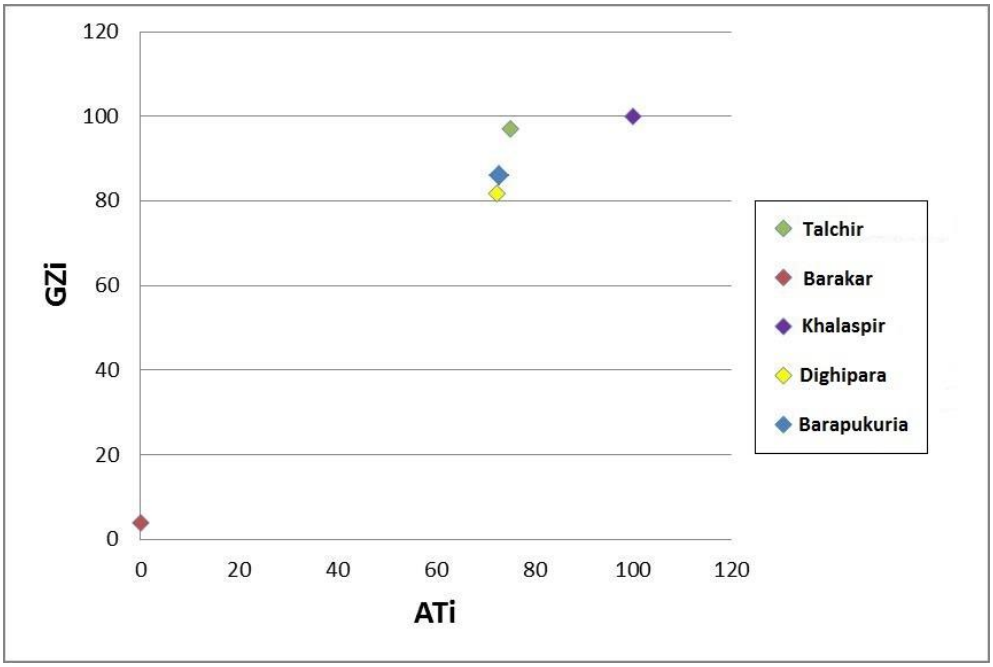

Figure 4.8 Plotted ATi (apatite, tourmaline) versus to GZi (garnet, zircon) indices of Gondwanan sandstones from different basins.

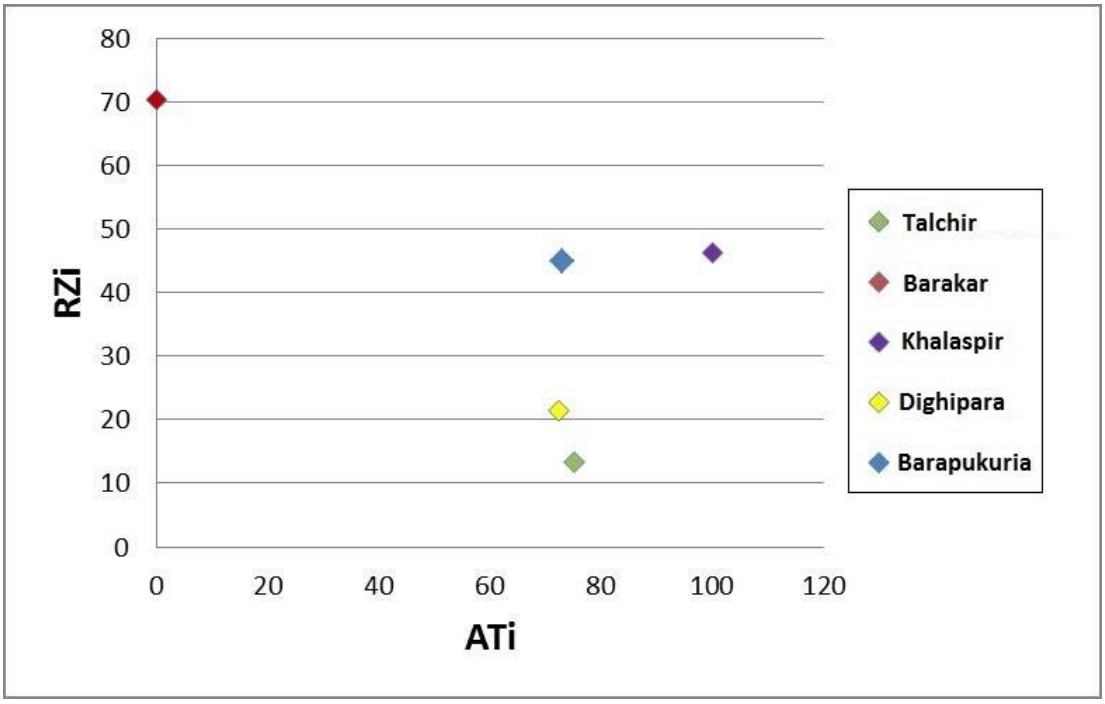

Figure 4.9 Plotted ATi (apatite, tourmaline) versus to RZi (rutile, zircon) indices of Gondwanan sandstones from different basins.

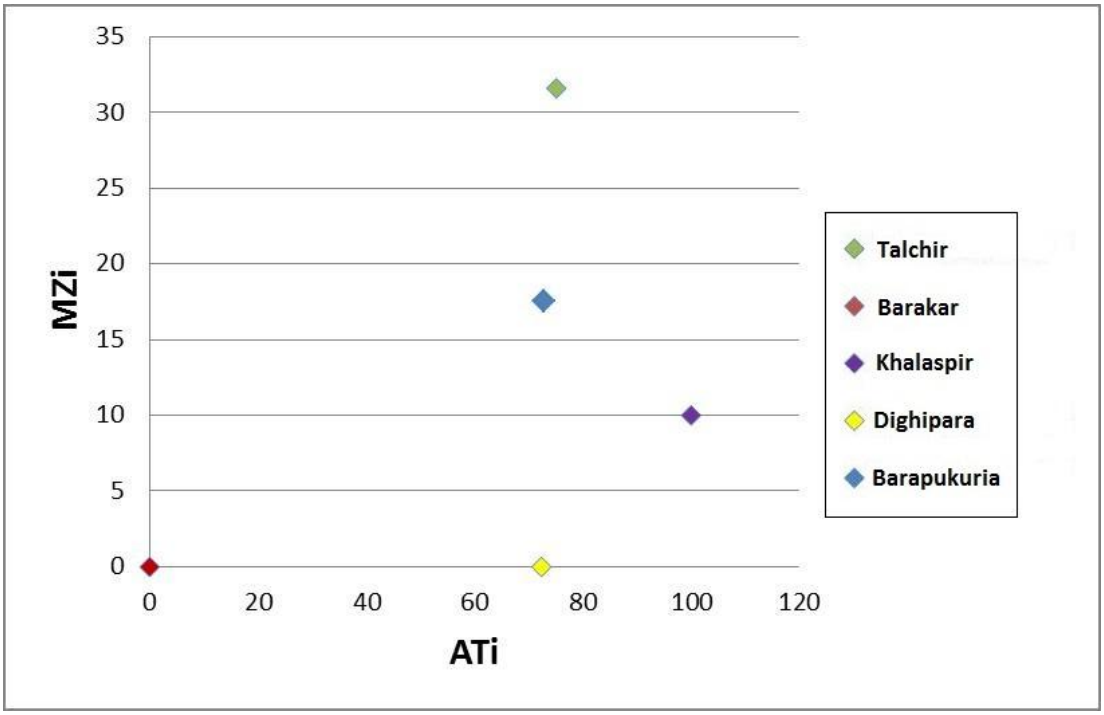

Figure 4.10 Plotted ATi (apatite, tourmaline) versus to MZi (monazite, zircon) indices of Gondwanan sandstones from different basins.

CHAPTER 5: MICROPROBE ANALYSES

5.1 INTRODUCTION

Studies of heavy mineral suits can be used as a powerful tool to decipher provenance information from sandstones. However, density and stability (both chemical and mechanical) variations among different heavy minerals may obscure the signature of the source. Reliability of provenance interpretation can be increased greatly by eliminating or reducing these variations in the heavy minerals. Density and stability of a specific mineral species are relatively homogeneous. Thus, varieties of key minerals present in a sedimentary unit are independent of influences such as hydrodynamic sorting and diagenesis. Hence, they can provide a more reliable guide to provenance than the simple presence, absence or relative abundance of different mineral species.

Electron microprobe is commonly used for chemical analysis of single mineral grains. The advancement of the electron microprobe made it possible to determine the compositional variations in a particular species of heavy mineral accurately and quickly. Studies of mineral chemistry using electron microprobe provide more detail information on source rock than the conventional petrographic studies of heavy mineral assemblages. This is also an effective method to study detrital opaque minerals.

Mineral chemistry of some specific minerals can be utilized to discriminate source rock types. Garnet chemistry can help differentiate grades of metamorphic source rocks, whereas tourmaline chemistry can aid in distinguishing plutonic rock types in the source terrane (Henry and Guidotti, 1985; Henry and Dutrow, 1990). Different

types of mafic igneous rocks can be distinguished using single grain chemistry of chrome-spinel.

Mineral chemistries of selected heavy minerals were analyzed to constrain provenance(s) of Permo-Carboniferous Gondwanan sediments from India and Bangladesh.

5.2 MINERAL CHEMISTRY

Some specific heavy minerals, like garnet, tourmaline, chrome-spinel, and amphibole have been used by several workers to determine provenance of sediments (Henry and Guidotti, 1985; Morton, 1985; Henry and Dutrow, 1990; Morton and Taylor, 1991; Nanayama, 1997; Kumar, 2004; Zahid, 2005; Rahman, 2008).

In this project, three mineral groups (garnet, tourmaline, and chrome-spinel) were used for microprobe analysis. Compositional variations in their mineral chemistry can be used to discriminate various source rocks (Henry and Guidotti, 1985; Morton, 1985; Henry and Dutrow, 1990; Morton and Taylor, 1991; Nanayama, 1997).

Garnet is commonly found in a variety of metamorphic rocks, as well as in plutonic igneous rocks, pegmatites, and some volcanic igneous rocks (Mange and Maurer, 1989). The chemical formula of garnet is $[X_3Y_2(SiO4)_3]$; where X is replaced by bivalent cations like Fe^{2+}, Mg^{2+}, Ca^{2+}, or Mn^{2+}, and Y is replaced by trivalent cations like Al^{3+}, Fe^{3+} or Cr^{3+}. The specific cations in the garnet structure can be related to the type of source rocks. The ratio of $(Fe^{2+} + Mg^{2+})/(Ca^{2+} + Mn^{2+})$ in the garnet structure increases

with the degree of metamorphism in the metamorphic source terrane (Sturt, 1962; Nandi, 1967).

Tourmaline can be found in various rock types as a common accessory mineral (Henry and Guidotti, 1985). The general formula of tourmaline is $XY_3Z_6(BO_3)Si_6O_{18}(OH)_4$; where X is occupied by Na^+, Ca^{2+}; Y is occupied by Mn^{2+}, Fe^{2+}, Al^{3+}, Li^{2+}, Mg^{2+}; and Z is occupied by Al^{3+}, Cr^{3+}, Mn^{2+}or Mg^{2+} (Deer et al., 1992). Tourmaline occurs in granites, granite pegmatites, and in contact- or regionally metamorphosed metamorphic rocks (Mange and Maurer, 1989). End-member calculations of tourmaline chemistry can help in distinguishing source rock types. Several workers have used Al-Fe(tot)-Mg and Ca-Fe(tot)-Mg plots for provenance analysis (e.g., Henry and Guidotti, 1985; Henry and Dutrow, 1992; Kumar, 2004; Zahid, 2005; Rahman, 2008; Sitaula, 2009; Alam, 2011).

The general structural formula of chrome-spinel which can be expressed as $[XY_2O_4]$; where X-site is usually occupied by Fe^{2+}, Mg^{2+}, Ca^{2+}, or Mn^{2+} and Y-site is occupied by Al^{3+}, Cr^{3+}, Ti^{4+}or Si^{4+} (Dick and Bullen, 1984). End members for chrome-spinel can be calculated based on cation occupancy in these X and Y sites and are useful in discriminating different types of mafic and ultramafic rocks in provenance studies (Irvine, 1974, 1977; Dick and Bullen, 1984).

5.3 SAMPLE PREPARATION

Polished thin sections prepared for conventional heavy mineral study were also used for microprobe studies. The preparation process is described in the heavy mineral section (chapter 4). To remove contamination (e.g., from fingerprints), polished thin

sections were washed carefully with detergent before microprobe analyses. Conduction of the electron beam was ensured by carbon coating all the thin sections.

5.4 ELECTRON MICROPROBE

The electron microprobe (EPM) provides a complete micron-scale quantitative chemical analysis of solids. This method utilizes characteristic x-rays excited by an electron beam incident on a flat surface of the sample. If the electron beam hits the surface of grains it responses in two different ways. Some of the beam electrons will be scattered backward. These backscattered electrons carry information about chemical composition of the grain. Backscattered electrons are a result of multiple elastic scattering and have energies between 0 and E_0 (the beam energy). When the electron beam hits the sample, it loses some energy which will be received by the electrons in the outer shell of atoms of the sample. By receiving this energy, electrons in the sample become excited and jump from one shell to another and emit certain amount of energy. This emitted energy (thrown by the sample electrons) is related to chemical composition. Some secondary electrons are also mobilized by the beam through inelastic scattering. These electrons have energies in the range 0-50 eV with a most probable energy of 3-5 eV. Different detector setups are required to detect different types of signals as there are energy differences between backscattered X-rays and secondary electrons.

EPM analyses provide a complete quantitative chemical analysis of microscopic volumes of solid materials, as well as high-resolution scanning electron and scanning x-ray images (concentration maps). There are two types of scanning electron images:

backscattered electron (BSE) images and secondary electron (SE) images. BSE images show compositional contrast, while SE images show enhanced surface and topographic features.

A JEOL JXA 8600 microprobe at the University of Georgia microprobe lab was used for this study. The probe is automated by Geller Micro analytical laboratory dQANT automation and uses an accelerating voltage of 15 K. V. and a beam current of 15 nanno amps. Both natural and synthetic standards were used to calibrate the data.

Standard Intensity Calibration:

Appropriate standards were chosen to obtain standard X-ray intensities of the substances measured during microprobe analysis. Different standards were used for different substances. Secondary standards were analyzed as unknowns to check if their known compositions are reproduced. A analytical conditions (e.g., accelerating voltage, beam current, etc.) were maintained throughout the session.

The standards used for this analysis are listed in Table 5.1. Most of them come from the C. M. Taylor Corp. The USNM standards come from the National Museum of Natural History, a branch of the Smithsonian Institution. This study used two synthetic standards obtained from the University of Oregon microprobe lab, and an almandine standard obtained from the Harvard Mineral Museum. Calibration for each analytical session was checked using the Kakanui Hornblende (USNM) and Pryope #39 (C. M. Taylor) standards.

Table 5.1 Electron microprobe standards used for this study.

Electron Microprobe Standards			
Element	Standard	Source	Comment
Cr	Chromite#5	C M Taylor Corp	
Mn	Spessartine#4b	C M Taylor Corp	
TiO2	Rutile	C M Taylor Corp	
Ca	Sohene# 1A	C M Taylor Corp	
Fe	Hematite# 2	C M Taylor Corp	Used for oxide (spinel) analysis
Fe	Syn. Fayalite Ol-11	Univ. of Oregon	Used for silicate analysis
Ni	Ni metal	C M Taylor Corp	
Si	Diopside 5A	C M Taylor Corp	Si standard for all phases except garnet
Mg	Olivine #1	C M Taylor Corp	
Al	Syn. Spinel	C M Taylor Corp	
K	Orthoclase MAD-10	C M Taylor Corp	
Na	Ameila Albite	USNM	This is a ubiquitous Na Standard
Si	Almandine	Harvard Mineral Museum oxygen standard # 112140	Si standard for garnet analyses
F	Syn. Fluoro-Phologopite	University of Oregon M-6	
Cl	Scapolite	USNM R 6600-1	

5.5 RESULTS

A total of twenty eight (28) grains (19 garnets, 5 tourmalines, 4 chrome-spinels) were analyzed to study their mineral chemistry. Owing to the absent of garnet, the Barakar Sandstone was excluded from garnet analyses. Chrome-spinels were analyzed only from Dighipara coal basin.

5.5.1 Garnet

Among the nineteen (19) garnet grains have been analyzed, seven (7) were from Barapukuria coal basin, six (6) from Talchir Sandstone, four (4) from Khalaspir basin, and two (2) from Dighipara basin. Garnet grains are abundant in Talchir Formation and all Gondwanan basins in the northwest Bangladesh contain significant amounts of garnets. Six garnet grains were identified during microscopic study of heavy mineral assemblages of the Barakar samples, but none were identified during microprobe study.

Different end members have been calculated using the data obtained from chemical analyses of garnet. These end members are plotted on different ternary diagrams (Fig 5.1 – 5.5) to evaluate variations in chemical composition. All of the grains show high almandine content. End member data plotted on the Sp+Gro-Alm-Py ternary diagram (Fig 5.1) fall in the Alm end showing high almandine content. Almandine contents range from 79.45% (sample B-K-6 from Khalaspir) to 60.56% (sample I-T-2 from Talchir), with an overall average of 68.69%. Most of the grains show high pyrope content after almandine. The other end members are grossular, spessartine, andradite, uvarovite, schrolmite-Al and NaTi garnet, in decreasing order of abundance. Pyrope

contents range from 33.80% (sample I-T-1 from Talchir) to 4.42% (sample B-B-6 from Barapukuria) and average of 20.46%. Sample I-T-2 from Talchir Formation shows the highest grossular content (18.69%) whereas sample B-K-9 from Khalaspir basin shows the lowest grossular content (0.78%). The average grossular and spessartine contents are 5.31% and 4.24%, respectively. The Py+Alm-Gro-Sp plot (Fig 5.2) shows most of the grains have high Py+Alm.

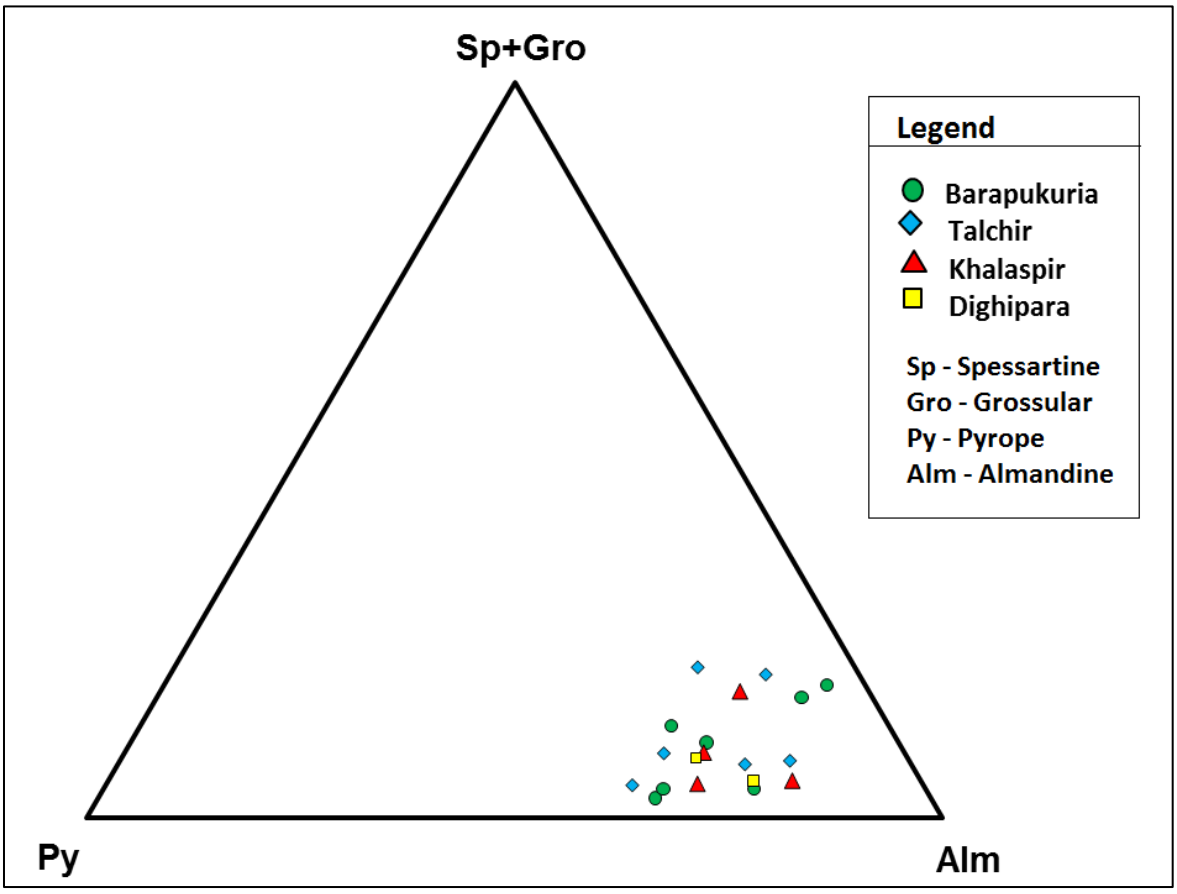

Figure 5.1 Chemical compositions of garnets from Gondwanan sequences of Barapukuria, Khalaspir, and Dighipara basins in Bangladesh and Talchir Formation in Jharia basin, India plotted on (Sp+Gro)-Py-Alm ternary diagram (adapted from Nanayama, 1997).

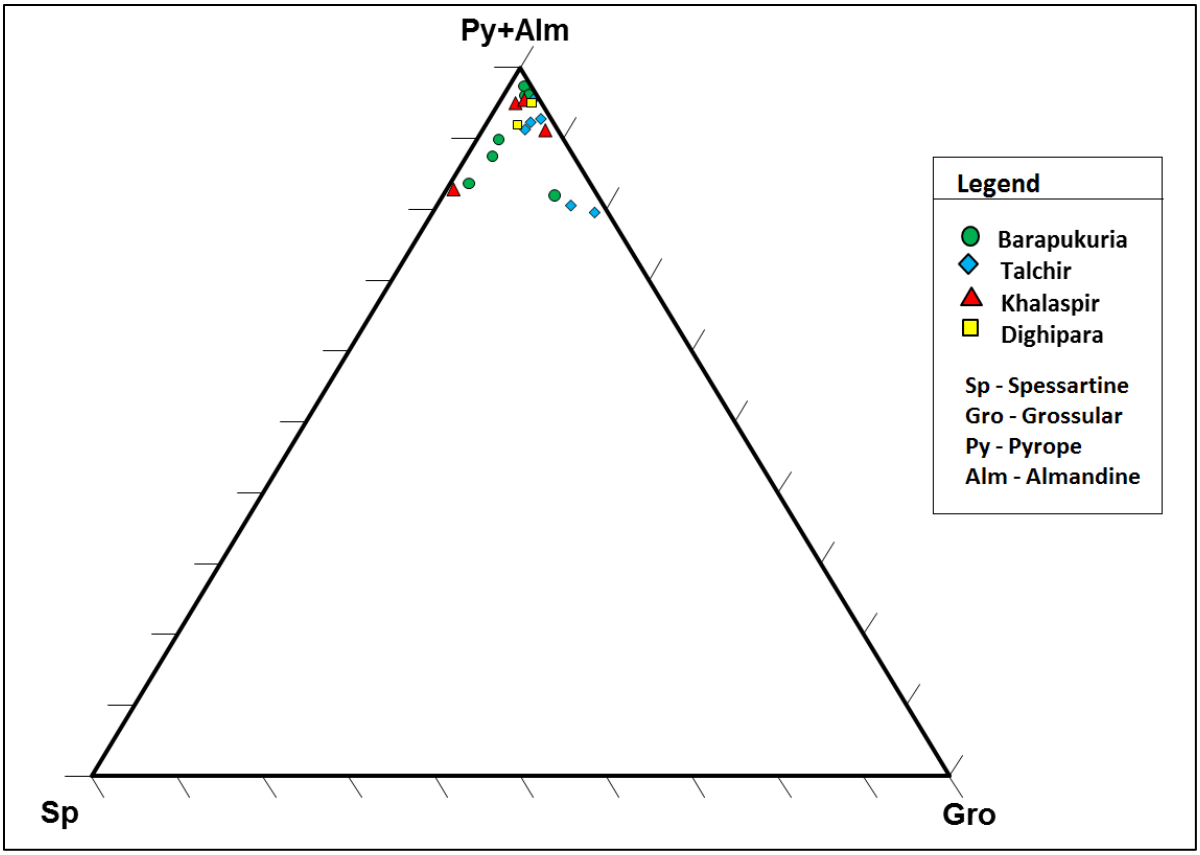

Figure 5.2 Chemical compositions of garnets from Gondwanan sequences of Barapukuria, Khalaspir, and Dighipara basins in Bangladesh and Talchir Formation in Jharia basin, India plotted on (Py+Alm)-Gro-Sp ternary diagram (adapted from Nanayama, 1997).

On the Sp-Py-Alm plot (Fig. 5.3), all analyzed grains plot either in the amphibolite facies (APF) or in the granulite facies (GNF) fields. The majority of the grains plot in the overlapping field of amphibolite facies and granulite facies. Similarly, the Gro+And-Py-Alm plot (Fig 5.4) shows that some of the grains plot in the granulite facies (GNF) field and others plot in pegmatite plus metamorphic rock (PG+Met) fields. The Alm+Sp-Py-Gro plot (Fig 5.5) shows that most of the grains fall at the Alm+Sp end within field II, which contains garnets with almandine and pyrope where grossular is less than 10%.

Only one (1) grain from Barapukuria falls within field I, which corresponds to garents with almandine and grossular where pyrope is less than 10%. Two (2) grains from the Talchir Formation fall within field III, where both pyrope and grossular content are more than 10%.

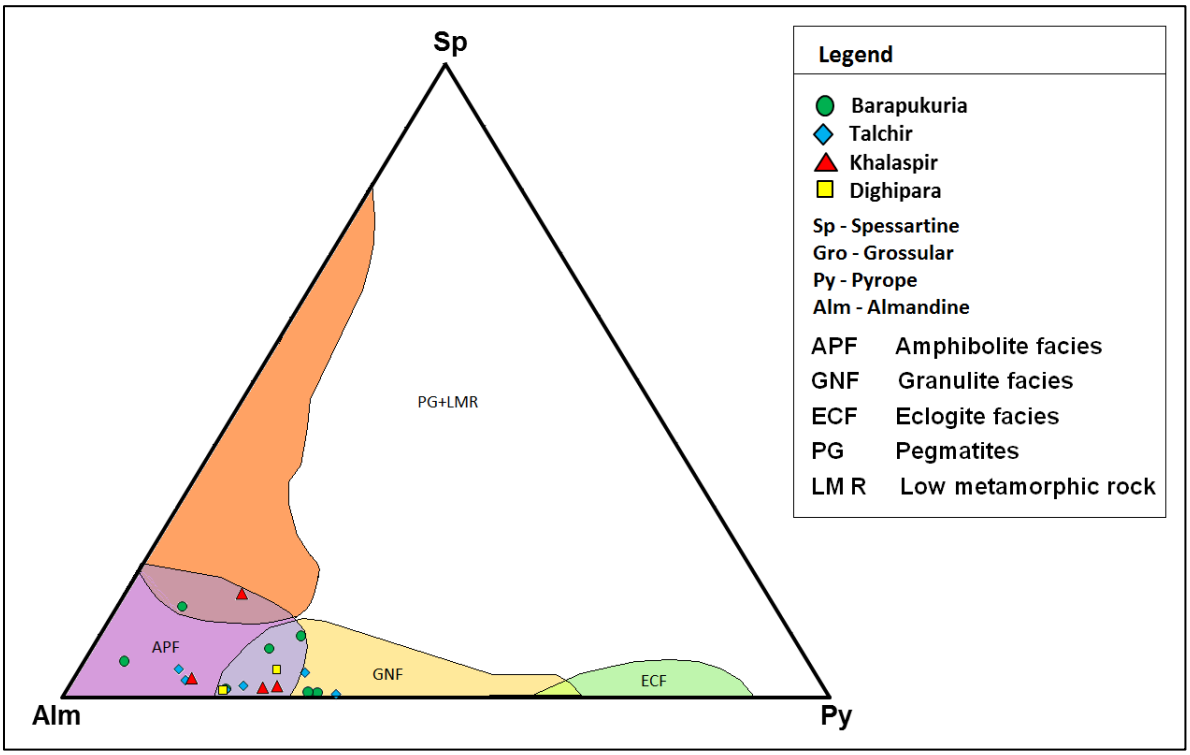

Figure 5.3 Chemical compositions of garnets from Gondwanan sequences of Barapukuria, Khalaspir, and Dighipara basins in Bangladesh and Talchir Formation in Jharia basin, India plotted on Sp-Py-Alm ternary diagram (adapted from Nanayama, 1997).

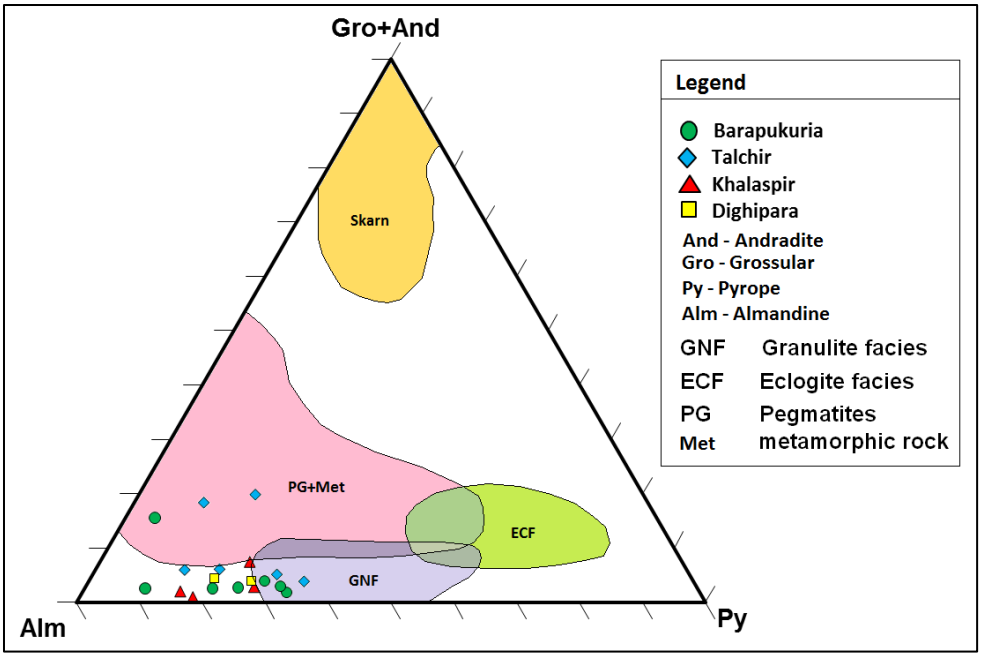

Figure 5.4 Chemical compositions of garnets from Gondwanan sequences of Barapukuria, Khalaspir, and Dighipara basins in Bangladesh and Talchir Formation in Jharia basin, India plotted on (Gro+And)-Py-Alm ternary diagram (adapted from Nanayama, 1997).

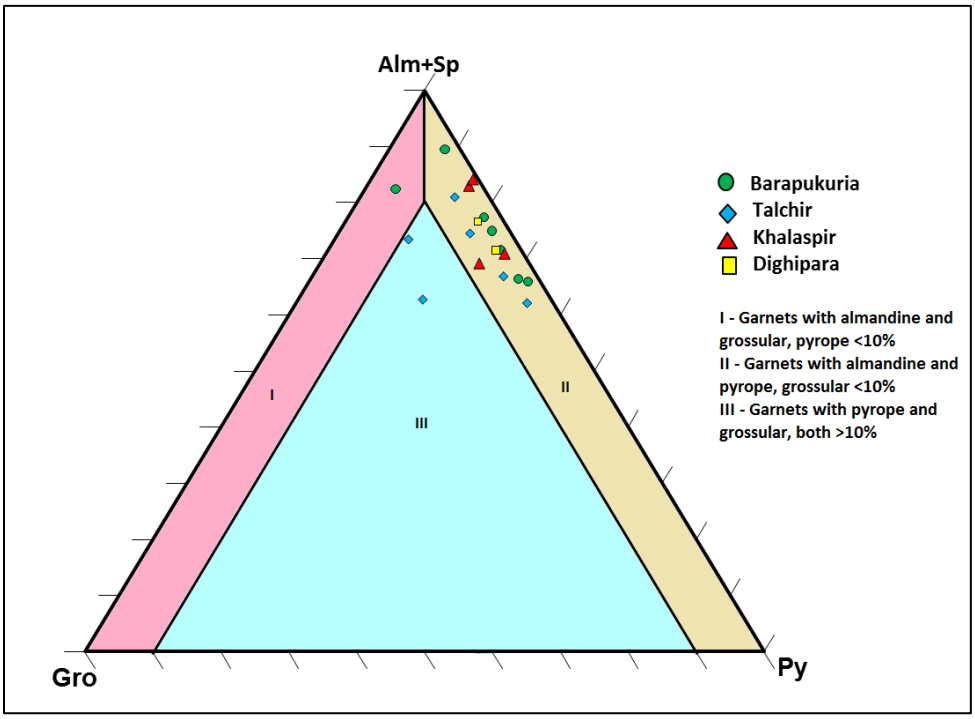

Figure 5.5 Chemical compositions of garnets from Gondwanan sequences of Barapukuria, Khalaspir, and Dighipara basins in Bangladesh and Talchir Formation in Jharia basin, India plotted on (Alm+Sp)-Py-Gro ternary diagram (adapted from Nanayama, 1997).

5.5.2 Tourmaline

The chemical structure of tourmaline is very complex. Due to significant of potential substitution in its structure, tourmaline is considered in terms of end members. End members usually are described based on their position in the schorl-elbaite or schorl-dravite series. A total five (5) tourmaline grains were analyzed; two (2) from the Talchir Sandstone, two (2) from the Dighipara basin and one (1) from the Barapukuria basin. Calculated end members are plotted on ternary diagrams Ca-Fe(tot)-Mg and Al-$Al_{50}Fe(tot)_{50}$-$Al_{50}Mg_{50}$ (Fig 5.6 and 5.7).

According to the Al-$Al_{50}Fe(tot)_{50}$-$Al_{50}Mg_{50}$ plot, all five grains fall in the Al-rich metapelite and metapsammite fields.

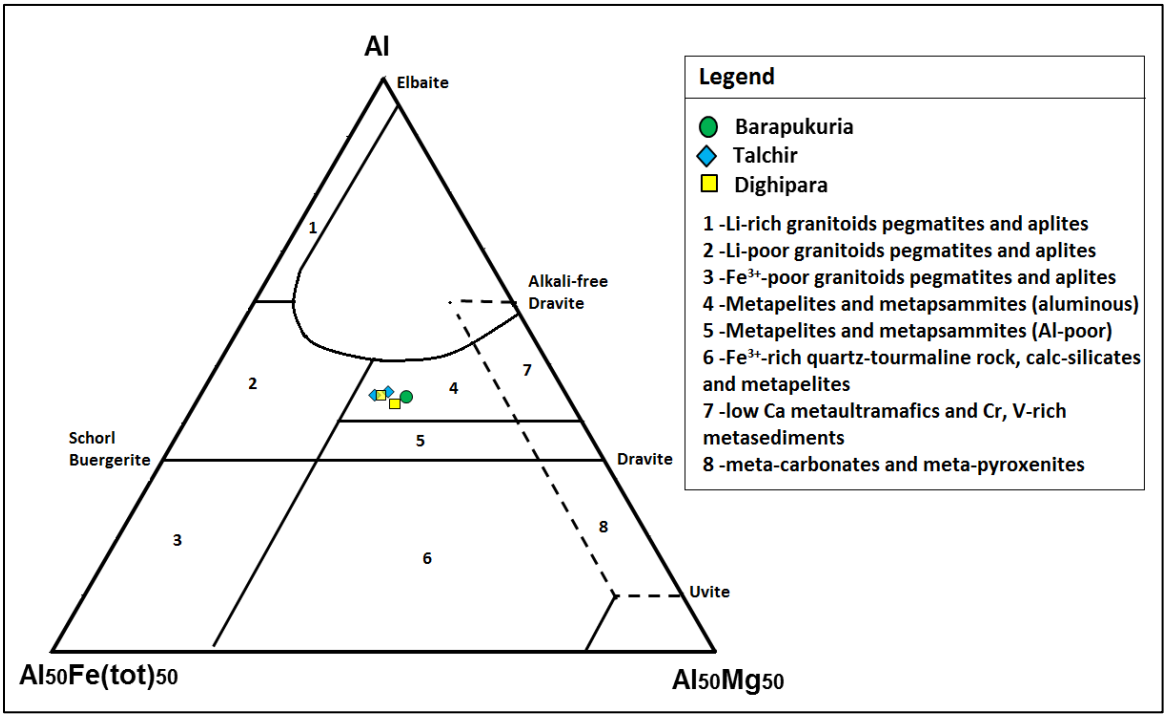

Figure 5.6 Chemical composition of tourmaline from Gondwanan sequences of Dighipara and Barapukuria basin, Bangladesh and Talchir Formation, India is plotted (in molecular proportion) on Al-$Al_{50}Fe(tot)_{50}$-$Al_{50}Mg_{50}$ ternary diagram (adapted from Henry and Guidotti, 1985).

The Ca-Fe(tot)-Mg plot (Fig 5.7) shows that all but one grain falls within Ca-poor metapelite, metapsammite, and quartz tourmaline rock fields. The exception from the Dighipara falls within the Ca-rich metapelite, metapsammite, and calc-silicate rock fields.

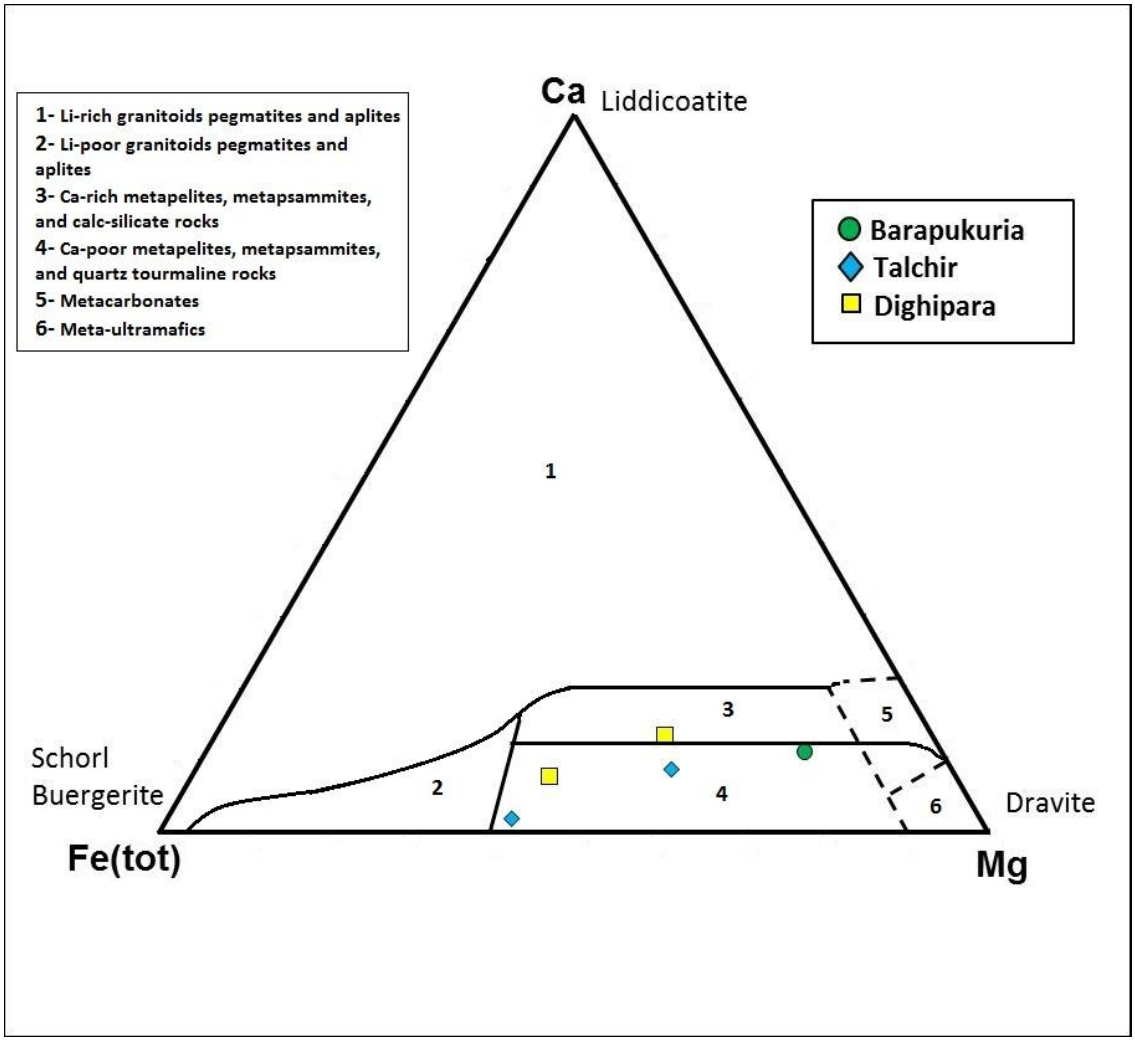

Figure 5.7 Chemical composition of tourmaline from Gondwanan sequences of Dighipara and Barapukuria basin, Bangladesh and Talchir Formation, India is plotted (in molecular proportion)on Al-Fe (tot)-Mg ternary diagram (adapted from Henry and Guidotti, 1985).

5.5.3 Chrome spinel

Four (4) grains of chrome spinel were analyzed from the Dighipara coal basin in Bangladesh. No chrome spinel grains were found from other basins during microprobe analysis. A ternary plot of Fe^{3+} -Cr^{3+}-Al^{3+} (Fig. 5.8) discriminates Alpine-type peridotites from Alaskan-type and stratiform peridotite complexes (Dick and Bullen, 1984). Alpine-type peridotites consist of over 95% harzburgite and originate as the depleted residues of partial melting. In these peridotites, Cr increases with increasing Fe^{3+}, but Fe^{3+} concentrations overall remain quite low. Both stratiform and Alaskan-type complexes generally exhibit much higher concentrations of Fe^{3+} than the Alpine-type peridotites, and greater scatter of Fe^{3+} concentrations relative to Cr concentrations.

Three major trivalent cations (Fe^{3+}, Cr^{3+}, and Al^{3+}) have been calculated from major oxide percentages. The Cr^{3+} contents are very high, whereas Al^{3+} contents are very low. The highest Cr^{3+} content is 70.34% and the lowest is 51.93% with an average of 62.82%. The highest Al^{3+} content is 13.60% and the lowest is 8.73% with an average of 11.36%. The average Fe^{3+} content is 25.82%. The Fe^{3+} -Cr^{3+}-Al^{3+} plot (Fig. 5.8) shows that grains fall within the Alaskan-type complex, close to the Cr^{3+}-end.

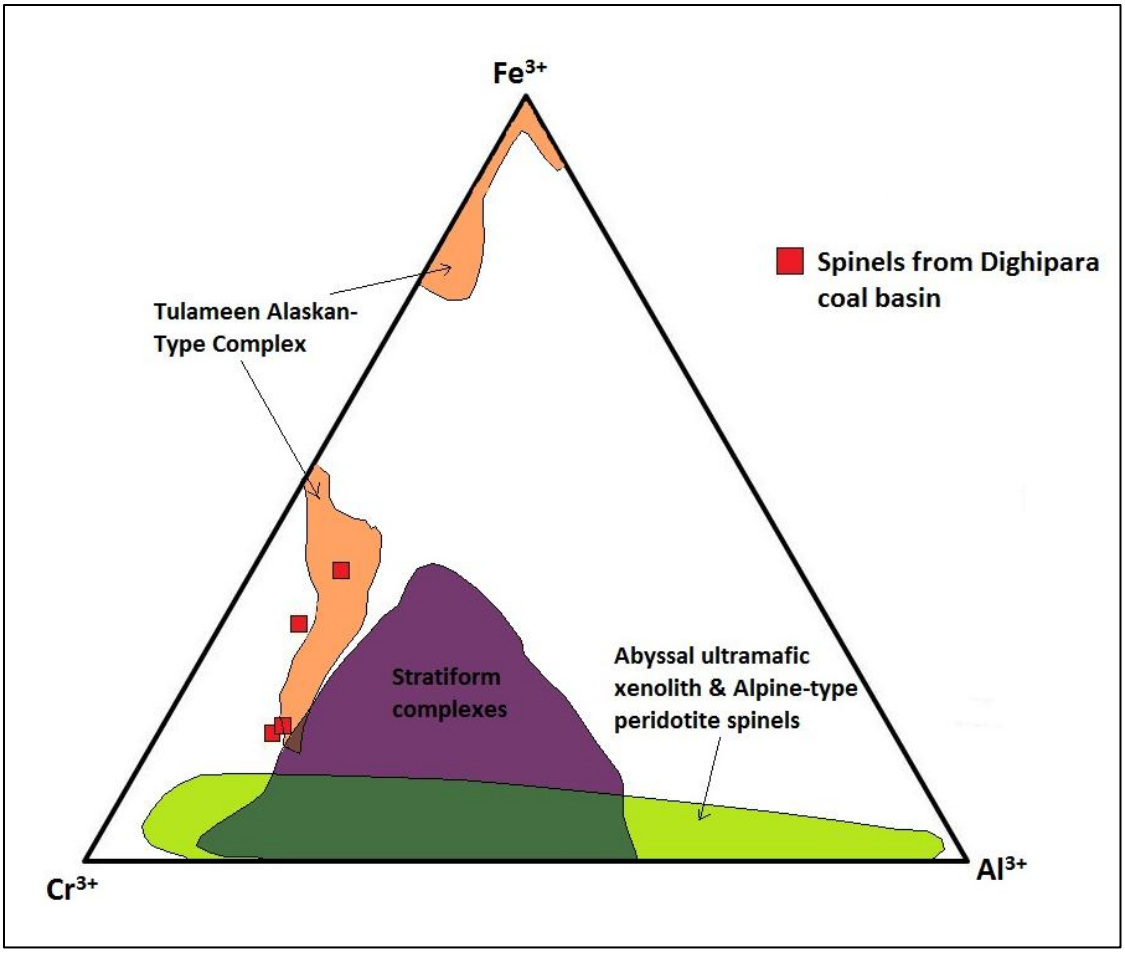

Figure 5.8 Ternary plot of major trivalent cations in chrome spinels from the Dighipara basin. Three major provenance fields have been drawn to show the data distribution (adapted from Nixon et al., 1990).

5.6 Provenance

5.6.1 Garnet

Garnets are characteristic minerals of metamorphic rocks but also can be found in some igneous rocks (Deer et al., 1992). Eight (8) different garnet species have been identified from the studied samples based on major oxide content. These are almandine, pyrope, grossular, spessartine, andradite, uvarovite, schorlomite-Al, and

NaTi garnet. All grains are almandine rich. Garnet composition suggests a mixing of source terranes. Most of the plots indicate amphibolite and granulite facies metamorphic rocks and pegmatites as source rocks.

5.6.2 Tourmaline

Compositional analyses of tourmaline suggest that aluminous metapelites and metapsammites are the probable source rocks for these minerals (Fig 5.6). The Ca-Fe (tot)-Mg plot shows that most of the grains came from Ca-poor metapelites, metapsammites, and quartz-tourmaline rocks (Fig 5.7). One (1) tourmaline grain from Dighipara shows Ca-rich metapelites, metapsammites, and calc-silicates source rocks.

5.6.3 Chrome-spinel

Microprobe data of chrome spinel shows that two of the studied grains from Dighipara basin sourced from an Tulameen Alaskan Type complex.

CHAPTER 6: WHOLE ROCK GEOCHEMISTRY

6.1 INTRODUCTION

Provenance interpretation of sedimentary suits by studying whole-rock geochemistry is well established by several workers (e.g. Bhatia, 1983; Condie et al., 1995; Cullers, 1994a, 1994b; Cullers et al., 1987, 1988; McLennan et al., 1990, 1993; Roser and Korsch, 1986, 1988; Wronkiewicz and Condie, 1987, 1990; Roy and Roser, 2013). The characteristics of detrital sediments greatly depend on various geological processes involved in four major environments/settings encountered during the sediment's entire path of denudation from the source to deposition and burial (Sageman and Lyons, 2003). These are: 1) the source area, where climate and tectonic setting might influence weathering and erosion of bed rock; 2) the transportation route, where different factors can modify the textural and compositional properties of sediments; 3) the depositional site, where different physical, chemical and biological processes constrain the amount of sediment accumulation; and 4) the conditions after deposition, where diagenesis may alter sediment characteristics further. Detrital sediments record geochemical signatures from these geological processes which can be archived for reconstructing ancient climatic conditons (McLennan et al., 1993).

Geochemical studies of sediments provide insight into the sedimentary processes affecting the rocks and may provide constraints on tectonic settings of source areas (McLennan et al., 1993). Provenance information deduced from petrographic study or other techniques can be complemented by geochemical approaches

(McLennan et al., 1993). All chemical constituents present in a source rock do not act uniformly under weathering regimes. Some get depleted early, while others remain almost constant, depending on their relative resistance. Some major oxides, such as SiO_2, Al_2O_3, K_2O (Bhatia, 1983; Roser and Korsch, 1986), some trace elements, like Zr, Th, Sc, Nb, Ga, and some rare earth elements remain constant from source to the basin due to their low solubility in water during weathering (McLennan et al., 1993; Bhatia and Crook, 1986). Hence, geochemical analyses of major oxides and trace and rare earth elements, combined with petrographical data, can help evaluate tectonic history of sedimentary provenance (Bhatia, 1985; Bhatia and Crook, 1986; Roser and Korsch, 1986; McLennan et al., 1993).

Whole-rock geochemical analyses of Gondwanan sediments from India and Bangladesh were performed in order to discriminate source rock weathering and provenance of these Permo-Carboniferous sediments.

6.2 METHODS

Fourteen (14) sandstones samples (six from Barakar, two from Talchir, three from Barapukuria, and three from Dighipara) were analyzed for whole-rock geochemistry. Samples were not used from Khalaspir basin because Roy and Roser (2013) already worked on these sediments. Samples were crushed using pestle and mortar at the Himalayan Research Laboratory (HRL), Auburn University. Crushed samples were sieved using a 200-mesh screen. Approximately 10 grams of samples (from the less than 200-mesh fraction) were sent to ACME Laboratories Limited. Forty

eight (48) parameters, including major oxides, minor elements, trace elements (rare earth and refractory elements), and precious and base metals, were analyzed from each sample. 'Inductively Coupled Plasma' mass spectrometry following lithium metaborate/tetraborate fusion and nitric acid digestion of 0.2 gm sub-samples was used for the determination of major oxides, minor elements, rare earth, and trace elements.

6.3 RESULTS

Average major, trace and rare earth elemental compositions of fourteen samples analyzed from different Gondwanan basins of Bangladesh and India are shown in Table 6.1.

6.3.1 Major Elements

Some of the major element compositions (e.g., SiO_2) of sediments, which are usually measured in the form of oxides, remain approximately the same amount as in the source rock (Bhatia, 1983; Roser and Korsch, 1986, 1988). Ratios of some oxides can be useful in provenance interpretation (Gotze, 1998, Rahman and Suzuki, 2007). Some major oxides (e.g., CaO) can be depleted during the weathering process. Hence major oxides should not be used alone to evaluate provenance. Rather, analyses should be accompanied by conventional petrographic studies and other geochemical analyses.

Table 6.1 Whole-rock chemistry of Gondwanan sediments from India and Bangladesh.

			Barakar						Talchir		Barapukuria			Dighipara		
Analyte	Unit	MDL	I-B-2	I-B-4	I-B-7	I-B-10	I-B-13	I-B-16	I-T-1	I-T-2	B-B-2	B-B-4	B-B-6	B-D-3	B-D-7	B-D-10
SiO2	%	0.01	77.42	59.19	55.39	61.04	34.76	69.93	61.59	63.93	56.57	58.60	49.59	58.73	48.43	53.17
Al2O3	%	0.01	13.10	24.76	17.65	22.36	8.57	14.20	14.73	11.16	24.09	24.87	19.14	27.53	13.48	13.25
Fe2O3	%	0.04	0.96	2.07	8.77	2.01	26.91	2.87	7.17	6.56	2.12	1.59	4.64	0.46	5.22	5.17
MgO	%	0.01	0.19	0.34	2.22	0.73	5.22	1.18	2.12	2.95	0.79	0.46	2.97	0.18	1.36	2.94
CaO	%	0.01	0.26	0.14	0.48	0.18	0.94	0.98	1.12	5.15	1.61	0.66	5.53	0.15	12.04	8.02
Na2O	%	0.01	0.02	0.07	0.07	0.06	0.04	0.05	3.19	1.44	0.08	0.10	0.57	0.02	<0.01	2.08
K2O	%	0.01	3.30	6.51	4.31	2.88	1.87	3.28	2.75	1.53	3.09	3.07	3.54	0.74	1.87	3.56
TiO2	%	0.01	0.33	1.06	0.91	1.39	0.34	0.47	0.99	0.58	0.71	0.33	0.57	0.88	0.85	0.57
P2O5	%	0.01	0.04	0.07	0.05	0.06	0.05	0.04	0.22	0.13	0.05	0.05	0.47	0.09	0.14	0.18
MnO	%	0.01	<0.01	0.02	0.13	0.04	0.35	0.05	0.11	0.14	0.04	0.03	0.09	<0.01	0.09	0.13
Cr2O3	%	0	0.004	0.023	0.018	0.022	0.015	0.011	0.012	0.011	0.017	0.014	0.005	0.006	0.147	0.002
Ni	PPM	20	<20	134	49	29	66	21	20	28	37	32	<20	<20	22	<20
Sc	PPM	1	7	16	22	11	49	8	19	13	8	6	17	11	15	8
LOI	%	-5.1	4.3	5.5	9.7	9.0	20.8	6.8	5.6	6.2	10.6	10.0	12.6	11.1	16.2	10.6
Sum	%	0.01	99.88	99.76	99.76	99.81	99.86	99.84	99.63	99.77	99.80	99.80	99.71	99.84	99.85	99.71
Ba	PPM	1	291	594	865	350	180	305	1646	549	551	611	997	264	77	1163
Be	PPM	1	<1	3	1	<1	2	2	2	<1	3	3	3	2	2	1
Co	PPM	0.2	4.3	23.1	18.0	11.0	14.1	10.0	18.3	15.3	19.1	33.0	13.6	4.6	8.8	12.4
Cs	PPM	0.1	2.8	2.9	3.8	2.4	1.9	2.5	1.3	1.2	1.0	0.6	20.4	0.4	4.1	5.2
Ga	PPM	0.5	11.3	26.0	22.0	17.6	8.3	15.2	18.9	12.0	21.2	21.1	15.7	27.9	25.7	12.9
Hf	PPM	0.1	3.6	8.5	7.0	6.8	2.1	4.7	9.4	11.6	7.5	3.8	5.8	8.4	2.2	10.3
Nb	PPM	0.1	6.0	21.9	19.9	21.5	7.1	10.9	18.6	9.8	19.8	11.3	8.4	26.0	5.6	12.6
Rb	PPM	0.1	83.7	196.4	170.0	123.5	73.3	120.2	93.7	67.8	114.1	109.0	167.6	25.0	70.3	79.3
Sn	PPM	1	5	9	5	6	7	8	6	4	23	36	12	5	4	5
Sr	PPM	0.5	14.8	119.8	55.9	50.5	22.0	56.1	190.4	185.5	78.9	73.5	363.3	53.2	106.1	179.7
Ta	PPM	0.1	0.6	1.5	1.5	1.9	0.6	1.2	1.4	0.9	1.8	1.1	0.4	2.5	0.3	0.5
Th	PPM	0.2	4.2	20.8	13.9	18.5	6.2	10.9	15.4	9.7	11.2	7.0	3.3	17.5	3.1	6.6
U	PPM	0.1	1.0	3.4	3.0	4.1	1.5	2.2	3.1	2.6	1.4	1.1	1.4	6.0	3.6	3.5
V	PPM	8	49	127	118	99	203	56	114	61	89	91	84	82	173	65
W	PPM	0.5	6.4	2.8	1.9	2.6	1.4	1.1	0.8	0.8	0.9	<0.5	0.8	6.2	2.2	1.0
Zr	PPM	0.1	129.6	302.9	250.9	270.5	81.7	177.7	352.7	447.1	236.6	118.8	247.1	300.2	77.9	408.5
Y	PPM	0.1	11.1	36.5	33.3	41.0	27.4	22.3	38.1	37.3	29.8	19.7	29.0	13.1	17.4	21.9
La	PPM	0.1	9.4	47.4	36.4	46.5	21.7	26.3	46.7	37.2	32.7	22.9	50.7	21.2	17.1	26.8
Ce	PPM	0.1	15.6	73.8	54.8	77.6	40.1	39.9	90.2	62.2	50.8	34.1	90.3	28.2	27.6	45.6
Pr	PPM	0.02	2.08	9.89	7.72	9.52	4.95	5.39	10.03	7.56	6.69	4.60	10.56	3.74	3.93	4.98
Nd	PPM	0.3	8.5	36.3	28.8	37.1	19.5	19.5	38.2	29.6	26.1	18.1	40.7	14.0	15.4	18.0
Sm	PPM	0.05	1.60	6.91	5.78	7.60	3.90	3.72	7.84	6.17	4.82	3.32	6.81	3.16	3.31	3.53
Eu	PPM	0.02	0.36	1.60	1.20	1.33	0.90	0.96	1.63	1.38	1.22	0.95	1.97	0.82	0.93	0.89
Gd	PPM	0.05	1.74	6.24	5.46	6.81	4.00	3.60	7.32	6.11	5.10	3.31	6.63	2.83	3.32	3.51
Tb	PPM	0.01	0.27	1.00	0.84	1.17	0.82	0.62	1.12	1.00	0.86	0.55	0.96	0.41	0.52	0.58
Dy	PPM	0.05	1.78	6.06	5.38	7.08	5.62	3.84	6.44	6.03	5.15	3.41	5.10	2.39	3.03	3.51
Ho	PPM	0.02	0.46	1.40	1.18	1.43	1.03	0.81	1.36	1.13	1.00	0.68	1.01	0.43	0.65	0.75
Er	PPM	0.03	1.27	3.73	3.81	4.55	3.25	2.16	4.27	3.46	3.28	2.03	2.73	1.34	1.57	2.34
Tm	PPM	0.01	0.20	0.59	0.56	0.70	0.46	0.35	0.63	0.46	0.52	0.31	0.40	0.20	0.22	0.37
Yb	PPM	0.05	1.25	4.21	3.87	4.39	3.26	2.30	4.31	3.55	3.24	2.13	2.66	1.28	1.49	2.72
Lu	PPM	0.01	0.19	0.66	0.57	0.68	0.48	0.36	0.66	0.50	0.51	0.35	0.43	0.22	0.22	0.40
TOT/C	%	0.02	0.09	0.11	1.76	0.84	6.38	1.09	0.07	1.07	0.95	0.65	0.62	0.88	3.08	1.66
TOT/S	%	0.02	0.07	<0.02	<0.02	<0.02	<0.02	<0.02	<0.02	<0.02	<0.02	<0.02	<0.02	<0.02	<0.02	<0.02

(MDL = Minimum Detection Limit)

The ratios of $\log(SiO_2/Al_2O_3)$ vs $\log(Fe_2O_3/K_2O)$ of studied sandstone samples are plotted in Figure 6.1. Most of the samples plot in highly feldspathic sandstone to wacke fields, while two other samples from the Barakar sandstone fall within the arkose and Fe-rich graywacke fields. Due to high iron content, one Talchir sample falls in Fe-sandstone area.

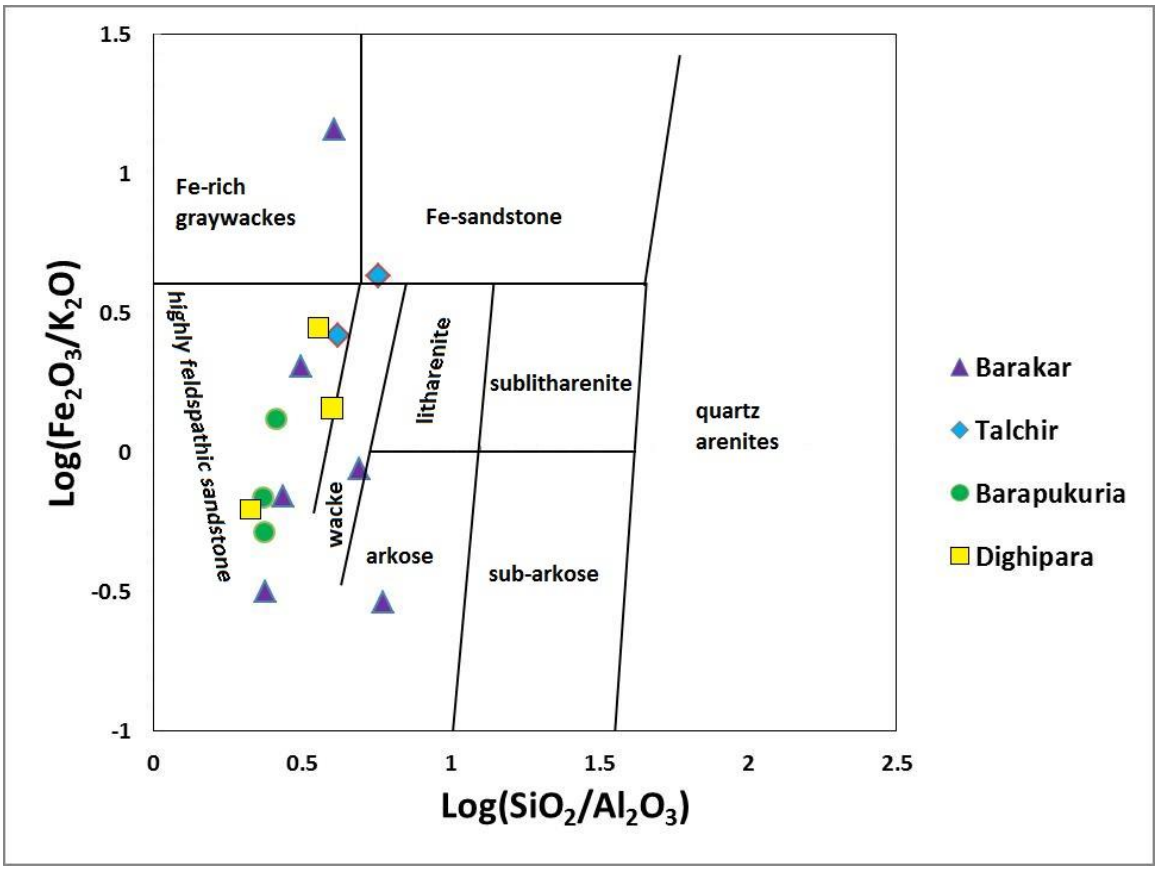

Figure 6.1 Chemical classifications of Gondwanan sandstones from India and Bangladesh (adapted from Herron, 1988).

Harker's variation diagrams of TiO_2, Al_2O_3, Fe_2O_3, MgO, Na_2O, and CaO do not show any linear correlation with SiO_2 content (Fig. 6.2). This is may be due to variations in the source terranes for these sediments.

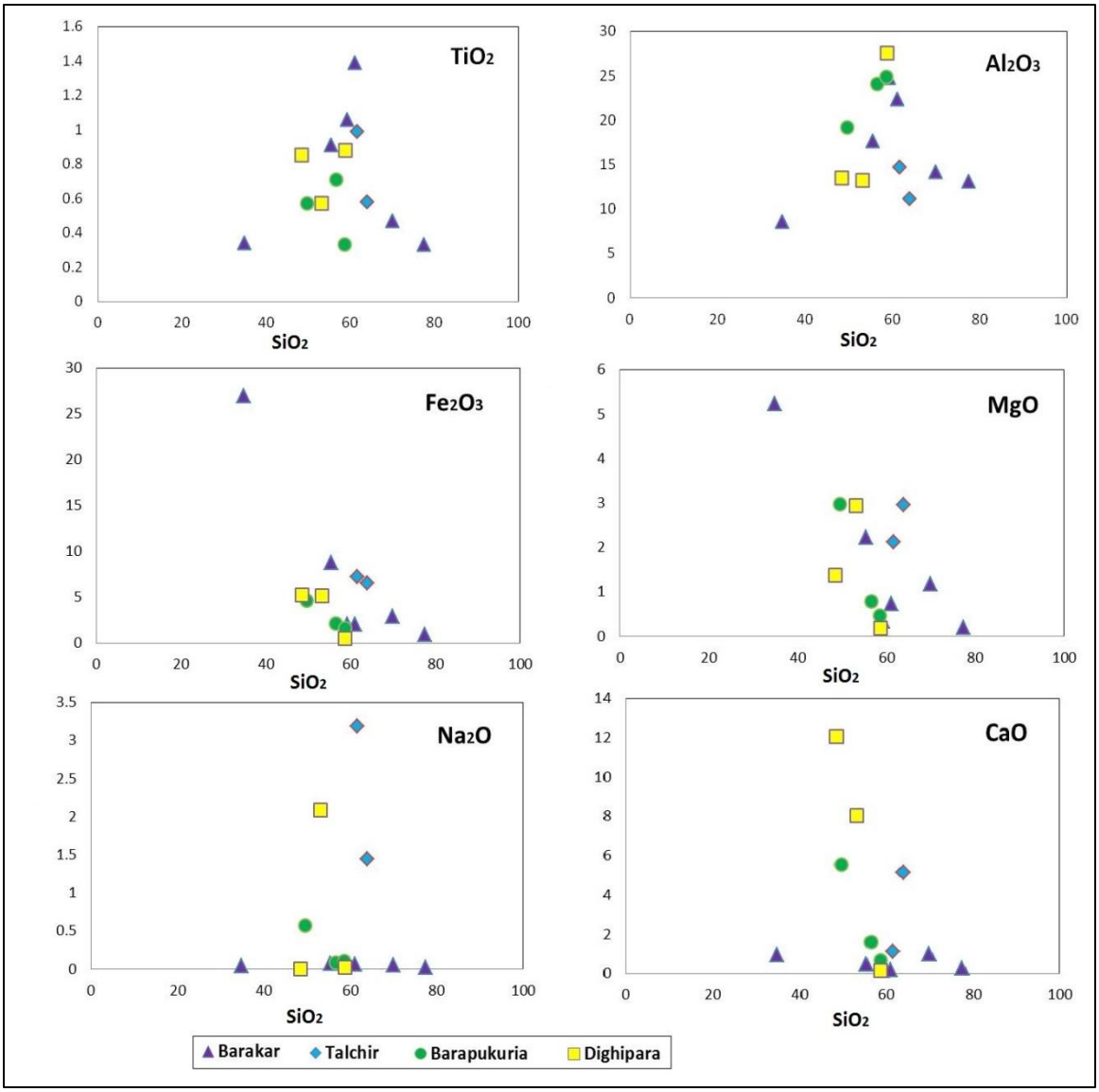

Figure 6.2 Harker variation diagrams for major oxides of Gondwanan sandstones from India and Bangladesh.

Major oxide patterns usually reflect the mineralogy of the sediments. Distribution patterns of eight major oxides are plotted in Figure 6.3. The weight percentages of oxides are normalized to PAAS (Post-Archean Australian Shales) values according to Taylor and McLennan (1985). The PAAS normalized trend of major oxides (patterns compared from Condie, 1993) suggests mixing of various sources for studied Gondwanan sediments. Even samples from same basin show variability of sources.

Major oxide composition of Talchir sandstones suggests cratonic source(s). Barakar samples show variation in sources; sample I-B-2 suggests granitic sources, samples I-B-4 and I-B-7 andesitic sources, I-B-10 cratonic shale, and I-B-13 and I-B-16 Fe-rich graywackes and graywackes, respectively (patterns compared from Condie, 1993). In contrast, Bengal samples from Barapukuria and Dighipara coal basins suggest andesitic and basaltic sources.

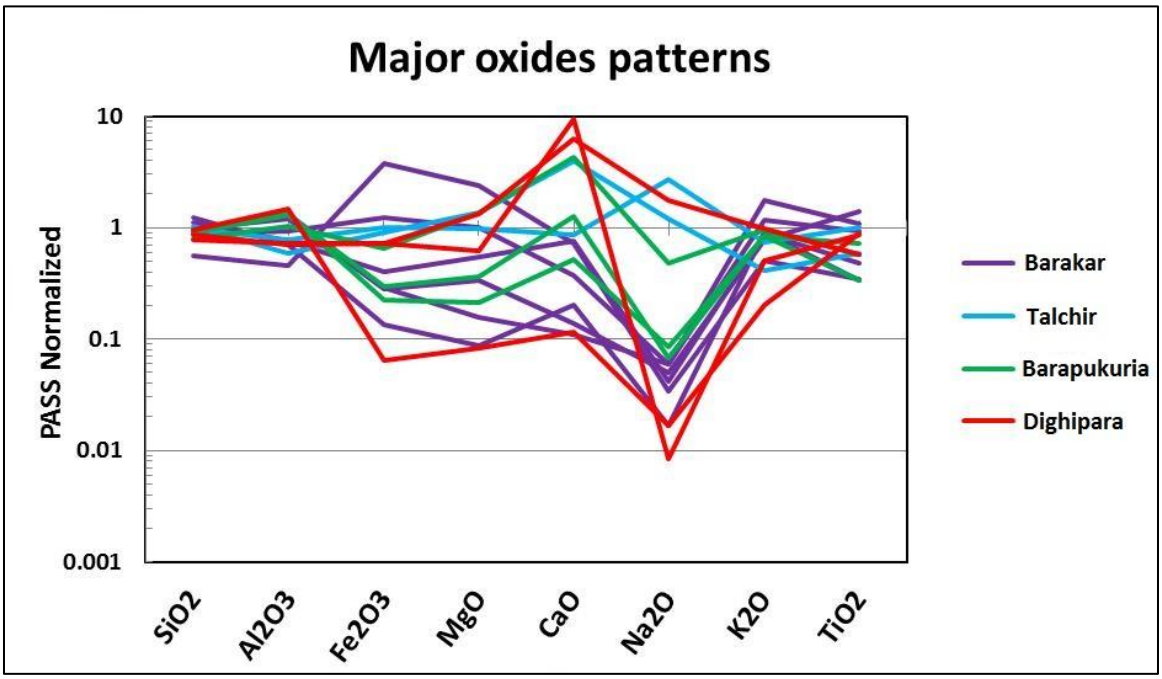

Figure 6.3 Major oxides distribution patterns in Gondwanan sandstones from India and Bangladesh. Plotted data are PAAS (Post Archean Australian Shale) normalized (Taylor and McLennan, 1995).

Indian sandstone samples have moderate silica (SiO_2) content (34.76% to 77.42% with an average of 60.41%), whereas Bengal samples show low silica content (49.59% to 58.73% with an average of 54.18%). Alumina (Al_2O_3) content in Indian samples is moderate to low while Bengal samples contain moderate to high alumina. Average Al_2O_3 content, in Barakar, Talchir, Barapukuria, and Dighipara sandstones are 16.77%, 12.95%,

22.70%, and 18.09%, respectively. CaO is very low in all of the samples from the Barakar sandstone (average of 0.5%). Significant CaO depletion in all samples indicates that most of the plagioclage feldspar was altered due to weathering (Sifeta et al., 2005).

6.3.2 Trace Elements and Rare Earth Elements

High field strength elements like Zr, Nb, Hf, Th, and Y reflect compositions of source rocks because of their immobile characteristics (Taylor and McLennan, 1985). These elements are rich in almost all studied samples, indicating felsic rather than mafic sources for these sediments. The range of chemical ratios of Gondwanan sandstones from India and Bangladesh are compared to the similar elemental ratios derived from felsic rocks, mafic rocks, and upper continental crust (Table 6.2).

Table 6.2 Range of chemical ratios of Gondwanan sandstones from India and Bangladesh (Data compared from Cullers, 1994a; Taylor and McLennan, 1985).

Range of elemental ratio	Barakar sandstone (n=6)	Talchir sandstone (n=2)	Sandstones from Barapukuria (n=3)	Sandstones from Dighipara (n=3)	Sediment from felsic sources	Sediment from mafic sources	Upper Continental Crust
La/Sc	0.44-4.23	2.46-2.86	2.98-4.09	1.14-3.35	2.5-16.3	0.43-0.86	2.21
Th/Sc	0.13-1.68	0.75-0.81	0.19-1.40	0.21-1.59	0.84-20.5	0.05-0.22	0.79
La/Co	1.54-4.22	2.43-2.55	0.69-3.73	1.94-4.61	1.80-13.8	0.14-0.38	1.76
Th/Co	0.44-1.68	0.63-0.84	0.21-0.59	0.35-3.8	0.04-3.25	0.04-1.40	0.63
Cr/Th	6.52-16.56	5.33-7.76	10.37-13.69	2.04-324.6	4.00-15.0	25-500	7.76

During fractional crystallization, major elements in silicate structures are replaced by different trace elements (Krauskopf and Bird, 1995). Transition trace elements (TTE), such as Cr, Ni, Ti, and V, replace Fe and Mg in the major oxides during the early stage of crystallization. Large ion lithophile elements (LILE), like Ba, Rb, Sr,

replace K during late stages of crystallization. TTE elements are enriched in mafic rocks, whereas LILE are enriched in felsic rocks. High field strength elements like Zr, Nb, and Hf are also rich in felsic rock. Figure 6.4 shows the distribution pattern of trace elements of Gondwanan sandstones from India and Bangladesh. Unusual patterns of trace element distribution indicate mixing of sources. Some distribution patterns indicate felsic sources but some trends indicate intermediate to mafic sources (Fig. 6.4).

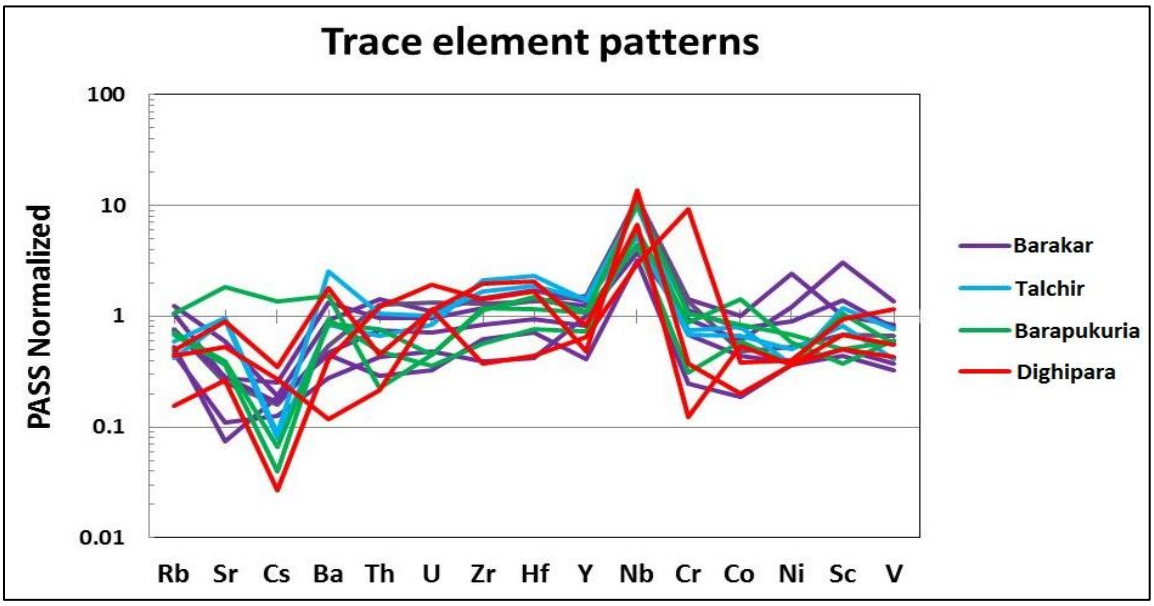

Figure 6.4 PAAS (Post-Archean Australian Shales) normalized trace element distribution patterns for Gondwanan sediments of Bangladesh and India (Taylor and McLennan, 1995).

6.4 Weathering and Diagenesis in the Source Terranes

Weathering and diagenesis in source terranes can be estimated based on chemical composition of sediments. The A-CN-K (Al_2O_3 – CaO+Na_2O-K_2O) plot in Figure 6.5 shows that most samples fall on the Al_2O_3 - K_2O line close to the Al_2O_3 end, indicating highly weathered source terranes. Talchir samples and one Dighipara sample fall close

to Upper Continental Crust (UCC) and average granite, which is indicative of low weathering regimes (Fig. 6.5).

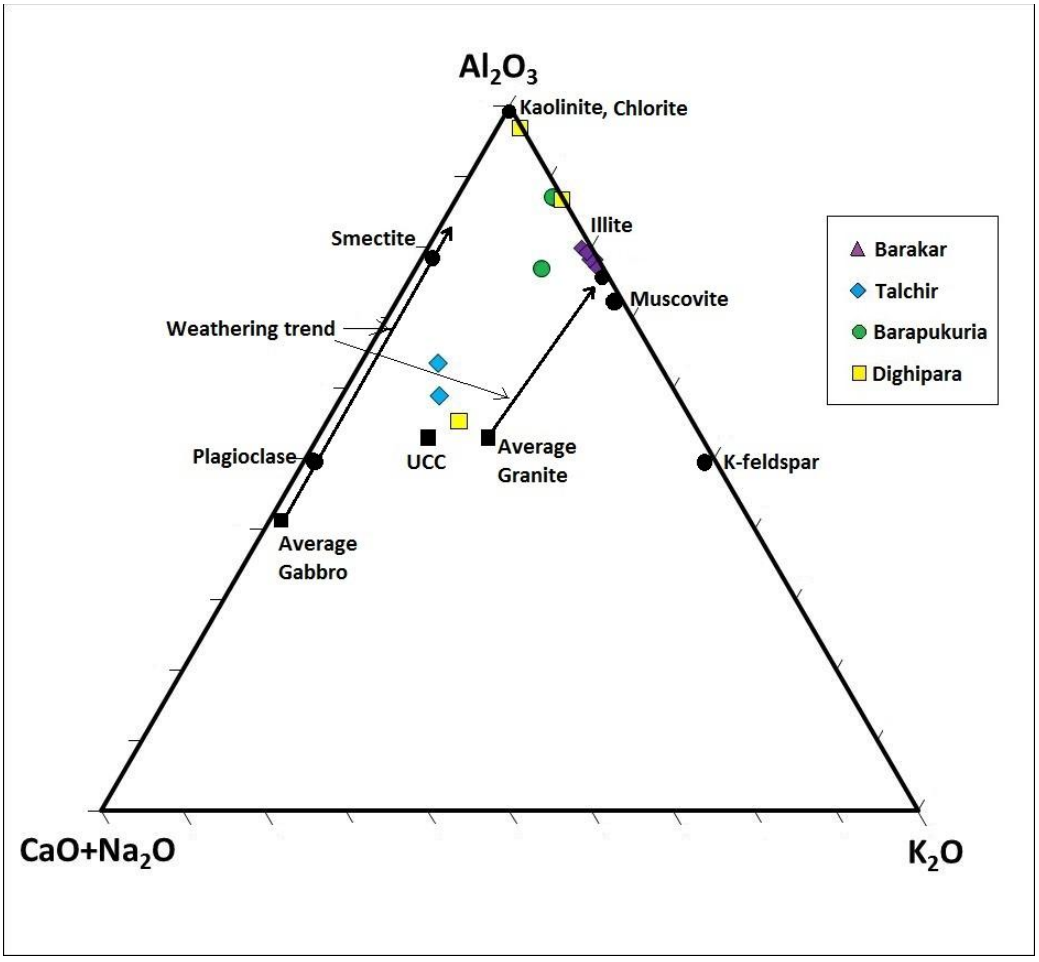

Figure 6.5 Chemical Index of Alteration (CIA) ternary plots of A-CN-K of Gondwanan sandstones from India and Bangladesh (from Nesbitt and Young, 1982, and Soreghan and Soreghan, 2007). The average composition of Upper Continental Crust is taken from Taylor and McLennan (1985). CaO is the amount of CaO present only in silicate phases.

Nesbitt and Young (1982) proposed that the Chemical Index of Alteration (CIA) can be used to evaluate intensity of weathering. The CIA is calculated by using the equation $[Al_2O_3/(Al_2O_3+CaO^*+Na_2O+K_2O)] \times 100$, where CaO* represents the amount of CaO incorporated in the silicate phase. If weight percent CaO is higher than Na_2O, then the CaO value is taken as equal to Na_2O. A high CIA value of 100 represents kaolinite and

chlorite, which is indicative of highly weathered source rocks. Very low CIA values (50 or less) indicate unweathered source, and moderate values (70-75) represent average shales (Nesbitt and Young, 1982). Most Gondwanan sandstones show intermediate to high CIA values. Exception include the Talchir samples (average of 61) and one Dighipara sample, which reflect lower CIA (B-D-10: CIA-55) (Fig 6.6). High to intermediate values of CIA in Barakar (77 – 87, on average 80), Barapukuria (77 – 87, on average 84), and the two Dighipara samples (55 – 97, on average 80) indicate intense weathering in source areas (Fig 6.6). Significant changes in various samples of Dighipara from different stratigraphic level may be due to changes in source terranes.

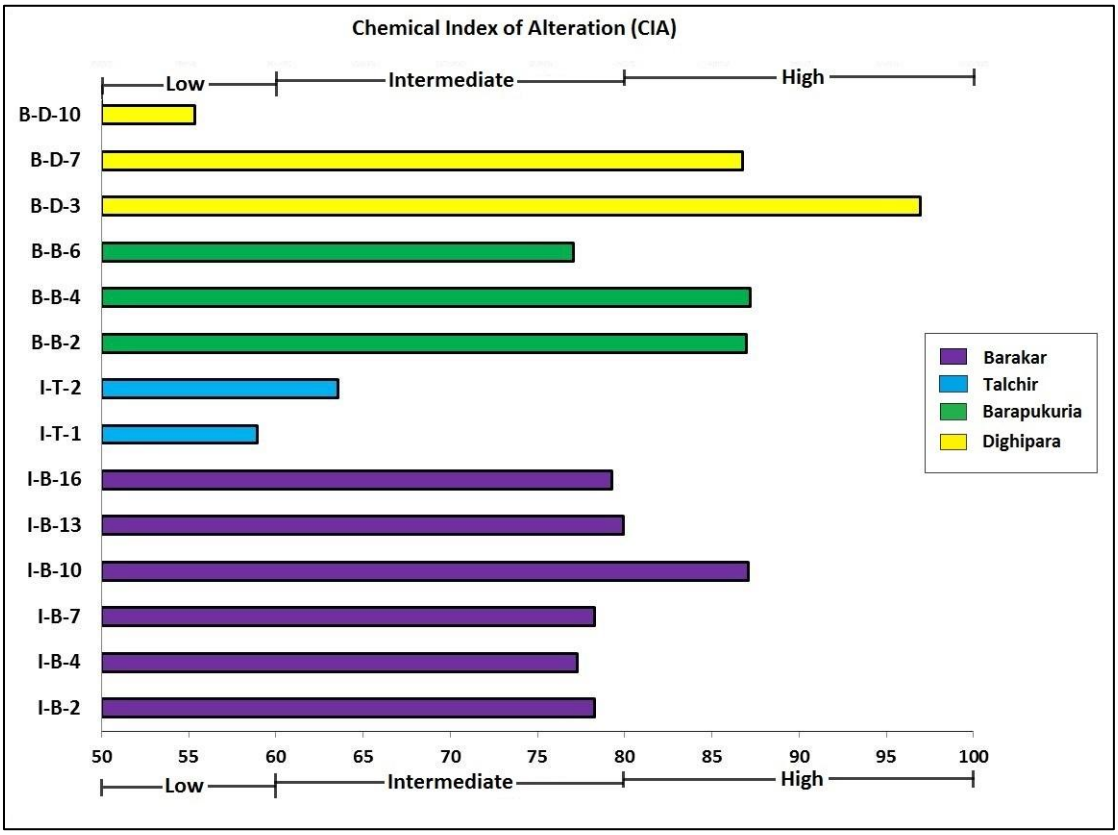

Figure 6.6 CIA values of Gondwanan sandstones from India and Bangladesh (adapted from Nesbitt and Young, 1982, and Soreghan and Soreghan, 2007).

6.5 Provenance and Tectonic Settings

Sandstones from specific tectonic regimes possess characteristic chemical compositions. SiO_2 content and K_2O/Na_2O ratios have been utilized by several workers (e.g., Roser and Korsch, 1986; Osae et al., 2006; Sitaula, 2009) to discriminate tectonic settings of the source area. The SiO_2 vs K_2O/Na_2O plot for studied samples in Figure 6.7 reflects multiple tectonic settings. Most of the samples fall in the passive- margin field. However, one Barakar sample, one Barapukuria sample, and Talchir samples fall in the active continental field. One sample from Dighipara basin falls in the volcanic arc field.

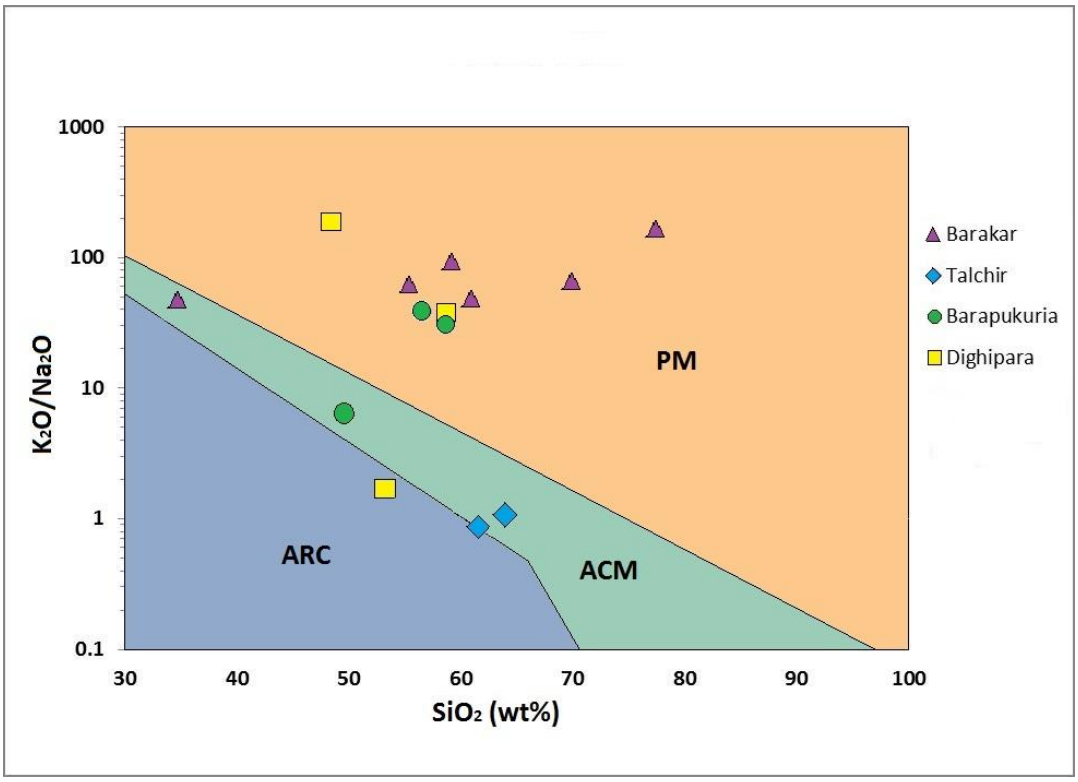

Figure 6.7 Tectonic discrimination diagram (SiO_2 vs K_2O/Na_2O) plotted from Roser and Korsch (1986). [Tectonic fields: PM – Passive Margin, ACM – Active Continental Margin, ARC – Volcanic Island Arc].

According to Bhatia and Crook (1986), trace element plots of La-Th-Sc can be useful in evaluation of tectonic settings of source areas. The La-Th-Sc plot in Figure 6.8 shows that most of the Gondwanan samples fall in a continental island arc field. Two samples (one Barakar and one Dighipara sample) fall in oceanic island arc area, and one Barapukuria sample does not fall in any previously recognized field.

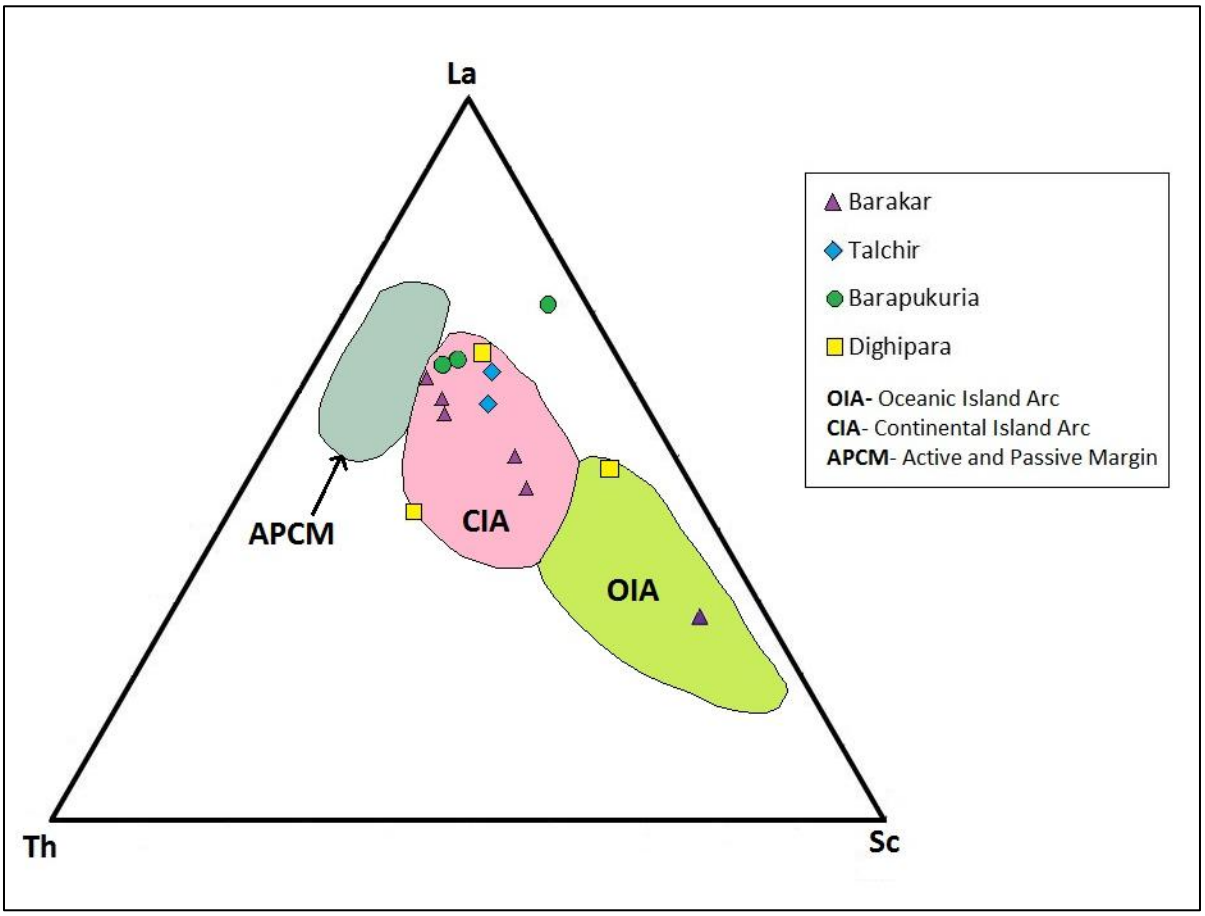

Figure 6.8 La-Th-Sc plots of Gondwanan sandstones from India and Bangladesh. Tectonic fields are taken from Bhatia and Crook (1986).

Ratios of some major oxides, such as K_2O/Na_2O and Al_2O_3/TiO_2, may help to interpret tectonic settings of the source area. K_2O/Na_2O ratios (Table 6.3) for all but one studied samples are higher than 1, which reflects passive-margin settings for source

terranes. The one exception, sample I-T-1 from Talchir, has a K_2O/Na_2O ratio expected for an active margin setting (McLennan et al., 1990). High values of Al_2O_3/TiO_2 in all samples indicate felsic source rocks (Sugitani et al., 1996).

Table 6.3 Ratios of some major oxides.

Samples	K2O/Na2O	Al2O3/TiO2
I-B-2	165.00	39.70
I-B-4	93.00	23.36
I-B-7	61.57	19.40
I-B-10	48.00	16.09
I-B-13	46.75	25.21
I-B-16	65.60	30.21
I-T-1	0.86	14.88
I-T-2	1.06	19.24
B-B-2	38.63	33.93
B-B-4	30.70	75.36
B-B-6	6.21	33.58
B-D-3	37.00	31.28
B-D-7	187.00	15.86
B-D-10	1.71	23.25

Due to their immobility, TiO_2 and the trace element Zr can be used to discriminate among igneous source-rock types (Hayashi et al., 1997). The TiO_2 vs Zr plot in Figure 6.9 indicates felsic rather than mafic source rocks for the studied samples. All but two of the Gondwanan samples fall in the felsic igneous rock field. Two exceptions, one from the Barakar and one from the Dighipara fall in the intermediate igneous rock field.

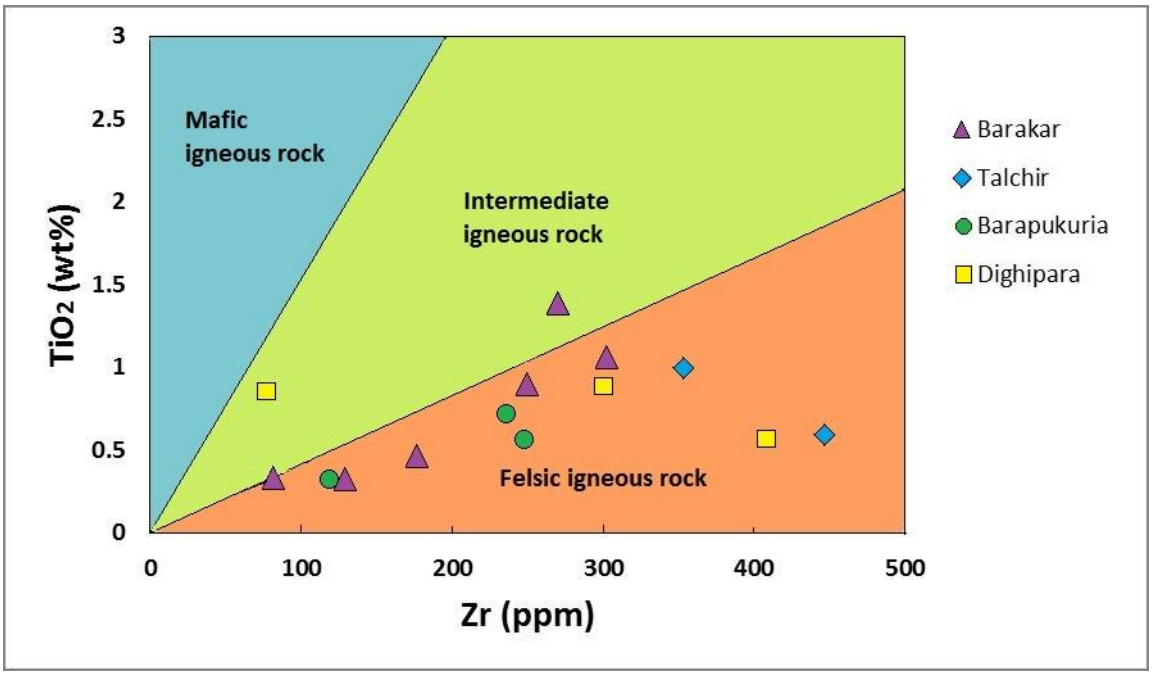

Figure 6.9 TiO_2 vs Zr plots of Gondwanan sandstone samples from India and Bangladesh. Fields are taken from Hayashi et al. (1997).

CHAPTER 7: DETRITAL $^{40}Ar/^{39}Ar$ GEOCHRONOLOGY

7.1 INTRODUCTION

Detrital sediments and sedimentary rocks provide information on the erosional history of active and ancient orogenic systems. Information on tectonic activity and provenance history can be extracted by detrital geochronology of sediments (Hodges et al., 1994, 2005; De Celles et al., 2004). Among the existing detrital age-dating techniques, U-Pb and $^{40}Ar/^{39}Ar$ thermochronology are the most widely used methods.

Age dating of detrital grains using single crystals of specific minerals is very helpful in evaluating the exhumation histories of orogens (Hodges et al., 1994, 2005; Najman, 2006). This technique of thermochronology yields information on key parameters including timing, magnitude and variations in erosional activities (Burbank et al., 2007). Reconstruction of cooling/unroofing histories of orogens is based on two common applications. First, samples analyzed from different stratigraphic levels of a section help reconstruct sequential changes in the suite of mineral cooling ages coming up from an orogen (Carter and Moss, 1999; White et al., 2002; Reiners et al., 2004; Burbank et al., 2007). Second, study of detrital rock fragments in modern streams yields a broad sampling of the realm of cooling ages presently exposed within a tributary catchment (Bernet et al. 2004; Burbank et al., 2007). Single crystal $^{40}Ar/^{39}Ar$ geochronologic methods have been used to reveal the cooling history of muscovite grains for possible provenance information (i.e., Uddin et al., 2010). The difference in

age between isotopic closure and deposition reflects the time required to remove 8-10 km of sediment (Cerveny, 1986).

7.2 $^{40}Ar/^{39}Ar$ GEOCHRONOLOGY OF DETRITAL MUSCOVITE

The detrital $^{40}Ar/^{39}Ar$ age-dating technique is a powerful tool to help constrain sedimentary provenance and to decipher paleotectonic history of a basin. While other techniques such as detrital fission-track and (U-Th)/He) thermochronology also offer such insights, the $^{40}Ar/^{39}Ar$ technique provides considerably higher precision and more rapid sample throughput (Hodges et al., 2005). Minerals like muscovite, biotite, K-feldspar, and amphibole that are rich in potassium (K) are commonly used in $^{40}Ar/^{39}Ar$ age dating (Tapsoba et al., 2013). Such minerals record the time at which the source rock passed the closure temperature and thus yield $^{40}Ar/^{39}Ar$ ages younger than the crystallization age of the rock sample (Dodson, 1979).

Muscovite is the best mineral for detrital $^{40}Ar/^{39}Ar$ analyses (Hodges et al., 2005). K-feldspars are very susceptible to secondary alteration and, in some cases (if derived from metamorphic or intrusive igneous province) they are too structurally complex to show a narrow range of $^{40}Ar/^{39}Ar$ closure temperatures (Parsons et al., 1999; Lovera et al., 2002). Micas other than muscovites, like biotites and phengites, are not preferable for $^{40}Ar/^{39}Ar$ dating because they might contain excess ^{40}Ar that was not produced by in situ decay of ^{40}K. As a result, they might yield geologically meaningless $^{40}Ar/^{39}Ar$ ages (Kelley, 2002). Biotites are also very susceptible to secondary alteration (Mitchell et al.; 1988, Murphy et al., 1998).

7.3 ANALYTICAL TECHNIQUES

7.3.1 ANALYTICAL PRINCIPLES

The inert gas argon volumetrically constitutes 0.94% of the earth's atmosphere. Argon naturally forms in the atmosphere and can prevail in various isotopic structures ranging from ^{30}Ar to ^{53}Ar. However, stable and common isotopes of argon are ^{40}Ar (99.6%), ^{36}Ar (0.34%), and ^{38}Ar (0.06%). Naturally forming ^{40}K (half-life=1.25×10^{9} years) decays to stable ^{40}Ar (11.2%) and stable ^{40}Ca (88.8%) through the emission of a positron and beta particles, respectively. Due to natural decay of ^{40}K to ^{40}Ar, the proportion of ^{40}Ar to other isotopes of argon will increase through time. The ^{40}Ar/^{36}Ar in the atmosphere is 295.5 which is used as a reference for ^{40}Ar/^{39}Ar in rock samples (McDougall and Harrison, 1999). The radioactive isotope ^{38}Cl decays to ^{38}Ar, while ^{37}Ar and ^{36}Ar form by the radioactive decay of ^{40}Ca (Dickin, 2005).

7.3.2 SAMPLE IRRADIATION

Before the development of ^{40}Ar/^{39}Ar age dating method, the ^{40}K/^{40}Ar dating technique was being used which is based on the decay of ^{40}K to ^{40}Ar with a half-life of 1.25 Ga (McDougall and Harrison, 1999). However, the ^{40}Ar/^{39}Ar method yields more precise and accurate results than the ^{40}K/^{40}Ar method. Moreover, the ^{40}Ar/^{39}Ar method decreases the effects of sample inhomogeneity and permits the use of smaller sample sizes (McDougall and Harrison, 1999). In the ^{40}Ar/^{39}Ar technique, ^{39}Ar is produced by neutron irradiation of the sample, and the proportions of ^{40}Ar with ^{39}Ar are measured simultaneously. The following nuclear reaction takes place during the irradiation:

$^{39}_{19}K$ [$^{39}_{19}K$ (n,p) $^{39}_{18}Ar$]

Where, n denotes neutron capture and p indicates proton emission (Faure, 1986).

During the irradiation process, multiple isotopes are produced along with ^{39}Ar. Some of these isotopes are beneficial while others are undesirable (Table 7.1). The effects of these reactions are corrected using laboratory salt and glasses (Scherer, 2007).

Table 7.1 Various isotopes produced during the irradiation process of muscovite.

Argon produced	Calcium	Potassium	Argon	Chlorite
^{36}Ar	^{40}Ca	---	---	---
^{37}Ar	^{40}Ca	^{39}K	^{36}Ar	---
^{38}Ar	^{42}Ca	^{39}K ^{40}K	^{40}Ar	^{37}Cl
^{39}Ar	^{42}Ca ^{43}Ca	^{39}K ^{40}K	^{38}Ar ^{40}Ar	---
^{40}Ar	^{43}Ca ^{44}Ca	^{40}K ^{41}K	---	---

Beneficial reactions

Insignificant reactions

Undesirable reactions

7.3.3 AGE DETERMINATION

According to McDougall and Harrison (1999), the equation for $^{40}Ar/^{39}Ar$ age dating is as follows:

$$t = (1/\lambda)\ln(^{40}Ar^*/^{39}Ar(J)+1)$$

Where, λ = decay constant for $^{40}K \rightarrow ^{40}Ar$, (=5.543 X 10-10/year)

J = neutron flux (fluence) constant

$^{40}Ar^*$ = ^{40}Ar formed due to radioactive decay of ^{40}K in situ

^{39}Ar = ^{39}Ar formed artificially by bombardment

Age-dating techniques using detrital mineral grains show a range of ages that reflect different source contributions. The maximum age population in a probability plot suggests greater contribution of detritus from source rocks having that age. Shorter time gaps are related to high relief, which results in rapid transport of sediments (Hodges et al., 2005). While studying sediments, the $^{40}Ar/^{39}Ar$ dating method is most commonly applied on muscovites. The $^{40}Ar/^{39}Ar$ dates of muscovite grains provide the time of cooling of source rocks through a closure temperature interval of 300-400˚ C (Hames and Bowring, 1994). It is assumed that no additional ^{40}Ar is added or lost during transportation and deposition (Hodges et al., 2005).

7.4 METHODOLOGY

Muscovite grains from five (5) sandstone samples were subjected to $^{40}Ar/^{39}Ar$ analyses. Three (3) of those samples (I-B-4, and I-B-13, from the Barakar Formation and

I-T-1 from the Talchir Formation) were selected from the Jharia (Damodar) basin, India (Fig. 7.4). The other two (2) samples (B-B-2 and B-D-1) are from the Dighipara (Fig. 7.1) and Barapukuria (Fig. 7.2) cores respectively, from northwestern Bangladesh.

Sandstone samples preparation was completed in the Himalayan Research Laboratory at Auburn University. Samples were crushed in a manner so as not damage individual mineral grains. Crushed samples were sieved to extract the grain size fraction of 0-4 phi. Samples were processed by heavy mineral separation and the lighter portions were used for muscovite extraction. According to Versmeesch (2004), in excess of 100 detrital muscovite grains need to be analyzed to ensure statistically valid $^{40}Ar/^{39}Ar$ results. A total of more than 100 muscovite grains were collected from each sample under a binocular microscope. Separated muscovite grains were then sent to the United States Geological Survey (USGS) Reactor in Denver, CO for irradiation.

Irradiated muscovite grains were analyzed by fusing single muscovite crystals with a CO_2 laser. From each sample, one hundred and twelve (112) muscovite grains were loaded into a copper holding disc. Data reductions were done using Isoplot 3 (Ludwig, 2003). All samples were corrected for atmospheric argon contamination and interfering nuclear reactions. Mass fractionation was evaluated by measuring multiple air aliquots daily, and procedural blanks were measured after every sample analyses. These analyses were carried out at the Auburn Noble Isotope Mass Analysis Laboratory (ANIMAL) at Auburn University. ANIMAL is equipped with a low-volume, high-sensitivity, and 10-cm radius sector mass spectrometer and automated sample extraction system

(based on CO_2 laser) for analysis of single crystals (Uddin et al., 2007). A filament current of 2.240 Amp, and source and multiplier potentials of 2000 V and –1300 V, respectively were used for this study. The high sensitivity and low blank of the instrument permits measurement of 10-14 mole samples to within 0.2% precision. The GA-1550 biotite (9.879 Ma; Renne et al., 1998) was used as a flux monitor for this study.

7.5 $^{40}Ar/^{39}Ar$ RESULTS

Data obtained from $^{40}Ar/^{39}Ar$ analyses are shown in Appendix D. Distributions of relative probability of $^{40}Ar/^{39}Ar$ age populations are plotted in Figures 7.1 through 7.7. Probability plots reflect plolymodal distribution patterns of ages. Sample B-D-1 collected from ~397 m depth in the Dighipara coal basin shows an almost unimodal distribution of ages. The distribution of ages ranges from 478 Ma to 504 Ma with the mode at 490 Ma (Fig. 7.1).

Sample B-B-2 was collected from drill well GDH-41 in the Barapukuria coal field at ~187 m of depth (Fig. 7.2). The relative probability pattern of this sample shows a polymodal distribution of ages but a significant distribution of ages ranges from 480 Ma to 520 Ma with the principal mode at 495 Ma (Fig. 7.3). Several muscovite grains from sample B-B-2 show unreasonable ages; two grains show an age of 150 Ma, one grain plots at 170 Ma, and other two grains plot at 230 Ma. These ages are younger than their depositional age (Permian - Carboniferous).

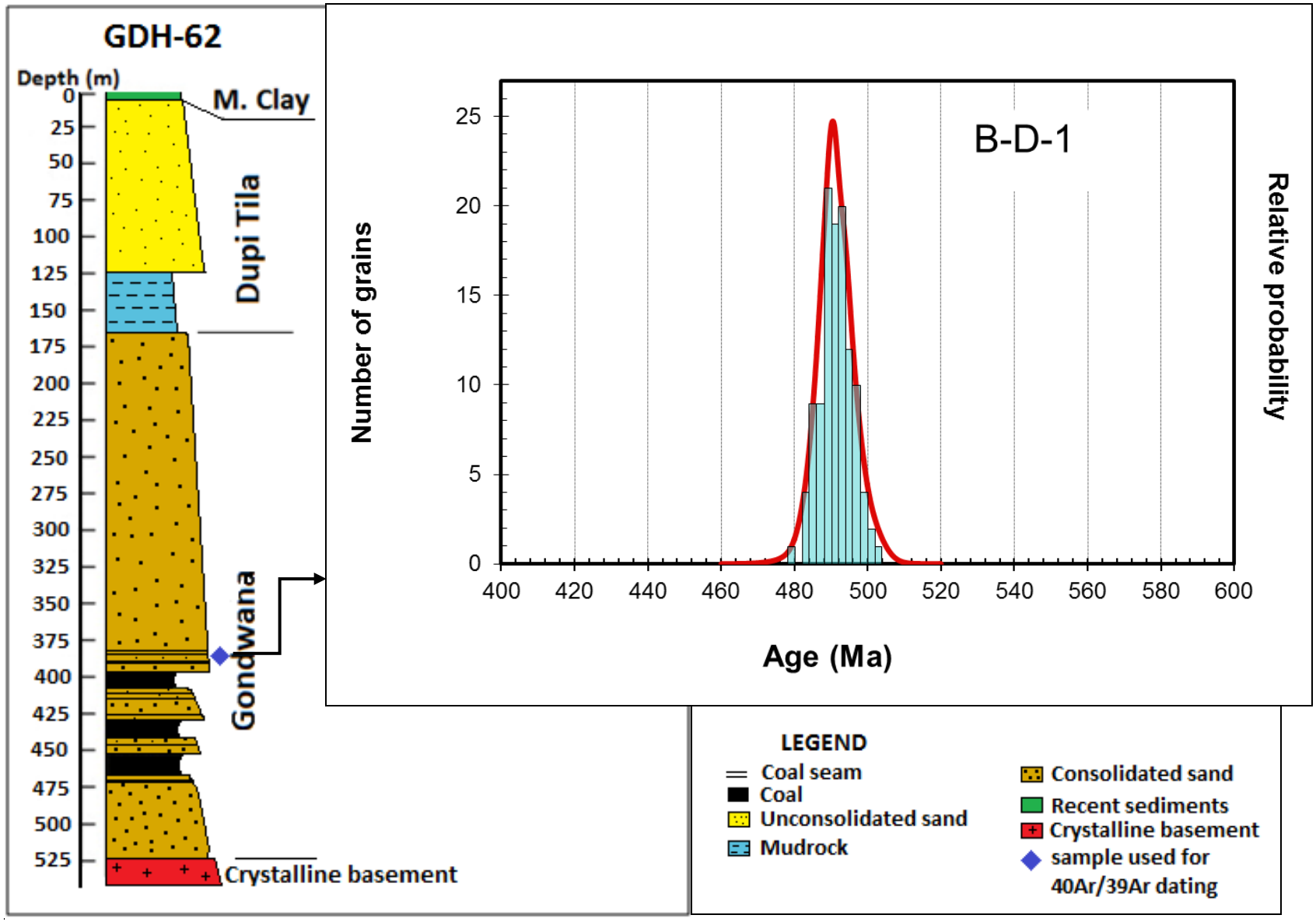

Figure 7.1 Stratigraphic positions of samples used for $^{40}Ar/^{39}Ar$ analyses of single muscovite crystals from Dighipara sample B-D-1.

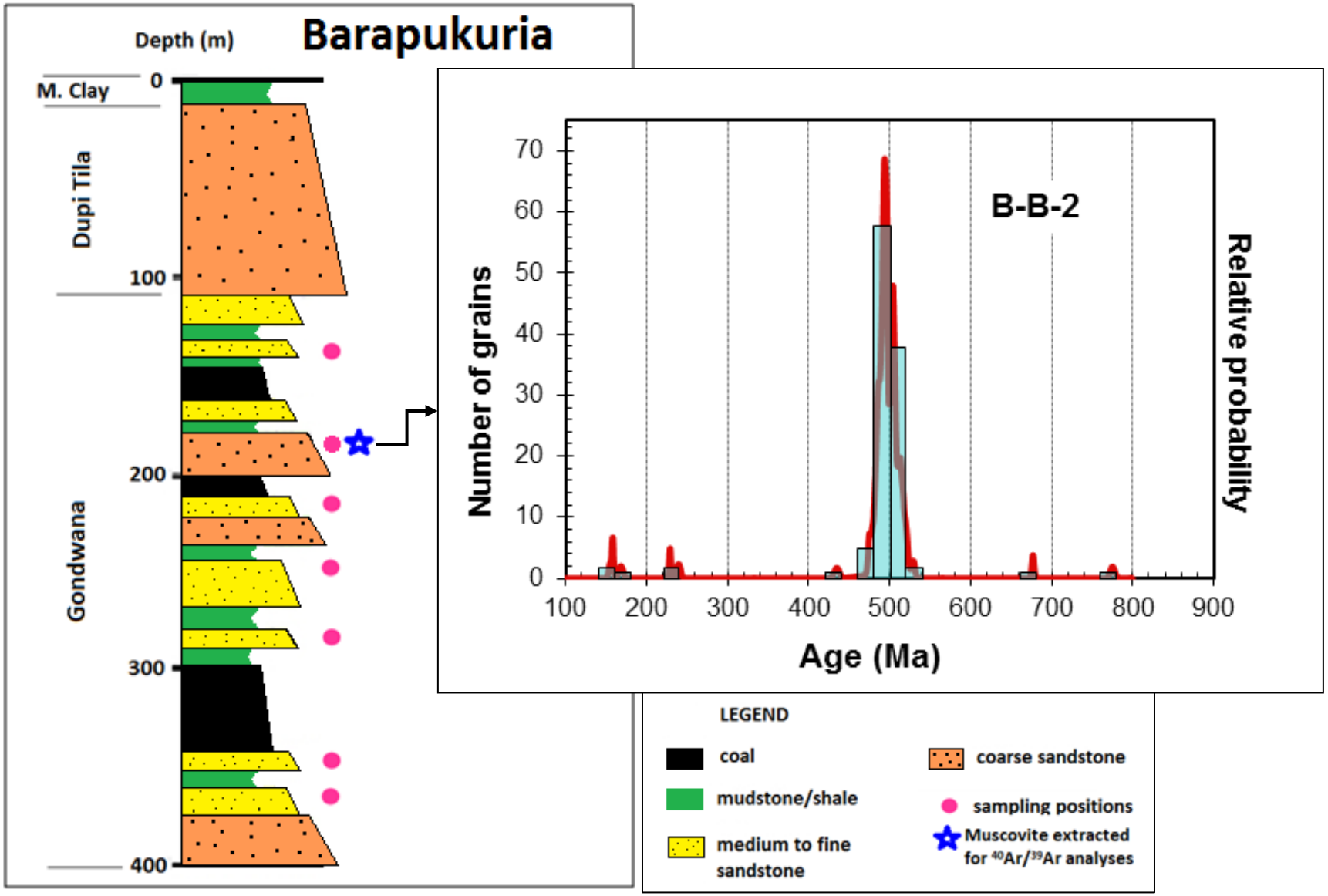

Figure 7.2 Stratigraphic positions of samples used for $^{40}Ar/^{39}Ar$ analyses of single muscovite crystals from Barapukuria sample B-B-2.

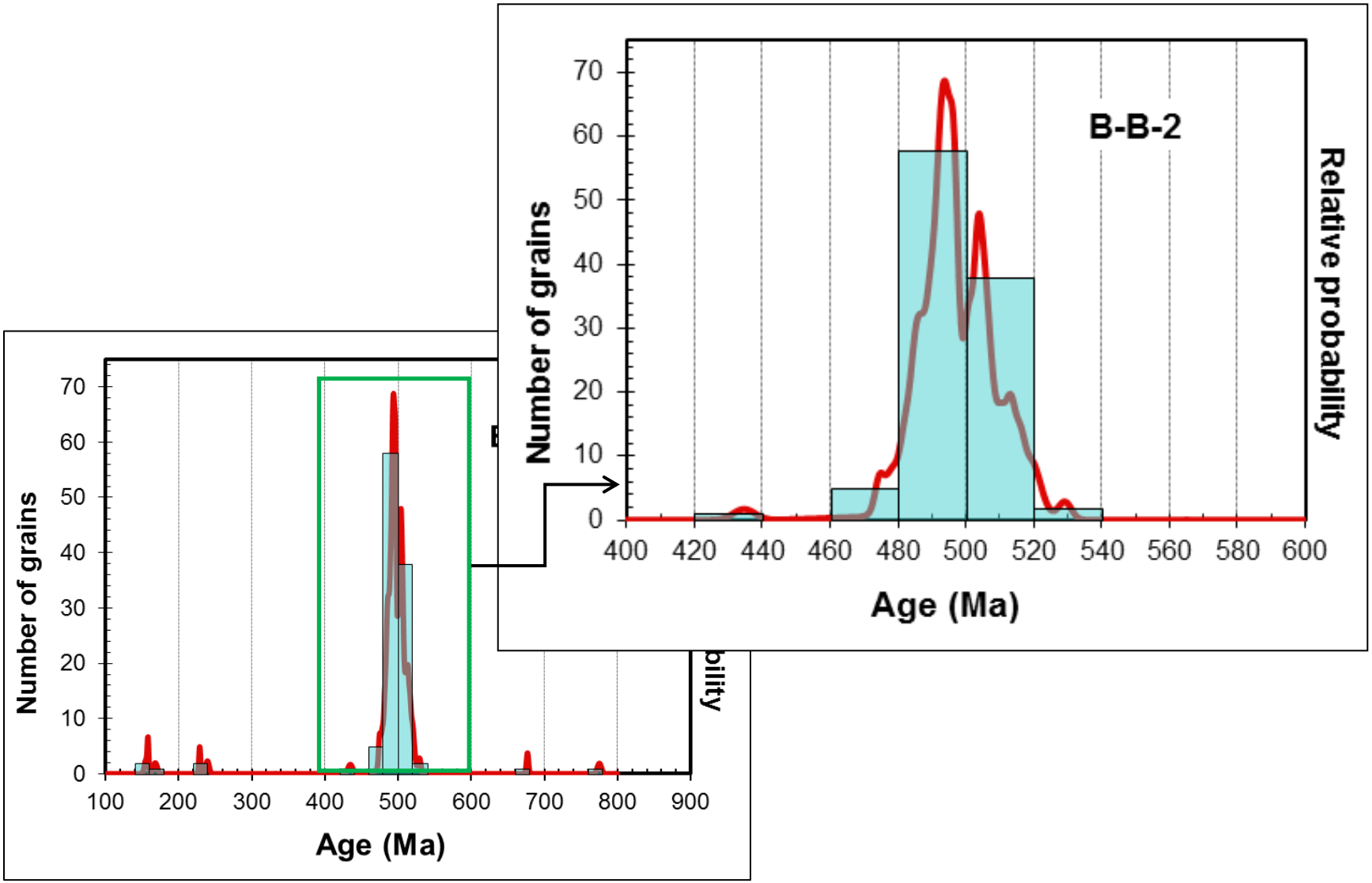

Figure 7.3 Probability plot for $^{40}Ar/^{39}Ar$ analyses of single muscovite crystals of sample B-B-2 from drill well GDH- 41, Barapukuria.

From Appendix D the youngest ages obtained tend to be for data from crystals with the highest air correction and the lowest yield of ^{40}Ar (signals below 0.7 volts). The results for these ages younger than 250 Ma are excluded from further discussion. This is because they are interpreted to be for crystal fragments that may have lost radiogenic ^{40}Ar following deposition, and that are more susceptible to errors arising from blank corrections and the statistical fit of the ^{36}Ar measurement.

Stratigraphic levels of samples from Jharia basin of eastern India (Talchir and Barakar sandstones) used for muscovite extraction are displayed in Figure 7.4. Detrital muscovites from the Talchir sandstone (sample I-T-1) show the most significant distribution of age populations at a range of 825 Ma to 875 Ma with the principal mode at 855 Ma. A single grain yielded a much younger age of 400 Ma relative to the other age distributions (Fig. 7.5).

Both Barakar samples used for $^{40}Ar/^{39}Ar$ analyses yielded non-uniform polymodal distributions of ages. Sample I-B-4, which was collected from a relatively stratigraphically lower level in the Barakar Formation (Fig. 7.4), shows several age distributions including a range from 420 Ma to 600 Ma with the principal mode at 500 Ma, and 620 Ma to 980 Ma with the mode at 770 Ma (Fig. 7.6). One grain plots at 1830 Ma. Sample I-B-13, collected from a stratigraphically higher position in the Barakar Formation (Fig. 7.4), also yielded several modes of age distribution. Two significant age distributions were observed in the probability plot; one from 480 Ma to 680 Ma with the mode at 520 Ma, and another from 700 Ma to 940 Ma with the mode at 780 Ma (Fig. 7.7). Three grains show relatively older cooling ages of 1010 Ma, 1050 Ma, and 1100 Ma.

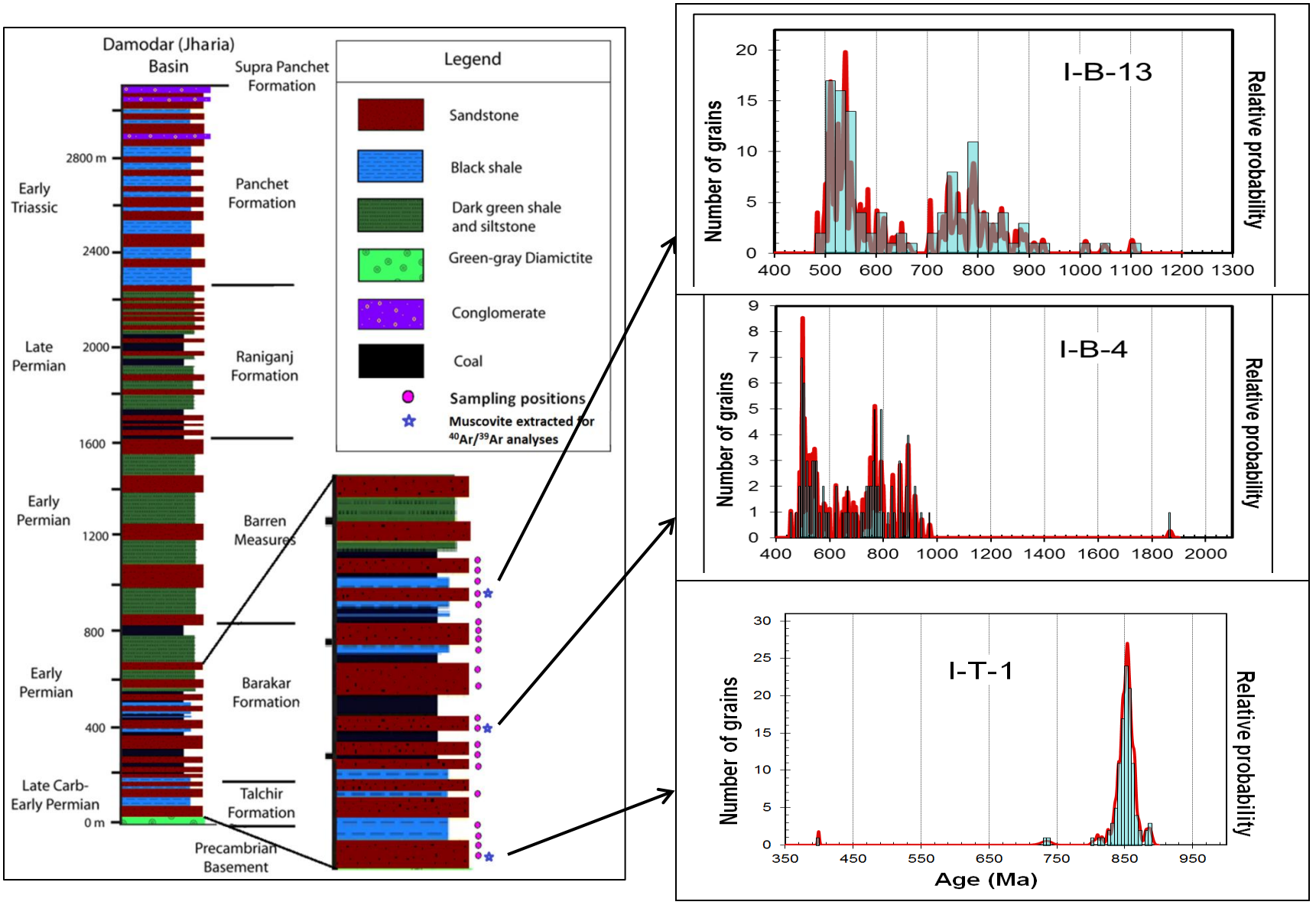

Figure 7.4 Stratigraphic positions of samples used for $^{40}Ar/^{39}Ar$ analyses from Barakar (samples I-B-13 and I-B-4) and Talchir (sample I-T-1) sandstones.

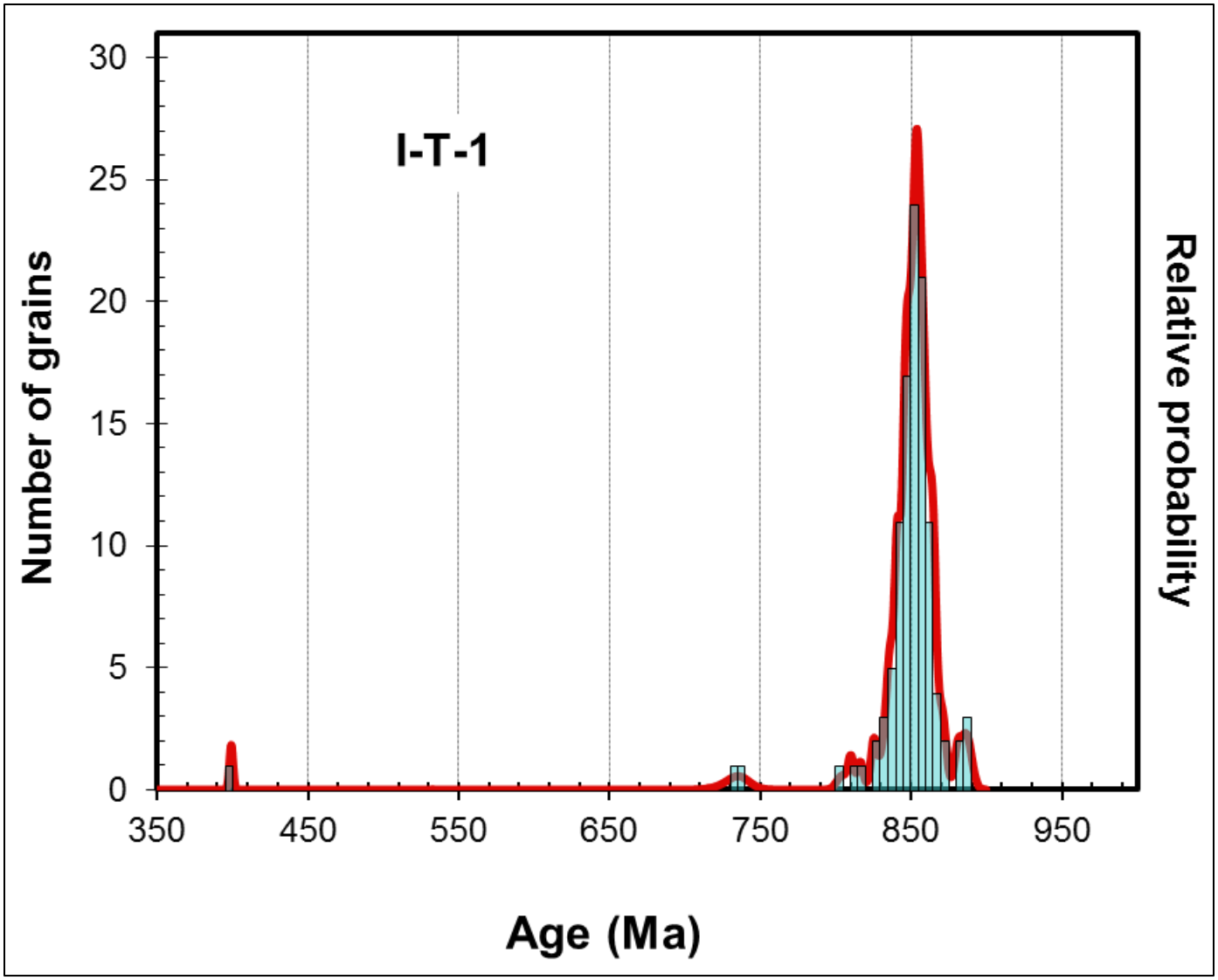

Figure 7.5 Probability plot for $^{40}Ar/^{39}Ar$ analyses of single muscovite crystals from sample I-T-1 from Talchir Fromation, Jharia basin.

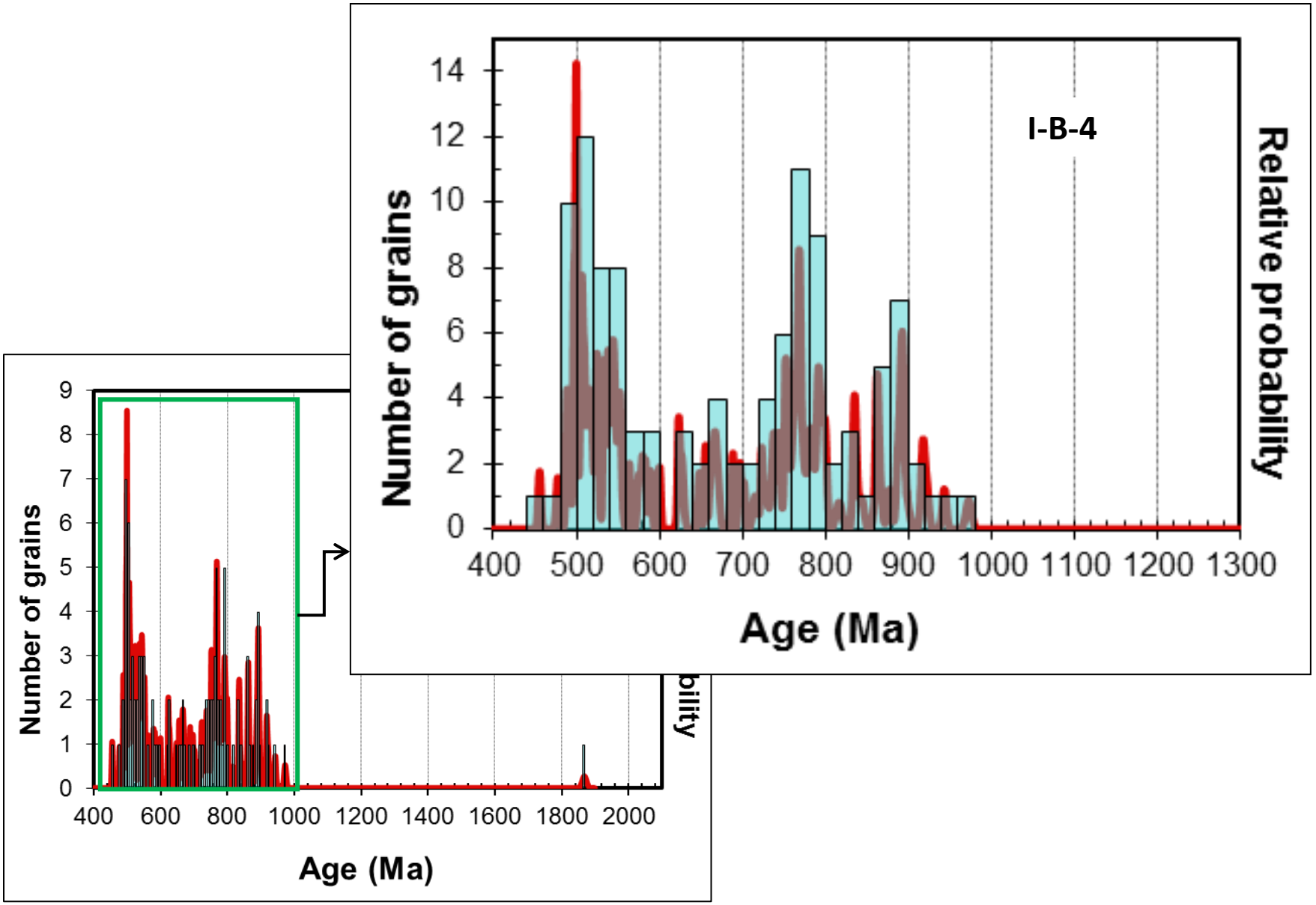

Figure 7.6 Probability plot for $^{40}Ar/^{39}Ar$ analyses of single muscovite crystals in sample I-B-4 from Barakar Formation, Jharia basin.

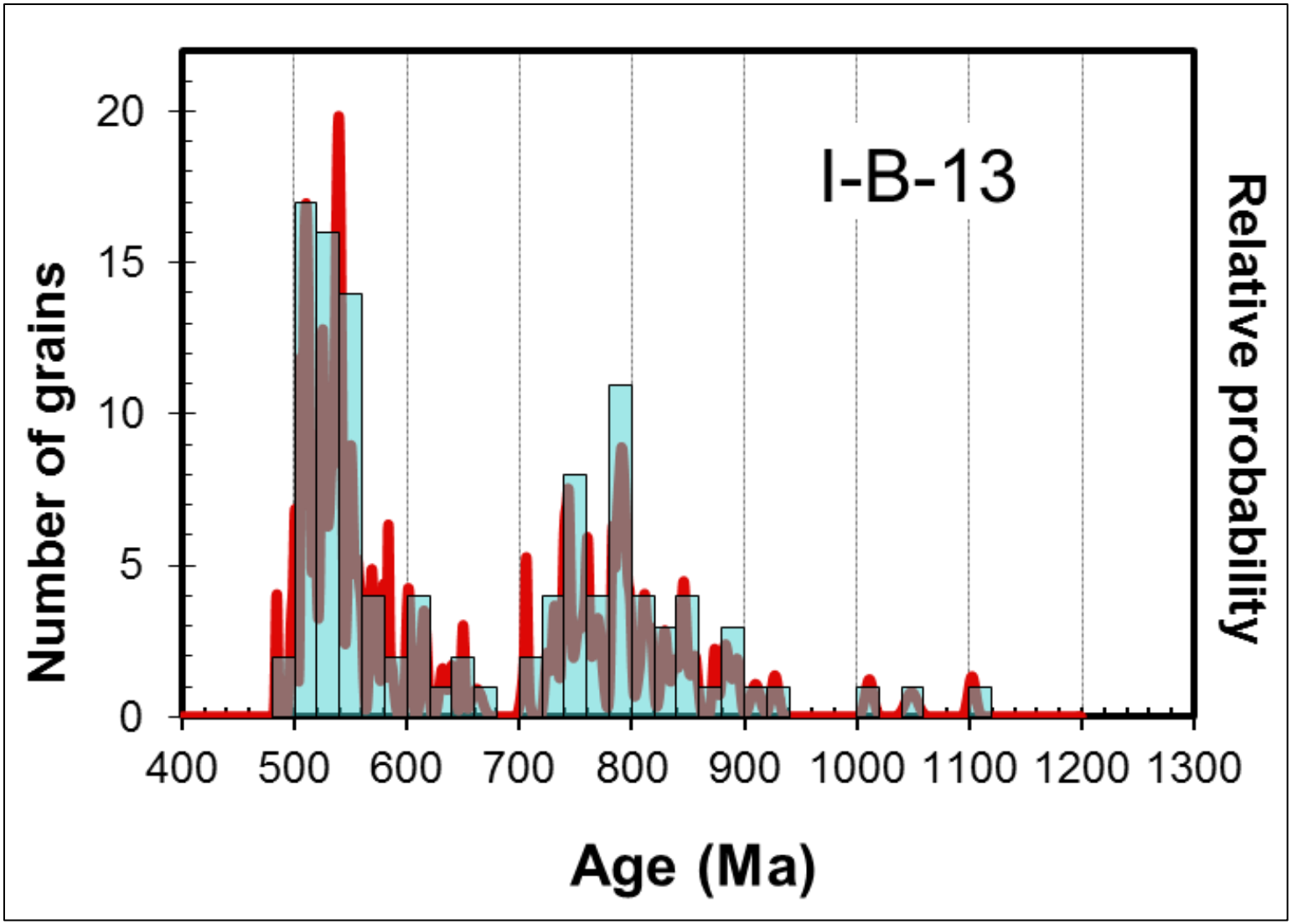

Figure 7.7 Probability plot for $^{40}Ar/^{39}Ar$ analyses of single muscovite crystals in sample I-B-13 from Barakar Formation, Jharia basin.

7.6 PROVENANCE INTERPRETATION

Various modes in the probability plots of age distribution indicate multiple sources for the studied Gondwanan sediments. Distinct differences in age distributions were observed between the Indian and Bengal samples indicating differences in their source terranes. Indian Gondwanan sediments (both Talchir and Barakar sanstones) reveal older ages than the Bengal sediments.

Both Bengal samples display the principal mode of age distribution at ca. 490 Ma demonstrating a similar source terrane, although the Barapukuria sample shows few other minor distribution modes. The Kuunga orogenic belt that developed during the Cambrian to Ordovician ages (Meert, 2001) and the adjacent Meghalayan craton (Shingbhum Plateau) may be a probable source of these sediments (Figs. 3.17 and 8.1). The Eastern Ghats Foldbelt that developed during the collision of India and Napier complex in the eastern Antarctica (Meert, 2001) might be another possible source. Several studies reveal that the Ross orogenic belt (Fig. 8.1) in the east Antarctica consists of several metamorphic terranes containing rocks with these age ranges (Wright and Dallmeyer, 1991; Fioretti et al., 2003; Alam, 2011). However, during Permo-Carboniferous time, the Ross orogenic belt was too far away from the Indian subcontinent to supply sediments into these basins. Moreover, petrographic study (sharp and angular grains) does not support long distant source of these sediments.

Strong polymodal distributions of ages in the probability plots for Indian samples indicate mixing of sediments from various sources. Although the Indian samples reflect

older and more variable ages than do the Bengal samples, Barakar sediments show a distribution pattern that matches with the muscovite grains from the analyzed Bengal samples. These similarities in age distribution may indicate that some sediments in the Barakar Formation were derived from the same source as Bengal sediments. The Talchir sample shows significant distribution of ages ranges from 830 Ma to 870 Ma, which differs significantly from the other studied samples. The Kuunga orogenic belt and Eastern Ghats Fold belt in eastern India are the most probable sources of these sediments. Muscovite grains representing Early Proterozoic to Early Cambrian age may have been derived from nearby Bastar and Shingbhum cratonic areas of Indian shield. Rayner Complex or Prydz Bay Belt in the eastern Antarctica also may have contributed to these basins in the Indian subcontinent. The age distributions for Gondwanan sediments from the Indian subcontinent analyzed in this study and for probable source terranes from various literatures are shown in Figure 7.8.

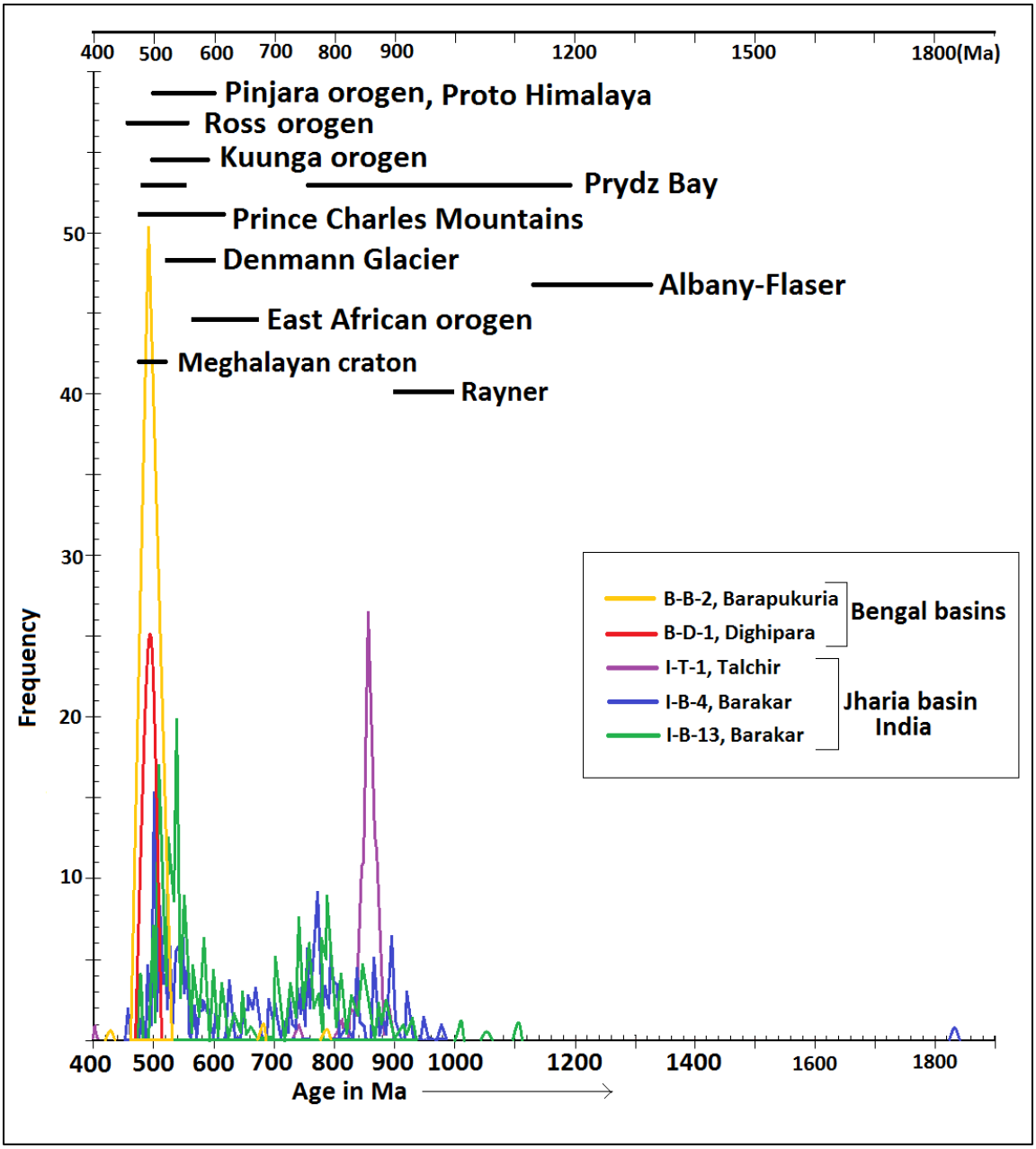

Figure 7.8 Distribution patterns of $^{40}Ar/^{39}Ar$ cooling ages of detrital muscovites from Gondwanan sandstones of Bangladesh and India. Black bars reflect the ages of potential source terranes as derived from the following previous works: Collerson and Sheraton, 1986; Sheraton et al., 1992; Black et al., 1992; Nelson et al., 1995; Carson et al., 1996; Veevers, 2000a, 2004; Boger et al., 2001; Meert, 2001; Gehrels et al., 2003; Collins and Fitzsimons, 2001; Fitzsimons, 2003; Yoshida and Upreti, 2006; Chatterjee et al., 2007; Meert et al., 2010 and references therein.

CHAPTER 8: SUMMARY AND DISCUSSION

8.1 SANDSTONE PETROGRAPHY

Sandstone petrographic studies of Permo-Carboniferous Gondwanan sequences reveal differences in sandstone modes between sediments from India and Bengal Basin. Modal compositions vary among various basins as well as among sandstones from different stratigraphic levels of the same basin (e.g., Talchir and Barakar formations). Sandstones from Barapukuria and Khalaspir coal basin of northwest Bangladesh and Talchir Formation from Jharia basin, India are lithic subarkoses. In contrast, the Barakar sandstones are sublitharenites, and the Dighipara samples are subarkoses (Fig. 3.10). These compositional differences among basins and different stratigraphic levels may be attributed to differences in source rocks. Sandstones from Bangladesh are angular to subangular and more texturally immature than coeval sandstones from India. Monocrystalline quartz was dominant over polycrystalline quartz in both Indian and Bengal samples. However, Bengal samples contain higher percentage of polycrystalline quartz with >3 crystals per grain, which indicates low-rank metamorphic source rocks (Blatt, 1967; Basu et al., 1975). High amount of monocrystalline nonundulose quartz in Barakar sandstones indicate plutonic sources (Blatt and Christie, 1963; Blatt, 1967; Basu et al., 1975). Although feldspars are common in the Bangladesh samples and the Talchir Formation of India, no feldspar was identified in the Barakar Formation (India). Feldspars from the Barakar sandstone may have been altered into clay minerals due to weathering effects. Based on modal compositional analyses, several tectonic

provenance fields have been identified for these sediments. These include recycled orogenic, craton interior and transitional continental provenances (Fig. 3.11).

Petrographic studies suggest that Gondwanan sequences of Bangladesh and India were derived from multiple sources. Textural and compositional immaturity in the Bengal samples indicates proximal source(s), whereas more matured Indian samples may have traveled further from the source(s). The nearby Shingbhum and Meghalayan cratons in the Indian shield and the Eastern Ghats Mobile Belt, all located at the southern boundary of these basins, were the most probable sources. However, the Kuunga orogen between India and Antarctica, the Pinjara orogen between India and Australia, and rocks in the Antarctic shield also may have contributed sediments to these Gondwanan basins.

8.2 HEAVY MINEARAL ASSEMBLAGES

Heavy mineral assemblages in Gondwanan sequences of Bangladesh and India are dominated by a few mineral groups such as garnet, apatite, zircon, rutile, tourmaline, sphene, epidote, siderite and opaques. Heavy mineral contents of Indian samples are relatively high compared to Bengal samples (Fig. 4.1). Garnet content is very high in Bengal samples. However, Barakar samples show a scarcity of garnets; only six garnet grains were identified in two Barakar samples, which is only ~1.6% of overall heavy mineral assemblages (Table 4.5). Although both Bengal and Indian samples share common mineral assemblages, there are distinct differences in relative abundances of various heavy mineral suites, indicating differences in source terranes and/or sediment

routing systems. Contrasts in textural maturity of similar heavy mineral suites indicate the existence of both proximal and distal sources for these Permo-Carboniferous successions. Like the petrographic studies, heavy mineral analyses suggest that the sediments from India are texturally and compositionally more matured than the Bengal samples. The average abundance of ultrastable minerals (zircon, tourmaline, and rutile) in Barakar samples, India (~16.84%) is higher than Bengal samples (Fig. 4.7). In the Indian sandstones, tourmaline content is high followed by rutile and zircon, whereas in Bengal sandstones zircon content is higher followed by rutile and tourmaline.

Heavy mineral assemblages suggest differences in source terranes or sediment routing systems among Gondwanan sediments from Bangladesh and India. Ratios of highly stable mineral indices also indicate variations in sources among the studied basins. Within Bangladesh, heavy mineral assemblages of Dighipara samples differ from those of other Gondwanan coal basins in Bangladesh (Barapukuria and Khalaspir basins), indicating dissimilarities in source rocks. Based on this study, several source terranes may be inferred; the Shingbhum and Bastar cratons in the Indian shield, Eastern Ghats Mobile Belt, and the East Antarctic shield.

8.3 MICROPROBE ANALYSES

Specific heavy minerals -- garnet, tourmaline and chrome spinel-- were chosen for microprobe analyses of single grain mineral chemistry. All garnets are mostly almandine and pyrope rich (Fig. 5.5). Based on major oxide content, eight (8) different garnet species are identified: almandine, pyrope, grossular, spessartine, andradite,

uvarovite, schorlomite-Al and NaTi garnet. Garnet compositions suggest a variety of source terranes. Most of the ternary plots using garnet end members indicate amphibolite facies, granulite facies, and pegmatites as source rocks (Figs. 5.3 and 5.4).

Compositional analyses of tourmaline suggest that probable source rocks are aluminous metapelites and metapsammites (Fig 5.6). Ca-Fe (tot)-Mg plot shows that most grains came from Ca-poor metapelites, metapsammites, and quartz-tourmaline rocks (Fig 5.7).

Chrome spinels are not common in the studied Gondwanan sequences. Chrome spinels were identified only from Dighipara sandstones. Microprobe data of chrome spinel suggests a Tulameen Alaskan Type complex for Dighipara samples.

8.4 WHOLE ROCK GEOCHEMISTRY

Major oxides plotted in $\log(SiO_2/Al_2O_3)$ vs $\log(Fe_2O_3/K_2O)$ show that most of the samples fall in highly feldspathic sandstone to wacke zones. Harker's variation diagrams do not show any linear correlation suggesting that Gondwanan sediments are not genetically related.

Al_2O_3 – $(CaO+Na_2O)$-K_2O plots show that most of the studied sediments derived from highly weathered source terranes. Talchir sandstones are exception and apparently were derived from unweathered source rocks (Fig. 6.5). High to moderate CIA values of the Barakar, Barapukuria, and Dighipara samples also indicate highly

weathered source rocks. In contrast, low CIA values for Talchir samples indicate unweathered source terranes.

Major oxide compositions of studied Gondwanan sediments suggest derivation mostly from a passive-margin setting, although some samples indicate active continental margin and volcanic island arc sources. Trace and rare earth element ratios of Gondwanan sediments suggest felsic sources (Table 6.2). High Al_2O_3/TiO_2 values (Table 6.3) and TiO_2 vs Zr plots (Fig. 6.9) also indicate felsic sources of Gondwanan sediments from India and Bangladesh. Studies of whole-rock chemistry suggest probable sources from gneissic complexes of nearby Shingbhum craton and/or felsic gneisses of Leeuwin metamorphic complex in the Pinjara orogen.

8.5 DETRITAL $^{40}Ar/^{39}Ar$ GEOCHRONOLOGY

$^{40}Ar/^{39}Ar$ analyses of detrital muscovites show mostly polymodal distributions of ages. The populations of age distributions from Indian samples significantly differ from those of the Bengal samples. Modes of ages from Bengal samples fall in a narrow zone, whereas age modes for Indian samples are more scattered. The Dighipara sample shows an almost unimodal distribution of ages ranging from 480 to 500 Ma with the principal mode at 490 Ma (Fig. 7.1). The Barakar sample shows a significant distribution of ages ranging from 480 to 520 Ma with the principal mode at 495 Ma (Fig. 7.3). The age distributions of Bengal samples are consistent with multiple potential sources: the Millie granite or gneissic complex of Meghalayan craton, Kuunga orogen, Prydz Bay and Prince

Charles Mountain in the east Antarctica. The Pinjarra orogen and/or Proto-Himalayan orogen also could be probable source(s).

$^{40}Ar/^{39}Ar$ analyses of Indian samples show polymodal age distributions indicating mixing of sediments from multiple sources. The age distributions of Talchir Formation significantly differ from Barakar sandstones. Age distributions from Talchir sandstone fall in a narrow zone ranging from 800 to 900 Ma, whereas Barakar sandstones show multiple significant modes of age distributions. Changes in the modes of age distributions from different stratigraphic levels may be due to changes of source terranes through time. Along with the source terranes mentioned above for Bengal sediments, the Rayner Complex and Denmann Glacier in the Eastern Antarctica are potential sources for the Indian samples.

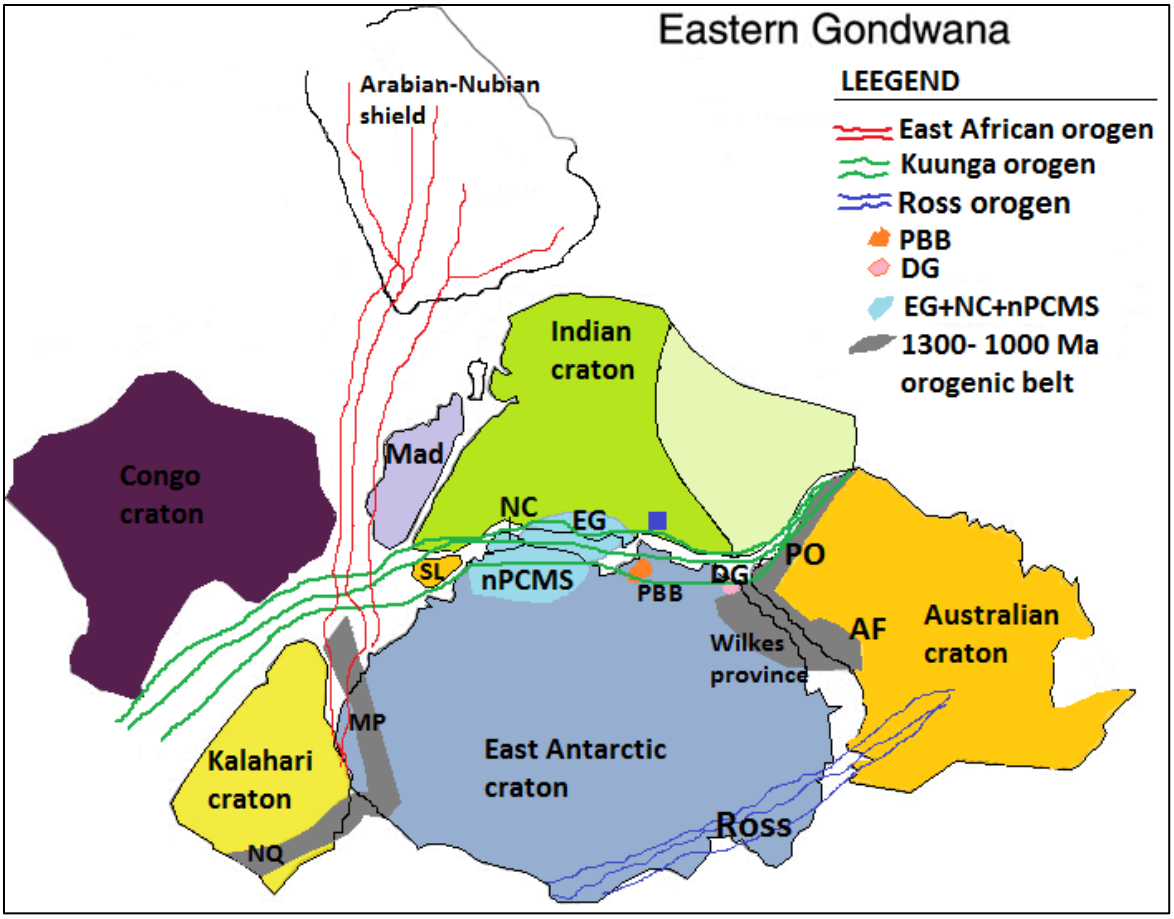

Figure 8.1 Paleogeographic map of Eastern Gondwana and probable source terranes for Gondwanan sequences of Bangladesh and India (compiled after Fitzsimons, 2000a; Meert, 2003; Yoshida and Upreti, 2006). Blue shaded square represent the study area. AF= Albany Fraser (Australia), EG= Eastern Ghats (India), DG= Denmann Glacier (Antarctica), Mad= Madagascar, MP= Maud Province (Antarctica), NC= Napier Complex (Antarctica), nPCMS= Northern Prince Charles Mountains (Antarctica), NQ= Namaqua Belt (Africa), SL= Sri Lanka. A closer view of Indian subcontinent is shown in Figure 3.17.

8.6 COMPARISONS WITH OTHER GONDWANAN BASINS OF SOUTH ASIA

Sandstone compositions from this study can be compared with previous studies done in different Gondwanan basins of south Asia (Bangladesh, India, and Nepal) (Fig. 8.2). There are dissimilarities in the composition of sediments among these basins of

similar depositional age. Differences in sandstone compositions among various basins may be attributed to changes/differences in source terranes, sediment dispersal systems, and geomorphic and structural settings of the basins.

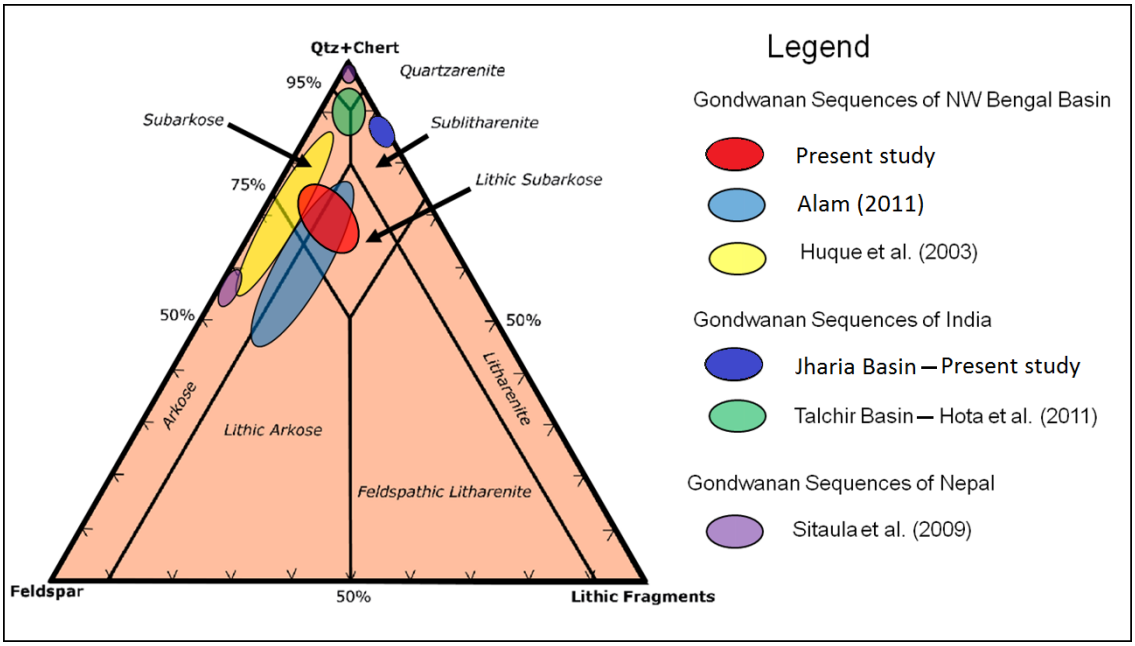

Figure 8.2 Comparision of average sandstone modes of Gondwanan sandstones from different areas of south Asia.

Differences in modal composition of Gondwanan sandstones from different areas in the Indian subcontinent are also reflected in Q_tFL ternary plots. Although recycled orogenic setting appears to be dominant some areas are suggestive of sandstone compositions from transitional continental, craton interior, and/or dissected arc settings (Fig. 8.3).

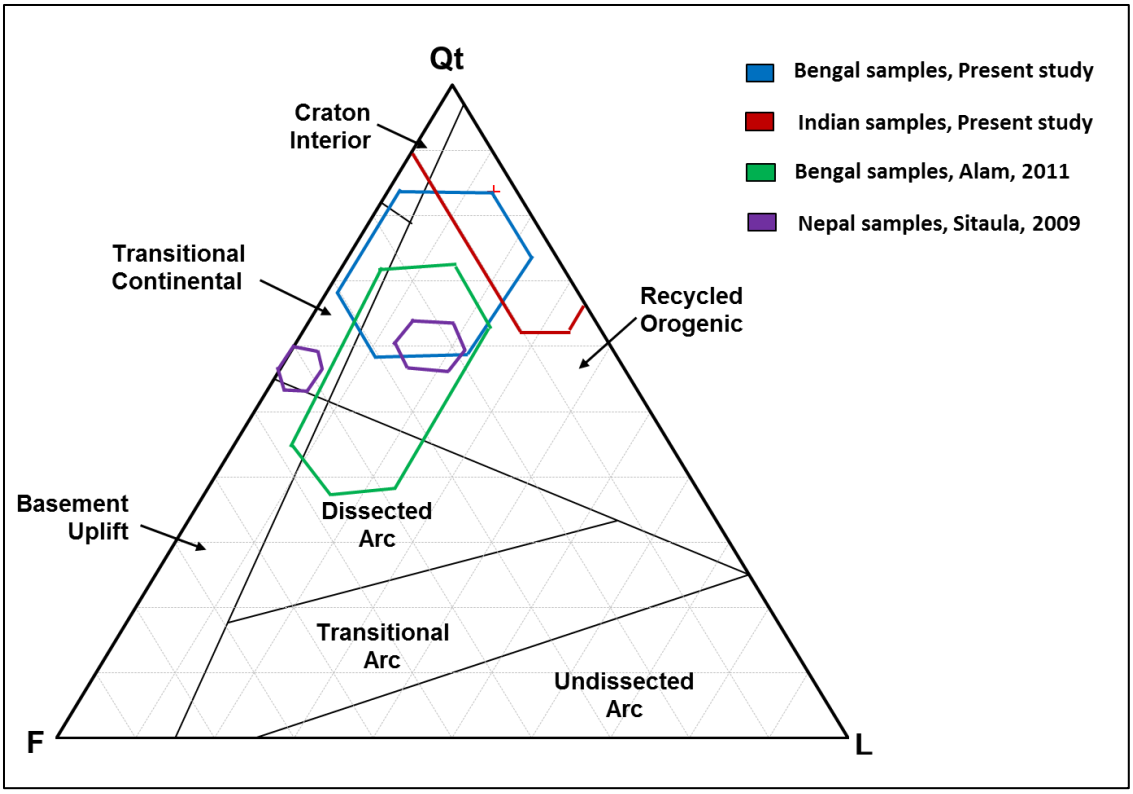

Figure 8.3 Q_tFL plots of Gondwanan sandstone samples from different areas of south Asia showing standard deviation polygons (fields are taken from Dickinson, 1985).

Comparison of $^{40}Ar/^{39}Ar$ analyses from different Gondwanan basins show differences in cooling ages of detrital muscovites (Fig. 8.4). All three analyses (Sitaula, 2009; Alam, 2011; and Present study) reveal there is a common modal distribution of ages ranging from 480 Ma to 520 Ma (Fig. 8.4). This common distribution of ages indicates that all of these basins received sediments from an orogenic belt that extensively developed around Indian subcontinent during the Cambrian. Muscovite age distribution patterns indicate mixing of sediment sources in most of these basins.

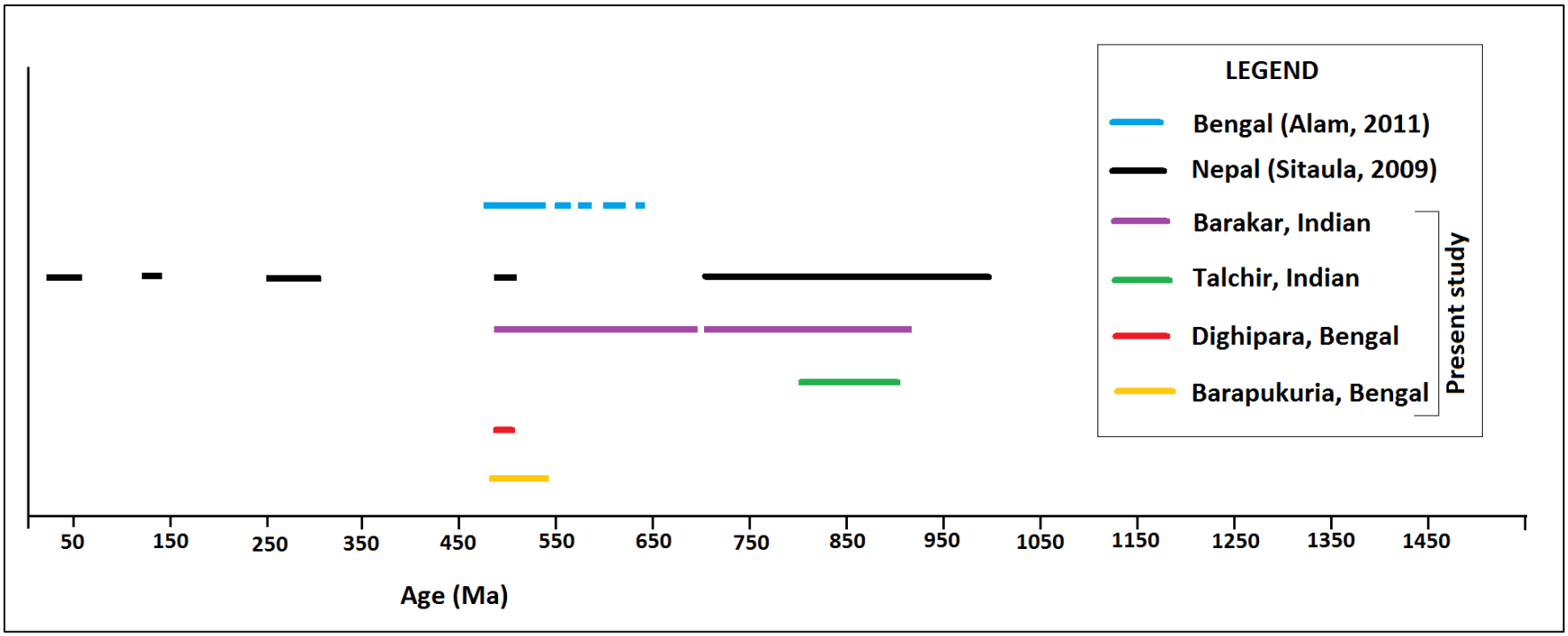

Figure 8.4 Comparison of detrital muscovite ages of Gondwanan sandstones from different areas of south Asia.

8.7 CONCLUSIONS

This study indicates that, Gondwanan sediments of Indian subcontinent derived from multiple source terranes. Permo-Carboniferous Gondwanan sediments of different Gondwanan basins on the Indian subcontinent differ from each other. Indian sediments are compositionally and texturally more matured than Bengal sediments.

Geochemical analyses suggest derivation mostly from felsic igneous rocks of passive-margin settings. High Chemical Index of Alteration values indicate highly weathered source terranes except for Dighipara samples. High mineralogical maturity of Barakar samples is reflected by very high ZTR indices (~17%). Garnet is one of the most common heavy minerals of Permo-Carboniferous Gondwanan sediments, except for in the Barakar sandstones.

Geochronologic analysis indicate several potential source terranes, including the Ross orogen, Kuunga orogen, Proto-Himalayan orogen, Pinjarra orogen, Meghalayan craton, Shingbhum craton, Eastern Ghats mobile belt, Kuunga orogen, Denmann Glacier, Prydz Bay belt, and Northern Prince Charles Mountains. Considering paleoslope direction and sandstone petrographic characteristics along with geochronologic data, the Meghalayan craton (Shilong Plateau) and Kuunga orogen are the most probable sources of Gondwanan sediments in Bengal Basin. In contrast, the Shingbhum craton, Eastern Ghats mobile belt, Kuunga orogen, Denmann Glacier, Prydz Bay belt, and/or Northern Prince Charles Mountain areas are probable sources of Permo-Carboniferous Gondwanan sediments of Jharia Basin, India.

REFERENCES

Acharyya, S.K., 2000, Coal and lignite resources of India: an overview: Geological Society of India, Bangalore, 50 p.

Akhtar, A., 2000, Coal and hard rock resources in Bangladesh: Episodes, v. 23, p. 25-28.

Akhtar, A., and Kosanke, R.M., 2000, Palynomorphs of Permian Gondwana coal from borehole GDH-38, Barapukuria Coal Basin, Bangladesh: Journal of Asian Earth Sciences, v. 31, p. 107-117.

Alam, M.I., 2011, Petrofacies and Paleotectonic Evolution of Permo-Carboniferous Gondwanan Sequences of the Bengal Basin, Bangladesh [unpublished M.S. Thesis]: Auburn University, Auburn, AL, 134 p.

Alam, M., Alam, M.M., Curray, J.R., Chowdhury, M.L.R., and Gani, M.R., 2003, An overview of the sedimentary geology of the Bengal Basin in relation to the regional tectonic framework and basin-fill history: Sedimentary Geology, v. 155, p. 179-208.

Bakr, M.A., Rahman, Q.M.A., Islam, M.M., Islam, M.K., Uddin, M.N., Resan, S.A., Haider, M.J., Sultan-Ul-Islam, M., Ali, M.W., Chowdhury, M., Mannan, K.H., and Anam, A.N.M.H., 1996, Geology of coal deposit of Barapukuria basin, Dinajpur District, Bangladesh: Records of The Geological Survey of Bangladesh, v. 8, 16 p.

Basu, A., 1976, Petrology of Holocene fluvial sand derived from plutonic source rocks: implications to paleoclimatic interpretation: Journal of Sedimentary Research, v. 46.

Basu, A., Young, S. W., Suttner, L. J., James, W. C., and Mack, G. H., 1975, Re-evaluation of the use of undulatory extinction and polycrystallinity in detrital quartz for provenance interpretation: Journal of Sedimentary Research, v. 45.

Bateman, R.M., and Catt, J.A., 1985, Modification of heavy mineral assemblages in English coversands by acid pedochemical weathering: Catena, v. 12, p. 1-21.

Bernet, M., Brandon, M.T., Garver, J.I. and Molitor, B.R., 2004, Fundamentals of detrital zircon fission-track analysis for provenance and exhumation studies with examples from the European Alps *in* Detrital Thermochronology-Provenance Analysis, Exhumation, and Landscape Evolution of Mountain Belts (Eds M. Bernet and C. Spiegel): Geological Society of America Special Paper, v. 378, p. 25-36.

Bhatia, M., 1983, Plate tectonics and geochemical composition of sandstones: Journal of Geology, v. 91, p. 611-627.

Bhatia, M.R., 1985, Rare earth element geochemistry of Australian Paleozoic graywackes and mudrocks: Provenance and tectonic control: Sedimentary Geology, v. 45, p. 97–113.

Bhatia, M. R., and Crook, K. A. W., 1986, Trace element chracteristics of graywacke and tectonic setting discrimination of sedimentary basins: Contributions to Mineralogy and Petrology, v. 92, p. 181-193.

Black, L.P., Sheraton, J.W., Tingey, R.J., and Mcculloch, M.T., 1992, New U-Pb zircon ages from the Denman Glacier area, East Antarctica, and their significance for Gondwana reconstruction: Antarctic Science, v. 4, p. 447–460.

Blatt, H., 1967, Provenance determinations and recycling of sediments: Journal of Sedimentary Research, v. 37.

Blatt, H., and Christie, J. M., 1963, Undulatory extinction in quartz of igneous and metamorphic rocks and its significance in provenance studies of sedimentary rocks: Journal of Sedimentary Research, v. *33*.

Boger, S.D., Wilson, C.J.L., and Fanning, C.M., 2001, Early Paleozoic tectonism within the East Antarctic craton: The final suture between east and west Gondwana?: Geology, v. 29, p. 463–466.

Burbank, D.W., Brewer, I.D., Sobel, E.R., and Bullen, M.E., 2007, Single-crystal dating and the detrital record of orogenesis, in sedimentary processes, environments and basins: A tribute to Peter Friend, G. Nichols, E. Williams and C. Paola, John Wiley and Sons (Eds.), p. 253-281.

Carson, C.J., Fanning, C.M., and Wilson, C.J.L., 1996, Timing of the progress granite, Larsemann hills: Additional evidence for early Palaeozoic orogenesis within the east Antarctic Shield and implications for Gondwana assembly: Australian Journal of Earth Sciences, v. 43, p. 539–553.

Carter, A., and Moss, S.J., 1999, Combined detrital-zircon fission-track and U-Pb dating: A new approach to understanding hinterland evolution: Geology, v. 27, p. 235–238.

Casshyap, S. M., and Tewari, R. C., 1988, Depositional model and tectonic evolution of Gondwana basins: Palaeobotanist, v. 36, p. 59-66.

Casshyap, S.M. and Tewari, R.C., 1991, Depositional model and tectonic evolution of Gondwana basins, In: Venkatachala, B.S., Maheswari, H.K. (Eds.), Indian Gondwana Memoir of Geological Society of India, v. 21, p. 95-206.

Casshyap, S.M., Tewari, R.C., and Srivastava, V.K., 1993, Origin and evolution of intracratonic Gondwana basins and their depositional limits in relation to Son-Narmada Lineament: Rifted Basins and Aulacogens: Geological and Geophysical Approach. Gyanodya Prakashan, Nainital, India, p. 200–215.

Cawood, P.A., 2005, Terra Australis Orogen: Rodinia breakup and development of the Pacific and Iapetus margins of Gondwana during the Neoproterozoic and Paleozoic: Earth Science Reviews, v. 69, p. 249-279.

Cerveny, P.F., 1986, Uplift and Erosion of the Himalaya over the past 18 Million years: Evidence from fission track dating of detrital zircons and heavy mineral analysis: unpublished M.S. thesis, Dartmouth College, 198 p.

Chakraborty, C., and Ghosh, S. K., 2005, Pull-apart origin of the Satpura Gondwana basin, central India: Journal of earth system science, v. 114, p. 259-273.

Chakraborty, C., and Ghosh, S.K., 2008, Pattern of sedimentation during the Late Paleozoic, Gondwanaland glaciation: An example from the Talchir Formation, Satpura Gondwana basin, central India: Journal of earth system science, v. 117, p. 499.

Chakraborty, C., Mandal, N., and Ghosh, S.K., 2003, Kinematics of the Gondwana basins of peninsular India: Tectonophysics, v. 377, p. 299-324.

Chatterjee, G. C., and Ghosh, P. K., 1970, Tectonic framework of the Peninsular Gondwanas of India: Rec. Geol. Surv. India, v. 98, p. 1-15.

Chatterjee, N., Mazumdar, A.C., Bhattacharya, A., and Saikia, R.R., 2007, Mesoproterozoic granulites of the Shillong–Meghalaya Plateau: Evidence of westward continuation of the Prydz Bay Pan-African suture into Northeastern India: Precambrian Research, v. 152, p. 1–26.

Collerson, K.D., and Sheraton, J.W., 1986, Age and geochemical characteristics of a mafic dyke swarm in the Archaean Vestfold Block, Antarctica: inferences about Proterozoic dyke emplacement in Gondwana: Journal of Petrology, v. 27, p. 853–886.

Collins, A.S., 2003, Structure and age of the northern Leeuwin Complex, Western Australia: constraints from field mapping and U-Pb isotopic analysis: Australian Journal of Earth Sciences, v. 50, p. 585-599.

Collins, A. S., and Fitzsimons, I. C. W., 2001, Structural, isotopic and geochemical constraints on the evolution of the Leeuwin Complex, SW Australia *in* Sircombe K.

N. & Li Z. X. eds. From Basins to Mountains: Rodinia at the Turn of the Century, Geological Society of Australia Abstracts 65, p. 16–19.

Collins, A.S., and Pisarevsky, S.A., 2005, Amalgamation eastern Gondwana: The evolution of the Circum-Indian Orogens: Earth-Science Reviews, v. 79, p. 229-270.

Condie, K. C., 1993, Chemical composition and evolution of the upper continental crust: Contrasting results from surface samples and shale: Chemical Geology, v. 104, p. 1-37.

Condie, K.C., Dengate, J., and Cullers, R.L., 1995, Behavior of rare earth elements in a paleoweathering profile on granodiorite in the Front Range, Colorado, USA: Geochimica et Cosmochimica Acta, v. 59, p. 279–294.

Cullers, R.L., 1994a, The chemical signature of source rocks in size fractions of Holocene stream sediment derived from metamorphic rocks in the Wet Mountains region, Colorado, U.S.A.: Chemical Geology, v. 113, p. 327–343.

Cullers, R.L., 1994b, The controls on the major and trace element variation of shales, siltstones, and sandstones of Pennsylvanian-Permian age from uplifted continental blocks in Colorado to platform sediment in Kansas, USA: Geochimica et Cosmochimica Acta, v. 58, p. 4955–4972.

Cullers, R.L., Barrett, T., Carlson, R., and Robinson, B., 1987, Rare-earth element and mineralogic changes in Holocene soil and stream sediment: A case study in the Wet Mountains, Colorado, U.S.A.: Chemical Geology, v. 63, p. 275–297.

Cullers, R.L., Basu, A., and Suttner, L.J., 1988, Geochemical signature of provenance in sand-size material in soils and stream sediments near the Tobacco Root Batholith, Montana, U.S.A: Chemical Geology, v. 70, p. 335-348.

Dasgupta, P., 2002, Architecture and facies pattern of a sublacustrine fan, Jharia basin, India: Sedimentary Geology, v. 148, p. 373– 387.

Decelles, P.G., Gehrels, G.E., Najman, Y., Martin, A.J., Carter, A., Garzanti., E., 2004, Detrital geochronology and geochemistry of Cretaceous-Early Miocene strata of Nepal: implications for timing and diachroneity of initial Himalayan orogenesis: Earth and Planetary Science Letters, v. 277, p. 313-330.

Deer, W.A., Howie, R.A., and Zussman, J., 1992, An introduction to the rock-forming minerals: Longman Scientific Technical, Harlow, United Kingdom, 696 p.

Dick, H.J.B., and Bullen, T., 1984, Chromian spinel as a petrogenetic indicator in abyssal and alpine-type peridotites and spatially associated lavas: Contributions to Mineralogy and Petrology, v. 86, p. 54-76.

Dickin, A.P., 2005, Radiogenic Isotope Geology: Cambridge University Press, 510 p.

Dickinson, W.R., 1985, Interpreting provenance relations from detrital modes of sandstones, in Zuffa, G.G., ed., Reading Provenance from Arenites: Dordecht, The Netherlands, Riedel, p. 333-361.

Dickinson, W.R., and Suczek, C.A., 1979, Plate tectonics and sandstone compositions: AAPG Bulletin, v. 63, p. 2164–2182.

Dickinson, W.R., Beard, L.S., Brakenridge, G.R., Erjavec, J.L., Ferguson, R.C., Inman, K.F., Knepp, R.A., Lindberg, F.A., and Ryberg, P.T., 1983, Provenance of North American Phanerozoic sandstones in relation to tectonic setting: Geological Society of America Bulletin, v. 94, p. 222–235.

Dodson, M.H., 1979, Theory of Cooling Ages, *in* Jäger, P.D.E. and Hunziker, P.D.D.J.C. eds., Lectures in Isotope Geology, Springer Berlin Heidelberg, p. 194–202.

Dorsey, R. J., 1988, Provenance evolution and unroofing history of a modern arc continent collision: Evidence from petrography of Plio-Pleistocene sandstones, eastern Taiwan: Journal of Sedimentary Petrology, v. 58, p. 208-218.

Dryden, A.L., and Dryden, C., 1946, Comparative rates of weathering of some common heavy minerals: Journal of Sedimentary Petrology, v. 16, p 91-96.

Dutta, P., 2002, Gondwana lithostratigraphy of Peninsular India: Gondwana Research (Gondwana Newsletter Sec), v. 5, p. 540-553.

Farhaduzzaman, M., Abdullah, W.H., and Islam, M.A., 2013, Petrographic characteristics and paleoenvironment of the Permian coal resources of the Barapukuria and Dighipara Basins, Bangladesh: Journal of Asian Earth Sciences, v. 64, p. 272-287.

Faure, G., 1986, Principles of Isotope Geology, second edition: New York, John Wiley and Sons, 589 p.

Fioretti, A.M., Black, P., Henjes-Kunst, F. and Visona`, D., 2003, Detrital zircon age patterns from a large gneissic xenolith from Cape Phillips granite and from Robertson Bay Group metasediments, northern Victoria Land, Antarctica: 9th International Symposium on Antarctic earth Science, 8–12 September, Potsdam, Terra Nostra, 2003/4, p. 94–95.

Fitzsimons, I. C. W., 2000a, A review of tectonic events in the East Antarctic Shield and their implications for Gondwana and earlier supercontinents: Journal of African Earth Sciences, v. 31, p. 3-23.

Fitzsimons, I.C.W., 2003, Proterozoic basement provinces of southern and southwestern Australia, and their correlation with Antarctica: Geological Society, London, Special Publications, v. 206, p. 93–130.

Fleet, W.F., 1926, Petrological notes on the Old Red Sandstones of the West Midlands: Geological Magazine, v. 63, p. 505-516.

Frakes, L.A., Francis, J.E., and Syktus, J.I., 1992, Climate modes for the Phanerozoic: Cambridge University Press, Cambridge, 274 p.

Frakes, L.A., Kemp, E.M., and Crowell, J.C., 1975, Late Paleozoic Glaciation: Part VI, Asia: Geological Society of America Bulletin, v. 86, p. 454-464.

Freise, F.W., 1931, Untersuchung von Mineralen auf Ab-nutzbarkeit bei Verfrachtung im Wasser: Tschermaks Mineralogy of Petrology, v. 41, p. 1-7

Fox, C. S., 1930, The Jharia Coalfield: Geological Survey of India, Memoir no. 56, 255 p.

Fox, C. S., 1931, The Gondwana System and related formations: Mem. Geological Survey of India 58 (iv), p. 241.

Garzanti, E., Vezzoli, G., Ando, S., Lave, J., Attal, M., France-Lanord, C., and DeCelles, P., 2007, Quantifying sand provenance and erosion (Marsyandi River, Nepal Himalaya): Earth and Planetary Science Letters, v. 258, p. 500-515.

Gehrels, G.E., DeCelles, P.G., Martin, A., Ojha, T.P., Pinhassi, G., and Upreti, B.N., 2003, Initiation of the Himalayan orogen as an early Paleozoic thin-skinned thrust belt: GSA today, v. 13, p. 4–9.

Ghosh, S.C., 2002, The Raniganj Coal Basin: an example of an Indian Gondwana rift: Sedimentary Geology, v. 147, p. 155-176.

Ghosh, P. K., and Bandyopadhyay, S. K., 1967, Palaeogeography of India during the Lower Gondwana times: Gondwana stratigraphy, IUGS symposium in Buenos Aires, p. 1-15.

Ghosh, P.K. and Mitra, N.D., 1970, A review of recent progress in the studies of the Gondwanas of India: Proc. 2nd Gondwana Symp., South Africa, p. 29–47.

Ghosh, S.K., and Mukhopadhyay, A., 1985, Tectonic history of the Jharia Basin–an intracratonic Gondwana basin of Eastern India: QJ Geol. Min. Metall. Soc. India, v. 57, p. 33–58.

Gotze, J., 1998, Geochemistry and provenance of the Altendorf feldspathic sandstone in the Middle Bunter of the Thuringian basin (Germany): Chemical Geology, v. 150, p. 43-61.

Graham, S.A., Ingersoll, R.V., and Dickinson, W.R., 1976, Common provenance for lithic grains in Carboniferous sandstones from Ouachita Mountains and Black Warrior Basin: Journal of Sedimentary Petrology, v. 46, p. 620–632.

Grimm, W.D., 1973, Stepwise heavy mineral weathering in the residual quartz gravel, Bavarian Molasse (Germany): Contribution to Sedimentology, v. 1, p 103-125.

Hames, W.E., and Bowring, S.A., 1994, An empirical evaluation of the argon diffusion geometry in muscovite: Earth and Planetary Science Letters, v. 124, p. 161-167.

Hasan, M.N., and Islam, M.N., 2003, Geophysical exploration for sub-surface geology and mineral resources in the Rangpur Platform, Bangladesh: GSB/AGID International Conference NESDA, GSB/AGID, Dhaka, Bangladesh, p. 1-8.

Hayashi, K. I., H.Fujisawa, Holland, H. D., and H.Ohmoto, 1997, Geochemistry of 1.9 Ga sedimentary rocks from northeastern Labrador, Canada: Geochimica et Cosmochimica Acta, v. 61, p. 4115–4137.

Henry, D.J., and Dutrow, B.L., 1992, Tourmaline in a low grade clastic metasedimentary rock: an example of the petrogenetic potential of tourmaline: Contributions to Mineralogy and Petrology, v. 112, p. 203–218.

Henry, D.J., and Dutrow, B.L., 1990, Tourmaline as a low grade clastic metasedimentary rock: an example of the petrogenetic potential of tourmaline: Contributions to Mineralogy and Petrology, v. 112, p. 203-218.

Henry, D.J., and Guidotti, C.V., 1985, Tourmaline as a petrogenetic indicator mineral: an example from the staurolite grade metapelites of NW Maine: American Mineralogists, v. 70, p. 1-15.

Herron, M. M., 1988, Geochemical classification of terrigenous sands and shales from core or log data: Journal of Sedimentary Research, v. *58*.

Hess, H.H., 1966, Notes on operation of Frantz isodynamic magnetic separator, Princeton University: User manual guide, 6 p.

Hodges, K. V., Hames, W. E., Olszewski, W., Burchfiel, B. C., Royden, L. H., and Chen, Z., 1994, Thermobarometric and $^{40}Ar/^{39}Ar$ geochronologic constraints on Eohimalayan metamorphism in the Dinggye area, Southern Tibet: Contributions to Mineralogy and Petrology, v. 117, p. 151-163.

Hodges, K.V., Rhul, K.W., Wobus, C.W., and Pringle, M.S., 2005, $^{40}Ar/^{39}Ar$ thermochronology of the detrital minerals, *in* Reiners, P.W., and Ehlers, T.A., eds., Thermochronology, Reviews in Mineralogy and Geochemistry, Mineralogical Society of America, Washington, D.C., v. 58, p. 235-257.

Hossain, H.M.Z., Islam, M.S.U., Ahmed, S.S., and Hossain, I., 2002, Analysis of sedimentary facies and depositional environments of the Permian Gondwana sequence in borehole GDH-45, Khalaspir Basin, Bangladesh: Geosciences Journal, v. 6, p. 227-236.

Hota, R.N., Das, B.K., Sahoo, M., and Maejima, W., 2011, Provenance variability during Damuda sedimentation in the Talchir Gondwana Basin, India – A statistical assessment: International Journal of Geosciences, v. 2, p. 120-137.

Hota, R.N., and Maejima, W., 2009, Heavy minerals of the Barakar Formation, Talchir Gondwana Basin, Orissa: Journal of the Geological Society of India, v. 74, p. 375–384.

Hubert, J. F., 1962, A zircon-tourmaline-rutile maturity index and the interdependence of the composition of heavy mineral assemblages with the gross composition and texture of sandstones: Journal of Sedimentary Research, v. 32.

Huque, M.A., Rahman, M.Z., Akhter, S.H., and Bhuiyan, A.H., 2003, Thin-section petrography of the Permian Gondwana coal bearing sandstones of the Barapukuria Basin, Dinajpur, Bangladesh: Bangladesh Journal of Geology, v. 22, p. 71-82.

Imam, B., 2005, Energy Resources of Bangladesh: University Grants Commission of Bangladesh, Dhaka.

Ingersoll, R.V., 1978, Submarine fan facies of the Upper Cretaceous Great Valley sequence, northern and central California: Sedimentary Geology, v. 21, p. 205–230.

Ingersoll, R.V., Bullard, T.F., Ford, R.L., Grimm, J.P., Pickle, J.D., and Sares, S.W., 1984, The effect of grain size on detrital modes: A test of the Gazzi-Dickinson point-counting method: Journal of Sedimentary Petrology, v. 54, p. 103-116.

Ingersoll, R.V., and Busby, C., 1995, Tectonics of sedimentary basins: Blackwell science.

Ingersoll, R.V., Graham, S.A., and Dickinson, W.R., 1995, Remnant ocean basins: Tectonics of sedimentary basins, p. 363–391.

Ingersoll, R.V., and Suczek, C.A., 1979, Petrology and provenance of Neogene sand from Nicobar and Bengal fans, DSDP sites 211 and 218: Journal of Sedimentary Research, v. 49.

Islam, M.S., 1990, Palynology of the Permian strata in the borehole GDH – 38 in Barapukuria basin, Dinajpur, Bangladesh: Bangladesh Journal of Geology, v. 9, p. 29-39.

Islam, M.M., Resan, S.A., Haider, M.J., Islam, M.S., Ali, M.W., and Chwodhury, M-E-A., 1987, Subsurface geology and coal deposit of Barapukuria area, Parbatipur Upazila, Dinajpur District, Bangladesh: Geological Survey Report (Unpublished).

Islam, M.N., Uddin, M.N., Resan, S.A., Sultan-ul-Islam, M., and Ali, M.W., 1992, Geology of the Khalashpir coal basin, Pirganj, Rangpur, Bangladesh: Combined report of Government of the People's Republic of Bangladesh, Ministry of Energy and Mineral Resources and Geological Survey of Bangladesh, 59 p.

Irvine, T.N., 1974, Petrology of the Duke Island ultramafic complex, southern Alaska: Geological Society of America Bulletin, v. 138, p. 240.

Irvine, T.N., 1977, Origin of chromite layers in the Muskox Intrusion and other stratiform intrusions; a new interpretation: Geology, v. 5, p. 273-277.

Johnsson, M.J., 1993, The system controlling the composition of clastic sediments, *in* Geological Society of America Special Papers, Geological Society of America, p. 1–20.

Kelley, S., 2002, Excess argon in K–Ar and Ar–Ar geochronology: Chemical Geology, v. 188, p. 1–22.

Khan, A. and Shahnawaz A., 2013, Petrography and Provenance of Early Triassic Pachmarhi Formation Sandstones, Satpura Gondwana Basin, Madhya Pradesh, Central India: Open Journal of Geology v. 3, p. 83-93.

Krauskopf, K. B., and D. K. Bird, 1995, Introduction to geochemistry: McGraw-Hill, New York, 647 p.

Kumar, P., 2004, Provenance history of Cenozoic sediments near Digboi-Margherita area, eastern syntaxis of the Himalayas, Assam, northeast India [M.S. Thesis]: Auburn University, Auburn, Alabama, 131 p.

Lovera, O.M., Grove, M., and Harrison, T.M., 2002, Systematic analysis of K-feldspar 40Ar/39Ar step heating results II: relevance of laboratory argon diffusion properties to nature: Geochimica et Cosmochimica Acta, v. 66, p. 1237–1255, doi: 10.1016/S0016-7037(01)00846-8.

Ludwig, K.R., 2003, User's manual for Isoplot, v. 3.0, a geochronological toolkit for Microsoft Excel: Berkeley Geochronological Center, Special Publication no. 4.

Maejima, W., Das, R., Pandya, K. L., and Hayashi, M., 2004, Deglacial Control on Sedimentation and Basin Evolution of Permo-Carboniferous Talchir Formation, Talchir Gondwana Basin, Orissa, India: Gondwana Research, v. 7, p. 339-352.

Mange, M. A., and Maurer, H. F. W., 1989, Heavy Minerals in Color: London, Chapman & Hall, London, 147 p.

Mange, M. A., and Maurer, H. F. W., 1992, Heavy Minerals in Color: London, Chapman & Hall, London, 147 p.

McBride E.F., 1963, A classification of common sandstones: Journal of Sedimentary Research, v. 33, p. 664-669.

McDougall, I., and Harrison, M.T., 1999, Geochronology and Thermochronology by the $^{40}Ar/^{39}Ar$ Method: New York, Oxford University Press, 269 p.

McLennan, S.M., Taylor, S.R., McCulloch, M.T., Maynard, J.B., 1990, Geochemical and Nd-Sr isotopic composition of deep-sea turbidites: Crustal evolution and plate tectonic associations, Geochemica et Cosmochemica Acta, v. 54. p. 2015-2050.

McLennan, S. M., Hemming, S., McDaniel, D. K., and Hanson, G. N., 1993, Geochemical approaches to sedimentation, provenance and tectonics. i*n* Johnson, M. J., Basu, A., eds, processes controlling the composition of the clastic sedimemts: Geological Society of America., Boulder, Colorado, Special Paper, v. 284, p. 21-40.

Medlicott, H.B., 1873, Notes on the Satpura Coal Basin: Geol. Survey of India, memoir no. 10, p. 133-188.

Meert, J.G., 2001, Growing Gondwana and Rethinking Rodinia: A Paleomagnetic Perspective: Gondwana Research, v. 4, p. 279–288.

Meert, J. G., 2003, A synopsis of events related to the assembly of eastern Gondwana: Tectonophysics, v. 362, p. 1-40.

Meert, J. G., Pandit, M. K., Pradhan, V. R., Banks, J., Sirianni, R., Stroud, M., and Gifford, J., 2010, Precambrian crustal evolution of Peninsular India: a 3.0 billion year odyssey: Journal of Asian Earth Sciences, v. 39, p. 483-515.

Milkov, A.V., 2000, World wide distribution of submarine mud volcanoes and associated gas hydrate: Marine Geology, v. 167, p. 29 -42.

Mitchell, J.G., Penven, M.-J., Ineson, P.R., and Miller, J.A., 1988, Radiogenic argon and major-element loss from biotite during natural weathering: A geochemical approach to the interpretation of potassium—argon ages of detrital biotite: Chemical Geology: Isotope Geoscience section, v. 72, p. 111–126.

Moore, M. F., 2012, $^{40}Ar/^{39}Ar$ Dating of Detrital Muscovite and Sediment Compositional Analysis of the Pottsville Formation in the Black Warrior basin in Alabama: Implications for Tectonics and Sedimentation [unpublished M.S. Thesis]: Auburn University, Auburn, AL, 132 p.

Morton, A.C., 1984, Stability of detrital heavy minerals in Tertiary sandstones of the North Sea Basin: Clay Mineralogy, v. 19, p 287-308.

Morton, A.C., 1985, Heavy minerals in provenance studies, in Zuffa, G.G., eds., Provenance of Arenites: Boston, D. Reidel Publishing Company, p. 249-277.

Morton, A.C., 1986, Dissolution of apatite in North Sea Jurassic sandstone: Implications for the generation of secondary porosity: Clay Mineralogy, v. 21, p 711-733.

Morton, A. C., and Hallsworth, C., 1994, Identifying provenance-specific features of detrital heavy mineral assemblages in sandstones: Sedimentary Geology, v. 90, p. 241-256.

Morton, A.C., and Hallsworth, C.R., 1999, Processes controlling the composition of heavy mineral assemblages in sandstones: Sedimentary Geology, v. 124, p. 3-30.

Morton, A.C., and Taylor, P.N., 1991, Geochemical and isotopic constraints on the nature and age of basement rocks from Rockall Bank, NE Atlantic: Journal of the Geological Society, London, v. 148, p. 630-634.

Mukhopadhyay, G., Mukhopadhyay, S.K., Roychowdhury, M., and Parui, P.K., 2010, Stratigraphic correlation between different Gondwana basins of India: Geological Society of India, v. 76, p. 251-266.

Murphy, S.F., Brantley, S.L., Blum, A.E., White, A.F., and Dong, H., 1998, Chemical Weathering in a Tropical Watershed, Luquillo Mountains, Puerto Rico: II. Rate and

Mechanism of Biotite Weathering: Geochimica et Cosmochimica Acta, v. 62, p. 227–243.

Najman, Y., 2006, The detrital record of orogenesis: A review of approaches and techniques used in the Himalayan sedimentary basins: Earth-Science Reviews, v. 74, p. 1–72.

Najman, Y., and Garzanti, E., 2000, Reconstructing early Himalayan tectonic evolution and paleogeography from Tertiary foreland basin sedimentary rocks, northern India: Geological Society of America Bulletin, v. 112, p. 435-449.

Nanayama, F., 1997, An electron microprobe study of the Amazon Fan: Proceedings of the Ocean Drilling Program, Scientific Results, v. 155, p. 147-168.

Nandi, K., 1967, Garnets as indices of progressive regional metamorphism: Mineralogical Magazine, v. 36, p. 89-93.

Nelson, D.R., Myers, J.S., and Nutman, A.P., 1995, Chronology and evolution of the Middle Proterozoic Albany-Fraser Orogen, Western Australia: Australian Journal of Earth Sciences, v. 42, p. 481–495.

Nesbitt, H.W., and Young, G.M., 1982, Early Proterozoic climates and plate motions inferred from major element chemistry of lutites: Nature, v. 299, p. 715–717.

Nixon, G.T., Cabri, L.J., and Laflamme, J.H.G, 1990, Platinum-group-element mineralization in lode and placer deposits associated with the Tulameen Alaskan-type complex, British Columbia: The Canadian Mineralogist, v. 28, p. 503-535.

Osae, S., Asiedu, D.K., Banoeng-Yakubo, B., Koeberl, C., and Dampare, S.B., 2006, Provenance and tectonic setting of Late Proterozoic Buem sandstones of southeastern Ghana: Evidence from geochemistry and detrital modes: Journal of African Earth Sciences, v. 44, p. 85–96.

Parsons, I., Brown, W.L., and Smith, J.V., 1999, 40Ar/39Ar thermochronology using alkali feldspars: real thermal history or mathematical mirage of microtexture?: Contributions to Mineralogy and Petrology, v. 136, p. 92–110.

Peavy, T., 2008, Provenance of lower Pennsylvanian Pottsville Formation, Cahaba synclinorium, Alabama [unpublished M.S. Thesis]: Auburn University, Auburn, AL, 106 p.

Pettijohn, F.J., 1941, Persistence of heavy minerals and geologic age: Journal of Geology, v. 49, p 610-625.

Pettijohn, T.J., Potter, P.E., and Siever, R., 1973, Sand and Sandstones: New York, Springer-Verlag, 618 p.

Rahman, M.W., 2008, Sedimentation and tectonic evolution of Cenozoic sequence from Bengal and Assam foreland basin, Eastern Himalayas [Unpublished M.S. Thesis]: Auburn, Auburn University, 180 p.

Rahman, M.H., and Ahmed, F., 1996, Scanning electron microscopy of quartz grain surface textures of the Gondwana Sediments, Barapukuria, Dinajpur, Bangladesh: Journal of the Geological Society of India, v. 47, p. 207-214.

Rahman, M. J. J., and Suzuki, S., 2007, Geochemistry of sandstones from the Miocene Surma Group, Bengal Basin, Bangladesh: Implications for Provenance, tectonic setting and weathering: Geochemical Journal, v. 41, p. 415-428

Reiners, P.W., Spell, T.L., Nicolescu, S., and Zanetti, K.A., 2004, Zircon (U-Th)/He thermochronometry: Geochemical Cosmochemial Acta, v. 68, p. 1857-1887.

Renne, P.R., Swisher, C.C., Deino, A.L., Karner, D.B., Owens, T.L., and DePaolo, D.J., 1998, Intercalibration of standards, absolute ages, and uncertainties in 40Ar/39Ar dating: Chemical Geology, v. 145, p. 117-152.

Rogers, J.J.W., Unrug, R., and Sultan, M., 1995, Tectonic assembly of Gondwana: Journal of Geodynamics, v. 19, p. 1-34.

Roser, B.P., and Korsch, R.J., 1986, Determination of tectonic setting of sandstone-mudstone suites using content and ratio: The Journal of Geology, p. 635–650.

Roser, B. P., and Korsch, R. J., 1988, Provenance signatures of sandstone-mudstone suites determined using discriminant function analysis of major-element data: Chemical Geology, v. 67, p. 119-139.

Roy, D.K., and Roser, B.P., 2013, Climatic control on the composition of Carboniferous-Permian Gondwana sediments, Khalaspir basin, Bangladesh: Gondwana Research, v. 23, p 1163–1171.

Sageman, B. B., and Lyons, T. W., 2003, Geochemistry of Fine-grained Sediments and Sedimentary Rocks: Treatise on Geochemistry, v. 7, p.115-158.

Scherer, A., 2007, $^{40}Ar/^{39}Ar$ dating and errors, www.geoberg.de.

Sevastjanova, I., Hall, R., and Alderton, D., 2012, A detrital heavy mineral viewpoint on sediment provenance and tropical weathering in SE Asia: Sedimentary Geology, v. 280, p. 179–194.

Sheraton, J.W., Black, L.P., and Tindle, A.G., 1992, Petrogenesis of plutonic rocks in a Proterozoic granulite-facies terrane—the Bunger Hills, East Antarctica: Chemical Geology, v. 97, p. 163–198.

Sifeta, K., Roser, B.P., and Kimura, J.-I., 2005, Geochemistry, provenance, and tectonic setting of Neoproterozoic metavolcanic and metasedimentary units, Werri area, Northern Ethiopia: Journal of African Earth Sciences, v. 41, p. 212–234.

Sitaula, R.P., 2009, Petrofacies and paleotectonic evolution of Gondwanan and post-Gondwanan sequences of Nepal [unpublished M.S. Thesis]: Auburn University, Auburn, AL, 186 p.

Soreghan, M. J., and Soreghan, G. S. L., 2007, Whole-rock geochmistry of upper Paleozoic loessite, western Pangaea: Implication for paleo-atmospheric circulation: Earth and Planetary Science Letters, v. 255, p. 117-132.

Stover, L.E., 1964, Palynology of coals from the EDH-5 bore, East Pakistan: Jersy Production Research Company, Geological Division, JS 64, p. 126.

Strut, B.A., 1962, The composition of garnets from pelitic schists in relation to the grade of regional metamorphism: Journal of Petrology, v. 3, p. 181-191.

Sugitani, K., Horiuchi, Y., Adachi, M., and Sugisaki, R., 1996, Anomalously low Al_2O_3/TiO_2 values for Archean cherts from the Pilbara Block, Western Australia--possible evidence for extensive chemical weathering on the early earth: Precambrian Research, v. 80, p. 49–76.

Suttner, L.J., 1974, Sedimentary petrologic provinces: An evaluation, *in* Ross, C.A., ed., Paleogeographic Provinces and Provinciality, Society of Economic Paleontologists and Mineralogists, Special Publication, v. 21, p. 75-84.

Tapsoba, N., Sauzéat, C., and Benedetto, H., 2013, Analysis of Fatigue Test for Bituminous Mixtures: Journal of Materials in Civil Engineering, v. 25, p. 701–710.

Taylor, S.R., and McLennan, S.M., 1995, The geochemical evolution of the continental crust: Reviews of Geophysics, v. 33, p. 241–265.

Taylor, S. R., and McLennan, S. M., 1985, The continental crust: Its composition and evolution: Oxford, Blackwell Scientific Publication, 312 p.

Tewari, R.C., 1999, Sedimentary - Tectonic Status of Permian - Triassic Boundary (250 Ma) in Gondwana Stratigraphy of Peninsular India: Gondwana Research, v. 2, p. 185-189.

Tewari, R.C., and Maejima, W., 2010, Origin of Gondwana Basins of Peninsular India: Journal of geosciences, Osaka City University, v. 53, p. 43–49.

Tiwari, R., and Yadav, R.N.S., 1993, Significance of heavy minerals: A case study from the Siwaliks of the Garhwal Himalaya: Jour. Ind. Acad. Geoscience, v. 36, p. 1-10.

Uddin, A., Hames, W.E., and Zahid, K.M., 2010, Laser 40Ar/39Ar age constraints on Miocene sequences from the Bengal basin: Implications for middle Miocene denudation of the eastern Himalayas: Journal of Geophysical Research: Solid Earth, v. 115, p. B07416.

Uddin, A., Kumar, P., Sarma, J.N., and Akhter, S.H., 2007, Heavy-mineral constraints on provenance of Cenozoic sediments from the foreland basins of Assam, India and Bangladesh: Erosional history of the eastern Himalayas and the Indo-Burman ranges, in Mange, M.A., and Wright, D.T., (Eds.), Heavy Minerals in Use, Development in Sedimentology, Elsevier, Amsterdam, v. 58, p. 823-847.

Uddin, A., and Lundberg, N., 1998, Cenozoic history of the Himalayan-Bengal system: Sand composition in the Bengal basin, Bangladesh: Geological Society of America Bulletin, v. 110, p. 497-511.

Uddin, A., and Lundberg, N., 2004, Miocene sedimentation and subsidence during continent–continent collision, Bengal Basin, Bangladesh: Sedimentary Geology, v. 164, p. 131-146.

Uddin, M.N., 1996, Structure and sedimentation in the Gondwana basins of Bangladesh: Proc. 9th International Gondwana Symposium, Oxford and IBH Pub, New Delhi. p. 805–819.

Uddin, M.N., and Islam, M.S., 1992, Gondwana Basins and their coal resources in Bangladesh: Geology in South Asia -1: Proceedings of First South Asian Geological Congress, Pakistan, p. 224-230.

Vaidyanadhan, R., and Ramakrishnan, M., 2008, Geology of India: Geological Society of India, Bangalore.

Veevers, J.J., 2000a, Billion-Year Earth History of Australia and Neighbours in Gondwanaland: GEMOC Press, Sydney, 400 p.

Veevers, J.J., 2004, Gondwanaland from 650–500 Ma assembly through 320 Ma merger in Pangea to 185–100 Ma breakup: supercontinental tectonics via stratigraphy and radiometric dating: Earth-Science Reviews, v. 68, p. 1–132.

Veevers, J.J., and Tewari, R.C., 1995, Gondwana Master Basin of peninsular India between Tethys and the interior of the Gondwanaland province of Pangea: Geological Society of America, Memoir no. 187, 71 p.

Velbel, M.A., 1985, Mineralogically mature sandstone in accretional prisms: Journal of Sedimentary Petrology, v. 55, p. 685-690.

Verma, R.K., Bhuin, N.C., and Mukhopadhyay, M., 1979, Geology, structure and tectonics of the Jharia coalfield, India — A three-dimensional model: Geoexploration, v. 17, p. 305–324.

Verma, R.K., and Ghosh, D., 1974, Gravity survey over Jharia coalfield, India: Geophysical Research Bulletin, v. 124, p. 165-175.

Vermeesch, P., 2004, How many grains needed for a provenance study?: Earth and Planetary Science Letters, v. 224, p. 441-451.

Wadia, D.N., 1919, Geology of India, 3rd edition: Macmillan and Co Ltd., London, 536p.

Weller, J.M., 1958, Stratigraphic facies differentiation and nomenclature: American Association of Petroleum Geologists Bulletin, v. 42, p. 609-639.

White, N.M., Pringle, M., and Garzanti, E., 2002, Constraints on the exhumation and erosion of the High Himalayan Slab, NW India, from foreland basin deposits: Earth and Planetary Science Letters, v. 195, p. 29-44.

Wright, T.O., and Dallmeyer, R.D., 1991, The age of cleavage development in the Ross orogen, northern Victoria Land, Antarctica: Evidence from $^{40}Ar/^{39}Ar$ whole-rock slate ages: Journal of Structural Geology, v. 13, p. 677-690.

Wronkiewicz, D.J., and Condie, K.C., 1987, Geochemistry of Archean shales from the Witwatersrand Supergroup, South Africa: Source-area weathering and provenance: Geochimica et Cosmochimica Acta, v. 51, p. 2401–2416.

Wronkiewicz, D.J., and Condie, K.C., 1990, Geochemistry and mineralogy of sediments from the Ventersdorp and Transvaal Supergroups, South Africa: cratonic evolution during the early Proterozoic: Geochimica et Cosmochimica Acta, v. 54, p. 343-354.

Yoshida, M., and Upreti, B.N., 2006, Neoproterozoic India within East Gondwana: Constraints from recent geochronologic data from Himalaya: Gondwana Research, v. 10, p. 349–356.

Zaher, M.A., and Rahman, A., 1980, Prospects and investigations for minerals in the northern part of Bangladesh in Petroleum and Mineral Resources of Bangladesh, Seminar and Exhibition: Dhaka, Government of People's Republic of Bangladesh, p. 9-18.

Zahid, K.M., 2005, Provenance and basin tectonics of Oligocene-Miocene sequences of the Bengal Basin, Bangladesh [M.S. Thesis]: Auburn University, Auburn, Alabama, 142 p.

APPENDIX A (i): Microprobe data for garnet from the Gondwanan sequences of India and Bengal Basin.

Sample	BB3 C	IT2 D	IT2C	IT1 Garnet	BK6 A	BB1	BB1_1	BB1_2	BB1_3
SiO2	37.11	37.29	36.85	36.81	37.23	37.23	38.09	37.51	38.20
TiO2	0.023	0.025	0.063	0.027	0.017	0.013	0.02	0.02	0.17
Al2O3	21.088	20.885	21.026	20.43	21.268	21.072	21.99	21.71	21.92
Cr2O3	-0.144	-0.027	-0.046	0.044	0.075	0.109	0.11	-0.11	0.10
FeO / FeOtot	33.555	27.314	28.022	31.016	35.488	28.282	29.34	29.86	29.76
MnO	0.618	0.686	1.662	1.625	1.356	4.134	0.37	3.35	0.42
MgO	4.982	4.556	6.968	2.625	3.75	6.273	8.16	5.59	7.82
CaO	0.871	6.788	1.795	6.119	0.769	1.349	0.77	0.90	1.34
Na2O	0.029	0.021	-0.011	0.022	0	0.036	-0.04	0.03	0.00
Total	98.141	97.575	96.351	98.856	99.96	98.601	98.82	98.85	99.73

Sample	IT1_1	IT1_2	IT1_3	BK9_1	BK9_2	BK9_3	BB6_1	BB6_2	BD1_1	BD1_2
SiO2	36.79	36.90	38.34	37.65	36.83	37.66	36.21	36.52	37.04	37.38
TiO2	-0.03	-0.06	-0.05	0.00	0.01	0.00	0.04	0.00	0.07	0.04
Al2O3	21.25	21.11	21.91	21.75	21.07	21.25	20.28	20.86	21.11	21.44
Cr2O3	-0.08	-0.10	0.10	0.10	0.05	0.10	-0.07	0.05	-0.02	0.00
FeO / FeOtot	35.91	32.37	28.18	30.92	29.20	30.37	33.92	32.84	34.04	30.54
MnO	1.15	0.54	0.26	0.81	6.98	0.67	2.11	6.09	0.52	1.92
MgO	3.42	4.82	8.72	6.62	3.65	5.92	1.08	2.03	4.83	6.20
CaO	2.01	2.07	1.47	1.07	0.33	2.72	5.06	0.95	1.57	1.34
Na2O	-0.01	0.00	0.01	-0.06	0.04	-0.03	0.00	-0.08	0.01	0.02
Total	100.43	97.64	98.93	98.85	98.16	98.66	98.63	99.26	99.17	98.85

APPENDIX A (ii): Microprobe data for garnet from the Gondwanan sequences of India and Bengal Basin.

End Members									
Schorlomite-Al			0.19%	0.08%	0.05%	0.04%	0.06%	0.07%	0.49%
NaTi garnet	0.07%	0.08%							
Uvarovite				0.14%	0.24%	0.34%	0.34%		0.31%
Spessartine	1.41%	1.56%	3.80%	3.72%	3.07%	9.32%	0.82%	7.55%	0.93%
Pyrope	20.03%	18.22%	28.05%	10.57%	14.97%	24.89%	31.83%	22.19%	30.30%
Almandine	75.69%	60.56%	62.68%	67.22%	79.45%	60.69%	64.23%	66.46%	64.63%
Grossular	2.49%	18.69%	4.89%	15.08%	1.92%	2.90%	1.76%	2.50%	2.92%
Andradite		0.79%		2.40%		0.56%			
Remainder	0.31%	0.11%	0.39%	0.80%	0.30%	1.25%	0.95%	1.23%	0.42%
Total	100.00%	100.01%	100.00%	100.01%	100.00%	99.99%	99.99%	100.00%	100.00%
Quality Index	Good	Excellent	Excellent	Superior	Superior	Excellent	Excellent	Good	Superior

End Members										
Schorlomite-Al				0.01%		0.01%	0.13%		0.21%	0.10%
NaTi garnet					0.02%					
Uvarovite			0.31%	0.30%	0.17%	0.31%		0.17%		
Spessartine	2.60%	1.23%	0.57%	1.82%	16.09%	1.52%	4.90%	14.09%	1.17%	4.30%
Pyrope	13.61%	19.43%	33.80%	26.11%	14.82%	23.42%	4.42%	8.26%	19.26%	24.51%
Almandine	76.21%	73.07%	61.04%	68.41%	66.52%	67.44%	75.23%	75.00%	74.09%	66.41%
Grossular	4.92%	5.99%	3.78%	2.71%	0.78%	7.30%	12.63%	2.20%	3.73%	3.69%
Andradite	0.77%						2.05%		0.55%	
Remainder	1.89%	0.29%	0.50%	0.64%	1.59%	0.00%	0.64%	0.28%	0.98%	0.98%
Total	100.00%	100.01%	100.00%	100.00%	99.99%	100.00%	100.00%	100.00%	99.99%	99.99%
Quality Index	Excellent	Superior	Superior	Excellent	Fair	Excellent	Superior	Excellent	Superior	Superior

APPENDIX B: Microprobe data for tourmaline from the Gondwanan sequences of India and Bengal Basin.

Weight percentage of oxides from micropobe analysis											
Sample No.	**SiO_2**	**TiO_2**	**Al_2O_3**	**MgO**	**FeO**	**CaO**	**MnO**	**K_20**	**Na_2O**	**Cr_2O_3**	**Total**
IT2-1	33.839	0.289	31.315	4.238	10.281	0.264	0.065	-0.04	2.088	-0.028	82.312
IT2-2	33.835	0.169	31.059	7.122	7.491	1.509	0.06	-0.031	1.559	0.095	82.869
BB6	35.711	0.867	30.665	9.617	3.921	2.078	-0.053	-0.053	1.525	0.06	84.339
BD1-1	34.689	0.841	31.2	5.381	10.914	1.346	0.012	-0.053	1.585	0.094	86.008
BD1-2	34.128	0.929	27.741	8.505	9.014	2.942	-0.012	0.006	1.223	-0.059	84.418

End member calculation								
					Percentage			
Sample No.	Ca	Mg	Fe (tot)	Total	Ca	Mg	Fe (tot)	Total
IT2-1	0.049615	1.10821	1.508147	2.665972	1.861052	41.56869	56.57026	100
IT2-2	0.278497	1.828877	1.07912	3.186494	8.739925	57.39464	33.86543	100
BB6	0.373149	2.402852	0.549581	3.325582	11.22056	72.25358	16.52586	100
BD1-1	0.244865	1.362055	1.549755	3.156675	7.75704	43.14841	49.09455	100
BD1-2	0.537907	2.163664	1.286413	3.987984	13.48819	54.25458	32.25723	100

End member calculation								
					Percentage			
Sample No.	Al	Al50Fe(tot)50	Al50Mg50	Total	Al	Al50Fe(tot)50	Al50Mg50	Total
IT2-1	6.47382	3.990984	3.791014733	14.2558181	45.41177	27.99547238	26.59275	100
IT2-2	6.305465	3.692293	4.067171065	14.064929	44.83112	26.25176879	28.91711	100
BB6	6.057278	3.30343	4.230064989	13.5907727	44.56905	24.30641454	31.12454	100
BD1-1	6.243577	3.896666	3.802816071	13.9430592	44.7791	27.94699532	27.2739	100
BD1-2	5.579365	3.432889	3.871514218	12.8837678	43.30538	26.64506959	30.04955	100

APPENDIX C: Microprobe data for chrome spinel from the Gondwanan sequences of Dighipara drill well, Bengal Basin.

Weight percentage of oxides from micropobe analysis

Sample No.	SiO_2	TiO_2	Al_2O_3	MgO	FeO	CaO	MnO	Cr_2O_3	Total
BD7-1	0.11	0.76	2.31	0.11	47.64	0.02	0.32	17.66	68.93
BD7-2	-0.01	1.52	2.81	0.05	59.63	0.05	0.81	28.95	93.80
BD7-3	0.06	0.85	4.71	0.18	47.65	0.02	0.70	38.13	92.30
BD7-4	0.01	0.69	5.12	0.17	49.82	0.03	0.98	38.52	95.32
K-1 CrSp5	0.14	0.68	41.89	17.31	16.78	0.04	0.23	23.08	100.15

End Member Calculation

Sample No.	Al3+	Cr3+	Fe3+	Total	Fe3+/Fe3++Cr+Al	Mg#(Mg/Mg+Fe^{2+})	Cr#(Cr/Cr+Al)	TiO2 (wt%)
BD7-1	10.13741	51.9291	37.9334416	100	0.379334416	0.005402554	0.836668649	0.76
BD7-2	8.728103	60.2737	30.9982026	100	0.309982026	0.001874807	0.873509046	1.522
BD7-3	12.95895	70.3405	16.7005224	100	0.167005224	0.008050599	0.84442935	0.852
BD7-4	13.60492	68.728	17.6670921	100	0.176670921	0.007217638	0.834757249	0.688

APPENDIX D: $^{40}Ar/^{39}Ar$ age data of detrital muscovite from the Gondwanan sequences of India and Bengal Basin.

Sensitivity (Moles/volt):	1.62E-14	± 0.000
J-Value:	28020000	± 112080.00
Measured 40/36 of Air:	291	± 1.50
Mass Discrimination (% per amu):	-0.002115	± 0.0010
(36/37)Ca:	0.0002900	± 0.00001
(39/37)Ca:	0.0006800	± 0.00011
(40/39)K:	0	± 0.00040
(38/39)Cl:	0.01	± 0.01000
% of Sample in Split	0.58	
Date of Irradiation:	9/9/2013	
Date of Analysis:	4/28/2014	

Samples were irradiated in the central core positon of the USGS TRIGA reactor in Denver, CO. Synthetic CaF2 was included with the irradiation to determine calcium production factors, and biotite GA1550 (from an aliquot prepared by Mike Cosca) was used to monitor production of 39ArK. Monitors were placed four positions (3 radial positions and one central position, 'S') for each layer of the irradiation package. All samples of the present study are from a single irradiation layer. Aliquots of air from an air pipette were measured daily to evaluate mass discrimination, and procedural blanks were measured following every five analyses of unknowns. Samples were analyzed in the Auburn Noble Isotope Mass Analysis Laboratory (ANIMAL) following gas extraction with a CO2 laser using an automated extraction line. Data were collected with the 10-cm radius of curvature GLM-110 mass spectrometer using an electron multiplier. Data presented are in volts unless otherwise indicated, and are corrected for backgrounds, mass discrimination, and decay of short-lived isotopes. 'P' refers to the laser power and 't' to seconds for laser heating; 'R' is the 40Ar*/39ArK ratio. Errors in measurement, individual calculated ages and plateau ages are 1 standard deviation; means are reported at the 95% confidence level. Plateau and biweight mean calculations were made using Isoplot (Ludwig, K.R., 2003, Isoplot v. 3.0, A geochronology toolkit for Microsoft Excel, Special Publication #4, Berkeley Geochronology Center).

Representative photographs are provided for muscovite grains of each sample.

Data For Standards, Blanks, and Monitors

Representative Air Analysis	P	t	40 V	39 V	38 V	37 V	36 V	Moles 40Ar*	40/36	40/38	M. Fract	Date
air.4.2.14.a.txt	0	0	23.57225 0.01316	0.00025 0.00016	0.01572 0.00010	0.00041 0.00003	0.0808418 0.0002738	3.83E-13	**291.6**	**1500**	0.9966878	########
Representative Blank	**P**	**t**	**40 V**	**39 V**	**38 V**	**37 V**	**36 V**	**Moles 40Ar***				
blank.4.28.14.m.txt	0	0	0.01318 ± 0.000228	0.00112 ± 0.000045	0.00027 ± 0.000009	0.00048 ± 0.000016	0.0001293 ± 0.000006	2.14E-16	102	214.3		

GA-1550 Biotite Flux Monitor, Single Crystal Analyses and J-Values

Monitor	P	t	40	39	38	37	36	Moles 40Ar*	% Rad	R	J-value	% -sd
au24.4c.bio.75a.txt	2.2	10	5.84002 ± 0.004231	1.54799 ± 0.001209	0.12849 ± 0.000502	0.00415 ± 0.000399	0.002113 ± 0.000030	9.48E-14	89.31%	3.36946	0.01670485 ± 0.000034	0.21%
au24.4c.bio.76a.txt	2.2	10	8.91857 ± 0.005501	2.30971 ± 0.003341	0.17116 ± 0.000481	0.00556 ± 0.000318	0.003872 ± 0.000055	1.45E-13	87.17%	3.36613	0.01672140 ± 0.000046	0.28%
au24.4c.bio.77a.txt	2.2	10	3.03094 ± 0.002976	0.84629 ± 0.000918	0.07276 ± 0.000424	0.00269 ± 0.000264	0.000583 ± 0.000027	4.92E-14	94.32%	3.37832	0.01666102 ± 0.000053	0.32%
au24.4c.bio.78a.txt	2.2	10	2.77984 ± 0.002630	0.71169 ± 0.001067	0.06476 ± 0.000383	0.03550 ± 0.000281	0.001285 ± 0.000025	4.51E-14	86.34%	3.37701	0.01666749 ± 0.000062	0.37%
au24.4c.bio.79a.txt	2.2	10	6.19983 ± 0.005957	1.55501 ± 0.001618	0.12926 ± 0.000391	0.00299 ± 0.000452	0.003170 ± 0.000032	1.01E-13	84.89%	3.38473	0.01662949 ± 0.000041	0.25%
au24.4g.bio.80a.txt	2.2	10	4.63722 ± 0.003849	1.32336 ± 0.001410	0.10390 ± 0.000518	0.00214 ± 0.000258	0.000527 ± 0.000022	7.53E-14	96.64%	3.38664	0.01662010 ± 0.000034	0.20%
au24.4g.bio.81a.txt	2.2	10	3.81051 ± 0.003783	0.97291 ± 0.000609	0.08510 ± 0.000282	0.00300 ± 0.000206	0.001709 ± 0.000026	6.19E-14	86.75%	3.39795	0.01656477 ± 0.000044	0.27%
au24.4g.bio.82a.txt	2.2	10	2.28831 ± 0.002812	0.59958 ± 0.000884	0.05310 ± 0.000256	0.00229 ± 0.000274	0.000864 ± 0.000025	3.72E-14	88.84%	3.39088	0.01659932 ± 0.000070	0.42%
au24.4g.bio.83a.txt	2.2	10	2.82057 ± 0.002925	0.75822 ± 0.000843	0.06667 ± 0.000480	0.00118 ± 0.000147	0.000858 ± 0.000028	4.58E-14	91.01%	3.38566	0.01662492 ± 0.000061	0.37%
au24.4g.bio.84a.txt	2.2	10	6.06454 ± 0.004093	1.60441 ± 0.001825	0.13838 ± 0.000635	0.01086 ± 0.000319	0.002162 ± 0.000027	9.85E-14	89.46%	3.38229	0.01664149 ± 0.000035	0.21%
au24.4k.bio.85a.txt	2.2	10	1.19134 ± 0.001452	0.34674 ± 0.000828	0.03011 ± 0.000319	0.00024 ± 0.000287	0.000041 ± 0.000022	1.93E-14	98.98%	3.40094	0.01655023 ± 0.000103	0.63%
au24.4k.bio.86a.txt	2.2	10	3.50356 ± 0.002877	1.02470 ± 0.001368	0.08467 ± 0.000389	0.00540 ± 0.000188	0.000141 ± 0.000021	5.69E-14	98.81%	3.37891	0.01665815 ± 0.000040	0.24%
au24.4k.bio.87a.txt	2.2	10	8.92129 ± 0.006849	2.35210 ± 0.002993	0.20992 ± 0.000396	0.00352 ± 0.000504	0.003343 ± 0.000034	1.45E-13	88.93%	3.37305	0.01668707 ± 0.000035	0.21%
au24.4k.bio.88a.txt	2.2	10	3.51452 ± 0.004210	0.90752 ± 0.001384	0.08017 ± 0.000403	0.00169 ± 0.000347	0.001441 ± 0.000026	5.71E-14	87.88%	3.40359	0.01653735 ± 0.000055	0.33%
au24.4k.bio.89a.txt	2.2	10	3.09813 ± 0.002315	0.85712 ± 0.000964	0.07467 ± 0.000306	0.00161 ± 0.000251	0.000689 ± 0.000021	5.03E-14	93.43%	3.37718	0.01666666 ± 0.000044	0.26%
au24.4s.bio.90a.txt	2.2	10	10.58952 ± 0.004149	2.90870 ± 0.003563	0.25269 ± 0.000828	0.06494 ± 0.000394	0.002612 ± 0.000073	1.72E-13	92.71%	3.37741	0.01666555 ± 0.000043	0.26%
au24.4s.bio.91a.txt	2.2	10	8.31076 ± 0.005414	2.06401 ± 0.002308	0.18281 ± 0.000422	0.00363 ± 0.000278	0.004399 ± 0.000030	1.35E-13	84.36%	3.39692	0.01656980 ± 0.000033	0.20%
au24.4s.bio.92a.txt	2.2	10	7.63464 ± 0.009196	2.09289 ± 0.001476	0.18262 ± 0.000488	0.10541 ± 0.001098	0.001876 ± 0.000026	1.24E-13	92.74%	3.38782	0.01661434 ± 0.000031	0.18%
au24.4s.bio.93a.txt	2.2	10	9.79036 ± 0.014622	2.79037 ± 0.004172	0.24191 ± 0.000536	0.02810 ± 0.000237	0.001178 ± 0.000027	1.59E-13	96.44%	3.38482	0.01662905 ± 0.000039	0.23%
au24.4s.bio.94a.txt	2.2	10	2.64900 ± 0.001833	0.73576 ± 0.001197	0.06535 ± 0.000208	0.00206 ± 0.000173	0.000508 ± 0.000023	4.30E-14	94.33%	3.39646	0.01657204 ± 0.000054	0.33%

Sample	P	t	40 V	39 V	38 V	37 V	36 V	Moles 40Ar*	% Rad	R	Age (Ma)	% -sd
I-B-4												
au25.4h.mus.3a.txt	1.8	10	14.29879 ± 0.010871	0.44551 ± 0.000686	0.00598 ± 0.000066	0.01768 ± 0.000519	0.000234 ± 0.000016	2.32E-13	99.5%	31.9453	768.88 ± 1.35	0.18%
au25.4h.mus.4a.txt	1.8	10	8.09664 ± 0.009452	0.28958 ± 0.000353	0.00372 ± 0.000057	0.00160 ± 0.000448	0.000029 ± 0.000017	1.31E-13	99.9%	27.9314	688.45 ± 1.24	0.18%
au25.4h.mus.5a.txt	1.85	10	10.59734 ± 0.007089	0.54257 ± 0.001267	0.00714 ± 0.000080	0.01464 ± 0.000976	0.000146 ± 0.000014	1.72E-13	99.6%	19.4551	505.83 ± 1.25	0.25%
au25.4h.mus.6a.txt	1.8	10	9.94676 ± 0.014303	0.38158 ± 0.000830	0.00494 ± 0.000061	0.00226 ± 0.000892	0.000110 ± 0.000010	1.61E-13	99.7%	25.9825	648.07 ± 1.71	0.26%
au25.4h.mus.7a.txt	1.85	10	20.05108 ± 0.009252	0.65907 ± 0.001289	0.00884 ± 0.000062	0.02026 ± 0.000625	0.000079 ± 0.000031	3.26E-13	99.9%	30.3915	738.17 ± 1.52	0.21%
au25.4h.mus.8a.txt	1.8	10	22.81786 ± 0.009625	1.18558 ± 0.001988	0.01539 ± 0.000114	0.02063 ± 0.000952	0.000232 ± 0.000013	3.70E-13	99.7%	19.1901	499.81 ± 0.87	0.17%
au25.4h.mus.11a.txt	1.8	10	9.99075 ± 0.019175	0.31935 ± 0.000980	0.00414 ± 0.000048	0.00235 ± 0.000491	0.000027 ± 0.000021	1.62E-13	99.9%	31.2610	755.42 ± 2.77	0.37%
au25.4h.mus.12a.txt	1.8	10	16.58383 ± 0.012225	0.57895 ± 0.001621	0.00836 ± 0.000079	0.01870 ± 0.000747	0.000164 ± 0.000016	2.69E-13	99.7%	28.5644	701.38 ± 2.05	0.29%
au25.4h.mus.13a.txt	1.8	10	13.35300 ± 0.010935	0.39623 ± 0.001014	0.00534 ± 0.000077	0.02011 ± 0.000920	0.000179 ± 0.000017	2.17E-13	99.6%	33.5719	800.48 ± 2.18	0.27%
au25.4h.mus.14a.txt	1.8	10	11.13369 ± 0.010794	0.42209 ± 0.000514	0.00595 ± 0.000066	0.01802 ± 0.000537	0.000064 ± 0.000027	1.81E-13	99.8%	26.3372	655.49 ± 1.12	0.17%
au25.4h.mus.15a.txt	1.8	10	3.28689 ± 0.003257	0.10150 ± 0.000443	0.00125 ± 0.000033	0.00040 ± 0.000680	-0.000011 ± 0.000013	5.34E-14	100.1%	32.3823	777.42 ± 3.60	0.46%
au25.4h.mus.16a.txt	1.8	10	7.03429 ± 0.005843	0.30896 ± 0.000679	0.00397 ± 0.000044	0.00033 ± 0.000764	-0.000003 ± 0.000019	1.14E-13	100.0%	22.7679	579.42 ± 1.43	0.25%
au25.4h.mus.17a.txt	1.8	10	5.58726 ± 0.007576	0.16242 ± 0.000666	0.00211 ± 0.000042	0.00150 ± 0.000837	-0.000009 ± 0.000018	9.07E-14	100.0%	34.4008	816.37 ± 3.61	0.44%
au25.4h.mus.18a.txt	1.8	10	10.86282 ± 0.018327	0.34179 ± 0.000685	0.00462 ± 0.000050	0.02020 ± 0.001086	0.000075 ± 0.000030	1.76E-13	99.8%	31.7236	764.53 ± 2.10	0.27%
au25.4h.mus.19a.txt	1.8	10	13.17617 ± 0.007739	0.34377 ± 0.000771	0.00462 ± 0.000054	0.01949 ± 0.001083	0.000025 ± 0.000027	2.14E-13	99.9%	38.3140	889.56 ± 2.14	0.24%
au25.4h.mus.20a.txt	1.8	10	9.77375 ± 0.006968	0.26353 ± 0.000743	0.00356 ± 0.000051	0.00022 ± 0.001190	0.000054 ± 0.000011	1.59E-13	99.8%	37.0279	865.83 ± 2.54	0.29%
au25.4h.mus.21a.txt	1.8	10	7.83622 ± 0.009578	0.31447 ± 0.000440	0.00417 ± 0.000042	0.00165 ± 0.000664	0.000137 ± 0.000011	1.27E-13	99.5%	24.7913	622.93 ± 1.19	0.19%
au25.4h.mus.22a.txt	1.8	10	6.18039 ± 0.008539	0.30493 ± 0.000817	0.00384 ± 0.000031	0.00223 ± 0.001047	-0.000044 ± 0.000017	1.00E-13	100.2%	20.2691	524.19 ± 1.64	0.31%
au25.4h.mus.23a.txt	1.8	10	4.80478 ± 0.005392	0.23640 ± 0.000661	0.00299 ± 0.000059	0.00005 ± 0.001022	-0.000044 ± 0.000020	7.80E-14	100.3%	20.3248	525.44 ± 1.71	0.32%
au25.4h.mus.24a.txt	1.8	10	3.31844 ± 0.002470	0.15672 ± 0.000434	0.00198 ± 0.000028	0.00039 ± 0.000993	0.000034 ± 0.000013	5.39E-14	99.7%	21.1110	542.99 ± 1.68	0.31%
au25.4h.mus.25a.txt	1.8	10	16.23190 ± 0.016260	0.39284 ± 0.000892	0.00528 ± 0.000065	0.01729 ± 0.000719	0.000050 ± 0.000033	2.64E-13	99.9%	41.2870	943.24 ± 2.41	0.26%
au25.4h.mus.26a.txt	1.8	10	7.67068 ± 0.007898	0.39200 ± 0.000683	0.00543 ± 0.000062	0.00258 ± 0.000625	-0.000010 ± 0.000022	1.25E-13	100.0%	19.5686	508.40 ± 1.12	0.22%
au25.4h.mus.27a.txt	1.8	10	12.63352 ± 0.006996	0.66045 ± 0.001128	0.00864 ± 0.000108	0.02076 ± 0.000909	0.000174 ± 0.000017	2.05E-13	99.6%	19.0542	496.72 ± 0.92	0.18%
au25.4h.mus.28a.txt	1.8	10	6.37054 ± 0.007840	0.23526 ± 0.000718	0.00310 ± 0.000045	0.00202 ± 0.000772	0.000016 ± 0.000019	1.03E-13	99.9%	27.0604	670.51 ± 2.29	0.34%
au25.4h.mus.29a.txt	1.8	10	16.64583 ± 0.006577	0.80031 ± 0.000953	0.01043 ± 0.000082	0.02232 ± 0.000895	0.000438 ± 0.000036	2.70E-13	99.2%	20.6405	532.51 ± 0.76	0.14%
au25.4h.mus.30a.txt	1.8	10	15.07390 ± 0.011002	0.39156 ± 0.001030	0.00542 ± 0.000079	0.01765 ± 0.000952	0.000045 ± 0.000026	2.45E-13	99.9%	38.4691	892.40 ± 2.48	0.28%
au25.4h.mus.31a.txt	1.8	10	21.46329 ± 0.013567	0.75684 ± 0.001534	0.01085 ± 0.000130	0.02035 ± 0.001235	0.000086 ± 0.000028	3.48E-13	99.9%	28.3286	696.57 ± 1.50	0.22%
au25.4h.mus.32a.txt	1.8	10	5.88030 ± 0.007227	0.19156 ± 0.000619	0.00250 ± 0.000039	0.00188 ± 0.000775	0.000004 ± 0.000015	9.55E-14	100.0%	30.6921	744.15 ± 2.64	0.35%
au25.4h.mus.33a.txt	1.8	10	13.02795 ± 0.012370	0.40732 ± 0.000667	0.00554 ± 0.000072	0.02060 ± 0.001069	0.000129 ± 0.000016	2.12E-13	99.7%	31.8974	767.94 ± 1.48	0.19%
au25.4h.mus.34a.txt	1.8	10	4.51761 ± 0.004801	0.13601 ± 0.000496	0.00182 ± 0.000039	-0.00061 ± 0.000962	-0.000028 ± 0.000018	7.33E-14	100.2%	33.2142	793.57 ± 3.16	0.40%
au25.4h.mus.35a.txt	1.8	10	4.57146 ± 0.003315	0.22847 ± 0.000503	0.00289 ± 0.000036	0.00137 ± 0.001156	-0.000035 ± 0.000019	7.42E-14	100.2%	20.0096	518.36 ± 1.37	0.26%
au25.4h.mus.36a.txt	1.8	10	10.77858 ± 0.007791	0.55904 ± 0.000993	0.00741 ± 0.000086	0.01597 ± 0.000961	0.000179 ± 0.000017	1.75E-13	99.5%	19.1887	499.78 ± 0.99	0.20%
au25.4h.mus.37a.txt	1.8	10	13.56582 ± 0.010271	0.35049 ± 0.000724	0.00489 ± 0.000048	0.01745 ± 0.000915	0.000319 ± 0.000036	2.20E-13	99.3%	38.4429	891.92 ± 2.10	0.24%
au25.4h.mus.38a.txt	1.8	10	12.19876 ± 0.008989	0.45125 ± 0.001319	0.00605 ± 0.000076	0.01809 ± 0.000583	0.000192 ± 0.000015	1.98E-13	99.5%	26.9123	667.45 ± 2.03	0.30%
au25.4h.mus.39a.txt	1.8	10	18.20629 ± 0.013964	0.45639 ± 0.001265	0.00618 ± 0.000075	0.01799 ± 0.001081	0.000054 ± 0.000028	2.96E-13	99.9%	39.8616	917.70 ± 2.67	0.29%
au25.4h.mus.40a.txt	1.8	10	9.80854 ± 0.008389	0.33043 ± 0.000515	0.00432 ± 0.000058	0.00365 ± 0.000944	0.000055 ± 0.000010	1.59E-13	99.8%	29.6356	723.04 ± 1.31	0.18%
au25.4h.mus.41a.txt	1.8	10	2.74899 ± 0.002214	0.12999 ± 0.000515	0.00168 ± 0.000031	0.00314 ± 0.000550	0.000026 ± 0.000010	4.46E-14	99.7%	21.0917	542.56 ± 2.27	0.42%
au25.4h.mus.42a.txt	1.8	10	9.39717 ± 0.011889	0.45135 ± 0.001060	0.00573 ± 0.000063	0.00326 ± 0.000967	0.000003 ± 0.000019	1.53E-13	100.0%	20.8190	536.49 ± 1.47	0.27%
au25.4h.mus.43a.txt	1.8	10	6.13094 ± 0.009481	0.24560 ± 0.000736	0.00322 ± 0.000036	0.00362 ± 0.000693	-0.000009 ± 0.000018	9.95E-14	100.0%	24.9651	626.62 ± 2.18	0.35%
au25.4h.mus.44a.txt	1.8	10	4.63954 ± 0.010906	0.13919 ± 0.000446	0.00178 ± 0.000037	0.00250 ± 0.000673	0.000062 ± 0.000010	7.53E-14	99.6%	33.2021	793.34 ± 3.21	0.40%
au25.4h.mus.45a.txt	1.8	10	15.00643 ± 0.007210	0.38965 ± 0.000891	0.00530 ± 0.000049	0.01712 ± 0.000515	0.000038 ± 0.000024	2.44E-13	99.9%	38.4890	892.76 ± 2.13	0.24%
au25.4h.mus.46a.txt	1.8	10	14.66176 ± 0.012032	0.47740 ± 0.000872	0.00640 ± 0.000089	0.01977 ± 0.000498	0.000098 ± 0.000035	2.38E-13	99.8%	30.6561	743.43 ± 1.58	0.21%
au25.4h.mus.47a.txt	1.8	10	10.67067 ± 0.009051	0.28212 ± 0.000731	0.00396 ± 0.000048	0.01714 ± 0.000808	0.000178 ± 0.000014	1.73E-13	99.5%	37.6439	877.23 ± 2.43	0.28%
au25.4h.mus.48a.txt	1.8	10	21.62150 ± 0.018001	0.60858 ± 0.001401	0.00824 ± 0.000105	0.01702 ± 0.000841	0.000089 ± 0.000035	3.51E-13	99.9%	35.4881	837.00 ± 2.09	0.25%
au25.4h.mus.49a.txt	1.8	10	19.65423 ± 0.019163	0.62133 ± 0.001327	0.00828 ± 0.000100	0.02111 ± 0.001320	0.000194 ± 0.000029	3.19E-13	99.7%	31.5441	761.00 ± 1.82	0.24%
au25.4h.mus.50a.txt	1.8	10	21.99679 ± 0.008353	0.55183 ± 0.001180	0.00737 ± 0.000074	0.02250 ± 0.001347	0.000051 ± 0.000025	3.57E-13	99.9%	39.8394	917.30 ± 2.02	0.22%
au25.4h.mus.51a.txt	1.8	10	3.19685 ± 0.005115	0.10659 ± 0.000391	0.00146 ± 0.000039	-0.00290 ± 0.001663	0.000035 ± 0.000010	5.19E-14	99.7%	29.8935	728.21 ± 3.00	0.41%
au25.4h.mus.52a.txt	1.8	10	4.12906 ± 0.003805	0.10293 ± 0.000245	0.00134 ± 0.000025	-0.00159 ± 0.001000	-0.000003 ± 0.000013	6.70E-14	100.0%	40.1126	922.23 ± 2.50	0.27%
au25.4h.mus.53a.txt	1.8	10	6.63844 ± 0.007050	0.21920 ± 0.000506	0.00294 ± 0.000041	-0.00101 ± 0.000594	-0.000021 ± 0.000021	1.08E-13	100.1%	30.2838	736.02 ± 1.99	0.27%
au25.4h.mus.54a.txt	1.8	10	6.88298 ± 0.006192	0.16025 ± 0.000523	0.00205 ± 0.000045	0.00051 ± 0.001026	-0.000028 ± 0.000014	1.12E-13	100.1%	42.9514	972.61 ± 3.35	0.34%
au25.4h.mus.55a.txt	1.8	10	7.32747 ± 0.005365	0.34381 ± 0.000993	0.00532 ± 0.000069	0.00024 ± 0.000980	0.000105 ± 0.000011	1.19E-13	99.6%	21.2228	545.47 ± 1.65	0.30%
au25.4h.mus.56a.txt	1.8	10	7.76966 ± 0.009693	0.20032 ± 0.000693	0.00250 ± 0.000039	0.00002 ± 0.000450	0.000015 ± 0.000021	1.26E-13	99.9%	38.7631	897.77 ± 3.39	0.38%
au25.4h.mus.57a.txt	1.8	10	9.23742 ± 0.014888	0.28240 ± 0.000700	0.00408 ± 0.000038	0.00140 ± 0.000477	0.000001 ± 0.000019	1.50E-13	100.0%	32.7095	783.79 ± 2.37	0.30%

18.46860	± 0.015375	0.52091	± 0.001060	0.00708	± 0.000112	0.01972	± 0.000668	0.000175	± 0.000020	3.00E-13	99.7%	35.3597	834.58	± 1.86	0.22%
7.37562	± 0.010704	0.39255	± 0.000710	0.00525	± 0.000058	0.00126	± 0.000981	0.000116	± 0.000016	1.20E-13	99.5%	18.7025	488.69	± 1.18	0.24%
9.05819	± 0.008488	0.27804	± 0.000706	0.00363	± 0.000039	0.00268	± 0.001230	0.000015	± 0.000021	1.47E-13	100.0%	32.5642	780.97	± 2.18	0.28%
3.20768	± 0.003009	0.15267	± 0.000534	0.00203	± 0.000037	0.00127	± 0.000862	0.000062	± 0.000017	5.21E-14	99.4%	20.8925	538.13	± 2.13	0.40%
15.28332	± 0.011628	0.65340	± 0.001704	0.00847	± 0.000121	0.01917	± 0.001796	0.000380	± 0.000021	2.48E-13	99.3%	23.2217	589.27	± 1.63	0.28%
8.32646	± 0.010790	0.43278	± 0.000795	0.00555	± 0.000063	0.00190	± 0.000930	0.000064	± 0.000017	1.35E-13	99.8%	19.1960	499.95	± 1.17	0.23%
15.16135	± 0.008276	0.78901	± 0.001629	0.01045	± 0.000155	0.01945	± 0.000539	0.000005	± 0.000032	2.46E-13	100.0%	19.2165	500.41	± 1.11	0.22%
5.23053	± 0.004440	0.16330	± 0.000467	0.00227	± 0.000051	0.00005	± 0.000783	0.000048	± 0.000015	8.49E-14	99.7%	31.9439	768.85	± 2.39	0.31%
7.44974	± 0.007685	0.23960	± 0.000308	0.00306	± 0.000039	0.00099	± 0.000772	0.000007	± 0.000022	1.21E-13	100.0%	31.0841	751.92	± 1.40	0.19%
13.53774	± 0.015635	0.36647	± 0.000583	0.00491	± 0.000058	0.01782	± 0.000932	0.000148	± 0.000018	2.20E-13	99.7%	36.8276	862.10	± 1.73	0.20%
5.23053	± 0.004440	0.16330	± 0.000467	0.00227	± 0.000051	0.00005	± 0.000783	0.000011	± 0.000009	8.49E-14	99.9%	32.0109	770.16	± 2.33	0.30%
7.44974	± 0.007685	0.23960	± 0.000308	0.00306	± 0.000039	0.00099	± 0.000772	-0.000030	± 0.000019	1.21E-13	100.1%	31.0932	752.10	± 1.36	0.18%
13.53774	± 0.015635	0.36647	± 0.000583	0.00491	± 0.000058	0.01782	± 0.000932	0.000111	± 0.000013	2.20E-13	99.8%	36.8574	862.66	± 1.72	0.20%
1.56516	± 0.001781	0.08043	± 0.000389	0.00102	± 0.000035	-0.00056	± 0.000807	-0.000017	± 0.000009	2.54E-14	100.3%	19.4592	505.92	± 2.65	0.52%
8.29163	± 0.013713	0.34892	± 0.000657	0.00445	± 0.000065	-0.00022	± 0.000905	0.000056	± 0.000011	1.35E-13	99.8%	23.7162	599.95	± 1.53	0.25%
10.83610	± 0.006232	0.32057	± 0.001325	0.00466	± 0.000059	0.01592	± 0.000712	0.000588	± 0.000017	1.76E-13	98.4%	33.2668	794.59	± 3.39	0.43%
3.39328	± 0.004125	0.17111	± 0.000549	0.00229	± 0.000042	-0.00418	± 0.001380	0.000006	± 0.000011	5.51E-14	99.9%	19.8175	514.03	± 1.83	0.36%
3.11553	± 0.002547	0.14733	± 0.000492	0.00199	± 0.000042	-0.00141	± 0.000586	-0.000027	± 0.000020	5.06E-14	100.3%	21.1452	543.75	± 2.14	0.39%
5.20500	± 0.003779	0.24275	± 0.000624	0.00352	± 0.000089	-0.00113	± 0.000840	0.000943	± 0.000013	8.45E-14	94.6%	20.2934	524.74	± 1.54	0.29%
4.27613	± 0.002937	0.21944	± 0.000413	0.00292	± 0.000051	-0.00076	± 0.000711	-0.000014	± 0.000018	6.94E-14	100.1%	19.4863	506.54	± 1.20	0.24%
4.03787	± 0.002975	0.19515	± 0.000677	0.00264	± 0.000047	0.00016	± 0.000465	-0.000007	± 0.000015	6.56E-14	100.0%	20.6916	533.65	± 1.98	0.37%
5.05954	± 0.004267	0.14125	± 0.000488	0.00196	± 0.000037	0.00135	± 0.000720	-0.000020	± 0.000017	8.21E-14	100.1%	35.8216	843.29	± 3.12	0.37%
3.29005	± 0.002776	0.16492	± 0.000602	0.00223	± 0.000038	0.00077	± 0.000674	0.000047	± 0.000010	5.34E-14	99.6%	19.8654	515.11	± 2.00	0.39%
4.62530	± 0.003585	0.10849	± 0.000524	0.00226	± 0.000043	0.00110	± 0.000993	0.003950	± 0.000045	7.51E-14	74.8%	31.8751	767.50	± 5.97	0.78%
4.33593	± 0.004069	0.22700	± 0.000738	0.00305	± 0.000029	0.00005	± 0.000948	0.000304	± 0.000012	7.04E-14	97.9%	18.7054	488.75	± 1.74	0.36%
5.23519	± 0.002942	0.24035	± 0.000552	0.00310	± 0.000047	-0.00028	± 0.000526	0.000191	± 0.000017	8.50E-14	98.9%	21.5458	552.62	± 1.42	0.26%
3.34219	± 0.004352	0.10669	± 0.000496	0.00142	± 0.000038	0.00086	± 0.000904	0.000027	± 0.000021	5.43E-14	99.8%	31.2537	755.27	± 3.92	0.52%
16.72489	± 0.009569	0.52245	± 0.001632	0.00719	± 0.000078	0.02187	± 0.000953	0.000251	± 0.000019	2.72E-13	99.6%	31.8752	767.50	± 2.46	0.32%
4.23620	± 0.005323	0.23102	± 0.000803	0.00278	± 0.000053	0.00151	± 0.000851	0.000098	± 0.000017	6.88E-14	99.3%	18.2121	477.43	± 1.87	0.39%
2.04946	± 0.002020	0.09376	± 0.000377	0.00101	± 0.000047	-0.00012	± 0.001011	0.000104	± 0.000017	3.33E-14	98.5%	21.5310	552.29	± 2.71	0.49%
24.15653	± 0.007363	0.22130	± 0.000772	0.00337	± 0.000044	0.01680	± 0.000934	0.000023	± 0.000030	3.92E-13	100.0%	109.1409	1867.51	± 6.58	0.35%
2.69874	± 0.003577	0.12632	± 0.000454	0.00159	± 0.000019	0.00067	± 0.000809	0.000037	± 0.000018	4.38E-14	99.6%	21.2785	546.71	± 2.36	0.43%
4.59748	± 0.005119	0.14020	± 0.000498	0.00176	± 0.000030	0.00018	± 0.000834	-0.000025	± 0.000017	7.46E-14	100.2%	32.7924	785.40	± 3.05	0.39%
14.30430	± 0.009238	0.53626	± 0.001286	0.00728	± 0.000114	0.02171	± 0.001048	0.000077	± 0.000024	2.32E-13	99.8%	26.6367	661.73	± 1.68	0.25%
12.48280	± 0.012023	0.32678	± 0.000590	0.00447	± 0.000060	0.02140	± 0.001102	0.000048	± 0.000030	2.03E-13	99.9%	38.1634	886.79	± 1.92	0.22%
3.36486	± 0.002474	0.16037	± 0.000189	0.00228	± 0.000027	-0.00020	± 0.000998	0.001018	± 0.000028	5.46E-14	91.1%	19.1064	497.91	± 1.53	0.31%
5.39778	± 0.003890	0.23534	± 0.000512	0.00307	± 0.000042	0.00045	± 0.000695	-0.000043	± 0.000017	8.76E-14	100.2%	22.9360	583.08	± 1.45	0.25%
4.65496	± 0.004978	0.24297	± 0.000443	0.00333	± 0.000027	0.00015	± 0.000862	0.000067	± 0.000011	7.56E-14	99.6%	19.0775	497.25	± 1.11	0.22%
2.89557	± 0.003366	0.08699	± 0.000190	0.00119	± 0.000042	-0.00057	± 0.000794	0.000028	± 0.000011	4.70E-14	99.7%	33.1901	793.11	± 2.16	0.27%
7.14584	± 0.007256	0.22491	± 0.000644	0.00303	± 0.000051	0.00207	± 0.000868	0.000052	± 0.000012	1.16E-13	99.8%	31.7039	764.14	± 2.35	0.31%
5.23577	± 0.003340	0.26562	± 0.000494	0.00345	± 0.000038	-0.00406	± 0.000520	0.000070	± 0.000010	8.50E-14	99.6%	19.6323	509.84	± 1.05	0.21%
3.45485	± 0.004379	0.11772	± 0.000440	0.00146	± 0.000030	-0.00169	± 0.001117	0.000035	± 0.000009	5.61E-14	99.7%	29.2568	715.41	± 2.89	0.40%
2.54577	± 0.002675	0.12870	± 0.000342	0.00173	± 0.000050	-0.00236	± 0.000760	0.000008	± 0.000019	4.13E-14	99.9%	19.7598	512.73	± 1.87	0.36%
3.25302	± 0.004069	0.12119	± 0.000228	0.00190	± 0.000041	-0.00263	± 0.000791	0.000008	± 0.000018	5.28E-14	99.9%	26.8197	665.53	± 1.85	0.28%
8.79335	± 0.006310	0.26509	± 0.000433	0.00352	± 0.000044	-0.00281	± 0.000819	0.000094	± 0.000020	1.43E-13	99.7%	33.0647	790.68	± 1.51	0.19%
5.13557	± 0.004198	0.22711	± 0.000666	0.00295	± 0.000052	0.00151	± 0.000945	0.000026	± 0.000011	8.34E-14	99.9%	22.5794	575.31	± 1.79	0.31%
2.68671	± 0.002608	0.12455	± 0.000472	0.00169	± 0.000038	0.00057	± 0.000721	0.000047	± 0.000010	4.36E-14	99.5%	21.4586	550.69	± 2.25	0.41%
8.23642	± 0.009566	0.43680	± 0.001085	0.00626	± 0.000101	0.00280	± 0.000922	0.000030	± 0.000020	1.34E-13	99.9%	18.8368	491.76	± 1.40	0.28%
9.74326	± 0.015768	0.27467	± 0.000365	0.00368	± 0.000057	0.00128	± 0.000862	0.000097	± 0.000012	1.58E-13	99.7%	35.3689	834.75	± 1.78	0.21%
13.68869	± 0.008480	0.35493	± 0.000686	0.00507	± 0.000055	0.02049	± 0.000815	0.000054	± 0.000028	2.22E-13	99.9%	38.5298	893.51	± 1.89	0.21%
4.89088	± 0.003376	0.23236	± 0.000319	0.00296	± 0.000034	-0.00037	± 0.000788	0.000108	± 0.000016	7.94E-14	99.3%	20.9114	538.55	± 0.99	0.18%
1.78612	± 0.001915	0.08827	± 0.000369	0.00113	± 0.000031	0.00091	± 0.000674	0.000052	± 0.000020	2.90E-14	99.1%	20.0636	519.58	± 2.85	0.55%
3.73449	± 0.002294	0.21569	± 0.000643	0.00282	± 0.000041	0.00025	± 0.000834	0.000036	± 0.000026	6.06E-14	99.7%	17.2641	455.46	± 1.67	0.37%
16.50286	± 0.010175	0.49194	± 0.001109	0.00677	± 0.000091	0.02110	± 0.000600	0.000102	± 0.000036	2.68E-13	99.8%	33.4905	798.91	± 1.94	0.24%
8.14901	± 0.012790	0.22079	± 0.000647	0.00289	± 0.000046	0.00079	± 0.001202	0.000092	± 0.000018	1.32E-13	99.7%	36.7870	861.35	± 2.92	0.34%
3.03129	± 0.003459	0.15529	± 0.000334	0.00195	± 0.000033	0.00447	± 0.000634	0.000043	± 0.000021	4.92E-14	99.6%	19.4427	505.55	± 1.60	0.32%
4.35325	± 0.003951	0.22632	± 0.000469	0.00287	± 0.000036	0.00028	± 0.000691	0.000054	± 0.000023	7.07E-14	99.6%	19.1642	499.22	± 1.39	0.28%
3.06639	± 0.002802	0.12283	± 0.000555	0.00162	± 0.000023	-0.00167	± 0.000842	0.000018	± 0.000022	4.98E-14	99.8%	24.9186	625.64	± 3.19	0.51%
3.48080	± 0.004328	0.10814	± 0.000427	0.00149	± 0.000034	-0.00114	± 0.000554	0.000011	± 0.000023	5.65E-14	99.9%	32.1588	773.06	± 3.54	0.46%
3.91772	± 0.002690	0.17691	± 0.000389	0.00225	± 0.000051	-0.00026	± 0.000931	0.000062	± 0.000016	6.36E-14	99.5%	22.0412	563.53	± 1.47	0.26%
													113		

B-D-1 Muscovite		40-80																
au25.4l.mus.3a.txt	1.8	10	5.09052	± 0.005772	0.26693	± 0.000573	0.00349	± 0.000029	0.00154	± 0.000558	0.000290	± 0.000010	8.26E-14	98.3%	18.7501	489.77	± 1.25	0.3%
au25.4l.mus.4a.txt	1.8	10	7.43867	± 0.009119	0.39307	± 0.000453	0.00511	± 0.000043	-0.00075	± 0.001471	0.000258	± 0.000008	1.21E-13	99.0%	18.7304	489.33	± 0.85	0.2%
au25.4l.mus.5a.txt	1.8	10	5.35527	± 0.003777	0.28215	± 0.000726	0.00364	± 0.000031	0.00143	± 0.001010	0.000182	± 0.000010	8.69E-14	99.0%	18.7902	490.69	± 1.35	0.3%
au25.4l.mus.6a.txt	1.8	10	1.99635	± 0.002261	0.10451	± 0.000313	0.00141	± 0.000024	0.00339	± 0.001308	0.000134	± 0.000018	3.24E-14	98.0%	18.7261	489.23	± 2.09	0.4%
au25.4l.mus.7a.txt	1.8	10	2.75704	± 0.002309	0.14656	± 0.000588	0.00190	± 0.000032	0.00241	± 0.000985	0.000131	± 0.000008	4.48E-14	98.6%	18.5495	485.18	± 2.06	0.4%
au25.4l.mus.8a.txt	1.8	10	2.47697	± 0.003201	0.12974	± 0.000431	0.00167	± 0.000043	0.00076	± 0.000603	0.000061	± 0.000010	4.02E-14	99.3%	18.9540	494.43	± 1.88	0.4%
au25.4l.mus.11a.txt	1.8	10	6.81817	± 0.008947	0.35472	± 0.000799	0.00455	± 0.000040	-0.00249	± 0.000787	0.000311	± 0.000013	1.11E-13	98.7%	18.9610	494.59	± 1.34	0.3%
au25.4l.mus.12a.txt	1.8	10	7.10272	± 0.009249	0.37535	± 0.000440	0.00499	± 0.000086	0.00050	± 0.000881	0.000313	± 0.000016	1.15E-13	98.7%	18.6771	488.10	± 0.93	0.2%
au25.4l.mus.13a.txt	1.8	10	4.84935	± 0.006368	0.25701	± 0.000646	0.00335	± 0.000046	0.00043	± 0.000663	0.000121	± 0.000020	7.87E-14	99.3%	18.7301	489.32	± 1.52	0.3%
au25.4l.mus.14a.txt	1.8	10	4.49074	± 0.003224	0.23454	± 0.000794	0.00308	± 0.000030	0.00172	± 0.001117	0.000252	± 0.000011	7.29E-14	98.3%	18.8305	491.61	± 1.77	0.4%
au25.4l.mus.15a.txt	1.8	10	2.88157	± 0.002006	0.15062	± 0.000420	0.00188	± 0.000023	0.00113	± 0.000771	0.000046	± 0.000024	4.68E-14	99.5%	19.0423	496.45	± 1.88	0.4%
au25.4l.mus.16a.txt	1.8	10	2.60225	± 0.001319	0.13190	± 0.000376	0.00175	± 0.000036	0.00227	± 0.001095	0.000398	± 0.000018	4.22E-14	95.5%	18.8394	491.82	± 1.83	0.4%
au25.4l.mus.17a.txt	1.8	10	4.37701	± 0.004931	0.22998	± 0.000383	0.00296	± 0.000052	0.00192	± 0.000516	0.000185	± 0.000018	7.11E-14	98.7%	18.7948	490.80	± 1.17	0.2%
au25.4l.mus.18a.txt	1.8	10	2.55297	± 0.002867	0.13476	± 0.000610	0.00170	± 0.000028	0.00211	± 0.000679	0.000138	± 0.000023	4.14E-14	98.4%	18.6440	487.35	± 2.66	0.5%
au25.4l.mus.19a.txt	1.8	10	1.14017	± 0.001453	0.05837	± 0.000272	0.00075	± 0.000020	-0.00047	± 0.000854	0.000111	± 0.000022	1.85E-14	97.1%	18.9716	494.84	± 3.78	0.8%
au25.4l.mus.20a.txt	1.8	10	1.23841	± 0.001753	0.06513	± 0.000336	0.00082	± 0.000024	-0.00060	± 0.000782	0.000049	± 0.000015	2.01E-14	98.8%	18.7897	490.68	± 3.18	0.6%
au25.4l.mus.21a.txt	1.8	10	0.94901	± 0.001364	0.04853	± 0.000187	0.00064	± 0.000030	-0.00180	± 0.000709	0.000092	± 0.000015	1.54E-14	97.1%	18.9905	495.27	± 3.17	0.6%
au25.4l.mus.22a.txt	1.8	10	3.21521	± 0.002895	0.16916	± 0.000572	0.00213	± 0.000033	-0.00301	± 0.000705	0.000123	± 0.000022	5.22E-14	98.9%	18.7894	490.67	± 2.00	0.4%
au25.4l.mus.23a.txt	1.8	10	7.84088	± 0.007576	0.40839	± 0.000846	0.00518	± 0.000056	-0.00017	± 0.000719	0.000546	± 0.000017	1.27E-13	97.9%	18.8045	491.02	± 1.19	0.2%
au25.4l.mus.24a.txt	1.8	10	9.98170	± 0.010882	0.53067	± 0.001131	0.00679	± 0.000086	0.00183	± 0.001104	0.000425	± 0.000016	1.62E-13	98.7%	18.5733	485.73	± 1.20	0.2%
au25.4l.mus.25a.txt	1.8	10	2.97713	± 0.003793	0.15475	± 0.000685	0.00209	± 0.000044	-0.00076	± 0.000836	0.000255	± 0.000017	4.83E-14	97.5%	18.7513	489.80	± 2.47	0.5%
au25.4l.mus.26a.txt	1.8	10	2.24474	± 0.002638	0.12031	± 0.000483	0.00153	± 0.000031	-0.00194	± 0.000504	0.000084	± 0.000016	3.64E-14	98.9%	18.4514	482.93	± 2.30	0.5%
au25.4l.mus.27a.txt	1.8	10	2.42112	± 0.001463	0.12553	± 0.000539	0.00161	± 0.000034	-0.00192	± 0.000571	0.000180	± 0.000017	3.93E-14	97.8%	18.8625	492.35	± 2.42	0.5%
au25.4l.mus.28a.txt	1.8	10	5.16059	± 0.004026	0.26705	± 0.000397	0.00349	± 0.000039	-0.00057	± 0.000919	0.000491	± 0.000018	8.38E-14	97.2%	18.7812	490.49	± 1.00	0.2%
au25.4l.mus.29a.txt	1.8	10	0.95530	± 0.001364	0.05031	± 0.000236	0.00059	± 0.000025	-0.00175	± 0.000757	0.000082	± 0.000017	1.55E-14	97.5%	18.5026	484.10	± 3.57	0.7%
au25.4l.mus.30a.txt	1.8	10	0.92051	± 0.001036	0.04880	± 0.000153	0.00062	± 0.000028	-0.00079	± 0.001098	0.000046	± 0.000015	1.49E-14	98.5%	18.5798	485.88	± 2.83	0.6%
au25.4l.mus.31a.txt	1.8	10	4.34897	± 0.004406	0.22725	± 0.000574	0.00297	± 0.000033	0.00073	± 0.000744	0.000289	± 0.000015	7.06E-14	98.0%	18.7622	490.05	± 1.46	0.3%
au25.4l.mus.32a.txt	1.8	10	1.81929	± 0.002797	0.09796	± 0.000330	0.00124	± 0.000028	0.00051	± 0.000907	0.000012	± 0.000023	2.95E-14	99.8%	18.5356	484.86	± 2.53	0.5%
au25.4l.mus.33a.txt	1.8	10	1.30581	± 0.002611	0.06922	± 0.000402	0.00093	± 0.000021	-0.00088	± 0.001292	0.000040	± 0.000022	2.12E-14	99.1%	18.6921	488.45	± 3.87	0.8%
au25.4l.mus.34a.txt	1.8	10	0.98509	± 0.001596	0.05099	± 0.000223	0.00070	± 0.000029	0.00041	± 0.001172	0.000075	± 0.000015	1.60E-14	97.7%	18.8840	492.84	± 3.25	0.7%
au25.4l.mus.35a.txt	1.8	10	1.82326	± 0.002290	0.09539	± 0.000279	0.00118	± 0.000027	-0.00032	± 0.000698	0.000073	± 0.000016	2.96E-14	98.8%	18.8854	492.87	± 2.04	0.4%
au25.4l.mus.36a.txt	1.8	10	3.26522	± 0.004664	0.17125	± 0.000444	0.00216	± 0.000043	0.00092	± 0.000973	0.000117	± 0.000018	5.30E-14	98.9%	18.8658	492.42	± 1.69	0.3%
au25.4l.mus.37a.txt	1.8	10	1.65325	± 0.001592	0.08574	± 0.000420	0.00108	± 0.000034	-0.00423	± 0.001174	0.000114	± 0.000011	2.68E-14	98.0%	18.8837	492.83	± 2.69	0.5%
au25.4l.mus.38a.txt	1.8	10	2.28921	± 0.002542	0.12087	± 0.000310	0.00159	± 0.000037	0.00071	± 0.000889	0.000094	± 0.000011	3.72E-14	98.8%	18.7105	488.87	± 1.54	0.3%
au25.4l.mus.39a.txt	1.8	10	2.70385	± 0.002019	0.14263	± 0.000478	0.00182	± 0.000036	0.00155	± 0.001016	0.000140	± 0.000010	4.39E-14	98.5%	18.6693	487.93	± 1.78	0.4%
au25.4l.mus.40a.txt	1.8	10	1.61861	± 0.001881	0.08526	± 0.000324	0.00110	± 0.000023	0.00263	± 0.000927	0.000072	± 0.000023	2.63E-14	98.7%	18.7387	489.51	± 2.86	0.6%
au25.4l.mus.41a.txt	1.8	10	2.21153	± 0.001858	0.11490	± 0.000276	0.00150	± 0.000025	0.00285	± 0.001247	0.000148	± 0.000015	3.59E-14	98.0%	18.8704	492.52	± 1.62	0.3%
au25.4l.mus.42a.txt	1.8	10	0.51976	± 0.000819	0.02719	± 0.000078	0.00034	± 0.000023	0.00155	± 0.000787	0.000057	± 0.000015	8.44E-15	96.7%	18.4949	483.93	± 4.53	0.9%
au25.4l.mus.43a.txt	1.8	10	1.81524	± 0.001579	0.09724	± 0.000396	0.00123	± 0.000034	-0.00042	± 0.000996	0.000062	± 0.000015	2.95E-14	99.0%	18.4795	483.58	± 2.37	0.5%
au25.4l.mus.44a.txt	1.8	10	2.95666	± 0.002956	0.15430	± 0.000362	0.00202	± 0.000033	0.00207	± 0.001028	0.000124	± 0.000019	4.80E-14	98.8%	18.9266	493.81	± 1.58	0.3%
au25.4l.mus.45a.txt	1.8	10	5.58850	± 0.003289	0.29262	± 0.000523	0.00373	± 0.000031	0.00006	± 0.000537	0.000320	± 0.000019	9.07E-14	98.3%	18.7750	490.35	± 1.07	0.2%
au25.4l.mus.46a.txt	1.8	10	3.42486	± 0.003177	0.18133	± 0.000476	0.00228	± 0.000042	0.00028	± 0.001092	0.000103	± 0.000021	5.56E-14	99.1%	18.7201	489.09	± 1.65	0.3%
au25.4l.mus.47a.txt	1.8	10	4.20547	± 0.002195	0.21986	± 0.000804	0.00284	± 0.000049	0.00149	± 0.000831	0.000158	± 0.000013	6.83E-14	98.9%	18.9160	493.57	± 1.90	0.4%
au25.4l.mus.48a.txt	1.8	10	3.13944	± 0.003750	0.16249	± 0.000657	0.00211	± 0.000043	0.00037	± 0.000821	0.000231	± 0.000012	5.10E-14	97.8%	18.9006	493.21	± 2.20	0.4%
au25.4l.mus.49a.txt	1.8	10	4.17118	± 0.006602	0.21922	± 0.000542	0.00275	± 0.000031	-0.00426	± 0.001689	0.000204	± 0.000016	6.77E-14	98.6%	18.7505	489.78	± 1.56	0.3%
au25.4l.mus.50a.txt	1.8	10	2.87221	± 0.002336	0.15257	± 0.000601	0.00218	± 0.000057	0.00090	± 0.000708	0.000097	± 0.000016	4.66E-14	99.0%	18.6393	487.24	± 2.13	0.4%
au25.4l.mus.51a.txt	1.8	10	10.81398	± 0.006903	0.57545	± 0.000940	0.00762	± 0.000081	0.02113	± 0.000726	0.000307	± 0.000030	1.76E-13	99.2%	18.6381	487.21	± 0.95	0.2%
au25.4l.mus.52a.txt	1.8	10	1.52052	± 0.002027	0.07985	± 0.000366	0.00107	± 0.000030	0.00028	± 0.000663	0.000020	± 0.000016	2.47E-14	99.6%	18.9687	494.77	± 2.85	0.6%
au25.4l.mus.53a.txt	1.8	10	1.27609	± 0.000949	0.06682	± 0.000320	0.00091	± 0.000034	0.00028	± 0.000727	0.000042	± 0.000019	2.07E-14	99.0%	18.9108	493.45	± 3.26	0.7%
au25.4l.mus.54a.txt	1.8	10	1.61336	± 0.001542	0.08689	± 0.000252	0.00113	± 0.000029	-0.00041	± 0.000946	-0.000013	± 0.000018	2.62E-14	100.2%	18.5667	485.58	± 2.16	0.4%
au25.4l.mus.55a.txt	1.8	10	1.33731	± 0.001611	0.06859	± 0.000409	0.00088	± 0.000025	0.00016	± 0.000692	0.000077	± 0.000015	2.17E-14	98.3%	19.1651	499.24	± 3.54	0.7%
au25.4l.mus.56a.txt	1.8	10	4.27758	± 0.005946	0.22456	± 0.000333	0.00293	± 0.000035	0.00114	± 0.001083	0.000270	± 0.000013	6.94E-14	98.1%	18.6931	488.47	± 1.11	0.2%
au25.4l.mus.57a.txt	1.8	10	1.60305	± 0.002236	0.08043	± 0.000456	0.00103	± 0.000036	0.00155	± 0.000706	0.000193	± 0.000012	2.60E-14	96.4%	19.2223	500.54	± 3.25	0.6%
au25.4l.mus.58a.txt	1.8	10	1.08554	± 0.001151	0.05661	± 0.000291	0.00074	± 0.000031	0.00045	± 0.000960	0.000061	± 0.000011	1.76E-14	98.3%	18.8590	492.26	± 3.01	0.6%
au25.4l.mus.59a.txt	1.8	10	2.18208	± 0.002182	0.11478	± 0.000520	0.00149	± 0.000030	-0.00051	± 0.000943	0.000060	± 0.000010	3.54E-14	99.2%	18.8563	492.20	± 2.41	0.5%
au25.4l.mus.60a.txt	1.8	10	1.56367	± 0.001291	0.07900	± 0.000297	0.00120	± 0.000047	0.00012	± 0.000365	0.000196	± 0.000009	2.54E-14	96.3%	19.0616	496.89	± 2.18	0.4%

au25.4l.mus.61a.txt	1.8	10	2.60136	± 0.001607	0.13898	± 0.000561	0.00180	± 0.000036	0.00096	± 0.000865	0.000009	± 0.000020	4.22E-14	99.9%	18.7002	488.63	± 2.30	0.5%
au25.4l.mus.62a.txt	1.8	10	1.64062	± 0.002395	0.08557	± 0.000346	0.00112	± 0.000029	-0.00031	± 0.000938	0.000041	± 0.000009	2.66E-14	99.3%	19.0321	496.21	± 2.28	0.5%
au25.4l.mus.63a.txt	1.8	10	2.50352	± 0.002175	0.13079	± 0.000423	0.00171	± 0.000035	0.00016	± 0.000627	0.000115	± 0.000010	4.06E-14	98.6%	18.8818	492.78	± 1.77	0.4%
au25.4l.mus.64a.txt	1.8	10	0.73512	± 0.000738	0.03794	± 0.000112	0.00044	± 0.000024	-0.00014	± 0.001163	0.000038	± 0.000010	1.19E-14	98.5%	19.0792	497.29	± 2.54	0.5%
au25.4l.mus.65a.txt	1.8	10	0.83097	± 0.001364	0.04276	± 0.000165	0.00056	± 0.000027	-0.00165	± 0.000799	0.000041	± 0.000010	1.35E-14	98.5%	19.1434	498.75	± 2.80	0.6%
au25.4l.mus.66a.txt	1.8	10	0.78032	± 0.000836	0.04180	± 0.000257	0.00051	± 0.000033	0.00505	± 0.001757	-0.000002	± 0.000016	1.27E-14	100.1%	18.6794	488.16	± 4.23	0.9%
au25.4l.mus.67a.txt	1.8	10	1.02697	± 0.000785	0.05265	± 0.000139	0.00066	± 0.000024	-0.00067	± 0.000960	0.000034	± 0.000018	1.67E-14	99.0%	19.3097	502.53	± 3.01	0.6%
au25.4l.mus.68a.txt	1.8	10	1.22268	± 0.001416	0.06360	± 0.000339	0.00078	± 0.000027	0.00047	± 0.000859	-0.000001	± 0.000016	1.99E-14	100.0%	19.2262	500.63	± 3.34	0.7%
au25.4l.mus.69a.txt	1.8	10	2.47220	± 0.002549	0.13219	± 0.000414	0.00167	± 0.000032	-0.00079	± 0.000981	0.000008	± 0.000018	4.01E-14	99.9%	18.6834	488.25	± 1.93	0.4%
au25.4l.mus.70a.txt	1.8	10	1.39638	± 0.001308	0.07256	± 0.000341	0.00094	± 0.000020	-0.00058	± 0.000714	0.000061	± 0.000011	2.27E-14	98.2%	18.8886	492.94	± 2.67	0.5%
au25.4l.mus.71a.txt	1.8	10	1.74482	± 0.002009	0.08996	± 0.000421	0.00117	± 0.000029	0.00169	± 0.001007	0.000106	± 0.000010	2.83E-14	98.2%	19.0494	496.61	± 2.59	0.5%
au25.4l.mus.72a.txt	1.8	10	2.63975	± 0.002992	0.13697	± 0.000355	0.00177	± 0.000027	0.00111	± 0.000844	0.000174	± 0.000021	4.29E-14	98.1%	18.8975	493.14	± 1.84	0.4%
au25.4l.mus.73a.txt	1.8	10	2.77655	± 0.001680	0.14374	± 0.000614	0.00183	± 0.000022	0.00081	± 0.000849	0.000166	± 0.000010	4.51E-14	98.2%	18.9768	494.95	± 2.24	0.5%
au25.4l.mus.74a.txt	1.8	10	1.34441	± 0.001473	0.07077	± 0.000325	0.00094	± 0.000023	0.00034	± 0.001094	0.000005	± 0.000019	2.18E-14	99.9%	18.9764	494.94	± 3.12	0.6%
au25.4l.mus.75a.txt	1.8	10	2.41529	± 0.001757	0.12899	± 0.000608	0.00165	± 0.000038	-0.00042	± 0.000923	0.000003	± 0.000016	3.92E-14	100.0%	18.7165	489.01	± 2.51	0.5%
au25.4l.mus.76a.txt	1.8	10	0.88264	± 0.000639	0.04730	± 0.000297	0.00061	± 0.000028	0.00115	± 0.000821	-0.000024	± 0.000014	1.43E-14	100.8%	18.6625	487.77	± 3.79	0.8%
au25.4l.mus.77a.txt	1.8	10	1.66652	± 0.002147	0.08717	± 0.000449	0.00109	± 0.000024	0.00025	± 0.000755	0.000067	± 0.000017	2.71E-14	98.8%	18.8923	493.03	± 3.03	0.6%
au25.4l.mus.78a.txt	1.8	10	1.02581	± 0.001519	0.05520	± 0.000409	0.00070	± 0.000024	0.00023	± 0.001173	0.000001	± 0.000010	1.67E-14	100.0%	18.5780	485.83	± 3.92	0.8%
au25.4l.mus.79a.txt	1.8	10	1.10342	± 0.001555	0.05852	± 0.000266	0.00071	± 0.000022	0.00035	± 0.000427	0.000012	± 0.000008	1.79E-14	99.7%	18.7956	490.82	± 2.59	0.5%
au25.4l.mus.80a.txt	1.8	10	1.27657	± 0.001471	0.06656	± 0.000289	0.00090	± 0.000028	0.00190	± 0.000638	0.000035	± 0.000010	2.07E-14	99.2%	19.0279	496.12	± 2.52	0.5%
au25.4l.mus.81a.txt	1.8	10	2.06588	± 0.001920	0.10817	± 0.000195	0.00146	± 0.000035	0.00149	± 0.001082	0.000063	± 0.000010	3.35E-14	99.1%	18.9271	493.82	± 1.23	0.2%
au25.4l.mus.82a.txt	1.8	10	0.95740	± 0.001190	0.05058	± 0.000468	0.00066	± 0.000031	0.00079	± 0.000381	0.000020	± 0.000009	1.55E-14	99.4%	18.8151	491.26	± 4.81	1.0%
au25.4l.mus.83a.txt	1.8	10	0.67913	± 0.000617	0.03593	± 0.000208	0.00045	± 0.000025	-0.00031	± 0.001238	0.000020	± 0.000010	1.10E-14	99.1%	18.7343	489.41	± 3.55	0.7%
au25.4l.mus.84a.txt	1.8	10	0.52150	± 0.000676	0.02712	± 0.000097	0.00041	± 0.000024	0.00201	± 0.000978	0.000025	± 0.000011	8.47E-15	98.6%	18.9600	494.57	± 3.71	0.8%
au25.4l.mus.85a.txt	1.8	10	0.48059	± 0.000866	0.02485	± 0.000093	0.00032	± 0.000017	0.00072	± 0.000891	0.000033	± 0.000011	7.80E-15	97.9%	18.9473	494.28	± 3.91	0.8%
au25.4l.mus.86a.txt	1.8	10	0.79768	± 0.000927	0.04028	± 0.000249	0.00054	± 0.000023	0.00023	± 0.001358	0.000105	± 0.000010	1.30E-14	96.1%	19.0331	496.24	± 3.80	0.8%
au25.4l.mus.87a.txt	1.8	10	1.49366	± 0.001648	0.07765	± 0.000469	0.00098	± 0.000030	-0.00188	± 0.000638	0.000060	± 0.000009	2.42E-14	98.8%	19.0068	495.64	± 3.22	0.6%
au25.4l.mus.88a.txt	1.8	10	1.83308	± 0.002408	0.09716	± 0.000251	0.00125	± 0.000025	0.00118	± 0.001250	0.000029	± 0.000010	2.98E-14	99.5%	18.7801	490.46	± 1.64	0.3%
au25.4l.mus.89a.txt	1.8	10	1.15608	± 0.000960	0.06109	± 0.000175	0.00079	± 0.000026	-0.00059	± 0.000937	0.000059	± 0.000010	1.88E-14	98.5%	18.6365	487.18	± 1.97	0.4%
au25.4l.mus.90a.txt	1.8	10	1.81006	± 0.002120	0.09576	± 0.000401	0.00126	± 0.000026	-0.00026	± 0.000916	0.000048	± 0.000009	2.94E-14	99.2%	18.7527	489.84	± 2.27	0.5%
au25.4l.mus.91a.txt	1.8	10	0.56215	± 0.000771	0.02985	± 0.000203	0.00040	± 0.000024	0.00085	± 0.000858	0.000042	± 0.000010	9.13E-15	97.8%	18.4247	482.32	± 4.33	0.9%
au25.4l.mus.92a.txt	1.8	10	0.44763	± 0.001159	0.02422	± 0.000255	0.00019	± 0.000035	0.00024	± 0.001058	0.000015	± 0.000010	7.27E-15	99.0%	18.2941	479.31	± 6.09	1.3%
au25.4l.mus.93a.txt	1.8	10	2.67086	± 0.002415	0.13883	± 0.000474	0.00178	± 0.000027	-0.00099	± 0.001072	0.000100	± 0.000009	4.34E-14	98.9%	19.0248	496.05	± 1.84	0.4%
au25.4l.mus.94a.txt	1.8	10	2.08927	± 0.001117	0.10863	± 0.000349	0.00145	± 0.000027	-0.00017	± 0.000910	0.000124	± 0.000010	3.39E-14	98.3%	18.8975	493.14	± 1.77	0.4%
au25.4l.mus.95a.txt	1.8	10	0.61972	± 0.000964	0.03093	± 0.000142	0.00041	± 0.000022	-0.00113	± 0.001083	0.000099	± 0.000017	1.01E-14	95.3%	19.0837	497.39	± 4.92	1.0%
au25.4l.mus.96a.txt	1.8	10	1.00532	± 0.000759	0.05213	± 0.000220	0.00077	± 0.000049	-0.00002	± 0.000986	0.000107	± 0.000017	1.63E-14	96.9%	18.6799	488.17	± 3.36	0.7%
au25.4l.mus.97a.txt	1.8	10	1.55573	± 0.001609	0.08087	± 0.000374	0.00105	± 0.000016	-0.00596	± 0.001548	0.000153	± 0.000017	2.53E-14	97.1%	18.6686	487.91	± 2.90	0.6%
au25.4l.mus.98a.txt	1.8	10	1.62504	± 0.001270	0.08494	± 0.000331	0.00103	± 0.000035	-0.00136	± 0.000473	0.000082	± 0.000011	2.64E-14	98.5%	18.8446	491.94	± 2.21	0.4%
au25.4l.mus.99a.txt	1.8	10	0.56303	± 0.000980	0.02954	± 0.000109	0.00036	± 0.000020	0.00043	± 0.001015	0.000020	± 0.000010	9.14E-15	98.9%	18.8572	492.22	± 3.35	0.7%
au25.4l.mus.100a.txt	1.8	10	2.72757	± 0.001775	0.14483	± 0.000405	0.00186	± 0.000038	0.00409	± 0.001136	0.000011	± 0.000015	4.43E-14	99.9%	18.8140	491.24	± 1.62	0.3%
au25.4l.mus.101a.txt	1.8	10	0.84410	± 0.000937	0.04392	± 0.000268	0.00065	± 0.000039	-0.00032	± 0.001135	0.000012	± 0.000015	1.37E-14	99.6%	19.1377	498.62	± 4.07	0.8%
au25.4l.mus.102a.txt	1.8	10	0.76464	± 0.001639	0.04028	± 0.000264	0.00053	± 0.000027	0.00022	± 0.000755	0.000034	± 0.000011	1.24E-14	98.7%	18.7330	489.39	± 3.98	0.8%
au25.4l.mus.103a.txt	1.8	10	1.29411	± 0.001926	0.06847	± 0.000234	0.00086	± 0.000026	-0.00051	± 0.001098	0.000083	± 0.000014	2.10E-14	98.1%	18.5393	484.95	± 2.42	0.5%
au25.4l.mus.104a.txt	1.8	10	0.96269	± 0.001137	0.05020	± 0.000367	0.00062	± 0.000023	0.00160	± 0.001214	-0.000015	± 0.000016	1.56E-14	100.5%	19.1787	499.55	± 4.44	0.9%
au25.4l.mus.105a.txt	1.8	10	0.52256	± 0.000802	0.02704	± 0.000171	0.00033	± 0.000030	-0.00254	± 0.001784	0.000028	± 0.000020	8.48E-15	98.4%	19.0129	495.78	± 6.55	1.3%
au25.4l.mus.106a.txt	1.8	10	0.40791	± 0.000700	0.02138	± 0.000108	0.00033	± 0.000024	0.00130	± 0.000815	-0.000010	± 0.000015	6.62E-15	100.7%	19.0842	497.40	± 5.98	1.2%
au25.4l.mus.107a.txt	1.8	10	1.20497	± 0.001646	0.06244	± 0.000359	0.00081	± 0.000028	0.00221	± 0.000970	0.000074	± 0.000008	1.96E-14	98.2%	18.9529	494.41	± 3.15	0.6%
au25.4l.mus.108a.txt	1.8	10	1.04015	± 0.001308	0.05554	± 0.000217	0.00076	± 0.000022	0.00285	± 0.001187	0.000030	± 0.000009	1.69E-14	99.2%	18.5766	485.80	± 2.36	0.5%
au25.4l.mus.109a.txt	1.8	10	2.58364	± 0.001586	0.13740	± 0.000296	0.00190	± 0.000052	0.00173	± 0.000736	-0.000018	± 0.000017	4.19E-14	100.2%	18.8051	491.03	± 1.44	0.3%
au25.4l.mus.110a.txt	1.8	10	1.39826	± 0.001802	0.07410	± 0.000258	0.00107	± 0.000053	0.00199	± 0.001041	-0.000004	± 0.000013	2.27E-14	100.1%	18.8719	492.56	± 2.28	0.5%
au25.4l.mus.113a.txt	1.8	10	1.74793	± 0.003449	0.09305	± 0.000233	0.00120	± 0.000028	0.00123	± 0.000698	0.000062	± 0.000011	2.84E-14	99.0%	18.5904	486.12	± 1.81	0.4%
au25.4l.mus.114a.txt	1.8	10	2.78114	± 0.003195	0.14686	± 0.000524	0.00184	± 0.000023	0.00005	± 0.000668	0.000102	± 0.000010	4.52E-14	98.9%	18.7324	489.37	± 1.93	0.4%
au25.4l.mus.115a.txt	1.8	10	1.21472	± 0.002075	0.06390	± 0.000367	0.00085	± 0.000025	0.00213	± 0.000997	0.000054	± 0.000009	1.97E-14	98.7%	18.7630	490.07	± 3.19	0.7%
au25.4l.mus.116a.txt	1.8	10	1.56921	± 0.002752	0.08335	± 0.000490	0.00101	± 0.000018	0.00102	± 0.001270	0.000015	± 0.000012	2.55E-14	99.7%	18.7756	490.36	± 3.23	0.7%
au25.4l.mus.117a.txt	1.8	10	7.33325	± 0.005210	0.39278	± 0.001030	0.00525	± 0.000077	0.00434	± 0.000828	0.000057	± 0.000017	1.19E-13	99.8%	18.6281	486.98	± 1.37	0.3%
au25.4l.mus.118a.txt	1.8	10	2.53540	± 0.002653	0.13495	± 0.000465	0.00173	± 0.000031	0.00119	± 0.001063	-0.000018	± 0.000019	4.12E-14	100.2%	18.7890	490.66	± 2.08	0.4%
																112		

I-T-1 Muscovite																		
au25.4s.mus.5a.txt	1.8	10	21.86646	± 0.019136	0.60024	± 0.001349	0.00803	± 0.000072	0.02046	± 0.001003	0.000200	± 0.000017	3.55E-13	99.7%	36.3352	852.92	± 2.07	0.2%
au25.4s.mus.7a.txt	1.8	10	19.29014	± 0.010827	0.52825	± 0.001237	0.00734	± 0.000104	0.02683	± 0.001175	0.000279	± 0.000018	3.13E-13	99.6%	36.3670	853.51	± 2.08	0.2%
au25.4s.mus.3a.txt	1.8	10	19.13754	± 0.018967	0.52155	± 0.000892	0.00704	± 0.000070	0.02869	± 0.001065	0.000284	± 0.000018	3.11E-13	99.6%	36.5397	856.74	± 1.72	0.2%
au25.4s.mus.4a.txt	1.8	10	6.16595	± 0.009098	0.17043	± 0.000540	0.00218	± 0.000027	0.00319	± 0.000985	0.000074	± 0.000011	1.00E-13	99.6%	36.0526	847.62	± 3.01	0.4%
au25.4s.mus.6a.txt	1.8	10	9.43974	± 0.011329	0.26148	± 0.000420	0.00337	± 0.000037	0.00325	± 0.000784	0.000077	± 0.000016	1.53E-13	99.8%	36.0163	846.94	± 1.76	0.2%
au25.4s.mus.8a.txt	1.8	10	20.76087	± 0.008089	0.57187	± 0.001130	0.00768	± 0.000070	0.02320	± 0.001207	0.000176	± 0.000015	3.37E-13	99.7%	36.2169	850.70	± 1.73	0.2%
au25.4s.mus.11a.txt	1.8	10	14.25700	± 0.010428	0.38764	± 0.000888	0.00536	± 0.000078	0.02112	± 0.001001	0.000447	± 0.000025	2.31E-13	99.1%	36.4446	854.96	± 2.12	0.2%
au25.4s.mus.12a.txt	1.8	10	24.13634	± 0.016223	0.65182	± 0.001040	0.00865	± 0.000085	0.01981	± 0.000886	0.000269	± 0.000033	3.92E-13	99.7%	36.9107	863.65	± 1.54	0.2%
au25.4s.mus.13a.txt	1.8	10	5.33899	± 0.007013	0.14304	± 0.000388	0.00190	± 0.000031	-0.00100	± 0.000971	0.000179	± 0.000011	8.67E-14	99.0%	36.9546	864.47	± 2.68	0.3%
au25.4s.mus.14a.txt	1.8	10	18.76713	± 0.021426	0.50101	± 0.001055	0.00666	± 0.000085	0.02456	± 0.000782	0.000227	± 0.000019	3.05E-13	99.6%	37.3310	871.45	± 2.11	0.2%
au25.4s.mus.15a.txt	1.8	10	18.48704	± 0.013482	0.50454	± 0.001478	0.00667	± 0.000089	0.01556	± 0.001636	0.000275	± 0.000014	3.00E-13	99.6%	36.4838	855.70	± 2.60	0.3%
au25.4s.mus.16a.txt	1.8	10	13.23593	± 0.012838	0.35668	± 0.000849	0.00487	± 0.000041	0.02222	± 0.001107	0.000241	± 0.000016	2.15E-13	99.5%	36.9164	863.76	± 2.25	0.3%
au25.4s.mus.17a.txt	1.8	10	16.69570	± 0.007203	0.44986	± 0.001124	0.00611	± 0.000060	0.02252	± 0.000814	0.000241	± 0.000017	2.71E-13	99.6%	36.9609	864.58	± 2.22	0.3%
au25.4s.mus.18a.txt	1.8	10	1.37216	± 0.001919	0.03851	± 0.000161	0.00051	± 0.000037	0.00149	± 0.001078	0.000049	± 0.000010	2.23E-14	98.9%	35.2561	832.62	± 4.16	0.5%
au25.4s.mus.19a.txt	1.8	10	24.17756	± 0.014758	0.67080	± 0.001828	0.00914	± 0.000047	0.02637	± 0.000649	0.000190	± 0.000016	3.93E-13	99.8%	35.9640	845.96	± 2.37	0.3%
au25.4s.mus.20a.txt	1.8	10	14.70274	± 0.007721	0.39785	± 0.000934	0.00548	± 0.000051	0.03264	± 0.001600	0.000252	± 0.000021	2.39E-13	99.5%	36.7785	861.19	± 2.11	0.2%
au25.4s.mus.21a.txt	1.8	10	17.26142	± 0.016251	0.46678	± 0.000945	0.00624	± 0.000078	0.02301	± 0.001256	0.000294	± 0.000019	2.80E-13	99.5%	36.7994	861.58	± 1.95	0.2%
au25.4s.mus.22a.txt	1.8	10	4.56564	± 0.002014	0.12960	± 0.000466	0.00174	± 0.000035	0.00075	± 0.000931	0.000143	± 0.000023	7.41E-14	99.1%	34.9025	825.92	± 3.28	0.4%
au25.4s.mus.23a.txt	1.8	10	18.46857	± 0.010030	0.51060	± 0.001221	0.00686	± 0.000073	0.02355	± 0.000846	0.000242	± 0.000029	3.00E-13	99.6%	36.0363	847.32	± 2.12	0.3%
au25.4s.mus.24a.txt	1.8	10	6.64978	± 0.008418	0.17363	± 0.000533	0.00222	± 0.000039	0.00182	± 0.001112	0.000073	± 0.000024	1.08E-13	99.7%	38.1752	887.01	± 3.10	0.3%
au25.4s.mus.25a.txt	1.8	10	8.80452	± 0.006325	0.24369	± 0.000396	0.00318	± 0.000042	-0.00067	± 0.000689	0.000060	± 0.000017	1.43E-13	99.8%	36.0563	847.69	± 1.59	0.2%
au25.4s.mus.26a.txt	1.8	10	8.70962	± 0.010997	0.24298	± 0.000697	0.00316	± 0.000030	0.00023	± 0.001075	0.000088	± 0.000017	1.41E-13	99.7%	35.7381	841.71	± 2.69	0.3%
au25.4s.mus.27a.txt	1.8	10	14.59174	± 0.009788	0.39882	± 0.000943	0.00530	± 0.000053	0.02322	± 0.000768	0.000177	± 0.000022	2.37E-13	99.6%	36.4628	855.30	± 2.14	0.3%
au25.4s.mus.28a.txt	1.8	10	11.79845	± 0.011704	0.32280	± 0.000824	0.00436	± 0.000060	0.01788	± 0.001113	0.000178	± 0.000018	1.92E-13	99.6%	36.3941	854.02	± 2.38	0.3%
au25.4s.mus.29a.txt	1.8	10	8.18235	± 0.008543	0.23112	± 0.000923	0.00299	± 0.000036	0.00123	± 0.001245	0.000067	± 0.000020	1.33E-13	99.8%	35.3183	833.80	± 3.51	0.4%
au25.4s.mus.30a.txt	1.8	10	16.38004	± 0.009930	0.44932	± 0.001312	0.00595	± 0.000068	0.02499	± 0.000760	0.000131	± 0.000014	2.66E-13	99.8%	36.3758	853.68	± 2.56	0.3%
au25.4s.mus.31a.txt	1.8	10	24.21998	± 0.015261	0.69256	± 0.001353	0.00925	± 0.000056	0.02578	± 0.000817	0.000270	± 0.000013	3.93E-13	99.7%	34.8609	825.13	± 1.70	0.2%
au25.4s.mus.32a.txt	1.8	10	13.42072	± 0.010994	0.37231	± 0.001079	0.00495	± 0.000067	0.02320	± 0.001076	0.000188	± 0.000015	2.18E-13	99.6%	35.9052	844.86	± 2.57	0.3%
au25.4s.mus.33a.txt	1.8	10	13.44633	± 0.012418	0.36672	± 0.001234	0.00493	± 0.000051	0.02317	± 0.000532	0.000254	± 0.000017	2.18E-13	99.4%	36.4691	855.42	± 3.02	0.4%
au25.4s.mus.34a.txt	1.8	10	13.63568	± 0.010832	0.37372	± 0.001008	0.00506	± 0.000074	0.02345	± 0.001039	0.000170	± 0.000018	2.21E-13	99.6%	36.3600	853.38	± 2.43	0.3%
au25.4s.mus.35a.txt	1.8	10	15.28054	± 0.012769	0.41802	± 0.000950	0.00571	± 0.000058	0.01779	± 0.001213	0.000266	± 0.000021	2.48E-13	99.5%	36.3717	853.60	± 2.10	0.2%
au25.4s.mus.36a.txt	1.8	10	6.16962	± 0.006228	0.17023	± 0.000446	0.00221	± 0.000031	-0.00357	± 0.001087	0.000095	± 0.000016	1.00E-13	99.5%	36.0752	848.05	± 2.48	0.3%
au25.4s.mus.37a.txt	1.8	10	16.19995	± 0.013590	0.44895	± 0.001235	0.00618	± 0.000054	0.01855	± 0.000794	0.000178	± 0.000019	2.63E-13	99.7%	35.9715	846.10	± 2.46	0.3%
au25.4s.mus.38a.txt	1.8	10	15.57345	± 0.014486	0.43094	± 0.001130	0.00583	± 0.000070	0.01663	± 0.000964	0.000147	± 0.000032	2.53E-13	99.7%	36.0422	847.43	± 2.42	0.3%
au25.4s.mus.39a.txt	1.8	10	6.29146	± 0.009169	0.17258	± 0.000649	0.00223	± 0.000023	-0.00382	± 0.001105	0.000104	± 0.000017	1.02E-13	99.5%	36.2756	851.80	± 3.52	0.4%
au25.4s.mus.40a.txt	1.8	10	4.60805	± 0.004839	0.12443	± 0.000384	0.00168	± 0.000040	0.00044	± 0.000871	-0.000009	± 0.000010	7.48E-14	100.1%	37.0348	865.96	± 2.88	0.3%
au25.4s.mus.41a.txt	1.8	10	6.69973	± 0.007203	0.17938	± 0.000473	0.00249	± 0.000035	0.00056	± 0.001125	0.000067	± 0.000012	1.09E-13	99.7%	37.2383	869.73	± 2.53	0.3%
au25.4s.mus.42a.txt	1.8	10	18.75428	± 0.017616	0.54923	± 0.001126	0.00735	± 0.000082	0.02069	± 0.001170	0.000144	± 0.000015	3.04E-13	99.8%	34.0734	810.11	± 1.84	0.2%
au25.4s.mus.43a.txt	1.8	10	16.00872	± 0.010507	0.44402	± 0.000751	0.00609	± 0.000064	0.02522	± 0.000836	0.000153	± 0.000026	2.60E-13	99.7%	35.9593	845.87	± 1.59	0.2%
au25.4s.mus.44a.txt	1.8	10	10.30883	± 0.017581	0.28409	± 0.000671	0.00373	± 0.000045	0.00015	± 0.001009	0.000064	± 0.000012	1.67E-13	99.8%	36.2204	850.77	± 2.50	0.3%
au25.4s.mus.45a.txt	1.8	10	18.30965	± 0.012779	0.50324	± 0.001155	0.00667	± 0.000054	0.02331	± 0.000541	0.000252	± 0.000022	2.97E-13	99.6%	36.2409	851.15	± 2.07	0.2%
au25.4s.mus.46a.txt	1.8	10	5.81833	± 0.006071	0.15869	± 0.000496	0.00204	± 0.000024	0.00086	± 0.000897	0.000103	± 0.000018	9.45E-14	99.5%	36.4723	855.48	± 2.94	0.3%
au25.4s.mus.47a.txt	1.8	10	7.02925	± 0.005895	0.19510	± 0.000459	0.00252	± 0.000033	0.00088	± 0.000484	0.000113	± 0.000018	1.14E-13	99.5%	35.8583	843.98	± 2.22	0.3%
au25.4s.mus.48a.txt	1.8	10	23.23872	± 0.014432	0.64932	± 0.001144	0.00874	± 0.000044	0.02249	± 0.001051	0.000286	± 0.000036	3.77E-13	99.6%	35.6633	840.31	± 1.62	0.2%
au25.4s.mus.49a.txt	1.8	10	15.64775	± 0.017144	0.42980	± 0.001029	0.00583	± 0.000068	0.02380	± 0.000739	0.000228	± 0.000023	2.54E-13	99.6%	36.2570	851.45	± 2.28	0.3%
au25.4s.mus.50a.txt	1.8	10	9.80099	± 0.013422	0.26999	± 0.000458	0.00358	± 0.000038	0.00250	± 0.000630	0.000075	± 0.000017	1.59E-13	99.8%	36.2208	850.78	± 1.91	0.2%
au25.4s.mus.51a.txt	1.8	10	4.93583	± 0.004891	0.13356	± 0.000438	0.00182	± 0.000038	0.00372	± 0.000965	0.000310	± 0.000020	8.01E-14	98.1%	36.2711	851.72	± 3.15	0.4%
au25.4s.mus.52a.txt	1.8	10	3.53189	± 0.003404	0.09533	± 0.000209	0.00138	± 0.000038	0.00156	± 0.000857	0.000126	± 0.000022	5.73E-14	98.9%	36.6616	859.01	± 2.62	0.3%
au25.4s.mus.53a.txt	1.8	10	13.25827	± 0.009808	0.35956	± 0.001222	0.00494	± 0.000060	0.02361	± 0.001219	0.000299	± 0.000019	2.15E-13	99.3%	36.6360	858.54	± 3.03	0.4%
au25.4s.mus.54a.txt	1.8	10	0.40978	± 0.000563	0.01346	± 0.000145	0.00021	± 0.000028	0.00250	± 0.000918	0.000018	± 0.000009	6.65E-15	98.7%	30.0704	731.76	± 9.51	1.3%
au25.4s.mus.55a.txt	1.8	10	20.76979	± 0.010267	0.56915	± 0.000876	0.00761	± 0.000048	0.02442	± 0.001087	0.000266	± 0.000018	3.37E-13	99.6%	36.3599	853.38	± 1.40	0.2%
au25.4s.mus.56a.txt	1.8	10	11.85592	± 0.015108	0.32273	± 0.000840	0.00446	± 0.000073	0.02564	± 0.001108	0.000157	± 0.000018	1.92E-13	99.6%	36.6023	857.91	± 2.52	0.3%
au25.4s.mus.57a.txt	1.8	10	10.55991	± 0.006666	0.29688	± 0.000593	0.00403	± 0.000062	0.01259	± 0.001520	0.000149	± 0.000016	1.71E-13	99.6%	35.4263	835.84	± 1.80	0.2%
au25.4s.mus.58a.txt	1.8	10	14.29627	± 0.010304	0.39032	± 0.000993	0.00527	± 0.000071	0.02343	± 0.001164	0.000293	± 0.000031	2.32E-13	99.4%	36.4124	854.36	± 2.34	0.3%
au25.4s.mus.59a.txt	1.8	10	15.35667	± 0.012257	0.41680	± 0.001031	0.00564	± 0.000047	0.02408	± 0.001114	0.000371	± 0.000019	2.49E-13	99.3%	36.5881	857.64	± 2.27	0.3%
au25.4s.mus.61a.txt	1.8	10	4.97243	± 0.003871	0.13647	± 0.000485	0.00162	± 0.000054	-0.00039	± 0.000449	0.000097	± 0.000018	8.07E-14	99.4%	36.2270	850.89	± 3.25	0.4%

au25.4s.mus.62a.txt	1.8	10	20.40649	± 0.015259	0.55475	± 0.001388	0.00753	± 0.000072	0.02320	± 0.000821	0.000246	± 0.000017	3.31E-13	99.6%	36.6590	858.96	± 2.26	0.3%
au25.4s.mus.63a.txt	1.8	10	5.37415	± 0.005393	0.14639	± 0.000465	0.00195	± 0.000027	0.00161	± 0.001228	0.000077	± 0.000020	8.72E-14	99.6%	36.5582	857.08	± 3.02	0.4%
au25.4s.mus.64a.txt	1.8	10	21.04655	± 0.009036	0.58478	± 0.001379	0.00771	± 0.000048	0.02395	± 0.000681	0.000216	± 0.000017	3.42E-13	99.7%	35.8865	844.51	± 2.04	0.2%
au25.4s.mus.65a.txt	1.8	10	16.18947	± 0.009304	0.45231	± 0.000746	0.00600	± 0.000101	0.02384	± 0.000724	0.000161	± 0.000014	2.63E-13	99.7%	35.6940	840.88	± 1.49	0.2%
au25.4s.mus.66a.txt	1.8	10	13.22792	± 0.012787	0.36068	± 0.000864	0.00497	± 0.000051	0.02182	± 0.000738	0.000134	± 0.000017	2.15E-13	99.7%	36.5723	857.35	± 2.25	0.3%
au25.4s.mus.67a.txt	1.8	10	7.52075	± 0.012105	0.20731	± 0.000406	0.00275	± 0.000036	0.00025	± 0.000631	0.000080	± 0.000010	1.22E-13	99.7%	36.1635	849.70	± 2.18	0.3%
au25.4s.mus.68a.txt	1.8	10	12.10329	± 0.013067	0.33057	± 0.000847	0.00453	± 0.000068	0.02288	± 0.001198	0.000203	± 0.000014	1.96E-13	99.5%	36.4400	854.88	± 2.41	0.3%
au25.4s.mus.69a.txt	1.8	10	10.88915	± 0.007697	0.28368	± 0.001060	0.00385	± 0.000035	0.02424	± 0.000906	0.000166	± 0.000016	1.77E-13	99.5%	38.2234	887.90	± 3.41	0.4%
au25.4s.mus.70a.txt	1.8	10	4.90012	± 0.006001	0.12854	± 0.000528	0.00170	± 0.000049	0.00229	± 0.000941	0.000018	± 0.000016	7.96E-14	99.9%	38.0817	885.29	± 3.90	0.4%
au25.4s.mus.71a.txt	1.8	10	12.95063	± 0.009916	0.35889	± 0.000929	0.00496	± 0.000067	0.02521	± 0.000742	0.000175	± 0.000023	2.10E-13	99.6%	35.9503	845.70	± 2.34	0.3%
au25.4s.mus.72a.txt	1.8	10	5.63282	± 0.008368	0.15391	± 0.000361	0.00210	± 0.000051	0.00077	± 0.000800	0.000057	± 0.000016	9.14E-14	99.7%	36.4884	855.78	± 2.49	0.3%
au25.4s.mus.73a.txt	1.8	10	9.64504	± 0.013082	0.26638	± 0.000459	0.00361	± 0.000046	0.00265	± 0.000798	0.000073	± 0.000018	1.57E-13	99.8%	36.1289	849.06	± 1.93	0.2%
au25.4s.mus.74a.txt	1.8	10	4.83588	± 0.006554	0.14186	± 0.000627	0.00192	± 0.000043	0.00196	± 0.000905	0.000147	± 0.000009	7.85E-14	99.1%	33.7841	804.56	± 3.78	0.5%
au25.4s.mus.75a.txt	1.8	10	16.20594	± 0.015175	0.45345	± 0.001473	0.00580	± 0.000081	0.02306	± 0.000792	0.000202	± 0.000017	2.63E-13	99.6%	35.6134	839.37	± 2.86	0.3%
au25.4s.mus.76a.txt	1.8	10	17.06952	± 0.014446	0.47104	± 0.001021	0.00621	± 0.000083	0.02517	± 0.001224	0.000200	± 0.000016	2.77E-13	99.7%	36.1189	848.87	± 2.00	0.2%
au25.4s.mus.77a.txt	1.8	10	2.83155	± 0.003440	0.07992	± 0.000171	0.00107	± 0.000022	0.00183	± 0.001253	-0.000005	± 0.000017	4.60E-14	100.1%	35.4333	835.97	± 2.54	0.3%
au25.4s.mus.78a.txt	1.8	10	4.97803	± 0.005916	0.33301	± 0.000898	0.00424	± 0.000044	0.00513	± 0.000954	0.000073	± 0.000011	8.08E-14	99.6%	14.8854	399.13	± 1.21	0.3%
au25.4s.mus.79a.txt	1.8	10	7.85603	± 0.011670	0.21369	± 0.000900	0.00274	± 0.000034	0.00371	± 0.001211	0.000084	± 0.000008	1.28E-13	99.7%	36.6493	858.78	± 3.86	0.4%
au25.4s.mus.80a.txt	1.8	10	4.67680	± 0.007251	0.12695	± 0.000454	0.00166	± 0.000048	0.00076	± 0.001050	0.000008	± 0.000011	7.59E-14	100.0%	36.8216	861.99	± 3.42	0.4%
au25.4s.mus.81a.txt	1.8	10	18.05100	± 0.026815	0.50168	± 0.001892	0.00682	± 0.000085	0.02366	± 0.000826	0.000257	± 0.000029	2.93E-13	99.6%	35.8350	843.54	± 3.46	0.4%
au25.4s.mus.82a.txt	1.8	10	23.23775	± 0.027237	0.65043	± 0.001933	0.00882	± 0.000092	0.02492	± 0.001012	0.000126	± 0.000035	3.77E-13	99.8%	35.6741	840.51	± 2.71	0.3%
au25.4s.mus.83a.txt	1.8	10	14.61474	± 0.013849	0.40966	± 0.000791	0.00546	± 0.000059	0.02345	± 0.001393	0.000017	± 0.000023	2.37E-13	100.0%	35.6699	840.43	± 1.85	0.2%
au25.4s.mus.84a.txt	1.8	10	8.48425	± 0.013898	0.22878	± 0.000753	0.00304	± 0.000061	0.00306	± 0.000666	0.000131	± 0.000013	1.38E-13	99.5%	36.9174	863.77	± 3.21	0.4%
au25.4s.mus.85a.txt	1.8	10	7.38580	± 0.004882	0.20211	± 0.000526	0.00270	± 0.000028	0.00347	± 0.000924	0.000050	± 0.000021	1.20E-13	99.8%	36.4734	855.50	± 2.41	0.3%
au25.4s.mus.86a.txt	1.8	10	0.87357	± 0.001299	0.02759	± 0.000194	0.00036	± 0.000025	0.00109	± 0.000796	0.000128	± 0.000013	1.42E-14	95.7%	30.2915	736.17	± 6.54	0.9%
au25.4s.mus.87a.txt	1.8	10	11.65981	± 0.007087	0.31967	± 0.000720	0.00430	± 0.000063	0.02322	± 0.001307	0.000147	± 0.000032	1.89E-13	99.6%	36.3467	853.13	± 2.11	0.2%
au25.4s.mus.88a.txt	1.8	10	9.85691	± 0.013392	0.26355	± 0.000715	0.00342	± 0.000037	0.00451	± 0.001066	0.000083	± 0.000019	1.60E-13	99.8%	37.3097	871.05	± 2.70	0.3%
au25.4s.mus.89a.txt	1.8	10	18.79876	± 0.016949	0.50759	± 0.000675	0.00667	± 0.000097	0.02797	± 0.001266	0.000077	± 0.000032	3.05E-13	99.9%	36.9972	865.26	± 1.46	0.2%
au25.4s.mus.90a.txt	1.8	10	23.92201	± 0.016980	0.65459	± 0.001471	0.00866	± 0.000082	0.02542	± 0.001233	0.000277	± 0.000030	3.88E-13	99.7%	36.4249	854.59	± 2.05	0.2%
au25.4s.mus.91a.txt	1.8	10	17.64872	± 0.014470	0.48380	± 0.001247	0.00648	± 0.000081	0.02329	± 0.001044	0.000218	± 0.000035	2.87E-13	99.6%	36.3518	853.23	± 2.37	0.3%
au25.4s.mus.92a.txt	1.8	10	5.99573	± 0.004618	0.16444	± 0.000324	0.00217	± 0.000047	-0.00041	± 0.001613	0.000266	± 0.000013	9.73E-14	98.7%	35.9816	846.29	± 1.89	0.2%
au25.4s.mus.93a.txt	1.8	10	14.27576	± 0.009378	0.37692	± 0.000817	0.00508	± 0.000044	0.02063	± 0.001120	0.000071	± 0.000031	2.32E-13	99.9%	37.8258	880.59	± 2.08	0.2%
au25.4s.mus.94a.txt	1.8	10	6.23403	± 0.008267	0.16365	± 0.000603	0.00211	± 0.000053	0.00083	± 0.001036	0.000064	± 0.000017	1.01E-13	99.7%	37.9790	883.41	± 3.54	0.4%
au25.4s.mus.95a.txt	1.8	10	8.83883	± 0.005807	0.24032	± 0.000761	0.00321	± 0.000030	0.00300	± 0.000907	0.000057	± 0.000019	1.43E-13	99.8%	36.7105	859.92	± 2.84	0.3%
au25.4s.mus.96a.txt	1.8	10	11.51325	± 0.007364	0.32129	± 0.000809	0.00451	± 0.000055	0.02361	± 0.000928	0.000132	± 0.000029	1.87E-13	99.7%	35.7222	841.42	± 2.28	0.3%
au25.4s.mus.97a.txt	1.8	10	13.47102	± 0.009458	0.37250	± 0.001103	0.00515	± 0.000061	0.02125	± 0.001069	0.000145	± 0.000024	2.19E-13	99.7%	36.0556	847.68	± 2.63	0.3%
au25.4s.mus.98a.txt	1.8	10	15.21674	± 0.012338	0.41127	± 0.001051	0.00573	± 0.000083	0.02673	± 0.000534	0.000207	± 0.000020	2.47E-13	99.6%	36.8580	862.67	± 2.35	0.3%
au25.4s.mus.99a.txt	1.8	10	7.58734	± 0.009045	0.20653	± 0.000440	0.00280	± 0.000039	0.00202	± 0.000921	0.000051	± 0.000019	1.23E-13	99.8%	36.6656	859.09	± 2.20	0.3%
au25.4s.mus.100a.txt	1.8	10	1.07213	± 0.001395	0.02930	± 0.000148	0.00037	± 0.000027	0.00145	± 0.001335	-0.000037	± 0.000015	1.74E-14	101.0%	36.6021	857.90	± 5.67	0.7%
au25.4s.mus.101a.txt	1.8	10	23.81780	± 0.012522	0.65100	± 0.001345	0.00871	± 0.000070	0.02598	± 0.001011	0.000209	± 0.000024	3.87E-13	99.7%	36.4965	855.93	± 1.85	0.2%
au25.4s.mus.102a.txt	1.8	10	2.92690	± 0.004508	0.08256	± 0.000202	0.00100	± 0.000049	0.00423	± 0.001300	0.000033	± 0.000012	4.75E-14	99.7%	35.3382	834.17	± 2.61	0.3%
au25.4s.mus.103a.txt	1.8	10	11.75272	± 0.011457	0.34109	± 0.000722	0.00469	± 0.000045	0.02184	± 0.001087	0.000082	± 0.000023	1.91E-13	99.8%	34.3929	816.22	± 1.97	0.2%
au25.4s.mus.104a.txt	1.8	10	8.64269	± 0.011031	0.24330	± 0.000718	0.00321	± 0.000039	0.00140	± 0.000768	-0.000009	± 0.000017	1.40E-13	100.0%	35.5237	837.67	± 2.74	0.3%
au25.4s.mus.105a.txt	1.8	10	7.67576	± 0.009127	0.21136	± 0.000564	0.00287	± 0.000048	0.00047	± 0.000950	0.000191	± 0.000012	1.25E-13	99.3%	36.0495	847.57	± 2.52	0.3%
au25.4s.mus.106a.txt	1.8	10	7.47119	± 0.010242	0.19208	± 0.000446	0.00278	± 0.000045	0.00288	± 0.001598	0.001236	± 0.000023	1.21E-13	95.1%	36.9961	865.24	± 2.59	0.3%
au25.4s.mus.107a.txt	1.8	10	7.10812	± 0.008339	0.19669	± 0.000717	0.00266	± 0.000046	0.00257	± 0.000729	0.000055	± 0.000017	1.15E-13	99.8%	36.0573	847.71	± 3.31	0.4%
au25.4s.mus.108a.txt	1.8	10	9.18422	± 0.014653	0.24930	± 0.000902	0.00326	± 0.000054	0.00289	± 0.000997	-0.000002	± 0.000016	1.49E-13	100.0%	36.8421	862.38	± 3.44	0.4%
au25.4s.mus.109a.txt	1.8	10	3.27395	± 0.002968	0.08887	± 0.000300	0.00123	± 0.000040	0.00071	± 0.000968	-0.000032	± 0.000023	5.32E-14	100.3%	36.8400	862.34	± 3.52	0.4%
au25.4s.mus.110a.txt	1.8	10	0.70209	± 0.000971	0.01920	± 0.000193	0.00027	± 0.000017	-0.00102	± 0.000781	0.000002	± 0.000010	1.14E-14	99.9%	36.5249	856.46	± 9.42	1.1%
au25.4s.mus.113a.txt	1.8	10	9.69337	± 0.008120	0.26578	± 0.000662	0.00350	± 0.000031	0.00209	± 0.000540	0.000146	± 0.000011	1.57E-13	99.6%	36.3096	852.44	± 2.27	0.3%
au25.4s.mus.114a.txt	1.8	10	7.74461	± 0.010096	0.21660	± 0.000493	0.00295	± 0.000043	0.00112	± 0.000986	0.000011	± 0.000019	1.26E-13	100.0%	35.7400	841.75	± 2.29	0.3%
au25.4s.mus.115a.txt	1.8	10	24.07332	± 0.016186	0.65197	± 0.000953	0.00878	± 0.000120	0.02385	± 0.001184	0.000621	± 0.000038	3.91E-13	99.2%	36.6467	858.74	± 1.45	0.2%
au25.4s.mus.116a.txt	1.8	10	7.34866	± 0.012094	0.20220	± 0.000591	0.00265	± 0.000041	0.00125	± 0.001456	0.000062	± 0.000010	1.19E-13	99.8%	36.2536	851.39	± 2.89	0.3%
au25.4s.mus.117a.txt	1.8	10	9.57085	± 0.009887	0.26333	± 0.000548	0.00335	± 0.000038	0.00226	± 0.000727	0.000045	± 0.000016	1.55E-13	99.9%	36.2952	852.17	± 2.03	0.2%
au25.4s.mus.118a.txt	1.8	10	1.66879	± 0.001664	0.04708	± 0.000167	0.00061	± 0.000035	0.00083	± 0.001275	-0.000043	± 0.000015	2.71E-14	100.8%	35.4455	836.20	± 3.83	0.5%
																111.00		

B-B-2 Muscovite																		
au25.4j.mus.29a.txt	1.8	10	0.36246	± 0.000432	0.06343	± 0.000324	0.00101	± 0.000026	0.00172	± 0.001308	0.000067	± 0.000014	5.88E-15	94.6%	5.4062	155.36	± 2.11	1.4%
au25.4j.mus.85a.txt	1.8	10	0.24603	± 0.000522	0.01320	± 0.000157	0.00015	± 0.000022	0.00027	± 0.000598	0.000033	± 0.000018	3.99E-15	96.1%	17.9091	470.43	± 12.08	2.6%
au25.4j.mus.36a.txt	1.8	10	0.29223	± 0.000617	0.04809	± 0.000270	0.00075	± 0.000025	0.00168	± 0.001106	0.000034	± 0.000014	4.74E-15	96.5%	5.8702	168.09	± 2.70	1.6%
au25.4j.mus.23a.txt	1.8	10	0.64788	± 0.000931	0.11437	± 0.000406	0.00180	± 0.000038	0.00123	± 0.000871	0.000062	± 0.000010	1.05E-14	97.2%	5.5054	158.09	± 0.97	0.6%
au25.4j.mus.30a.txt	1.8	10	1.05962	± 0.001406	0.12704	± 0.000252	0.00167	± 0.000030	0.00692	± 0.001010	0.000094	± 0.000014	1.72E-14	97.4%	8.1276	228.78	± 1.10	0.5%
au25.4j.mus.97a.txt	1.8	10	1.29661	± 0.001860	0.06484	± 0.000378	0.00082	± 0.000029	0.00025	± 0.001119	0.000097	± 0.000024	2.11E-14	97.8%	19.5545	508.08	± 4.19	0.8%
au25.4j.mus.7a.txt	1.8	10	0.45016	± 0.000839	0.05164	± 0.000332	0.00101	± 0.000034	-0.00153	± 0.000754	0.000032	± 0.000010	7.31E-15	97.9%	8.5285	239.34	± 2.31	1.0%
au25.4j.mus.18a.txt	1.8	10	1.60725	± 0.001885	0.08347	± 0.000264	0.00106	± 0.000019	0.00038	± 0.001057	0.000089	± 0.000013	2.61E-14	98.4%	18.9419	494.16	± 2.06	0.4%
au25.4j.mus.102a.txt	1.8	10	1.77098	± 0.001615	0.08715	± 0.000525	0.00113	± 0.000035	0.00224	± 0.001404	0.000096	± 0.000009	2.88E-14	98.4%	19.9970	518.08	± 3.30	0.6%
au25.4j.mus.100a.txt	1.8	10	1.12696	± 0.001608	0.05941	± 0.000339	0.00072	± 0.000028	0.00048	± 0.001200	0.000056	± 0.000017	1.83E-14	98.5%	18.6918	488.44	± 3.63	0.7%
au25.4j.mus.81a.txt	1.8	10	1.12838	± 0.001584	0.05726	± 0.000260	0.00070	± 0.000029	-0.00189	± 0.000938	0.000052	± 0.000017	1.83E-14	98.6%	19.4364	505.41	± 3.38	0.7%
au25.4j.mus.99a.txt	1.8	10	1.41121	± 0.001841	0.07677	± 0.000360	0.00092	± 0.000036	-0.00095	± 0.000846	0.000056	± 0.000017	2.29E-14	98.8%	18.1674	476.40	± 2.92	0.6%
au25.4j.mus.82a.txt	1.8	10	1.16899	± 0.001553	0.06195	± 0.000262	0.00078	± 0.000023	-0.00050	± 0.001222	0.000043	± 0.000018	1.90E-14	98.9%	18.6653	487.83	± 3.17	0.6%
au25.4j.mus.46a.txt	1.8	10	3.01389	± 0.002407	0.14834	± 0.000653	0.00188	± 0.000039	0.00053	± 0.001022	0.000105	± 0.000011	4.89E-14	99.0%	20.1087	520.59	± 2.42	0.5%
au25.4j.mus.34a.txt	1.8	10	2.21362	± 0.001893	0.10928	± 0.000285	0.00139	± 0.000038	0.00296	± 0.000859	0.000073	± 0.000020	3.59E-14	99.0%	20.0615	519.53	± 2.02	0.4%
au25.4j.mus.22a.txt	1.8	10	5.96302	± 0.005282	0.31206	± 0.000823	0.00402	± 0.000044	0.00296	± 0.001232	0.000193	± 0.000020	9.68E-14	99.0%	18.9274	493.83	± 1.47	0.3%
au25.4j.mus.25a.txt	1.8	10	2.44154	± 0.001529	0.12918	± 0.000398	0.00164	± 0.000027	0.00025	± 0.001046	0.000076	± 0.000010	3.96E-14	99.1%	18.7253	489.21	± 1.66	0.3%
au25.4j.mus.114a.txt	1.8	10	1.04608	± 0.001321	0.05334	± 0.000170	0.00069	± 0.000024	0.00152	± 0.001336	0.000033	± 0.000011	1.70E-14	99.1%	19.4345	505.36	± 2.40	0.5%
au25.4j.mus.106a.txt	1.8	10	4.02577	± 0.002494	0.21389	± 0.000802	0.00279	± 0.000041	0.00187	± 0.000992	0.000120	± 0.000011	6.54E-14	99.1%	18.6563	487.63	± 1.91	0.4%
au25.4j.mus.66a.txt	1.8	10	3.20929	± 0.002762	0.16372	± 0.000326	0.00216	± 0.000029	0.00094	± 0.001592	0.000095	± 0.000012	5.21E-14	99.1%	19.4319	505.30	± 1.24	0.2%
au25.4j.mus.24a.txt	1.8	10	2.81744	± 0.003076	0.14738	± 0.000439	0.00199	± 0.000061	0.00173	± 0.001224	0.000083	± 0.000019	4.57E-14	99.1%	18.9522	494.39	± 1.87	0.4%
au25.4j.mus.83a.txt	1.8	10	1.09960	± 0.001604	0.05701	± 0.000188	0.00073	± 0.000028	-0.00058	± 0.001184	0.000032	± 0.000018	1.79E-14	99.2%	19.1237	498.30	± 3.06	0.6%
au25.4j.mus.75a.txt	1.8	10	1.12570	± 0.000997	0.05763	± 0.000308	0.00073	± 0.000029	0.00062	± 0.000830	0.000031	± 0.000009	1.83E-14	99.2%	19.3743	504.00	± 3.01	0.6%
au25.4j.mus.37a.txt	1.8	10	0.80124	± 0.001305	0.04201	± 0.000126	0.00056	± 0.000020	0.00266	± 0.001265	0.000022	± 0.000013	1.30E-14	99.2%	18.9259	493.79	± 2.95	0.6%
au25.4j.mus.92a.txt	1.8	10	3.24647	± 0.003787	0.17000	± 0.000718	0.00213	± 0.000040	0.00084	± 0.001176	0.000089	± 0.000010	5.27E-14	99.2%	18.9435	494.19	± 2.23	0.5%
au25.4j.mus.77a.txt	1.8	10	2.50508	± 0.002214	0.13063	± 0.000351	0.00164	± 0.000027	0.00163	± 0.001193	0.000068	± 0.000010	4.07E-14	99.2%	19.0245	496.04	± 1.53	0.3%
au25.4j.mus.19a.txt	1.8	10	1.71332	± 0.002035	0.08296	± 0.000253	0.00116	± 0.000030	0.00003	± 0.001105	0.000046	± 0.000009	2.78E-14	99.2%	20.4893	529.13	± 1.94	0.4%
au25.4j.mus.5a.txt	1.8	10	4.12840	± 0.003881	0.21028	± 0.000620	0.00276	± 0.000033	0.00045	± 0.000733	0.000107	± 0.000009	6.70E-14	99.2%	19.4821	506.44	± 1.61	0.3%
au25.4j.mus.57a.txt	1.8	10	0.89717	± 0.001253	0.04519	± 0.000166	0.00065	± 0.000032	0.00070	± 0.000821	0.000023	± 0.000015	1.46E-14	99.2%	19.7045	511.48	± 3.21	0.6%
au25.4j.mus.14a.txt	1.8	10	5.81898	± 0.007534	0.30395	± 0.000520	0.00451	± 0.000048	0.00228	± 0.001023	0.000134	± 0.000011	9.45E-14	99.3%	19.0153	495.83	± 1.11	0.2%
au25.4j.mus.42a.txt	1.8	10	5.69556	± 0.003888	0.30743	± 0.000680	0.00399	± 0.000047	0.00465	± 0.001369	0.000129	± 0.000021	9.25E-14	99.3%	18.4046	481.85	± 1.24	0.3%
au25.4j.mus.103a.txt	1.8	10	0.75517	± 0.001343	0.04582	± 0.000260	0.00065	± 0.000033	0.00083	± 0.000721	0.000017	± 0.000011	1.23E-14	99.4%	16.3761	434.64	± 3.17	0.7%
au25.4j.mus.13a.txt	1.8	10	7.90831	± 0.010385	0.41487	± 0.000682	0.00524	± 0.000034	0.00165	± 0.001073	0.000172	± 0.000010	1.28E-13	99.4%	18.9399	494.11	± 1.06	0.2%
au25.4j.mus.116a.txt	1.8	10	1.14714	± 0.001112	0.05886	± 0.000321	0.00074	± 0.000024	0.00089	± 0.000846	0.000025	± 0.000011	1.86E-14	99.4%	19.3675	503.84	± 3.14	0.6%
au25.4j.mus.80a.txt	1.8	10	3.50391	± 0.003346	0.17605	± 0.000398	0.00223	± 0.000032	0.00012	± 0.001269	0.000074	± 0.000010	5.69E-14	99.4%	19.7778	513.13	± 1.34	0.3%
au25.4j.mus.78a.txt	1.8	10	6.84950	± 0.007732	0.36545	± 0.001248	0.00551	± 0.000083	0.00102	± 0.000865	0.000145	± 0.000009	1.11E-13	99.4%	18.6257	486.93	± 1.77	0.4%
au25.4j.mus.12a.txt	1.8	10	15.31524	± 0.011927	0.79905	± 0.001728	0.01069	± 0.000176	0.02667	± 0.000805	0.000317	± 0.000017	2.49E-13	99.4%	19.0530	496.69	± 1.16	0.2%
au25.4j.mus.73a.txt	1.8	10	5.74841	± 0.004752	0.29711	± 0.000602	0.00378	± 0.000060	0.00056	± 0.001336	0.000116	± 0.000011	9.33E-14	99.4%	19.2329	500.79	± 1.14	0.2%
au25.4j.mus.68a.txt	1.8	10	0.82076	± 0.000877	0.04381	± 0.000234	0.00053	± 0.000025	0.00052	± 0.001050	0.000015	± 0.000012	1.33E-14	99.5%	18.6313	487.06	± 3.36	0.7%
au25.4j.mus.69a.txt	1.8	10	1.09087	± 0.001373	0.05756	± 0.000253	0.00069	± 0.000025	-0.00082	± 0.000975	0.000020	± 0.000012	1.77E-14	99.5%	18.8472	492.00	± 2.76	0.6%
au25.4j.mus.11a.txt	1.8	10	3.18435	± 0.003743	0.16642	± 0.000390	0.00210	± 0.000034	0.00043	± 0.001550	0.000058	± 0.000015	5.17E-14	99.5%	19.0319	496.21	± 1.49	0.3%
au25.4j.mus.63a.txt	1.8	10	1.25636	± 0.001118	0.06429	± 0.000211	0.00081	± 0.000025	0.00002	± 0.001003	0.000023	± 0.000014	2.04E-14	99.5%	19.4370	505.42	± 2.40	0.5%
au25.4j.mus.94a.txt	1.8	10	2.70513	± 0.003105	0.14434	± 0.000377	0.00188	± 0.000030	0.00295	± 0.001465	0.000049	± 0.000011	4.39E-14	99.5%	18.6438	487.34	± 1.51	0.3%
au25.4j.mus.15a.txt	1.8	10	17.21173	± 0.010848	0.86610	± 0.002164	0.01123	± 0.000099	0.02476	± 0.000917	0.000304	± 0.000016	2.79E-13	99.5%	19.7721	513.00	± 1.34	0.3%
au25.4j.mus.76a.txt	1.8	10	2.41031	± 0.002758	0.12936	± 0.000420	0.00164	± 0.000035	0.00105	± 0.001104	0.000042	± 0.000011	3.91E-14	99.5%	18.5371	484.90	± 1.80	0.4%
au25.4j.mus.79a.txt	1.8	10	1.41309	± 0.002019	0.07412	± 0.000358	0.00097	± 0.000026	0.00164	± 0.001098	0.000025	± 0.000009	2.29E-14	99.5%	18.9679	494.75	± 2.69	0.5%
au25.4j.mus.40a.txt	1.8	10	1.89530	± 0.001497	0.09543	± 0.000350	0.00121	± 0.000027	0.00134	± 0.000763	0.000033	± 0.000010	3.08E-14	99.5%	19.7616	512.77	± 2.10	0.4%
au25.4j.mus.50a.txt	1.8	10	4.24951	± 0.002426	0.21507	± 0.000423	0.00281	± 0.000044	-0.00041	± 0.000904	0.000073	± 0.000010	6.90E-14	99.5%	19.6590	510.45	± 1.11	0.2%
au25.4j.mus.35a.txt	1.8	10	1.20822	± 0.001073	0.06000	± 0.000336	0.00076	± 0.000029	0.00224	± 0.000889	0.000020	± 0.000019	1.96E-14	99.5%	20.0434	519.12	± 3.84	0.7%
au25.4j.mus.38a.txt	1.8	10	5.47839	± 0.005601	0.29406	± 0.000770	0.00374	± 0.000062	0.00281	± 0.001076	0.000091	± 0.000010	8.89E-14	99.5%	18.5402	484.97	± 1.39	0.3%
au25.4j.mus.93a.txt	1.8	10	1.17807	± 0.001389	0.06034	± 0.000395	0.00086	± 0.000034	0.00071	± 0.000913	0.000019	± 0.000009	1.91E-14	99.5%	19.4309	505.28	± 3.56	0.7%
au25.4j.mus.28a.txt	1.8	10	2.11666	± 0.003643	0.11466	± 0.000345	0.00147	± 0.000024	0.00189	± 0.000982	0.000034	± 0.000014	3.44E-14	99.5%	18.3740	481.15	± 1.92	0.4%
au25.4j.mus.96a.txt	1.8	10	6.93647	± 0.009166	0.36291	± 0.000516	0.00463	± 0.000053	0.00242	± 0.000996	0.000111	± 0.000018	1.13E-13	99.5%	19.0238	496.03	± 1.04	0.2%
au25.4j.mus.16a.txt	1.8	10	6.83368	± 0.008015	0.34173	± 0.000694	0.00436	± 0.000048	0.01219	± 0.001122	0.000107	± 0.000012	1.11E-13	99.5%	19.9089	516.09	± 1.24	0.2%
au25.4j.mus.39a.txt	1.8	10	3.56137	± 0.003615	0.18596	± 0.000197	0.00239	± 0.000030	0.00152	± 0.001283	0.000056	± 0.000019	5.78E-14	99.5%	19.0638	496.94	± 1.06	0.2%
au25.4j.mus.33a.txt	1.8	10	2.90612	± 0.003527	0.15378	± 0.000654	0.00192	± 0.000030	0.00138	± 0.000820	0.000045	± 0.000017	4.72E-14	99.5%	18.8123	491.20	± 2.35	0.5%

au25.4j.mus.108a.txt	1.8	10	1.91086	± 0.002725	0.10272	± 0.000344	0.00134	± 0.000030	0.00588	± 0.001496	0.000029	± 0.000011	3.10E-14	99.6%	18.5263	484.65	± 1.95	0.4%
au25.4j.mus.109a.txt	1.8	10	1.94091	± 0.002762	0.10584	± 0.000474	0.00139	± 0.000030	-0.00081	± 0.001873	0.000027	± 0.000010	3.15E-14	99.6%	18.2613	478.56	± 2.38	0.5%
au25.4j.mus.17a.txt	1.8	10	11.85212	± 0.008432	0.36609	± 0.001293	0.00490	± 0.000063	0.02715	± 0.000575	0.000156	± 0.000015	1.92E-13	99.6%	32.2575	774.99	± 2.82	0.4%
au25.4j.mus.115a.txt	1.8	10	5.45679	± 0.004801	0.28704	± 0.000519	0.00372	± 0.000051	0.00150	± 0.001238	0.000069	± 0.000012	8.86E-14	99.6%	18.9396	494.11	± 1.05	0.2%
au25.4j.mus.48a.txt	1.8	10	9.03474	± 0.009421	0.32898	± 0.000582	0.00452	± 0.000060	0.00289	± 0.001149	0.000113	± 0.000012	1.47E-13	99.6%	27.3623	676.75	± 1.42	0.2%
au25.4j.mus.86a.txt	1.8	10	2.11848	± 0.002061	0.11230	± 0.000493	0.00145	± 0.000024	0.00121	± 0.000892	0.000027	± 0.000010	3.44E-14	99.6%	18.7962	490.83	± 2.32	0.5%
au25.4j.mus.89a.txt	1.8	10	1.31983	± 0.001153	0.06745	± 0.000348	0.00087	± 0.000024	0.00075	± 0.000885	0.000016	± 0.000009	2.14E-14	99.6%	19.4987	506.82	± 2.87	0.6%
au25.4j.mus.45a.txt	1.8	10	4.51841	± 0.002845	0.23263	± 0.000233	0.00304	± 0.000045	0.00299	± 0.001186	0.000055	± 0.000018	7.34E-14	99.6%	19.3541	503.54	± 0.85	0.2%
au25.4j.mus.113a.txt	1.8	10	4.54301	± 0.007000	0.24815	± 0.000865	0.00311	± 0.000043	0.00253	± 0.001240	0.000055	± 0.000011	7.38E-14	99.6%	18.2425	478.13	± 1.86	0.4%
au25.4j.mus.32a.txt	1.8	10	3.23723	± 0.003144	0.17113	± 0.000544	0.00220	± 0.000036	0.00328	± 0.000859	0.000036	± 0.000016	5.26E-14	99.7%	18.8564	492.20	± 1.80	0.4%
au25.4j.mus.58a.txt	1.8	10	1.76157	± 0.002089	0.09286	± 0.000455	0.00125	± 0.000045	-0.00318	± 0.000873	0.000019	± 0.000011	2.86E-14	99.7%	18.9046	493.31	± 2.65	0.5%
au25.4j.mus.72a.txt	1.8	10	4.63051	± 0.004760	0.24492	± 0.000535	0.00342	± 0.000059	0.00136	± 0.000880	0.000051	± 0.000009	7.52E-14	99.7%	18.8455	491.96	± 1.23	0.2%
au25.4j.mus.27a.txt	1.8	10	5.22174	± 0.004460	0.27583	± 0.000461	0.00372	± 0.000063	0.00311	± 0.001284	0.000056	± 0.000019	8.48E-14	99.7%	18.8716	492.55	± 1.07	0.2%
au25.4j.mus.61a.txt	1.8	10	1.06819	± 0.001009	0.05467	± 0.000360	0.00074	± 0.000023	0.00144	± 0.000962	0.000011	± 0.000008	1.73E-14	99.7%	19.4808	506.41	± 3.54	0.7%
au25.4j.mus.20a.txt	1.8	10	2.12021	± 0.002371	0.11121	± 0.000520	0.00140	± 0.000029	0.00022	± 0.001067	0.000022	± 0.000009	3.44E-14	99.7%	19.0069	495.64	± 2.47	0.5%
au25.4j.mus.41a.txt	1.8	10	3.11446	± 0.002289	0.17175	± 0.000383	0.00233	± 0.000032	0.00355	± 0.001742	0.000031	± 0.000013	5.06E-14	99.7%	18.0823	474.43	± 1.26	0.3%
au25.4j.mus.26a.txt	1.8	10	2.21227	± 0.002479	0.11401	± 0.000196	0.00148	± 0.000030	0.00215	± 0.000882	0.000022	± 0.000019	3.59E-14	99.7%	19.3489	503.42	± 1.65	0.3%
au25.4j.mus.91a.txt	1.8	10	0.73177	± 0.001256	0.03751	± 0.000156	0.00046	± 0.000019	0.00129	± 0.000913	0.000006	± 0.000009	1.19E-14	99.7%	19.4613	505.97	± 2.99	0.6%
au25.4j.mus.49a.txt	1.8	10	5.60728	± 0.002302	0.29701	± 0.000819	0.00373	± 0.000055	0.00206	± 0.001154	0.000048	± 0.000010	9.10E-14	99.7%	18.8323	491.65	± 1.40	0.3%
au25.4j.mus.52a.txt	1.8	10	3.17210	± 0.002980	0.16737	± 0.000324	0.00211	± 0.000044	0.00274	± 0.001307	0.000026	± 0.000008	5.15E-14	99.8%	18.9089	493.41	± 1.13	0.2%
au25.4j.mus.101a.txt	1.8	10	1.83332	± 0.002056	0.09682	± 0.000263	0.00119	± 0.000031	0.00037	± 0.000757	0.000014	± 0.000010	2.98E-14	99.8%	18.8923	493.03	± 1.64	0.3%
au25.4j.mus.67a.txt	1.8	10	3.20423	± 0.003175	0.16913	± 0.000659	0.00209	± 0.000039	-0.00069	± 0.000949	0.000023	± 0.000012	5.20E-14	99.8%	18.9041	493.29	± 2.06	0.4%
au25.4j.mus.88a.txt	1.8	10	1.65076	± 0.001488	0.08639	± 0.000285	0.00108	± 0.000028	0.00057	± 0.001256	0.000012	± 0.000010	2.68E-14	99.8%	19.0688	497.05	± 1.92	0.4%
au25.4j.mus.95a.txt	1.8	10	6.11670	± 0.004964	0.32574	± 0.000595	0.00427	± 0.000043	0.00321	± 0.001093	0.000042	± 0.000017	9.93E-14	99.8%	18.7406	489.56	± 1.06	0.2%
au25.4j.mus.84a.txt	1.8	10	2.96403	± 0.003022	0.15521	± 0.000390	0.00194	± 0.000037	-0.00125	± 0.001300	0.000019	± 0.000022	4.81E-14	99.8%	19.0600	496.85	± 1.72	0.3%
au25.4j.mus.56a.txt	1.8	10	2.93559	± 0.002850	0.15273	± 0.000572	0.00199	± 0.000045	-0.00168	± 0.001025	0.000018	± 0.000010	4.77E-14	99.8%	19.1849	499.69	± 2.00	0.4%
au25.4j.mus.98a.txt	1.8	10	4.62541	± 0.001996	0.24029	± 0.000305	0.00316	± 0.000039	0.00027	± 0.000991	0.000028	± 0.000023	7.51E-14	99.8%	19.2149	500.38	± 1.01	0.2%
au25.4j.mus.3a.txt	1.8	10	2.58095	± 0.001380	0.12957	± 0.000558	0.00169	± 0.000033	-0.00348	± 0.001209	0.000015	± 0.000017	4.19E-14	99.8%	19.8817	515.48	± 2.44	0.5%
au25.4j.mus.4a.txt	1.8	10	4.68421	± 0.006141	0.24177	± 0.000677	0.00308	± 0.000031	0.00050	± 0.000915	0.000027	± 0.000017	7.60E-14	99.8%	19.3418	503.26	± 1.65	0.3%
au25.4j.mus.118a.txt	1.8	10	2.32360	± 0.001678	0.12378	± 0.000407	0.00162	± 0.000027	0.00062	± 0.000747	0.000013	± 0.000010	3.77E-14	99.8%	18.7408	489.56	± 1.76	0.4%
au25.4j.mus.117a.txt	1.8	10	1.65311	± 0.001765	0.08899	± 0.000306	0.00121	± 0.000030	-0.00008	± 0.001245	0.000007	± 0.000011	2.68E-14	99.9%	18.5520	485.24	± 1.99	0.4%
au25.4j.mus.53a.txt	1.8	10	2.84002	± 0.003403	0.15261	± 0.000712	0.00202	± 0.000036	-0.00119	± 0.000734	0.000012	± 0.000016	4.61E-14	99.9%	18.5855	486.01	± 2.47	0.5%
au25.4j.mus.31a.txt	1.8	10	1.20934	± 0.001238	0.06421	± 0.000148	0.00081	± 0.000033	0.00152	± 0.000621	0.000005	± 0.000010	1.96E-14	99.9%	18.8142	491.24	± 1.73	0.4%
au25.4j.mus.90a.txt	1.8	10	4.29940	± 0.003603	0.22171	± 0.000641	0.00300	± 0.000030	-0.00048	± 0.000594	0.000014	± 0.000018	6.98E-14	99.9%	19.3724	503.96	± 1.64	0.3%
au25.4j.mus.74a.txt	1.8	10	1.47043	± 0.001701	0.07588	± 0.000236	0.00095	± 0.000020	0.00055	± 0.000803	0.000002	± 0.000007	2.39E-14	100.0%	19.3695	503.89	± 1.82	0.4%
au25.4j.mus.104a.txt	1.8	10	1.91065	± 0.001915	0.09910	± 0.000390	0.00133	± 0.000034	0.00209	± 0.000978	0.000003	± 0.000016	3.10E-14	100.0%	19.2732	501.70	± 2.38	0.5%
au25.4j.mus.60a.txt	1.8	10	2.03377	± 0.001776	0.10652	± 0.000518	0.00149	± 0.000043	-0.00011	± 0.000824	-0.000001	± 0.000017	3.30E-14	100.0%	19.0931	497.61	± 2.76	0.6%
au25.4j.mus.44a.txt	1.8	10	1.30292	± 0.001416	0.06701	± 0.000265	0.00092	± 0.000023	0.00203	± 0.000533	-0.000002	± 0.000017	2.12E-14	100.1%	19.4479	505.67	± 2.83	0.6%
au25.4j.mus.105a.txt	1.8	10	3.30410	± 0.003141	0.17882	± 0.000694	0.00238	± 0.000038	0.00030	± 0.000969	-0.000011	± 0.000018	5.36E-14	100.1%	18.4777	483.53	± 2.08	0.4%
au25.4j.mus.47a.txt	1.8	10	1.63435	± 0.001483	0.08246	± 0.000321	0.00105	± 0.000030	0.00292	± 0.001177	-0.000006	± 0.000015	2.65E-14	100.1%	19.8243	514.18	± 2.49	0.5%
au25.4j.mus.110a.txt	1.8	10	3.04404	± 0.002594	0.16396	± 0.000502	0.00208	± 0.000025	0.00263	± 0.001489	-0.000013	± 0.000017	4.94E-14	100.1%	18.5676	485.59	± 1.74	0.4%
au25.4j.mus.71a.txt	1.8	10	3.22361	± 0.003623	0.16934	± 0.000391	0.00220	± 0.000044	-0.00138	± 0.000884	-0.000016	± 0.000012	5.23E-14	100.1%	19.0349	496.28	± 1.39	0.3%
au25.4j.mus.55a.txt	1.8	10	1.57829	± 0.001742	0.08327	± 0.000322	0.00104	± 0.000032	-0.00166	± 0.000700	-0.000009	± 0.000014	2.56E-14	100.2%	18.9524	494.40	± 2.37	0.5%
au25.4j.mus.87a.txt	1.8	10	0.88079	± 0.001373	0.04720	± 0.000197	0.00059	± 0.000022	-0.00056	± 0.001128	-0.000005	± 0.000015	1.43E-14	100.2%	18.6604	487.72	± 3.26	0.7%
au25.4j.mus.70a.txt	1.8	10	1.82205	± 0.002657	0.09382	± 0.000503	0.00120	± 0.000036	0.00080	± 0.001061	-0.000012	± 0.000015	2.96E-14	100.2%	19.4219	505.08	± 3.08	0.6%
au25.4j.mus.54a.txt	1.8	10	2.12786	± 0.001897	0.11023	± 0.000296	0.00140	± 0.000026	-0.00051	± 0.001170	-0.000019	± 0.000014	3.45E-14	100.3%	19.3039	502.40	± 1.71	0.3%
au25.4j.mus.43a.txt	1.8	10	1.47355	± 0.001444	0.07711	± 0.000359	0.00105	± 0.000034	0.00337	± 0.000456	-0.000016	± 0.000018	2.39E-14	100.3%	19.1150	498.10	± 2.97	0.6%
au25.4j.mus.21a.txt	1.8	10	0.91552	± 0.000814	0.04707	± 0.000160	0.00054	± 0.000022	0.00247	± 0.001107	-0.000011	± 0.000016	1.49E-14	100.4%	19.4557	505.85	± 3.19	0.6%
au25.4j.mus.8a.txt	1.8	10	1.81836	± 0.001822	0.09645	± 0.000170	0.00125	± 0.000037	-0.00289	± 0.001016	-0.000030	± 0.000016	2.95E-14	100.5%	18.8486	492.03	± 1.61	0.3%
au25.4j.mus.59a.txt	1.8	10	1.10396	± 0.001390	0.05804	± 0.000294	0.00083	± 0.000035	0.00055	± 0.001139	-0.000021	± 0.000015	1.79E-14	100.6%	19.0231	496.01	± 3.26	0.7%
au25.4j.mus.65a.txt	1.8	10	1.17259	± 0.001907	0.06188	± 0.000226	0.00075	± 0.000020	-0.00115	± 0.001332	-0.000031	± 0.000015	1.90E-14	100.8%	18.9465	494.26	± 2.76	0.6%
au25.4j.mus.62a.txt	1.8	10	0.92983	± 0.001290	0.04839	± 0.000231	0.00068	± 0.000026	0.00148	± 0.000811	-0.000028	± 0.000017	1.51E-14	100.9%	19.2196	500.48	± 3.68	0.7%
au25.4j.mus.64a.txt	1.8	10	1.33447	± 0.001179	0.07109	± 0.000325	0.00093	± 0.000026	0.00137	± 0.001368	-0.000045	± 0.000018	2.17E-14	101.0%	18.7740	490.32	± 3.02	0.6%
au25.4j.mus.51a.txt	1.8	10	0.59489	± 0.000952	0.02991	± 0.000205	0.00035	± 0.000025	-0.00054	± 0.000590	-0.000023	± 0.000015	9.66E-15	101.2%	19.8845	515.54	± 5.31	1.0%
au25.4j.mus.107a.txt	1.8	10	0.79508	± 0.000711	0.04086	± 0.000170	0.00054	± 0.000030	-0.00073	± 0.001220	-0.000048	± 0.000014	1.29E-14	101.8%	19.4588	505.92	± 3.45	0.7%
																111.00		

I-B-13 Muscovite																		
au25.4f.mus.3a.txt	1.8	10	17.91930	± 0.018801	0.49457	± 0.001372	0.00662	± 0.000083	0.02644	± 0.001002	0.000462	± 0.000020	2.91E-13	99.2%	35.9622	845.93	± 2.54	0.3%
au25.4f.mus.4a.txt	1.8	10	2.57266	± 0.004365	0.12946	± 0.000512	0.00170	± 0.000024	0.00269	± 0.001030	0.000100	± 0.000010	4.18E-14	98.9%	19.6462	510.16	± 2.30	0.5%
au25.4f.mus.5a.txt	1.8	10	6.19099	± 0.004194	0.31204	± 0.000857	0.00414	± 0.000054	0.00005	± 0.000963	0.000266	± 0.000016	1.01E-13	98.7%	19.5880	508.84	± 1.51	0.3%
au25.4f.mus.6a.txt	1.8	10	11.10765	± 0.007061	0.56709	± 0.000511	0.00740	± 0.000051	0.02472	± 0.000903	0.000254	± 0.000024	1.80E-13	99.3%	19.4594	505.93	± 0.65	0.1%
au25.4f.mus.7a.txt	1.8	10	9.25765	± 0.010745	0.44053	± 0.000670	0.00562	± 0.000078	0.00163	± 0.001072	0.000137	± 0.000016	1.50E-13	99.6%	20.9235	538.82	± 1.07	0.2%
au25.4f.mus.8a.txt	1.8	10	9.45983	± 0.009019	0.46477	± 0.001042	0.00596	± 0.000049	0.00281	± 0.000876	0.000087	± 0.000010	1.54E-13	99.7%	20.2988	524.86	± 1.29	0.2%
au25.4f.mus.11a.txt	1.8	10	9.75000	± 0.016887	0.48899	± 0.000710	0.00630	± 0.000054	0.00636	± 0.001107	0.000316	± 0.000011	1.58E-13	99.0%	19.7495	512.49	± 1.18	0.2%
au25.4f.mus.12a.txt	1.8	10	0.97690	± 0.001115	0.04637	± 0.000186	0.00068	± 0.000020	0.00295	± 0.001117	0.000014	± 0.000010	1.59E-14	99.6%	20.9834	540.15	± 2.79	0.5%
au25.4f.mus.13a.txt	1.8	10	18.72774	± 0.011830	0.56010	± 0.001034	0.00758	± 0.000066	0.02678	± 0.001266	0.000355	± 0.000016	3.04E-13	99.4%	33.2547	794.36	± 1.57	0.2%
au25.4f.mus.14a.txt	1.8	10	7.47054	± 0.009777	0.36120	± 0.000760	0.00454	± 0.000048	0.00473	± 0.000609	0.000125	± 0.000010	1.21E-13	99.5%	20.5814	531.19	± 1.34	0.3%
au25.4f.mus.15a.txt	1.8	10	11.24492	± 0.008424	0.34292	± 0.000400	0.00465	± 0.000045	0.02552	± 0.001405	0.000158	± 0.000027	1.83E-13	99.6%	32.6644	782.91	± 1.22	0.2%
au25.4f.mus.16a.txt	1.8	10	4.26065	± 0.004418	0.19854	± 0.000352	0.00256	± 0.000026	-0.00057	± 0.001029	0.000290	± 0.000014	6.92E-14	98.0%	21.0282	541.15	± 1.25	0.2%
au25.4f.mus.17a.txt	1.8	10	10.75028	± 0.006585	0.34781	± 0.000550	0.00470	± 0.000049	0.02784	± 0.001089	0.000269	± 0.000026	1.75E-13	99.3%	30.6890	744.09	± 1.38	0.2%
au25.4f.mus.18a.txt	1.8	10	7.13916	± 0.009943	0.32995	± 0.000505	0.00435	± 0.000053	0.00234	± 0.001303	0.000625	± 0.000017	1.16E-13	97.4%	21.0781	542.26	± 1.22	0.2%
au25.4f.mus.19a.txt	1.8	10	4.99633	± 0.006964	0.25161	± 0.000558	0.00325	± 0.000049	0.00345	± 0.001282	0.000142	± 0.000014	8.11E-14	99.2%	19.6921	511.20	± 1.41	0.3%
au25.4f.mus.20a.txt	1.8	10	7.69139	± 0.006538	0.24888	± 0.000627	0.00339	± 0.000034	0.00321	± 0.000880	0.000229	± 0.000014	1.25E-13	99.1%	30.6327	742.97	± 2.03	0.3%
au25.4f.mus.21a.txt	1.8	10	2.84262	± 0.003642	0.13665	± 0.000474	0.00171	± 0.000042	0.00046	± 0.001607	0.000017	± 0.000011	4.61E-14	99.8%	20.7660	535.31	± 2.07	0.4%
au25.4f.mus.22a.txt	1.8	10	11.08136	± 0.012366	0.57144	± 0.000899	0.00814	± 0.000107	0.02912	± 0.000882	0.000329	± 0.000036	1.80E-13	99.1%	19.2272	500.66	± 1.09	0.2%
au25.4f.mus.23a.txt	1.8	10	5.63316	± 0.013136	0.27962	± 0.000699	0.00358	± 0.000047	0.00241	± 0.001527	0.000096	± 0.000009	9.15E-14	99.5%	20.0456	519.17	± 1.80	0.3%
au25.4f.mus.24a.txt	1.8	10	16.46514	± 0.016568	0.53622	± 0.001023	0.00711	± 0.000057	0.02720	± 0.001172	0.000477	± 0.000030	2.67E-13	99.1%	30.4491	739.32	± 1.66	0.2%
au25.4f.mus.25a.txt	1.8	10	6.42376	± 0.003909	0.30242	± 0.000544	0.00388	± 0.000051	0.00033	± 0.001058	0.000266	± 0.000009	1.04E-13	98.8%	20.9810	540.10	± 1.06	0.2%
au25.4f.mus.26a.txt	1.8	10	8.77491	± 0.014644	0.33355	± 0.000416	0.00432	± 0.000054	0.00275	± 0.000900	0.000269	± 0.000022	1.42E-13	99.1%	26.0704	649.91	± 1.45	0.2%
au25.4f.mus.27a.txt	1.8	10	17.49479	± 0.014999	0.54539	± 0.001381	0.00741	± 0.000061	0.02799	± 0.001399	0.000201	± 0.000028	2.84E-13	99.7%	31.9743	769.45	± 2.10	0.3%
au25.4f.mus.28a.txt	1.8	10	7.45056	± 0.008263	0.24705	± 0.000509	0.00318	± 0.000039	0.00410	± 0.000715	0.000129	± 0.000024	1.21E-13	99.5%	30.0054	730.46	± 1.85	0.3%
au25.4f.mus.29a.txt	1.8	10	10.80803	± 0.010125	0.58094	± 0.001112	0.00775	± 0.000110	0.02725	± 0.000783	0.000197	± 0.000018	1.75E-13	99.5%	18.5093	484.26	± 1.07	0.2%
au25.4f.mus.30a.txt	1.8	10	12.92272	± 0.007993	0.64262	± 0.001135	0.00862	± 0.000070	0.02858	± 0.001402	0.000659	± 0.000022	2.10E-13	98.5%	19.8111	513.88	± 1.01	0.2%
au25.4f.mus.31a.txt	1.8	10	3.89528	± 0.003979	0.17795	± 0.000567	0.00232	± 0.000048	-0.00153	± 0.001175	0.000346	± 0.000017	6.32E-14	97.4%	21.3141	547.50	± 2.02	0.4%
au25.4f.mus.32a.txt	1.8	10	12.54024	± 0.008199	0.40049	± 0.001102	0.00545	± 0.000079	0.02465	± 0.001471	0.000252	± 0.000018	2.04E-13	99.4%	31.1332	752.89	± 2.16	0.3%
au25.4f.mus.33a.txt	1.8	10	19.58447	± 0.012587	0.67645	± 0.000940	0.00944	± 0.000121	0.02493	± 0.001387	0.000356	± 0.000020	3.18E-13	99.5%	28.8006	706.18	± 1.11	0.2%
au25.4f.mus.34a.txt	1.8	10	2.31653	± 0.003340	0.11704	± 0.000279	0.00154	± 0.000035	-0.00621	± 0.001840	0.000108	± 0.000015	3.76E-14	98.6%	19.5140	507.17	± 1.76	0.3%
au25.4f.mus.35a.txt	1.8	10	5.20350	± 0.004981	0.26149	± 0.000537	0.00342	± 0.000043	-0.00159	± 0.001190	0.000260	± 0.000016	8.45E-14	98.5%	19.6051	509.23	± 1.26	0.2%
au25.4f.mus.36a.txt	1.8	10	7.73775	± 0.012458	0.36909	± 0.000505	0.00470	± 0.000067	0.00518	± 0.001272	0.000146	± 0.000023	1.26E-13	99.4%	20.8492	537.17	± 1.23	0.2%
au25.4f.mus.37a.txt	1.8	10	13.05294	± 0.012261	0.38863	± 0.001241	0.00529	± 0.000043	0.02812	± 0.001199	0.000354	± 0.000020	2.12E-13	99.2%	33.3264	795.74	± 2.69	0.3%
au25.4f.mus.38a.txt	1.8	10	15.20744	± 0.011811	0.45601	± 0.001106	0.00624	± 0.000047	0.02730	± 0.000827	0.000370	± 0.000019	2.47E-13	99.3%	33.1165	791.68	± 2.05	0.3%
au25.4f.mus.39a.txt	1.8	10	15.85247	± 0.013670	0.50092	± 0.000690	0.00687	± 0.000078	0.02542	± 0.001228	0.000172	± 0.000033	2.57E-13	99.7%	31.5511	761.14	± 1.33	0.2%
au25.4f.mus.40a.txt	1.8	10	14.01064	± 0.017034	0.40922	± 0.000817	0.00560	± 0.000073	0.02802	± 0.000889	0.000165	± 0.000029	2.27E-13	99.7%	34.1265	811.12	± 1.97	0.2%
au25.4f.mus.41a.txt	1.8	10	8.33611	± 0.008418	0.42129	± 0.001043	0.00556	± 0.000090	0.00191	± 0.000940	0.000137	± 0.000010	1.35E-13	99.5%	19.6914	511.18	± 1.39	0.3%
au25.4f.mus.42a.txt	1.8	10	8.18720	± 0.012105	0.24625	± 0.000469	0.00324	± 0.000031	0.00141	± 0.001016	0.000128	± 0.000011	1.33E-13	99.5%	33.0935	791.24	± 1.95	0.2%
au25.4f.mus.43a.txt	1.8	10	14.93900	± 0.011731	0.48754	± 0.001170	0.00651	± 0.000067	0.02372	± 0.001210	0.000222	± 0.000015	2.43E-13	99.6%	30.5124	740.58	± 1.89	0.3%
au25.4f.mus.44a.txt	1.8	10	1.66605	± 0.001746	0.05402	± 0.000152	0.00072	± 0.000027	0.00076	± 0.000853	0.000041	± 0.000010	2.70E-14	99.3%	30.6192	742.70	± 2.59	0.3%
au25.4f.mus.45a.txt	1.8	10	4.68389	± 0.002742	0.22765	± 0.000464	0.00299	± 0.000036	0.00126	± 0.000955	0.000216	± 0.000011	7.60E-14	98.6%	20.2951	524.78	± 1.19	0.2%
au25.4f.mus.46a.txt	1.8	10	4.59328	± 0.008548	0.23781	± 0.000630	0.00306	± 0.000039	-0.00174	± 0.000963	0.000083	± 0.000008	7.46E-14	99.5%	19.2116	500.30	± 1.65	0.3%
au25.4f.mus.47a.txt	1.8	10	7.62065	± 0.010929	0.36060	± 0.001079	0.00471	± 0.000049	0.00298	± 0.000963	0.000365	± 0.000011	1.24E-13	98.6%	20.8353	536.86	± 1.82	0.3%
au25.4f.mus.48a.txt	1.8	10	12.55729	± 0.011923	0.33414	± 0.000662	0.00468	± 0.000058	0.02073	± 0.000793	0.000157	± 0.000013	2.04E-13	99.6%	37.4498	873.65	± 1.94	0.2%
au25.4f.mus.49a.txt	1.8	10	16.53150	± 0.017169	0.71774	± 0.001038	0.00953	± 0.000073	0.02421	± 0.001285	0.000667	± 0.000020	2.68E-13	98.8%	22.7618	579.29	± 1.07	0.2%
au25.4f.mus.50a.txt	1.8	10	12.16674	± 0.003490	0.52591	± 0.000613	0.00693	± 0.000066	0.02234	± 0.000936	0.000336	± 0.000028	1.98E-13	99.2%	22.9506	583.39	± 0.81	0.1%
au25.4f.mus.51a.txt	1.8	10	3.37853	± 0.005161	0.14977	± 0.000662	0.00194	± 0.000024	0.00257	± 0.001032	0.000020	± 0.000017	5.49E-14	99.8%	22.5198	574.01	± 2.83	0.5%
au25.4f.mus.52a.txt	1.8	10	7.48105	± 0.012725	0.22641	± 0.000530	0.00304	± 0.000027	0.00206	± 0.001562	0.000077	± 0.000011	1.21E-13	99.7%	32.9414	788.29	± 2.31	0.3%
au25.4f.mus.53a.txt	1.8	10	4.37633	± 0.006995	0.20657	± 0.000768	0.00274	± 0.000029	-0.00056	± 0.000845	0.000145	± 0.000011	7.10E-14	99.0%	20.9783	540.04	± 2.25	0.4%
au25.4f.mus.54a.txt	1.8	10	8.16889	± 0.011310	0.31740	± 0.001176	0.00407	± 0.000056	0.00323	± 0.001069	0.000141	± 0.000012	1.33E-13	99.5%	25.6067	640.18	± 2.56	0.4%
au25.4f.mus.55a.txt	1.8	10	13.30652	± 0.010280	0.29365	± 0.000965	0.00399	± 0.000044	0.02494	± 0.001435	0.000156	± 0.000035	2.16E-13	99.7%	45.1682	1011.00	± 3.51	0.3%
au25.4f.mus.56a.txt	1.8	10	14.25608	± 0.012186	0.36829	± 0.000935	0.00499	± 0.000060	0.02476	± 0.000786	0.000224	± 0.000023	2.31E-13	99.5%	38.5372	893.64	± 2.44	0.3%
au25.4f.mus.57a.txt	1.8	10	6.59602	± 0.010205	0.32198	± 0.000673	0.00425	± 0.000056	0.00274	± 0.001521	0.000281	± 0.000010	1.07E-13	98.7%	20.2290	523.29	± 1.40	0.3%
au25.4f.mus.58a.txt	1.8	10	1.33502	± 0.001603	0.06489	± 0.000309	0.00081	± 0.000023	-0.00213	± 0.000605	0.000024	± 0.000015	2.17E-14	99.5%	20.4627	528.53	± 3.14	0.6%
au25.4f.mus.59a.txt	1.8	10	9.59103	± 0.014352	0.38844	± 0.001118	0.00511	± 0.000051	0.00254	± 0.000788	0.000244	± 0.000009	1.56E-13	99.2%	24.5065	616.87	± 2.02	0.3%
au25.4f.mus.60a.txt	1.8	10	6.89422	± 0.007537	0.31805	± 0.000650	0.00407	± 0.000052	0.00353	± 0.001082	0.000169	± 0.000010	1.12E-13	99.3%	21.5212	552.08	± 1.31	0.2%

au25.4f.mus.61a.txt	1.8	10	6.21913	± 0.011478	0.17388	± 0.000389	0.00226	± 0.000037	0.00195	± 0.000986	0.000123	± 0.000009	1.01E-13	99.4%	35.5600	838.36	± 2.48	0.3%
au25.4f.mus.62a.txt	1.8	10	10.98226	± 0.014308	0.33317	± 0.000477	0.00444	± 0.000081	0.02646	± 0.001089	0.000124	± 0.000023	1.78E-13	99.7%	32.8626	786.76	± 1.60	0.2%
au25.4f.mus.63a.txt	1.8	10	5.51563	± 0.008278	0.23129	± 0.000698	0.00293	± 0.000055	0.00155	± 0.001581	0.000057	± 0.000018	8.95E-14	99.7%	23.7760	601.23	± 2.11	0.4%
au25.4f.mus.64a.txt	1.8	10	7.26525	± 0.009917	0.20079	± 0.000943	0.00266	± 0.000051	0.00297	± 0.000986	0.000029	± 0.000009	1.18E-13	99.9%	36.1430	849.32	± 4.17	0.5%
au25.4f.mus.65a.txt	1.8	10	2.48521	± 0.002783	0.10750	± 0.000416	0.00137	± 0.000038	0.00207	± 0.001188	0.000020	± 0.000009	4.03E-14	99.8%	23.0641	585.86	± 2.45	0.4%
au25.4f.mus.66a.txt	1.8	10	6.13314	± 0.005751	0.27862	± 0.000723	0.00366	± 0.000058	0.00399	± 0.001308	0.000149	± 0.000018	9.96E-14	99.3%	21.8556	559.45	± 1.63	0.3%
au25.4f.mus.67a.txt	1.8	10	2.46682	± 0.003226	0.11798	± 0.000375	0.00155	± 0.000031	-0.00104	± 0.001219	0.000013	± 0.000015	4.00E-14	99.8%	20.8739	537.72	± 2.09	0.4%
au25.4f.mus.68a.txt	1.8	10	8.03604	± 0.013868	0.21162	± 0.000494	0.00288	± 0.000047	0.00090	± 0.000835	0.000045	± 0.000016	1.30E-13	99.8%	37.9104	882.14	± 2.62	0.3%
au25.4f.mus.69a.txt	1.8	10	7.06107	± 0.008866	0.34263	± 0.001024	0.00442	± 0.000066	0.00281	± 0.001223	0.000153	± 0.000018	1.15E-13	99.4%	20.4777	528.87	± 1.77	0.3%
au25.4f.mus.70a.txt	1.8	10	8.42951	± 0.010535	0.23003	± 0.000595	0.00306	± 0.000045	0.00155	± 0.001225	0.000101	± 0.000012	1.37E-13	99.6%	36.5158	856.29	± 2.50	0.3%
au25.4f.mus.71a.txt	1.8	10	6.56711	± 0.009224	0.21183	± 0.000697	0.00284	± 0.000025	-0.00313	± 0.001474	0.000037	± 0.000018	1.07E-13	99.8%	30.9484	749.23	± 2.76	0.4%
au25.4f.mus.72a.txt	1.8	10	3.55689	± 0.004057	0.10476	± 0.000441	0.00138	± 0.000032	0.00278	± 0.001026	0.000011	± 0.000012	5.77E-14	99.9%	33.9250	807.26	± 3.62	0.4%
au25.4f.mus.73a.txt	1.8	10	4.69463	± 0.007187	0.22555	± 0.000294	0.00293	± 0.000041	0.00058	± 0.001042	0.000113	± 0.000009	7.62E-14	99.3%	20.6667	533.09	± 1.12	0.2%
au25.4f.mus.74a.txt	1.8	10	4.75679	± 0.006555	0.23264	± 0.000731	0.00292	± 0.000047	-0.00042	± 0.001111	0.000050	± 0.000015	7.72E-14	99.7%	20.3826	526.74	± 1.88	0.4%
au25.4f.mus.75a.txt	1.8	10	7.14669	± 0.006563	0.20723	± 0.000428	0.00276	± 0.000032	0.00022	± 0.001595	0.000039	± 0.000019	1.16E-13	99.8%	34.4318	816.96	± 1.95	0.2%
au25.4f.mus.76a.txt	1.8	10	6.79047	± 0.011882	0.17774	± 0.000620	0.00238	± 0.000038	0.00156	± 0.000768	0.000045	± 0.000018	1.10E-13	99.8%	38.1314	886.21	± 3.53	0.4%
au25.4f.mus.77a.txt	1.8	10	7.39648	± 0.009903	0.18217	± 0.000565	0.00242	± 0.000035	0.00077	± 0.001034	0.000137	± 0.000010	1.20E-13	99.5%	40.3806	927.04	± 3.17	0.3%
au25.4f.mus.78a.txt	1.8	10	3.61840	± 0.004122	0.18082	± 0.000498	0.00240	± 0.000047	0.00067	± 0.001359	-0.000004	± 0.000017	5.87E-14	100.0%	20.0117	518.41	± 1.70	0.3%
au25.4f.mus.79a.txt	1.8	10	3.80978	± 0.004680	0.18282	± 0.000577	0.00237	± 0.000045	-0.00089	± 0.001030	0.000036	± 0.000015	6.19E-14	99.7%	20.7812	535.65	± 1.92	0.4%
au25.4f.mus.80a.txt	1.8	10	4.60389	± 0.005463	0.18246	± 0.000734	0.00238	± 0.000028	0.00255	± 0.001434	0.000021	± 0.000016	7.47E-14	99.9%	25.2004	631.61	± 2.73	0.4%
au25.4f.mus.81a.txt	1.8	10	17.39622	± 0.014211	0.48193	± 0.001139	0.00660	± 0.000068	0.02633	± 0.001140	0.000256	± 0.000025	2.82E-13	99.6%	35.9464	845.63	± 2.15	0.3%
au25.4f.mus.82a.txt	1.8	10	1.75072	± 0.003702	0.06568	± 0.000396	0.00089	± 0.000030	-0.00003	± 0.001027	-0.000025	± 0.000019	2.84E-14	100.4%	26.6556	662.12	± 4.72	0.7%
au25.4f.mus.83a.txt	1.8	10	16.02198	± 0.010890	0.50610	± 0.000846	0.00685	± 0.000047	0.02848	± 0.001599	0.000333	± 0.000029	2.60E-13	99.4%	31.4703	759.54	± 1.44	0.2%
au25.4f.mus.84a.txt	1.8	10	6.37338	± 0.009136	0.13413	± 0.000640	0.00179	± 0.000040	0.00064	± 0.000962	0.000061	± 0.000021	1.03E-13	99.7%	47.3821	1048.55	± 5.34	0.5%
au25.4f.mus.85a.txt	1.8	10	6.37143	± 0.007432	0.18047	± 0.000814	0.00238	± 0.000048	-0.00005	± 0.000828	0.000132	± 0.000020	1.03E-13	99.4%	35.0891	829.46	± 3.97	0.5%
au25.4f.mus.86a.txt	1.8	10	11.01987	± 0.010642	0.34991	± 0.000732	0.00480	± 0.000067	0.02543	± 0.001064	0.000210	± 0.000015	1.79E-13	99.4%	31.3247	756.67	± 1.78	0.2%
au25.4f.mus.87a.txt	1.8	10	1.55979	± 0.001190	0.07147	± 0.000216	0.00091	± 0.000025	-0.00234	± 0.001073	0.000021	± 0.000010	2.53E-14	99.6%	21.7332	556.76	± 2.02	0.4%
au25.4f.mus.88a.txt	1.8	10	2.78346	± 0.003829	0.13980	± 0.000400	0.00177	± 0.000032	0.00088	± 0.001319	0.000188	± 0.000011	4.52E-14	98.0%	19.5128	507.14	± 1.76	0.3%
au25.4f.mus.89a.txt	1.8	10	5.34704	± 0.005625	0.15188	± 0.000401	0.00200	± 0.000035	-0.00123	± 0.001114	0.000071	± 0.000016	8.68E-14	99.6%	35.0653	829.01	± 2.48	0.3%
au25.4f.mus.90a.txt	1.8	10	5.45375	± 0.002980	0.18049	± 0.000479	0.00237	± 0.000040	0.00067	± 0.001115	0.000054	± 0.000018	8.85E-14	99.7%	30.1272	732.89	± 2.12	0.3%
au25.4f.mus.91a.txt	1.8	10	7.41773	± 0.010480	0.37632	± 0.001049	0.00501	± 0.000060	0.00343	± 0.001090	0.000067	± 0.000016	1.20E-13	99.7%	19.6600	510.47	± 1.63	0.3%
au25.4f.mus.92a.txt	1.8	10	7.45353	± 0.015468	0.35289	± 0.000980	0.00452	± 0.000068	0.00011	± 0.001187	0.000170	± 0.000008	1.21E-13	99.3%	20.9790	540.06	± 1.89	0.4%
au25.4f.mus.93a.txt	1.8	10	8.67214	± 0.013022	0.21921	± 0.000898	0.00291	± 0.000052	0.00373	± 0.001733	0.000100	± 0.000015	1.41E-13	99.7%	39.4281	909.86	± 4.01	0.4%
au25.4f.mus.94a.txt	1.8	10	4.29209	± 0.005522	0.19898	± 0.000350	0.00264	± 0.000050	0.00138	± 0.001627	0.000099	± 0.000010	6.97E-14	99.3%	21.4250	549.95	± 1.26	0.2%
au25.4f.mus.95a.txt	1.8	10	4.07790	± 0.005167	0.18633	± 0.000398	0.00248	± 0.000048	0.00015	± 0.001006	0.000133	± 0.000014	6.62E-14	99.0%	21.6742	555.46	± 1.51	0.3%
au25.4f.mus.96a.txt	1.8	10	5.99902	± 0.010264	0.24245	± 0.000561	0.00317	± 0.000055	0.00384	± 0.001049	0.000302	± 0.000011	9.74E-14	98.5%	24.3764	614.10	± 1.83	0.3%
au25.4f.mus.97a.txt	1.8	10	6.43881	± 0.010795	0.19918	± 0.000611	0.00258	± 0.000052	0.00259	± 0.000859	0.000128	± 0.000012	1.05E-13	99.4%	32.1387	772.66	± 2.75	0.4%
au25.4f.mus.98a.txt	1.8	10	8.26188	± 0.007833	0.24557	± 0.000422	0.00329	± 0.000055	0.00298	± 0.001341	0.000157	± 0.000010	1.34E-13	99.4%	33.4568	798.26	± 1.60	0.2%
au25.4f.mus.99a.txt	1.8	10	2.74576	± 0.005082	0.12705	± 0.000480	0.00167	± 0.000024	0.00340	± 0.000717	0.000067	± 0.000010	4.46E-14	99.3%	21.4590	550.70	± 2.42	0.4%
au25.4f.mus.100a.txt	1.8	10	2.82132	± 0.003390	0.14168	± 0.000605	0.00190	± 0.000026	0.00080	± 0.000921	0.000096	± 0.000020	4.58E-14	99.0%	19.7138	511.69	± 2.54	0.5%
au25.4f.mus.101a.txt	1.8	10	5.27834	± 0.007528	0.27608	± 0.000676	0.00357	± 0.000036	0.00133	± 0.000984	0.000037	± 0.000016	8.57E-14	99.8%	19.0794	497.29	± 1.48	0.3%
au25.4f.mus.102a.txt	1.8	10	2.73941	± 0.004984	0.11432	± 0.000285	0.00156	± 0.000047	0.00105	± 0.001136	0.000070	± 0.000010	4.45E-14	99.3%	23.7847	601.42	± 1.97	0.3%
au25.4f.mus.103a.txt	1.8	10	7.14460	± 0.012265	0.33942	± 0.001000	0.00449	± 0.000058	0.00143	± 0.001487	0.000123	± 0.000020	1.16E-13	99.5%	20.9423	539.24	± 1.90	0.4%
au25.4f.mus.104a.txt	1.8	10	2.97748	± 0.005071	0.13894	± 0.000461	0.00184	± 0.000034	-0.00114	± 0.001346	0.000020	± 0.000014	4.83E-14	99.8%	21.3875	549.12	± 2.18	0.4%
au25.4f.mus.105a.txt	1.8	10	6.06225	± 0.007629	0.26897	± 0.000791	0.00358	± 0.000042	0.00217	± 0.001797	0.000220	± 0.000011	9.84E-14	98.9%	22.2974	569.15	± 1.87	0.3%
au25.4f.mus.106a.txt	1.8	10	4.26959	± 0.005511	0.21121	± 0.000479	0.00277	± 0.000036	0.00029	± 0.001057	0.000191	± 0.000014	6.93E-14	98.7%	19.9475	516.96	± 1.45	0.3%
au25.4f.mus.107a.txt	1.8	10	6.89768	± 0.010215	0.20053	± 0.000770	0.00266	± 0.000027	0.00222	± 0.000890	0.000127	± 0.000012	1.12E-13	99.5%	34.2116	812.75	± 3.39	0.4%
au25.4f.mus.108a.txt	1.8	10	4.06179	± 0.005643	0.13310	± 0.000296	0.00177	± 0.000030	0.00325	± 0.001317	0.000363	± 0.000012	6.59E-14	97.4%	29.7130	724.59	± 2.06	0.3%
au25.4f.mus.109a.txt	1.8	10	4.16808	± 0.005936	0.12606	± 0.000322	0.00161	± 0.000026	0.00312	± 0.001068	0.000012	± 0.000018	6.77E-14	99.9%	33.0385	790.17	± 2.52	0.3%
au25.4f.mus.110a.txt	1.8	10	9.38962	± 0.012466	0.28633	± 0.000538	0.00373	± 0.000032	0.00096	± 0.000843	0.000123	± 0.000019	1.52E-13	99.6%	32.6658	782.94	± 1.87	0.2%
au25.4f.mus.113a.txt	1.8	10	4.50804	± 0.006489	0.13590	± 0.000408	0.00181	± 0.000035	0.00213	± 0.000978	0.000077	± 0.000011	7.32E-14	99.5%	33.0044	789.51	± 2.70	0.3%
au25.4f.mus.114a.txt	1.8	10	5.62707	± 0.010618	0.11096	± 0.000244	0.00158	± 0.000029	0.00354	± 0.000788	0.000033	± 0.000011	9.14E-14	99.8%	50.6284	1102.22	± 3.26	0.3%
au25.4f.mus.115a.txt	1.8	10	1.42465	± 0.001996	0.04959	± 0.000100	0.00075	± 0.000028	0.00153	± 0.000735	-0.000041	± 0.000016	2.31E-14	100.9%	28.7334	704.81	± 2.88	0.4%
au25.4f.mus.116a.txt	1.8	10	6.14205	± 0.008927	0.19279	± 0.000552	0.00253	± 0.000032	0.00282	± 0.001616	0.000071	± 0.000011	9.97E-14	99.7%	31.7508	765.06	± 2.50	0.3%
au25.4f.mus.117a.txt	1.8	10	4.50923	± 0.007762	0.20085	± 0.000485	0.00274	± 0.000054	0.00585	± 0.002036	0.000139	± 0.000009	7.32E-14	99.1%	22.2497	568.11	± 1.74	0.3%
au25.4f.mus.118a.txt	1.8	10	11.08356	± 0.006754	0.54126	± 0.001480	0.00712	± 0.000064	0.03116	± 0.001323	0.000215	± 0.000013	1.80E-13	99.4%	20.3663	526.37	± 1.49	0.3%
																N:112		

APPENDIX E: Photomicrographs of detrital muscovite grains analyzed for argon dating.

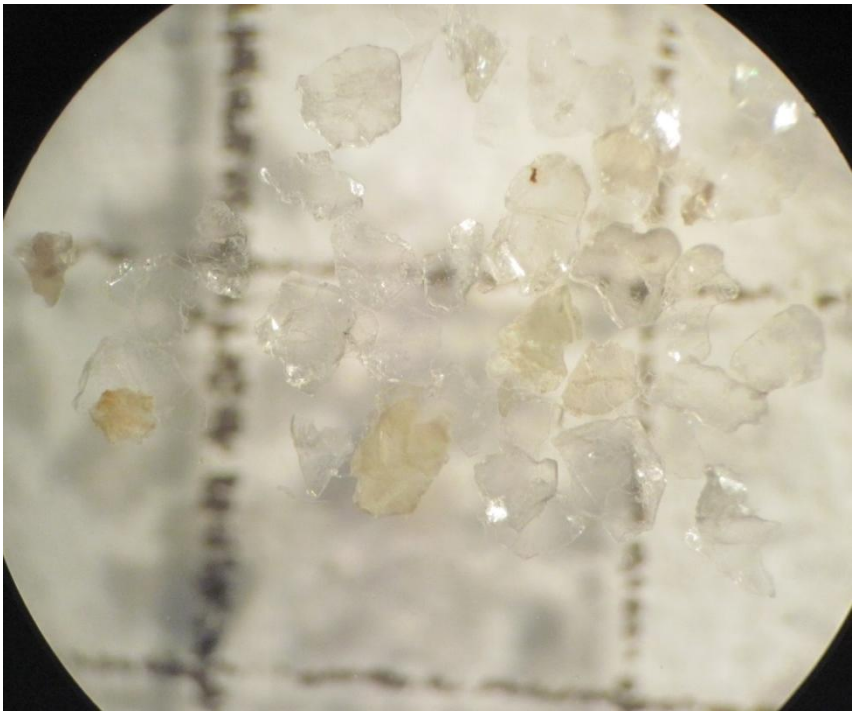

Sample B-B-2 from drill-well GDH-41, Barapukuria Basin, Bangladesh (shown in 1 mm grid).

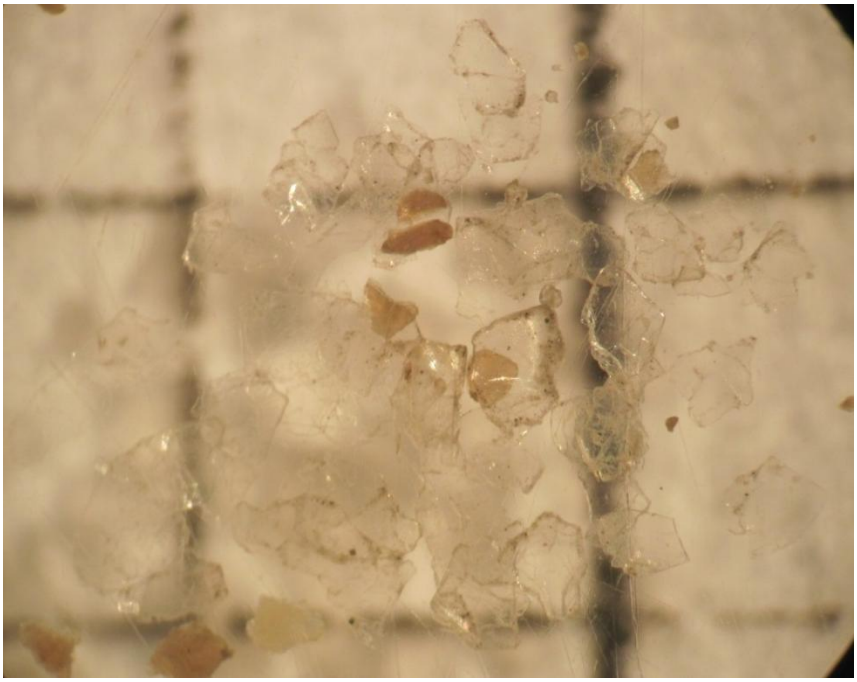

Sample B-D-1 from drill-well GDH-41, Barapukuria Basin, Bangladesh (shown in 1 mm grid).

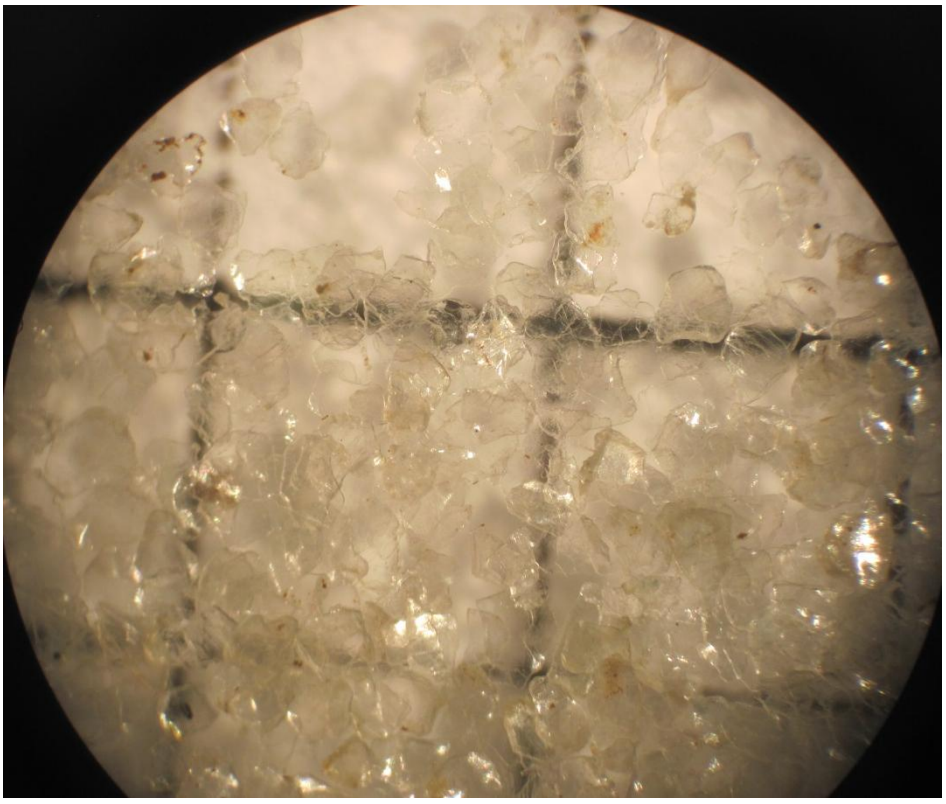

Sample I-B-4 from Barakar Sandstone in the Jharia coal field, India (shown in 1 mm grid).

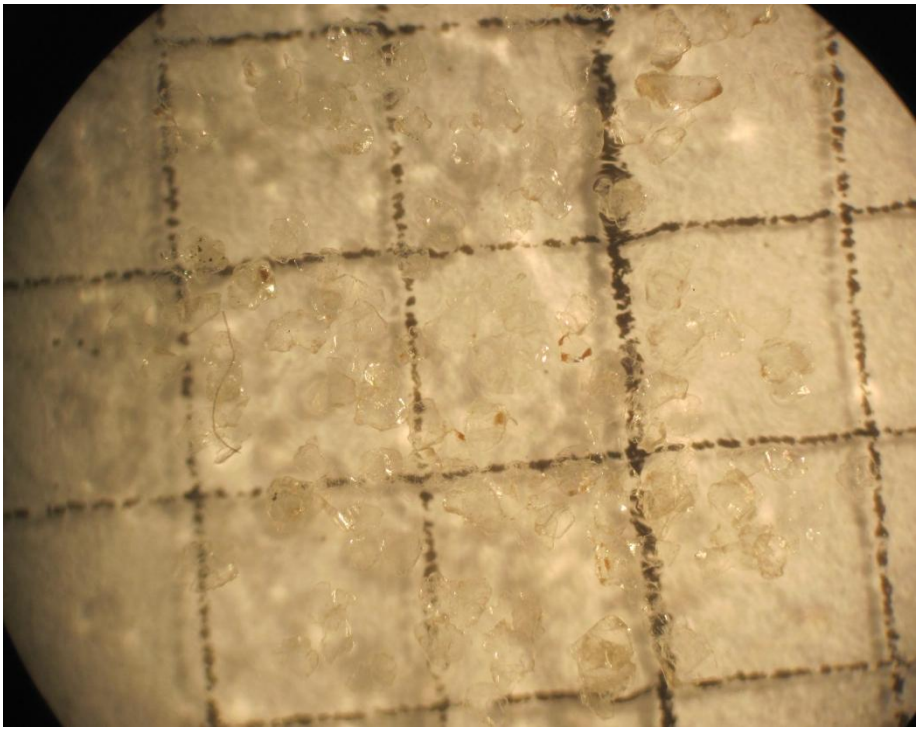

Sample I-B-13 from Barakar Sandstone in the Jharia Basin, India (shown in 1 mm grid).

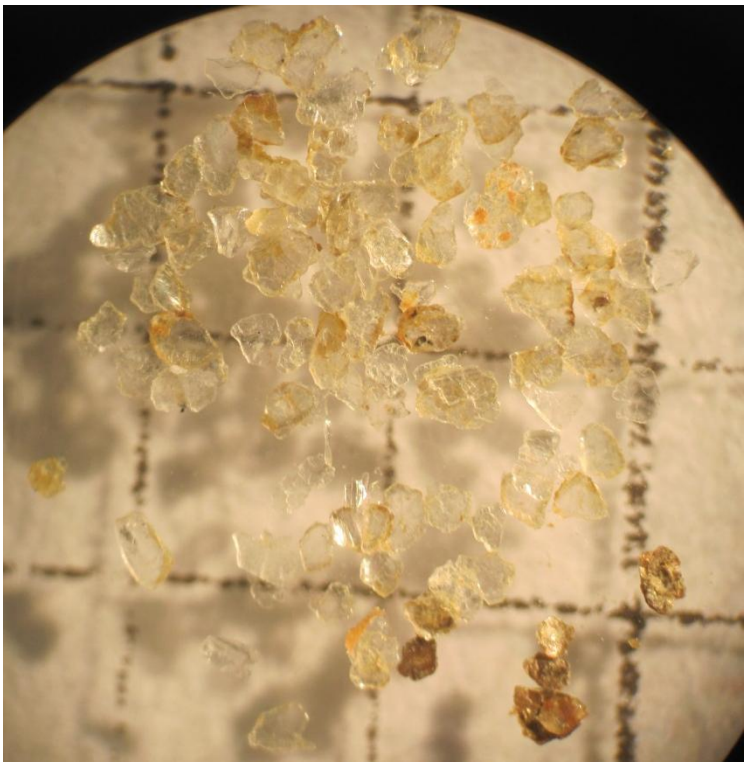

Sample I-T-1 from Talchir Formation in the Jharia Basin, India (shown in 1 mm grid).